Application of supramolecular chemistry for the design and experimentation in murine model of compounds with trypanocidal activity

/

Aplicación de la química supramolecular para el diseño y experimentación en modelo murino de compuestos con actividad tripanocida

Memoria de Tesis Doctoral presentada por ***D. Rubén Martín Escolano*** *para aspirar a la obtención del título de* ***Doctor Internacional*** *por la* ***Universidad de Granada*** *dentro del* ***Programa de Doctorado en Medicina Clínica y Salud Pública (B12.56.1)***

Rubén Martín Escolano

Departamento de Parasitología

Universidad de Granada

Directores de la Tesis Doctoral

Dr. Manuel Sánchez Moreno

Profesor Emérito de la

Universidad de Granada

Dra. Clotilde Marín Sánchez

Profesora Titular de la

Universidad de Granada

Editor: Universidad de Granada. Tesis Doctorales
Autor: Martín Escolano, Rubén
ISBN: 978-84-1306-647-9
URI: http://hdl.handle.net/10481/63923

INDEX

1. SUMMARY/RESUMEN

Chagas Disease, also known as American Trypanosomiasis, is a life-long and life-threatening illness caused by tropical infection with the insect-transmitted protozoan parasite *Trypanosoma cruzi*. According to the World Health Organization, Chagas Disease is classified as a neglected tropical disease, it is the most important parasitic disease in Latin America and, after acquired immune deficiency syndrome and tuberculosis, it is the third most spread infectious disease in this region.

Chagas Disease is an important public health problem in Latin America, it is the leading cause of morbimortality in many endemic regions and it generates a global expenditure of USD$627.5 million per year in health care costs. Moreover, Chagas Disease is the most prevalent of the poverty-caused and poverty-promoting neglected tropical disease in Latin America countries, where fewer than 10 % people are diagnosed and only a few number receive treatment. Recently, Chagas Disease has become more widespread due to the increase mobility and migration, with large numbers of infected individuals, particularly in North America and Europe (mainly Spain). Hence, Chagas Disease has converted into a global health problem, with 6–8 million infected people, 14–50 thousand deaths annually, and 70–100 million people at risk of infection worldwide.

The parasite *T. cruzi* is naturally transmitted by blood-sucking triatomine vectors, although congenital transmission, blood transfusion and organ transplantation from infected donors, parasite-contaminated food and drink, and laboratory accidents are other important means of transmission.

Despite many efforts over the past decades, the long-term nature of Chagas Disease and its complex pathology have resulted in a lack of effective vaccines, and currently approved treatments are still limited to two obsolete nitroheterocyclic drugs, benznidazole and nifurtimox. Hence, new safe and effective treatments for Chagas Disease are urgently needed.

For several years our group has colalborated with various chemical groups, which were responsible for the synthesis of the compounds. Subsequently, our group carried out the biological tests with the aim of determining the trypanocidal activity both *in vitro* and *in vivo* of the synthesized compounds. Our group also performed a preliminary analysis of the mechanism of action of the trypanocidal drug candidates at the energy metabolism level and the inhibition of the superoxide dismutase protein.

A complete screening strategy has been designed according to different authors. The reference drug benznidazole was also tested to compare the results obtained and to select only the compounds with enhanced efficacy. Assays were performed against extra- and intracellular forms of three different *T. cruzi* strains. For *in vivo* assays, the selected compounds were evaluated in infected BALB/c mice in both the acute and chronic phases of Chagas Disease. The methodology has been also improved according to the available instrumentation both *in vitro* and *in vivo*.

In addition, a novel, sensible, precise and simple fluorescence based-method has been developing for monitoring infected cultures over time to identify static/cidal and slow/fast-acting compounds. This is an important fact since fast-acting, long-lasting and cidal drugs are urgently needed.

The project developed during this pre-doctoral period, in collaboration with the chemical groups, has allowed us to evaluate a total of 519 compounds belonging to different chemical families. We have identified seven trypanocidal drug candidates for the treatment of Chagas Disease, some of which have already been published. These trypanocidal candidates show improved *in vitro* activity against the relevant forms from a clinical viewpoint and enhanced *in vivo* efficacy compared to the reference drug benznidazole. In addition, they fulfill the most stringent *in vitro* requirements stablished for ideal drugs against Chagas Disease, and most of the *in vivo* criteria of the target

product profile for Chagas Disease. Hence, these compounds provide a step forward in the development of new cost-effective anti-Chagas drugs for clinical trials. Three of them are included in this doctoral thesis.

The results obtained are summarized in several conclusions on the potential use and putative mechanism of action of candidates for the development of new treatments for Chagas Disease, and on the novel fluorescence-based method developed for the drug screening. Also, future guidelines are established to take a step further in this research in order to achieve better outcomes.

/

La Enfermedad de Chagas, también conocida como Tripanosomiasis americana, es una enfermedad crónica y potencialmente mortal. Se trata de una infección tropical causada por el protozoo parásito *Trypanosoma cruzi*, el cual es transmitido por insectos. De acuerdo con la Organización Mundial de la Salud, la Enfermedad de Chagas se clasifica como una enfermedad tropical desatendida, es la enfermedad parasitaria más importante de América Latina y, después del síndrome de inmunodeficiencia adquirida y la tuberculosis, es la tercera enfermedad infecciosa más extendida de esta región.

La Enfermedad de Chagas es un importante problema de salud pública en América Latina, es la principal causa de morbimortalidad en muchas regiones endémicas y genera un gasto global de 627.5 millones de dólares estadounidenses en atención médica al año. Además, la Enfermedad de Chagas es la mayor causa y consecuencia de pobreza de todas las enfermedades tropicales desatendidas en los países de América Latina, donde se diagnostican menos del 10 % de las personas y sólo unas pocas reciben tratamiento. Recientemente, la Enfermedad de Chagas se ha generalizado debido al aumento de la movilidad y la migración, con un gran número de personas infectadas, particularmente en América del Norte y Europa (principalmente España). Por lo tanto,

la Enfermedad de Chagas se ha convertido en un problema de salud global, con 6–8 millones de personas infectadas, 14–50 mil muertes anuales, y 70–100 millones de personas en riesgo de infección en todo el mundo.

El parásito *T. cruzi* se transmite de manera natural a través de vectores triatominos hematófagos, aunque la transmisión congénita, la transfusión de sangre y el trasplante de órganos de donantes infectados, los alimentos y bebidas contaminadas con el parásito, y los accidentes de laboratorio son otros medios de transmisión importantes.

A pesar de los muchos esfuerzos de las últimas décadas, la naturaleza a largo plazo de la Enfermedad de Chagas y su compleja patología han dado lugar a una falta de vacunas eficaces, y actualmente los tratamientos se limitan a dos fármacos nitroheterocíclicos obsoletos, el benznidazol y el nifurtimox. Por lo tanto, se necesitan urgentemente nuevos tratamientos seguros y eficaces para la Enfermedad de Chagas.

Durante varios años nuestro grupo ha colaborado con distintos grupos químicos, los cuáles fueron responsables de la síntesis de los compuestos. Posteriormente, nuestro grupo ha realizado los ensayos biológicos con el fin de determinar la actividad tripanocida tanto *in vitro* como *in vivo* de los compuestos sintetizados. Nuestro grupo también ha realizado un análisis preliminar del mecanismo de acción de los potenciales compuestos a nivel del metabolismo energético y la inhibición de la proteína superóxido dismutasa.

Se ha diseñado una estrategia completa de cribado de acuerdo con diferentes autores. El fármaco de referencia benznidazol también se ha ensayado para comparar los resultados obtenidos y seleccionar sólo los compuestos con mayor eficacia. Se realizaron ensayos frente a las formas extra e intracelulares de tres cepas diferentes de *T. cruzi*. Para los ensayos *in vivo*, los compuestos seleccionados se evaluaron en ratones BALB/c infectados tanto en la fase aguda como en la fase crónica de la Enfermedad de Chagas.

La metodología también se ha mejorado de acuerdo a la instrumentación disponible tanto *in vitro* como *in vivo*.

Además, se ha desarrollado un método novedoso, sensible, preciso y sencillo basado en fluorescencia para el seguimiento de cultivos infectados a lo largo del tiempo con el objetivo de identificar compuestos tripanostáticos/tripanocidas y de acción lenta/rápida. Este es un hecho importante ya que se necesitan urgentemente fármacos tripanocidas, de acción rápida y de larga duración.

El proyecto desarrollado en esta tesis doctoral, en colaboración con los grupos quimicos, ha permitido evaluar un total de 519 compuestos pertenecientes a diferentes familias químicas. Hemos identificado siete posibles candidatos para el tratamiento de la Enfermedad de Chagas, algunos de los cuáles ya han sido publicados. Estos potenciales compuestos muestran mejor actividad *in vitro* frente a las formas relevantes desde un punto de vista clínicos y mayor eficacia *in vivo* en comparación con el fármaco de referencia benznidazol. Además, estos compuestos cumplen con los requisitos *in vitro* más estrictos establecidos para los fármacos ideales, y la mayoría de los criterios *in vivo* establecidos para la Enfermedad de Chagas. Por lo tanto, estos compuestos suponen un paso adelante en el desarrollo de nuevos fármacos anti-Chagas rentables para ensayos clínicos. Tres de ellos se incluyen en esta tesis doctoral.

Los resultados obtenidos se resumen en varias conclusiones sobre el uso potencial y sobre el posible mecanismo de acción de los potenciales candidatos para el desarrollo de nuevos tratamientos para la Enfermedad de Chagas, y sobre el novedoso método basado en fluorescencia para el cribado de fármacos. Además, se establecen las pautas futuras para dar un paso más en esta investigación con el fin de lograr mejores resultados.

2. INTRODUCTION

2.1. Chagas Disease & Trypanosoma cruzi

2.1.1. Background

Chagas Disease (CD), also known as Chagas-Mazza or American Trypanosomiasis, is named after Carlos Ribeiro Justiniano Chagas, a Brazilian doctor who discovered the disease in 1909[1,2]. The discoveries of C. Chagas are unique in at least two senses. First, C. Chagas found the pathogen *Trypanosoma cruzi* in the triatomine vector *Panstrongylus megitus* before he described the clinical disease and isolated the organism from patients. Second, many aspects of the disease have been rapidly understood, largely by the efforts of a single individual. He described the clinical aspects of CD, its epidemiology, as well as the hosts, the insect vector, and different developmental stages of the parasite in the medical institute at the Manguinhos farm, under the directorship of Oswaldo Gonçalves Cruz[1,3]. This period is considered the founding stage[4].

In the 1930s, Dr Salvador Mazza opened the studies up to a large number of cases for the first time, confirming the endemic nature of CD and defining the anatomical-clinical stages of the disease[4].

On February, 1909, C. Chagas consulted a 2-year-old patient in Brazil that would be the first CD case described in the literature: the child had a high fever, face edema, presence of the parasite in the bloodstream, and hepatosplenomegaly[1]. Following this, there were first reports in: El Salvador (1913)[5], Peru (1919)[6], Venezuela (1919)[7], Costa Rica (1922)[8], Paraguay (1924)[9], and Chile (1937)[10], among others. Nevertheless, there is evidence that CD was present in Latin America from the beginning of the XIII century through Peruvian ceramics that show possible representations of CD[3,11]. In 1997, deoxyribonucleic acid (DNA) analysis have found the oldest evidence *T, cruzi* infection in mummies from the Atacama Desert, dating from 7,050 years B.C.[12]

After its discovery, CD was limited for many decades only in Latin America as a silent, rural and poorly visible disease[13,14]. The classical endemic region of CD ranges from the north Argentina and Chile to the southern USA, comprising 21 countries, in which vector borne transmission to man occurs[2,14]. In the 1980s, 17.4 million people were the estimated number of infected individuals in Latin America, and 100 million people were at risk of infection[13,15]. Since the 1990s, national and international health policies (e.g. compulsory blood-bank screening) and multinational initiatives (e.g. "Southern Cone Initiative", "Initiative of the Andean Countries", "Initiative of Central America and Mexico", and "Initiative of the Amazon Countries") have led to significant reductions in the number of cases of CD and the presence of triatomine vectors in many endemic regions of Latin America[16,17]. As a consequence of these initiatives, 7.7 million people were infected in 2005 and 5.7 million people in 2010 in Latin America, also reducing the percentage of population at risk of infection[13,15] (**Table 1**). In addition, the vectorial transmission, and indirectly blood-transfusion and congenital transmissions, were decreased[18], even declared interrupted in Uruguay (1997), Chile (1999) and Brazil (2006)[19].

In recent decades, CD has spread to other regions due mainly to the constant mobility and migration[16,20], with recorded outbreaks in Canada, USA, several European countries, Australia, New Zealand, and Japan[21,22] (**Figure 1**). While the prevalence of the disease has been reduced in Latin America, a dramatic increase in non-endemic countries have been observed in recent decades[23,24]. Hence, CD is currently a global health problem that affects 6–8 million people[13,16,25], causes about 28 thousand new cases and 14–50 thousand deaths annually, and it is hypothesized that 70–100 million people are living at risk of infection[2,13,26], most of them in Latin America. The current estimated number of infected people in non-endemic countries is large, particularly in

Table 1. Estimated number of infected individuals with *T. cruzi* and people at risk of infection in Latin America in 1980-1985, and in 2005 and 2010 after the health policies and initiatives. Taken from *Lidani KCF et al., 2019*[13].

	1980–1985		2005		2010	
	Infected individuals	Individuals at risk of infection (%)	Infected individuals	Individuals at risk of infection (%)	Infected individuals	Individuals at risk of infection (%)
SOUTHERN CONE						
Argentina	2,640,000 (10%)	23	1,600,000 (4.1%)	23	1,505,235 (3.64%)	5.42
Bolivia	1,300,000 (24%)	32	620,000 (6.8%)	32	607,186 (6.1%)	5.9
Brazil	6,180,000 (4.2%)	32	1,900,000 (1%)	32	1,156,821 (0.6%)	13.4
Chile	1,460,000 (16.9%)	63	160,200 (1%)	63	119,660 (0.7%)	0
Paraguay	397,000 (21.4%)	31	150,000 (2.5%)	31	184,669 (2.13%)	19.6
Uruguay	37,000 (3.4%)	33	21,700 (0.7%)	33	7,852 (0.23%)	0
ANDEAN INITIATIVE						
Colombia	900,000 (30%)	11	436,000 (1%)	11	437,960 (0.95%)	10.5
Ecuador	30,000 (10.7%)	41	230,000 (1.7%)	47	199,872 (1.38%)	28.9
Peru	621,000 (9.8%)	39	192,000 (0.7%)	12	127 282 (0.43%)	4.5
Venezuela	1,200,000 (3%)	72	310,000 (1.2%)	18	193,339 (0.71%)	3.8
CENTRAL AMERICA						
Belize	–	–	2,000 (0.7%)	50	1,040 (0.3%)	22.3
Costa Rica	130,000 (11.7%)	45	23,000 (0.5%)	23	7,667 (0.16%)	5.2
El Salvador	900,000 (20%)	45	232,000 (3.4%)	39	90,222 (1.3%)	15.9
Guatemala	1,100,000 (16.6%)	54	250,000 (2%)	17	166,667 (1.2%)	10.3
Honduras	300,000 (15.2%)	47	220,000 (3.1%)	49	73,333 (9.2%)	14.6
NICARAGUA	–	–	58,600 (1.1%)	25	29,300 (0.52%)	11.5
Panama	200,000 (17.7%)	47	21,000 (0.01%)	31	18,337 (5.2%)	13.1
Mexico	–	–	1,100,000 (1%)	28	876,458 (7.8%)	20.9
*Guianas/Suriname	–	–	–	–	12,600 (0.8%)	25.1
Total	17,395,000 (4.3%)	25	7,694,500 (1.4%)	20	5,742,167 (1.1%)	12.9

USA (>300,000)[13,27] and Spain (>70,000)[13,27,28]. Moreover, CD generates a global expenditure of USD$627.5 million per year in health care costs[29]. In this context, the Drugs for Neglected Diseases *Initiative* (DND*i*) launched the Chagas Clinical Research Platform (CCRP) in 2009 to develop new treatments of CD. This platform brings together experts and stakeholders to provide support for the evaluation and development of new drugs for CD, the standardization of methodology to assess drug efficacy, and the revision of alternatives for using current approved drugs (guidelines, doses, combination)[2].

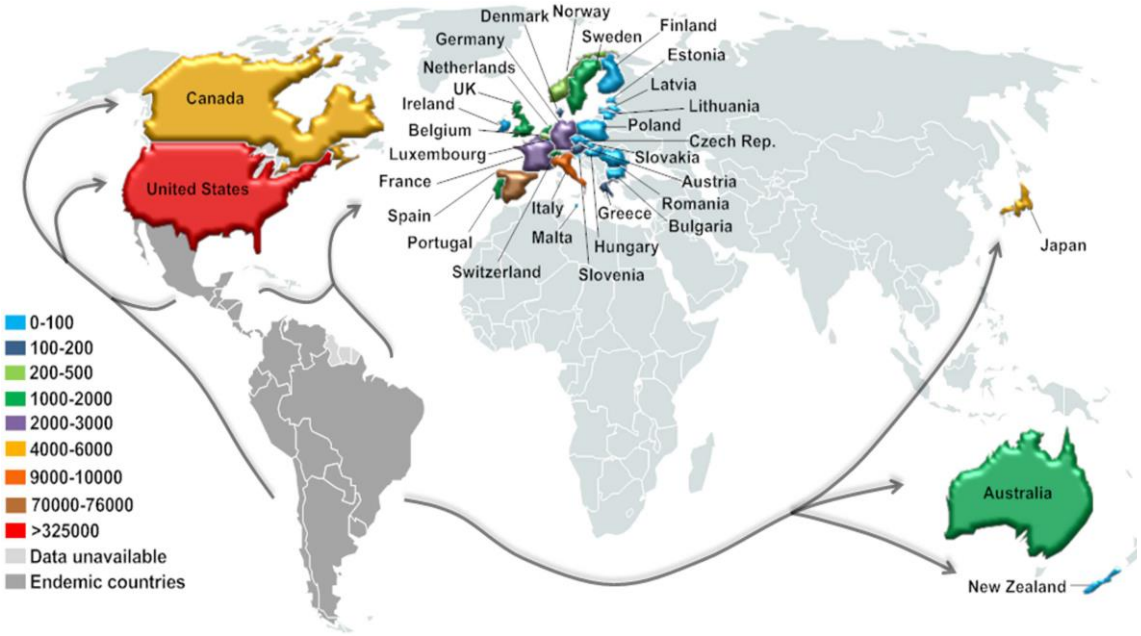

Figure 1. Estimated number of immigrants with *T. cruzi* infection in non-endemic countries. Taken from *Lidani KCF et al., 2019*[13].

According to the World Health Organization (WHO), CD is classified as the most prevalent of the poverty-caused and poverty-promoting neglected tropical disease (NTD), the most important parasitic disease, and after acquired immune deficiency syndrome (AIDS) and tuberculosis, the third most spread infectious disease in Latin America[13,30,31]. However, fewer than 10 % people are diagnosed and only a few number receive treatment[2,31,32].

2.1.2. T. cruzi: trypanosome cell

T. cruzi is an eukaryotic parasite belonging to the order Kinetoplastida (family Trypanosomatidae, genus *Trypanosoma*), a monophyletic group of unicellular parasitic protozoa[33]. Hence, *T. cruzi* has the classical features of eukaryotes (plasma membrane, membrane bound nucleus, endoplasmic reticulum, and Golgi apparatus) and several particular features in common with other kinetoplastids (a single mitochondrion, glycosomes, and DNA found within a single suborganellar structure – the kinetoplast)[34].

A schematic representation of epimastigote form of *T. cruzi* is shown in **Figure 2A**.

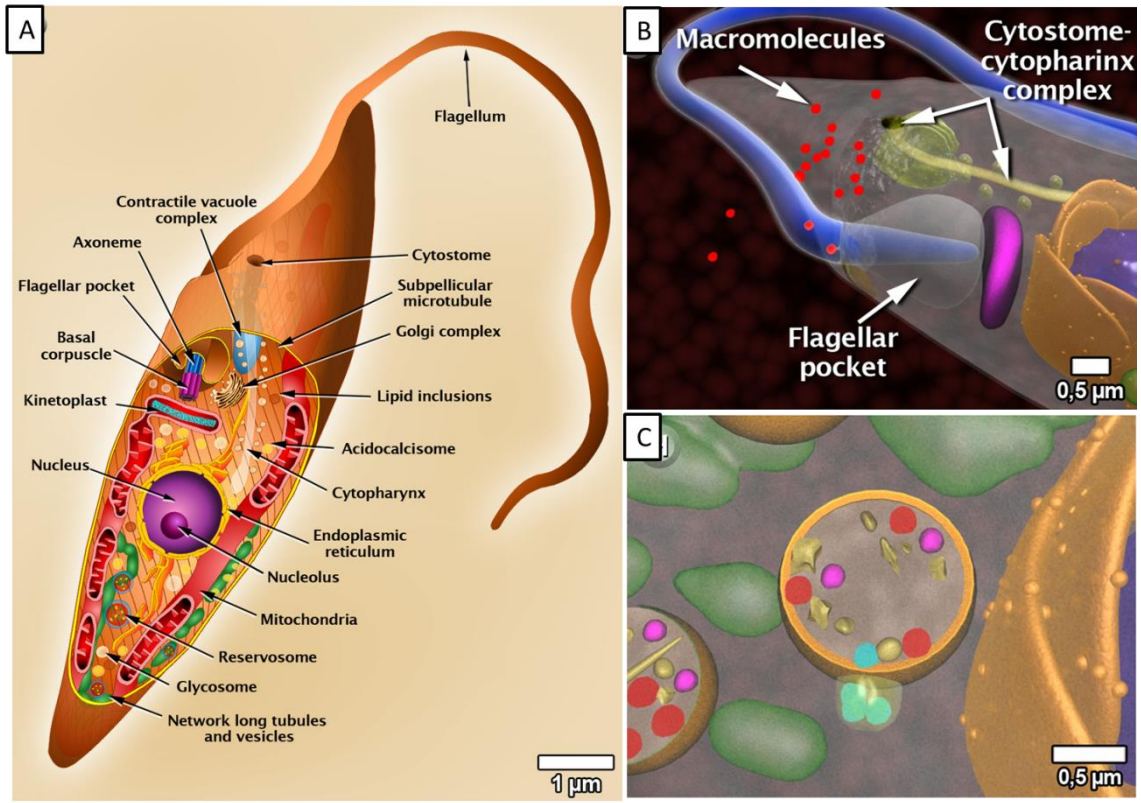

Figure 2. Schematic representations of (A) *T. cruzi* epimastigote organelles, (B) specialized invaginations: flagellar pocket and cytostome, and (C) cytostome containing macromolecules and cruzipain. Taken from *Teixeira DE et al., 2012*[35].

The kinetoplast is located in a well-defined region of the mitochondrion, forming a rounded or rod-like structure below the basis of the flagellum[36]. It is a linked network of hundreds of molecules that are catenated and compressed into a disc-like structure: the

minicircles and maxicircles. Minicircles carry the specific information for ribonucleic acid (RNA) editing in the form of guide RNAs (gRNAs). Maxicircles are the functional equivalent of the mitochondrial DNA of other eukaryotes, containing genes for mitochondrial ribosomal RNAs (rRNAs) and mitochondrial proteins involved in the membrane-bound oxidative phosphorylation pathway. This kinetoplast DNA (kDNA) comprises approximately 20–25 % of the total cellular DNA in *T. cruzi*[34].

The glycosome is a membrane-enclosed organelle that compartmentalizes glycolysis. This organelle concentrates and compartmentalizes the glycolitic enzymes, increasing the efficiency of this process[36]. It also store minerals in electrondense structures so-called acidocalcisomes, and sequesters membranes and macromolecules in vesicles known as reservosomes[34].

It is interesting to note that the cytoskeleton of *T. cruzi* is unusual: it is predominantly microtubular with no evidence of microfilament, intermediate filament systems or centrioles. The different *T. cruzi* stages are imposed by a sub-pellicular corset of microtubules which closely adheres to the plasma membrane, and the replicative forms undergo mitosis with a microtubule spindle which emerges from poorly defined structures in the nuclear membrane[34]. However, molecular analyses showed the presence of actin, myosin, and other related proteins located in rounded and punctuated structures in the cytoplasm and flagellum[37,38].

T. cruzi possesses a single flagellum subtended by the single defined microtubule organizing centre, the basal body, which lies within the cell. The flagellar motor is the typical ciliary axonemal complex (9 + 2 configuration of parallel microtubules), and it is appended by filaments to an unusual semi-crystalline structure so-called paraflagellar rod (PFR) (**Figure 3**). This PFR provides support to the flagellar axoneme, playing an

essential role in motility. The exterior flagellum is surrounded by a specialized sterol- and sphingolipid-rich membrane which contains domain-specific proteins[34].

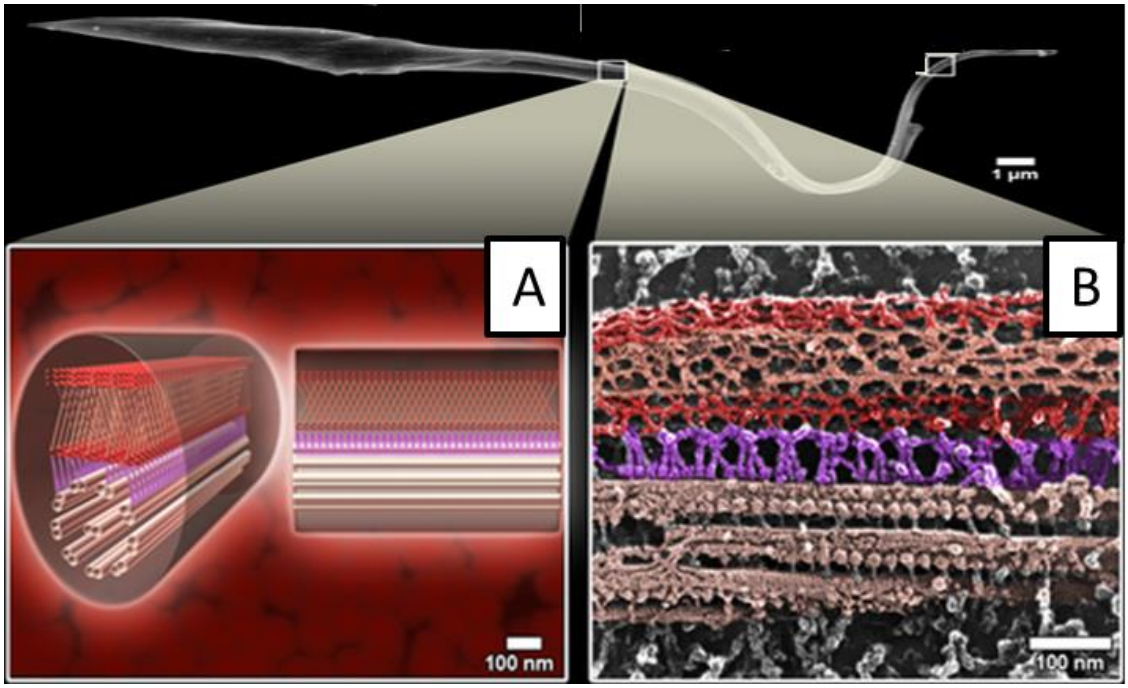

Figure 3. Paraflagellar rod (PFR). (A) Schematic 3D representation and (B) deep-etching replica images. Axoneme (light pink), filaments that link the PFR proteins to the axoneme (purple), PFR (red), and the intermediate domain (salmon). Taken from *Teixeira DE et al., 2012*[35].

The cell surface of *T. cruzi* can be considered as composed of three structures: the glycocalix, the lipid bilayer, and the sub-pellicular microtubules. Although the intramembranous particles are uniformly distributed throughout most of the plasma membrane, there are a few areas of membrane specialization[36]. These areas are two specialized invaginations: the flagellar pocket and the cytostome (**Figure 2B**). The flagellar pocket is the invagination that forms at the junction site between the sub-pellicular plasma membrane and flagellar membrane. The majority of vesicular trafficking and nutrient uptake is believed to occur in this area and many receptors are specifically located to this region. The cytostome is a smaller invagination proximal to the flagellar pocket which has also been implicated in nutrient uptake[34]. The cytostome

is found only in epimastigote and amastigote forms[36]. The nutrients ingested through these specialized sites are delivered to reservosomes, which are the last compartment of the endocytic pathway, provide storage for macromolecules and also concentrate cruzipain (**Figure 2C**)[39].

2.1.3. Genetic diversity of T. cruzi

T. cruzi belongs to a heterogeneous species consisting of a pool of strains and isolates that circulate among vectors and mammalian hosts[31]. This heterogeneity could explain the geographical differences in disease pathology, morbidity, and mortality, and it has been extensively studied by biological, biochemical, and molecular methods[40,41]. However, no definitive correlation between disease severity and parasite lineage has been established[31].

In 1982, the high genetic intraspecific diversity of *T. cruzi* was reported, showing a difference of up to 40 % in both nuclear and kinetoplast DNA content between strains[42]. Such difference would be equivalent to 73 Mb of DNA, an amazing finding for populations of the same species[43]. In 1999, phlylogenetic reconstructions by comparative analysis based on ribosomal DNA (rDNA) sequences suggest that *T. cruzi* strains diverged about 100 milllion years ago[44]. Since 2001, several articles reported the natural and habitual recombination in *T. cruzi*[43,45–48], as well as evidence that hybridization and genetic exchange are frequent between the dividing amastigote intracellular forms[49]. Moreover, similarly to that observed in other trypanosomatids, in which genetic exchange takes place in the vectors[50,51], it would be expected that this exchange also occurs in the digestive tract of triatomine vectors among the perimicrovilar membranes-adherent epimastigotes[52].

Taken as a whole, the traditional paradigm of the clonal evolution model is challenged: *T. cruzi* has been considered a clonal organism that replicates by binary fission and in

which new clones evolve with the accumulation of discrete mutations. Currently, the evidence indicates that recombination and genetic exchange have contributed to the present parasite population structures and to the evolution of distinct *T. cruzi* subgroups[53].

In 1999, two major lineages were described[54]: *T. cruzi* I, which is associated with human disease in all endemic countries north of the Amazon basin; and *T. cruzi* II, which predominates in the Southern Cone countries, and is subdivided into five discrete typing units (DTUs) – IIa, IIb, IIc, IId, and IIe[55–57]. In 2005, the whole-genome sequencing of the *T. cruzi* CL Brener strain was performed, which opens prospects for the development of novel therapeutic and diagnostic techniques[58]. In 2006, the existence of a *T. cruzi* III lineage was reported[59]. In 2009, an expert committee considered previous studies based on the pattern of genetic, biochemical and biological markers, and proposed a minimum of six genetic lineages or DTUs, named TcI to TcVI[60]. Finally, analyses from genealogies of mitochondrial sequences identified in 2016 three clades that hold a correlation with the DTUs: clade A corresponds to TcI; clade B, to TcIII, TcIV, TcV and TcVI strains; and clade C, exclusive to TcII strains[61].

TcI and TcV infections are the most commonly identified, although other DTUs predominate in some specific areas[62]. TcI is implicated with CD in Amazonia, the Andean countries, Central America, and Mexico, and clinical presentations mainly include chagasic cardiomyopathy; TcII, TcV and TcVI are the main causes of CD in the Southern Cone region, and clinical presentations include chagasic cardiomyopathy, and a proportion of cases megaoesophagus and megacolon[63,64]. **Figure 4** shows the approximate geographical distribution of all *T. cruzi* DTUs in the American continent.

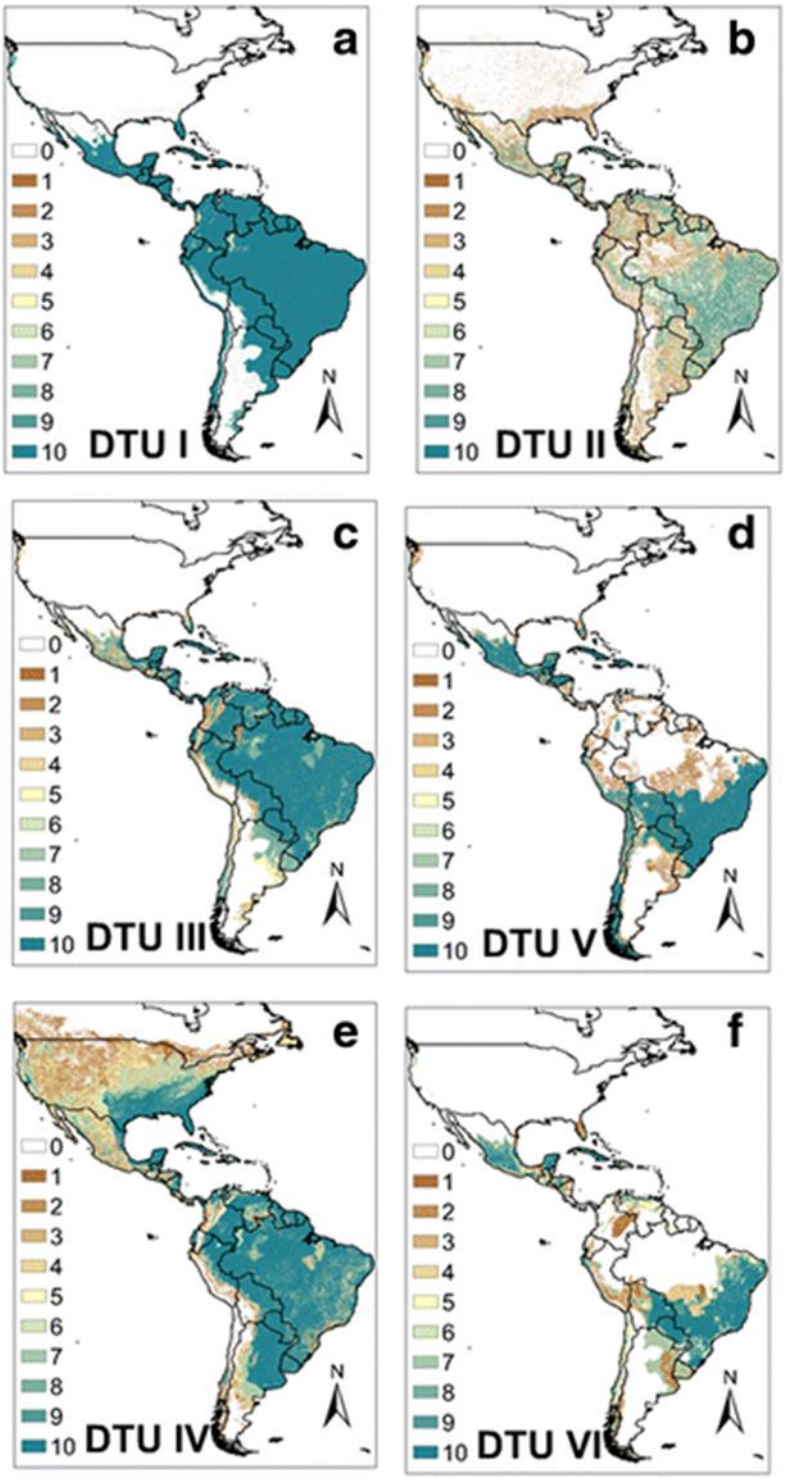

Figure 4. Approximate geographical distribution of *T. cruzi* discrete typing units (DTUs) in the American continent. (a) DTUI, (b) DTUII, (c) DTUIII, (d) DTUV, (e) DTUIV, (f) DTUVI. Taken from *Izeta-Alberdi A et al., 2016*[65].

The genetic diversity of *T. cruzi* is an important point since there have been several reports of wide divergence in the susceptibility of the current treatments – benznidazole (BZN) and nifurtimox (NFX) – to different *T. cruzi* strains, and independent of the mitochondrial nitroreductase (TcNTR) sequence – BZN and NFX are prodrugs that require NTR-catalyzed activation within the parasite to have trypanocidal effects[66,67]. This fact implies that this susceptibility must be associated with additional factors, which are not a consequence of the treatment. These factors must be studied to avoid drug resistance and treatment failures[66–68]. The division of *T. cruzi* strains into DTUs led to investigate whether certain DTUs were associated with natural drug resistance: some reports showed that TcI isolates were more resistant to BZN than others[69], while other authors concluded that this correlation does not exist[67,68].

2.1.4. Glucose metabolism of T. cruzi

It has been known for many years that epimastigotes of *T. cruzi* are able to uptake and consume both carbohydrates and amino acids, and glucose is preferred over amino acids when both are present[70]. Trypanosomatids are among the cells that have a higher rate of glucose consumption. This is associated with the peculiar metabolism that was called "aerobic fermentation of glucose"[71]: trypanosomatids produce and excrete into the medium still-reduced compounds from glucose catabolism (succinate and l-alanine), even under aerobic conditions, instead of oxidizing glucose completely to carbon dioxide (CO_2) and water[72]. A second peculiar feature of glucose catabolism in tripanosomatids is the lack of the Pasteur effect, that is, the transition from anaerobiosis to aerobiosis is not accompanied by a considerable decrease in glucose consumption. They even show a "reverse Pasteur effect", meaning that glucose utilization may be lower under anaerobic conditions. This is a result of the lack of effect of the normal inhibitors of hexokinase and phosphofructokinase[72]. The lack of normal inhibitors of

these enzymes, together with the fact that hexokinase is one of the enzymes with higher control on the pathway fluxes and is a key enzyme encoded by all morphological forms of *T. cruzi*[73–75], makes this enzyme a promising target for chemotherapy.

The glucose catabolism (glycolytic pathway) in tripanosomatids is partially compartmentalized in a peroxisome-like organelle, called glycosome, since the first six enzymes are found in this organelle[76]. The lack of the classical regulation of the above-mentioned enzymes has been proposed to be compensated by the compartmentation of these first six enzymes[77]. A schematic representation of glycolysis in *T. cruzi*, together with the tricarboxylic acid cycle, is shown in **Figure 5**. The balance between succinate and l-alanine (still-reduced end-products) shifts depending on the CO_2 concentration: if the CO_2 concentration is high, the production of succinate by the phosphoenolpyruvate carboxykinase (PEPCK) is favoured[78]; if the latter enzyme is inhibited, the production of l-alanine is favoured[79].

All glycolytic systems must have, in order to remain functional, an efficient system for the reoxidation of the nicotinamide adenine dinucleotide (NADH). *T. cruzi* has several possible ways for NADH reoxidation. These are, in addition to reoxidation in the respiratory chain, production of succinate and probably also of L-alanine[80].

T. cruzi metabolizes glucose through a second pathway, the so-called pentose phosphate pathway (PPP) or pentose phosphate cycle[74] (**Figure 6**). The PPP is involved in the production of the ribose 5-phosphate required for nucleotide synthesis and of reducing power in the form of NADPH – an essential coenzyme for biosynthetic pathways and also for protection against oxidative stress, due to reactive oxygen species (ROS)[81]. All seven enzymes of the PPP are present in the four major stages of the parasite life-cycle, and deletion[82] or inhibition[83] of some of them has been shown to be lethal for *T. cruzi*. All this makes these enzymes promising targets for the chemotherapy of CD.

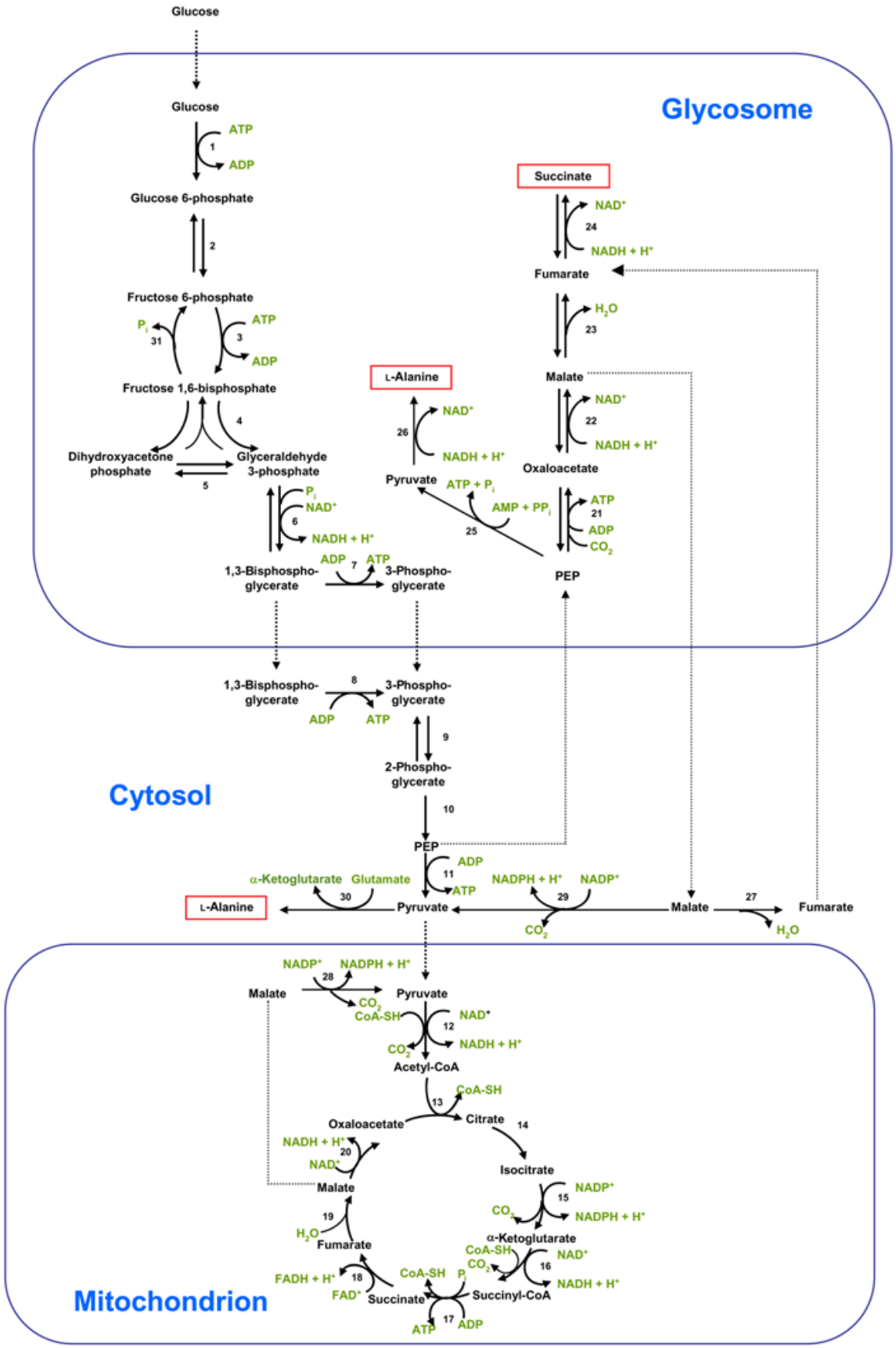

Figure 5. Schematic representation of glycolysis and the tricarboxylic acid cycle in *T. cruzi*. 1, Hexokinase K; 2, phosphoglucose isomerase; 3, phosphofructokinase; 4, aldolase; 5, triose

phosphate isomerase; 6, glyceraldehyde-3-phosphate dehydrogenase; 7, phosphoglycerate kinase (glycosomal); 8, phosphoglycerate kinase (cytosolic) 9, phosphoglycerate mutase; 10, enolase; 11, pyruvate kinase; 12, pyruvate dehydrogenase complex; 13, citrate synthase; 14, aconitase; 15, NADP-linked isocitrate dehydrogenase; 16, α-ketoglutarate dehydrogenase complex; 17, succinate thiokinase; 18, succinate dehydrogenase; 19, fumarate hydratase (mitochondrial); 20, malate dehydrogenase (mitochondrial); 21, phosphoenolpyruvate carboxykinase; 22, malate dehydrogenase (glycosomal); 23; fumarate hydratase (glycosomal); 24, NAD-linked fumarate reductase; 25, pyruvate, phosphate dikinase; 26, alcohol dehydrogenase; 27, fumarate hydratase (cytosolic); 28, NADP-linked malic enzyme (mitochondrial); 29, NADP-linked malic enzyme (cytosolic); 30, alanine aminotransferase; 31, fructose-1,6-bisphosphatase. Taken from *Maugeri DA et al., 2011*[74].

Glucose transport – via a facilitated transporter – has also been thoroughly studied in trypanosomatids. Bloodstream trypomastigotes (BTs), which obviously live in glucose-rich medium, express the only gene encoding a glucose transporter[84,85]. However, intracellular amastigotes live in the cytosol of mammalian cells, where free glucose cannot be abundant; in this sense, amastigote forms do not uptake glucose from the medium and the expression of the transporter has not been found. Amastigote forms obtain their energy mostly from amino acids. Epimastigote foms, although living in a medium in which glucose is supposed to be scarce, express the glucose transporter and prefer glucose to amino acids[85].

Finally, it is interesting to note that the two essential enzymes for gluconeogenesis are present in *T. cruzi*, but there is no reserve polysaccharide[74].

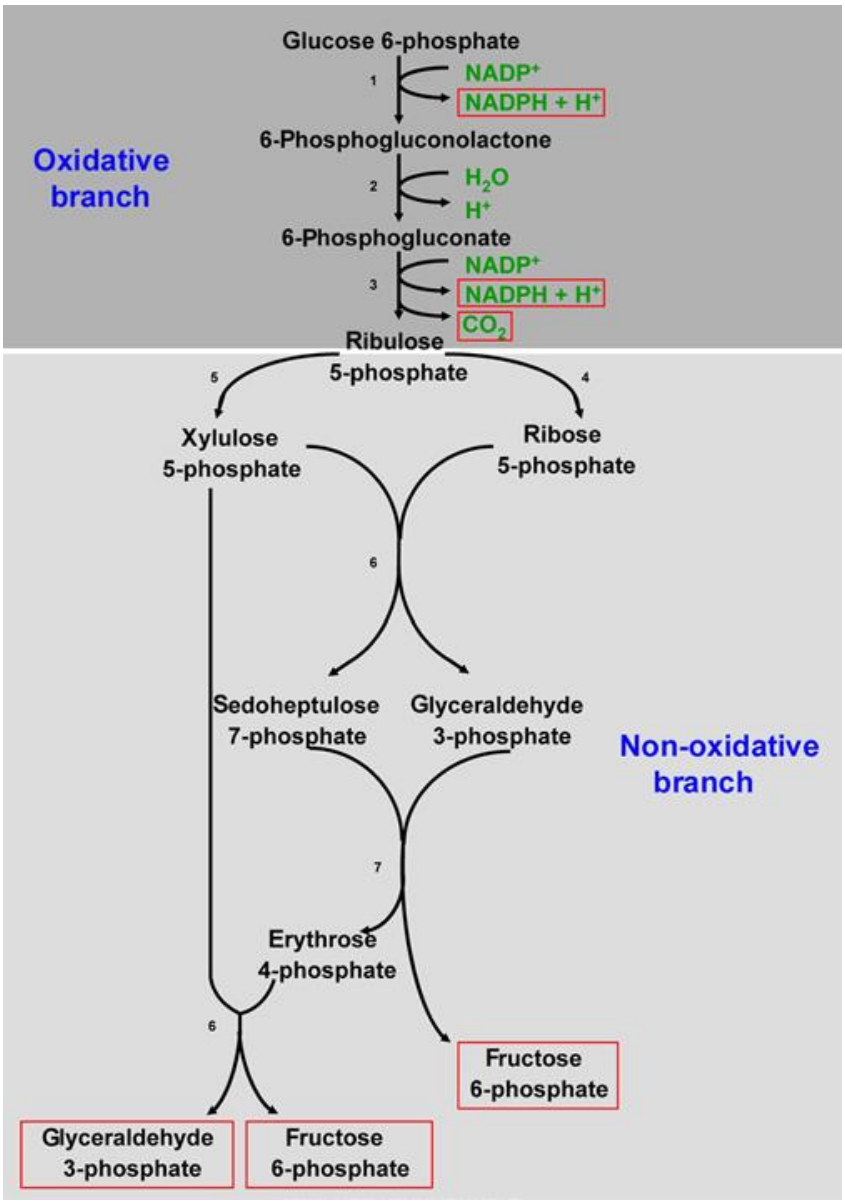

Figure 6. Schematic representation of the pentose phosphate pathway in *T. cruzi*. Taken from *Maugeri DA et al., 2011*[74].

2.1.5. Life-cycle of T. cruzi

T. cruzi is a heteroxenic protozoan, which means that it presents different stages of its life-cycle in distinct hosts. Hence, this parasite uses several strategies to survive in these diverse environmental conditions: *T. cruzi* undergoes changes in morphology, gene expression and metabolism as it passes from the replicative epimastigote stage in the insect to the non-replicative and infective metacyclic trypomastigote form for humans[86,87]. The replicative epimastigotes and the non-replicative metacyclic

trypomastigotes are the forms found in the insect vector. Meanwhile, the intracellular and replicative amastigotes and the extracellular and non-replicative BTs are the forms present in the vertebrate host[86] (**Figure 7**). In addition, intermediate forms are also observed during the *T. cruzi* life-cycle[88,89]. Cell differentiation in this parasite involves nuclear shape alterations, chromatin remodelling, mitochondrial DNA rearrangement, and relative volume alterations of the kinetoplast, reservosome and lipid bodies, among others[86,90].

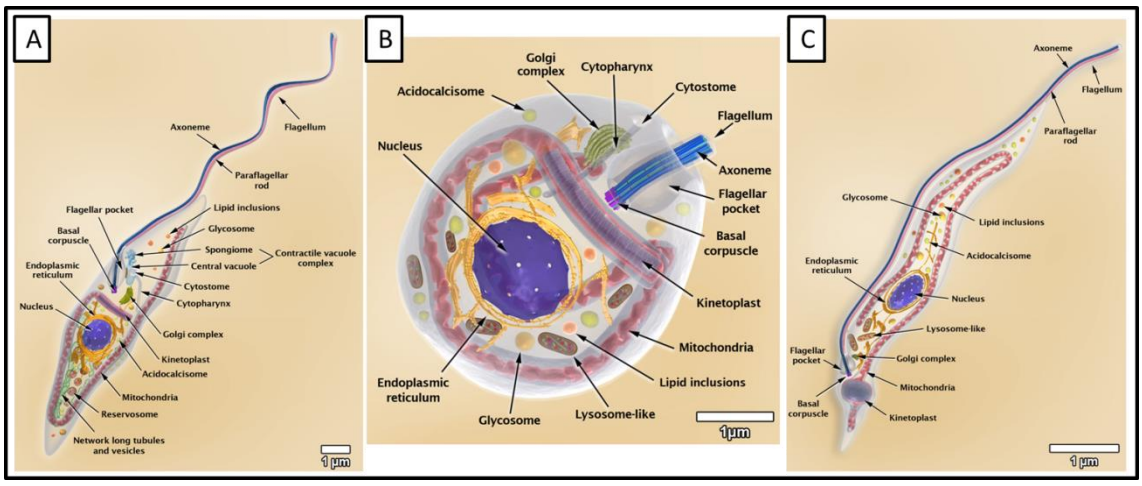

Figure 7. Schematic representations of (A) *T. cruzi* epimastigotes, (B) *T. cruzi* amastigotes, and (C) *T. cruzi* trypomastigotes. Taken from *Teixeira DE et al., 2012*[35].

T. cruzi fully embodies the characteristics of a successful parasite since it is maintained in nature by numerous vector species and mammal host species distributed almost all biomes and habitats in the Americas, such as marsupials, rodents, bats, armadillos, ranging carnivores, birds, domestic animals (dogs, cats, pigs or goats, among others), and primates[91].

In general, the classical description of *T. cruzi* life-cycle was reported more than 100 years ago[1], although it is still under study[31,35,62,89,92]. In the classical version, the infection of a mammalian host begins with the non-dividing metacyclic trypomastigotes present in the excreta (stercorarian trypanosomes) of the blood-feeding triatomine vector. These are introduced into the host by contamination of the vector bite wound or

a variety of mucosal membranes, and are able to invade a wide range of phagocytic and non-phagocytic nucleates cells. Initially, the parasites binds to receptors on the host cell surface and enter a membrane bound vacuole so-called parasitophorus vacuole (PV). Upon entry, the parasites begin to differentiate into small round-shaped amastigote forms and escape the PV into the cell cytoplasm where the morphologic transformation is completed, including flagellar involution. The amastigote forms re-enter the cell cycle and proliferate by binary fission until the cell fills with these replicative forms. At this point the amastigote forms elongate, reacquire their long flagella, and differentiate into non-replicative trypomastigote forms. These trypomastigote forms escape the cell and can invade adjacent cells; alternatively, they can enter the blood and lymph and disseminate. These BTs can be taken up by blood-feeding triatomine vectors. In the vector midgut, parasites become to the epimastigote forms and proliferate. Finally, after migration to the vector's hindgut, the late-log epimastigote forms attach to the waxy gut cuticle by their flagella and differentiate into trypomastigote forms, completing the life-cycle[31,34,62] (**Figure 8**).

Further research has revealed that this established view is rather superficial and that the process in mammalian host cells is certainly more complex (**Figure 9**): (A) the initial differentiation from the metacyclic trypomastigote forms involves an asymmetric cell division which results in one amastigote and one “zoid”. The zoid is a cell with kinetoplast, but no nucleus, and quickly dies and is degraded by the host cell[93] (steps 3 and 5 in **Figure 9**); (B) some amastigote forms may become metabolically quiescent – called quiescent or dormant amastigotes – and could reside long term in chronically infected tissues, although this is yet to be proven[62] (step 6 in **Figure 9**); (C) evidence for an intracellular epimastigote-like form has been reported, although it is unclear whether this form represents an obligate intracellular stage of the life-cycle, or is simply an

intermediate in the amastigote to trypomastigote transition[34,62] (steps 8 and 9 in **Figure 9**); (D) BTs are a pleomorphic population made up of a mixture of two basic morphologies: slender and broad[89]; (E) extracellular differentiation of trypomastigote forms to amastigote forms has also been observed, and a mixture of these forms may be present in the blood of infected individuals[89].

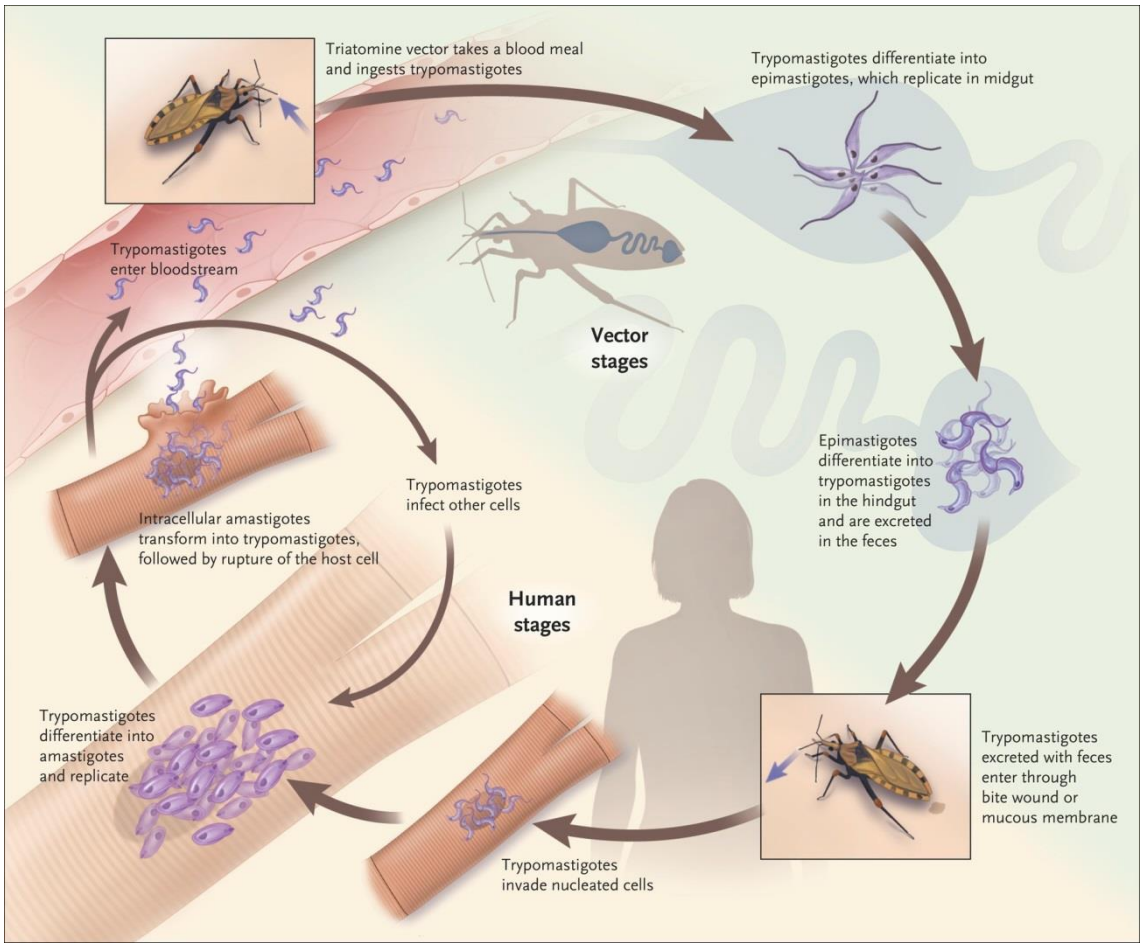

Figure 8. *T. cruzi* life-cycle. Taken from *Bern C., 2015*[32].

The process in the blood-feeding triatomine vector is also more complex. For example, bloodstream amastigote forms – produced after extracellular differentiation of trypomastigote forms – differentiate into forms with short flagella. These forms are called sphaeromastigotes, although probably represent intermediate in the transition to epimastigote forms[89]. Finally, trypomastigote forms have been shown to have the capacity to differentiate into epimastigote-like forms. These epimastigote forms display

a distinct proteomic fingerprint, are able to invade phagocytic and cardiac cells, and can initiate an infection in mice[94].

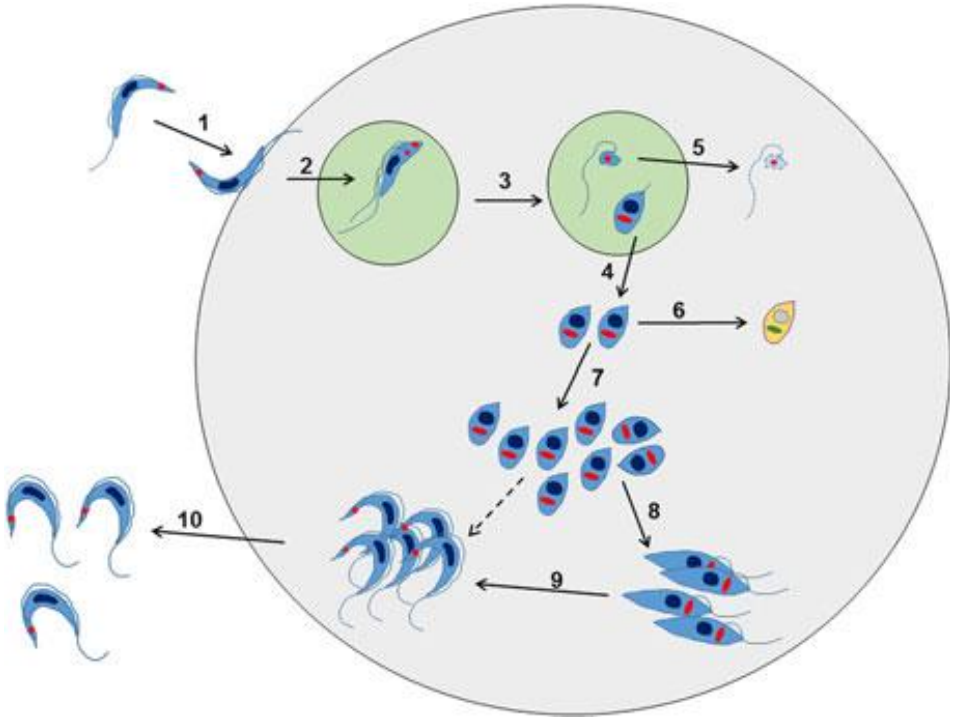

Figure 9. Intracellular life-cycle of *T. cruzi* in mammalian host cells. Taken from *Francisco AF et al., 2017*[62].

2.1.6. Immune evasion strategies of T. cruzi

The survival of the protozoan parasites owes much to their efficient reproductive mechanism, with its short generation times and rapid developmental sequence producing large numbers of progeny[91]. However, the acute-phase involves complex molecular and cellular interactions between the pathogen and its host that can be exploited to the parasite benefit[95,96].

In vertebrate hosts, *T. cruzi* confronts a sophisticated immune system involving circulating cells, molecules, and specialized tissues and organs[97–99]. *T. cruzi* has an arsenal of evasion strategies linked to alternation between intracellular proliferative amastigote forms and non-proliferative and extracellular BTs. The different morphological forms are associated with adaptive changes in gene expression[34] that are

responsible for the wide range of host cells targeted by the parasite, mainly non-phagocytic cells[100].

Immune evasion by *T. cruzi* relies primarily on subverting the complement system and inhibitory effects on the mononuclear phagocyte system[101,102]. Downregulation of phagocytic activity is also seen in other trypanosomatids[76,103]. However, these parasites inhibit the maturation of phagolysosomes, and *T. cruzi* evades macrophage microbicidal activity by escaping from the phagolysosome to the cell cytoplasm[104]. Moreover, *T. cruzi* also interferes with the transcription of cytokines secreted by infected macrophages[105] and a major parasite cysteine-protease prevents macrophage activation by blocking the NF-κB P65 pathway[106]. In this scenario, the macrophage infection favours the secretion of anti-inflammatory cytokines such as interleukin 10 (IL-10) and transforming growth factor β (TGF-β) that favour the spread of infection by impairing the development of protective immune responses[107,108].

The acute CD is characterized by strong inhibition of the host immune response by the *T. cruzi* virulence factors, which are crucial for creating a persistent infection and establishing the chronic CD[95,96]. This immunosuppression (IS) involves the induction of anergy and clonal deletion in the T cell compartment, together with strong polyclonal B cell stimulation which ultimately restricts the development of antigen-specific lymphocytes[109,110]. In addition, there are a variety of natural *T. cruzi* strains that coexist dynamically in natural reservoirs, and it appears that their immune modulatory effects are strain-dependent[91,111]. Hence, immune evasion may occur at the population level rather than at the level of a single strain.

Alternatively, *T. cruzi* membrane glycoproteins are critical for damping host protective immunity. The parasite surface is covered by mucin-like molecules with sialic acid residues which are transferred from host glycoconjugates by the parasite

transsialidase[112,113]. These hijacked sialylated forms are able to protect parasite antigenic determinants from host attack mediated by anti-galactosyl antibodies and complement factor B[114,115], and inhibit early events in T cell activation[116].

Besides, host cell invasion and parasite internalization are also important steps in the protection against the host immune response, in addition to access to microenvironment rich in metabolic products. Host cell intracellular signalling can combat the infection, but it can also favour parasite entry. Parasites hijack the host immune response and phagocytosis for their own survival and replication. The mechanisms that lead to the internalization of trypomastigote forms appear to be different when one considers the cell type where the internalization will occur. In cells considered as non-professional phagocytic there appears to be an internalization process where *T. cruzi* is the active agent of penetration[117,118]. In general, *T. cruzi* invades the host cell by an endocytic process where the firing of several signalling cascades culminates in the formation of a PV. This endocytic process can be performed by three different strategies: one lysosomal-dependent, one actin-dependent, and one phosphatidylinositol-3,4,5-triphosphate (PIP3)-dependent[92,118,119] (**Figure 10**). Subsequently, PV maturates with the acquisition of lysosome markers, and the trypomastigote form transform into an amastigote form with simultaneous lysis of the PV membrane[92]. Lysis of the PV membrane takes place most probably due to the increased concentration of the Tc-Tox perforin-like protein produced by the parasite and the generation of an acidic environment within the PV[120]. Finally, amastigote form in direct contact with the cytoplasm starts to divide[92].

Finally, since *T. cruzi* is exposed to oxidative stress imposed by ROS derived from its own aerobic metabolism and from the host immune response. To detoxify ROS, *T. cruzi* possesses several pathways making intricate network converging to reduced

trypanothione, which is maintained in its reduced form by trypanothione reductase, with the utilization of nicotinamide adenine dinucleotide phosphate (NADPH)[81].

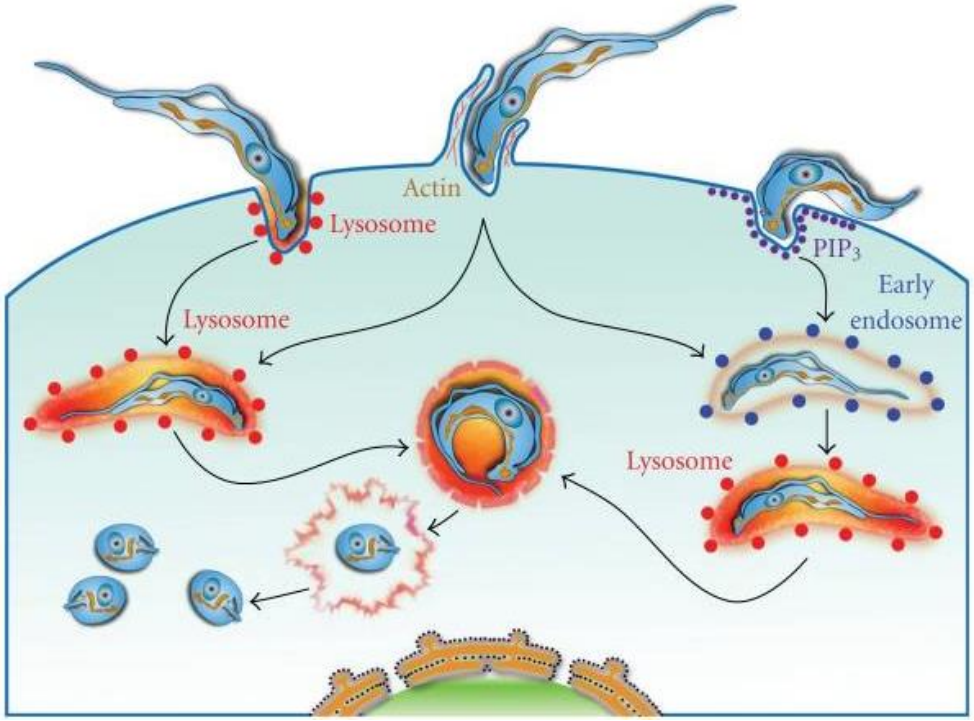

Figure 10. Strategies of *T. cruzi* invasion into host cell. Taken from *de Souza W et al., 2010*[92].

2.2. Clinical phases & Pathogenesis

CD has two clinical phases, an acute and a chronic-phase. It is interesting to note that the outcome of the infection in a particular individual is the result of a set of complex interactions among the host genetic background and the genetic composition of the parasite, and modulated by environmental and social factors; all of which can be complicated by mixed infections and re-infections[121].

The acute-phase occurs immediately after infection, and lasts for 4–8 weeks (**Figure 11**). Acute-phase is usually asymptomatic or mild – as a self-limiting febrile illness – and unrecognized, which is probably because the parasite load is fairly small[2,25,31]. When symptoms occur, there may be: prolonged fever; malaise; enlargement of the liver, spleen and lymph nodes; and, in the particular case of vector-borne transmission,

swelling around the site of inoculation (chagoma and Romaña sign)[31]. Rarely, acute-phase may result in severe myocarditis, meningoencephalitis and pneumonitis, but have a high risk of death[31,122]. Manifestations of this phase resolve spontaneously in about 90 % of infected people[31], although is fatal for 2–8 % of children[2,25]. During this phase, BTs may be found, and infected people can transmit the parasite to others[2,25].

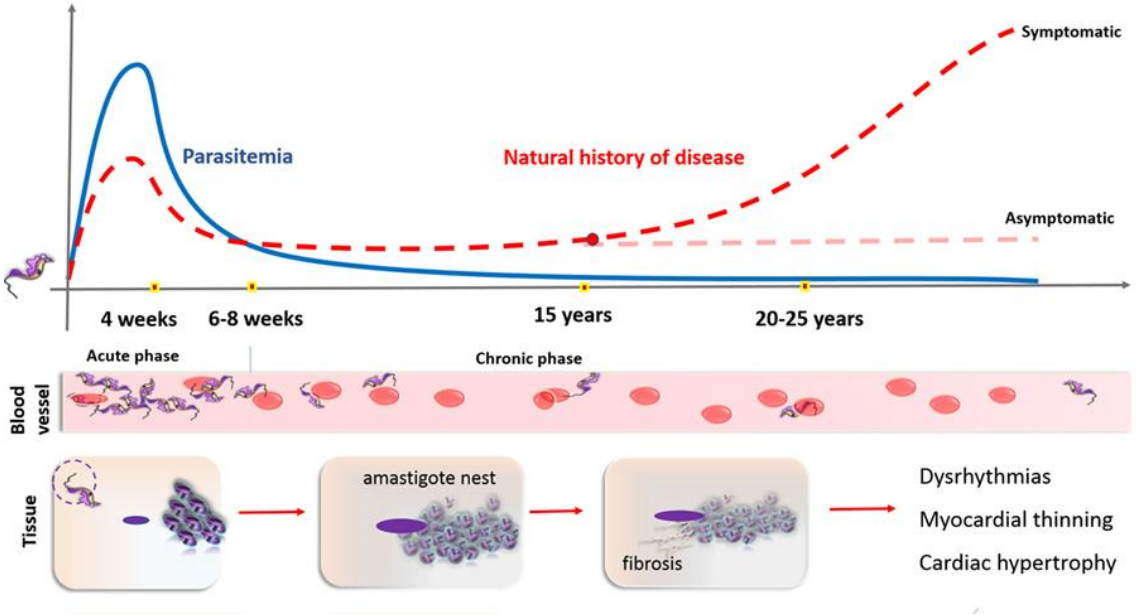

Figure 11. Natural history of Chagas Disease. Taken from *De Bona E et al., 2018*[123].

The chronic-phase can be divided into two stages, an asymptomatic (or indeterminate) and a symptomatic stage (**Figure 11**). The asymptomatic (or indeterminate) stage may last decades after infection, and most people are unaware of their disease. Many people may remain asymptomatic for life. During this time, few or no parasites are found in the blood. This stage is characterised by positivity for anti-*T. cruzi* antibodies, a normal electrocardiogram, and normal radiological examination of the oesophagus, chest and colon. The symptomatic stage, developing 10–30 years later in up to 30 % of infected people, causes severe and sometimes life-threatening medical problems: megaoesophagus and megacolon (leading to difficulties with eating or passing stool), and heart disease (cardiomyopathy and heart rhythm abnormalities) that may cause sudden death[2,25,31].

Typical clinical manifestations of the symptomatic stage are grouped into three major forms (**Figure 12**): digestive, cardiac and cardiodigestive[124,125]. The digestive form is seen almost exclusively south of the Amazon basin, probably due to differences in parasite strains[121], and develops in about 10–15% of chronically infected people. This clinical form mainly involves megaoesophagus and/or megacolon, causing dysphagia, epigastric pain, regurgitation, abdominal distension, and large bowel obstruction and malnutrition in severe cases. In addition, people with megaoesophagus have an increased prevalence of oesophagus cancer[31]. The cardiac form is the most frequent manifestation, developed in about 20–30 % of chronically infected people. It is the most serious manifestation of CD, and typically leads to bradyarrhythmias, tachyarrhythmias, aneurysms, cardiac failure, tromboembolism, and sudden death[124,125]. Heart failure ir often a late manifestation of CD, usually biventricular with a predominance of right-sided failure (peripheral oedema, hepatomegaly, and ascites)[31]. The association of heart disease with megaoesophagus and/or megacolon defines the cardiodigestive form of CD. In most countries, the development of megaoesophagus usually precedes heart and colon disease, but the prevalence of this form is not known because of the scarcity of appropriate studies[124,125].

A direct progression from the acute-phase to a chronic symptomatic stage has been recorded in 5–10 % of infected people. Reactivation of CD can also occur in chronically patients who have suppressed immune systems, e.g. due to AIDS or immunosuppressive treatment, causing severe neurological symptoms[25,31,126,127].

Tissue and organ damage during the acute-phase is caused by the parasite itself and by the host immunoinflammatory response[128]. Several studies have suggested that a strong T-helper-1 adaptive immuno reponse with both CD4 and C8 cells, characterised by the production of specific cytokines (such as tumour necrosis factor α (TNFα), interferon γ

and IL-12), is important in the control of parasitism[129–131]. The synthesis of the nitric oxide, a potent trypanocidal molecule produced by the T-helper-1 immuno reponse, has a protective role[132]. By contrast, production of TGF-β and IL-10 is related to parasite replication by inhibition of macrophage trypanocidal activity[133].

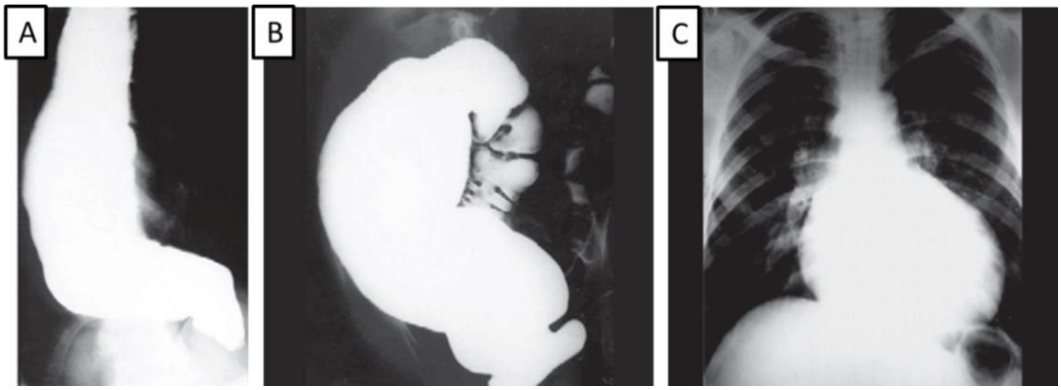

Figure 12. Typical clinical manifestations of Chagas Disease: (A) megaoesophagus, (B) megacolon, and (C) heart disease. Taken from *Rassi Jr A et al., 2010*[31].

Balance between immune-mediated parasite containment and damaging inflammation during chronic-phase probably determines the course of CD. If the immunological response is inefficient, or paradoxically leads to tissue damage, both parasite load and immunemediated inflammation increase. In contrast, a well-executed immune response reduces tissue damage and parasitism[134].

Currently, a growing consensus indicates that parasite persistence is needed for development of CD[135,136]. However, it is not yet known if tissue damage is caused by direct parasite factors, by a host immunoinflammatory response, or by both reasons[137,138]. Autoimmunity is the third possible cause of tissue damage, which could arise from polyclonal activation[139], molecular self-mimicry by immune cross-reactivity with parasite antigens[140], or cryptic epitopes shared by the host and parasites[141].

2.3. Diagnosis

The diagnosis can be performed both in the acute and chronic phases of CD and involves the analysis of clinical, epidemiological, and laboratory data. Currently, most cases are diagnosed during the chronic-phase of CD[16].

During the acute-phase of illness, diagnosis is based on the detection of BTs in peripheral blood or cerebral spinal fluid (CSF) by parasitological tests. This detection can be direct by microscopic examination as thick and thin blood smear, by multiplication as hemoculture, and xenodiagnosis[25,142]. In specialised centres, diagnosis is based on amplification of *T. cruzi* DNA by polymerase chain reaction (PCR) since the sensitivity of PCR is greater than other methods[143].

During the chronic-phase of illness, diagnosis is generally made by testing for *T. cruzi* specific antibodies since parasitaemia is low[25,142,144]. Diagnosis of chronic CD is based on serology at least two different serological tests, such as indirect immunofluorescence assay (IFA), enzyme-linked immunosorbent assay (ELISA), and haemagglutination[142,144]. Two serological tests based on different principles are needed to confirm diagnosis. However, a single ELISA test is sufficient for the exclusion of blood in blood banks[13]. PCR is not used for chronic diagnostic tests since this method is less sensitive than serological tests during this phase of CD[145].

In addition, electrocardiogram, chest radiography and hepatogram are requested at any stage of CD for clinical evaluation[146,147]. Alternatively, molecular diagnosis by PCR could be useful for cases of inconclusive serology in chronic CD, reactivation associated with IS, congenital CD, infection by transfusion or transplant transmission, and for monitoring of suspected laboratory exposures[25,31]. At Centers for Disease Control and Prevention (CDC) molecular detection of parasite DNA is performed using a combination of two real-time PCR assays using ethylenediaminetetraacetic acid

(EDTA) blood (minimum of 2.2 mL), saline or paraffin-embedded heart biopsy tissue, and CSF in cases of suspected central nervous system (CNS) involvement.

PCR is also used as an auxiliary method to identify treatment failure; PCR is not useful to identify treatment success sine even repeated negative PCR results do not necessarily indicate sterile cure[145]. Currently, assessment of cure is based on the seroconversion, that is, the disappearance of anti-*T. cruzi* antibodies, using serological tests. However, antibodies may take up to 5 years to disappear. Accordingly, positive serology does not mean active infection, whereas negative serology indicates cure (except for immunocompromised individuals)[127].

Over the past 35 years, the worldwide spread of human immunodeficiency virus (HIV), in combination with the changing epidemiology of *T. cruzi*, has led to the emergence of *T. cruzi*/HIV co-infections. Diagnosis of CD in these co-infections is particularly difficult. When CD reactivates, it behaves like a separate disease with acute features such as severe neurological symptoms. Moreover, traditional serological diagnostic tests are found to be weaker and less sensitive, as HIV-infected patients are less likely to build a strong antibody response[127].

2.4. Current treatments

Despite CD affects approximately 6–8 million people, causes 14–50 thousand deaths annually[2,13,16,25], represents a high economic burden, and becomes widespread, currently approved treatments are still limited to two obsolete nitroheterocyclic drugs, NFX and BZN[32,148,149] (**Figure 13**). These drugs were developed more than 50 years and present serious drawbacks, such as frequently treatment failures, toxic side-effects (dermatitis, pruritus, fever, and gastrointestinal intolerance, among others), and long treatment periods. For these reasons, treatment is often discontinued[150–152].

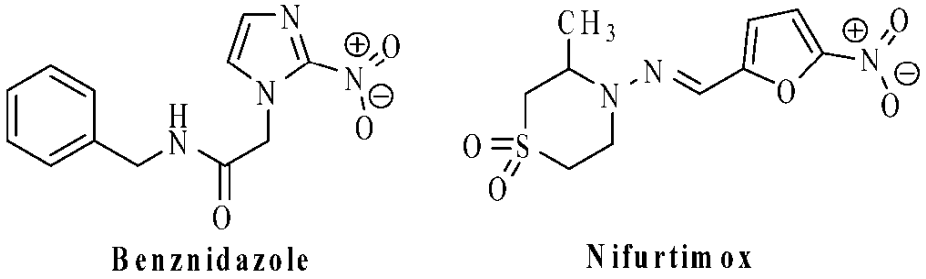

Figure 13. Benznidazole and nifurtimox, the first-line treatments for Chagas Disease. Taken from *Menezes JC et al., 2014*[153].

Adults should be daily treated with 5 mg/kg BZN or 8–10 mg/kg NFX for 60–90 days. For children, daily treatment with 5–10 mg/kg BZN or 15 mg/kg NFX in three divided doses is recommended for the same duration as for adults[154]. It is important to emphasize that the cure rate and its confirmation depend on factor such as phase of disease, age and immune response of the patient, associated comorbidities, and even the susceptibility of the parasite genotype to the drugs used[15].

Both drugs are almost 100 % effective in curing the disease if given soon after infection at the onset of the acute-phase, including congenital CD; however, the efficacy diminishes the longer a patient has been infected. According to recommendations in 2005[154] and 2007[144], treatment is strongly recommended for all cases of acute (including children) and congenital CD, and for patients up to 18 years old with chronic CD[16,144]. Treatment is also recommended for patients during the early chronic-phase and for patients suffering from reactivation. Asymptomatic infected adults aged 19–50 years should also be treated to prevent or delay disease progression or congenital infection in the cases of childbearing-aged women, although there is no consensus for the use of the treatment in the chronic-phase[16,155]. It is optional for those older than 50 years old because benefit has not been proven in this population[144]. In other cases the potential benefits of treatment should be weighed against possible adverse reactions, occurring in up to 40 % of patients.

These drugs are contraindicated during pregnancy, in people with kidney or liver insufficiency, and in people with advanced Chagas heart disease[31]. Moreover, NFX should not be taken by people with neurological and/or psychiatric disorders[16]. BZN has the best safety and efficacy profile, and therefore is usually used for first-line treatment[156].

Additionally, treatment also involves supportive symptomatic treatments in chronic CD: specific treatment for cardiac, digestive or neurological manifestations may be required[16]. Patients with chronic chagasic cardiomyopathy are recommended to follow the treatment protocol for heart failure according to cardiac commitment grade such as amiodarone[157,158], being heart transplantation the only course of action in case of advanced heart failure[159]. Patients with digestive manifestations are indicated to follow a conservative o even surgical treatment depending on the stage of the disease[160]. Digestive dysfunction treatments range from palliation using sublingual nitrates and nifedipine – which induce lower oesophageal-sphincter to help the transit of food and liquids through it[31] – to laparoscopic Heller's myotomy, fundoplication and oesophageal resection[161]. Colonic dysfunction treatments range from a fibre-rich diet, laxatives and occasional enema to surgical organ resection[162].

The aim is to find a specific treatment that allows the eradication of the parasite and, hence, the elimination of the signs and symptoms of CD. The development of new drugs, safer, more effective, that provide a shorter treatment course, and to devise paediatric formulations, preferably oral, is an important need[163]. In this way, the urgency to continue researching, in order to discover novel therapeutic alternatives, is justified. Other strategy that has emerged is the drug repositioning, a fructiferous strategy for improving the drug development process, but it has not obtained good

results either[164,165]. Even combination therapies of existing and new drugs with different mechanism of action (MoA) are recommemded to avoid drug resistance.

In recent years, target-based approaches have been used for screening, concentrating on putative targets and pathways of potential importance for *T. cruzi*. Among the most promising approaches are:

I) Inhibitors of trypanothione metabolism such as buthionine sulfoximine[166]. Trypanothione reductase is one of the main proteins involved in the antioxidant protective mechanisms of *T. cruzi*[30,167].

II) Inhibitors of the NADH reoxidation system. NADH is an essential coenzyme for biosynthetic pathways and also for protection against oxidative stress, due to ROS[81].

III) Inhibitors of cruzipain, such as the vinyl sulphone k777. Cruzipain is the main cysteine protease of the parasite able to cleave immunoglobulins (Igs) – immunoescape mechanism – and it plays an important role in the process of parasite internalization within mammalian cells[30,167].

IV) Polyamine transport inhibitors. In contrast with other protozoa, *T. cruzi* is auxotrophic for polyamines and its intracellular availability depends exclusively on polyamine transport. These polyamines are needed for the parasite viability parasite (cell growth and differentiation)[168].

V) Purine synthesis inhibitors, such as allopurinol[166].

VI) Phospholipid synthesis inhibitors, such as miltefosine[166].

VII) Ergosterol synthesis inhibitors, such as posaconazole and ravuconzole. Ergosterol is a critical sterol in the cell membranes of *T. cruzi*[30,167].

VIII) Bisphosphonates that inhibit the parasite's farnesyl-pyrophosphate synthase. Farnesyl-pyrophosphate synthase is a key enzyme that supplies precursors for

the biosynthesis of essential isoprenoids like carotenoids, sterols, and ubiquinones, among others[30,167].

IX) Inhibitors of pyrophosphate metabolism. Inorganic pyrophosphate is responsible for energy supply in *T. cruzi* and there are numerous pyrophosphate-dependent enzymes in this parasite. Pyrophosphate analogues such as alendronate or pamidronate are examples of these inhibitors[166].

Notwithstanding all the challenges described above, there is no doubt that the Chagas R&D environment has been very active in the last 10 years:

- From 2010 to 2013 (CHAGASAZOL, NCT01162967), a proof-of-concept phase II clinical study with posaconazole for the treatment of CD was under way in Spain. In 2011, patients began to be recruited into a second trial in Argentina and sponsored by Merck & Co. The results showed that posazonazole exhibited antitrypanosomal activity in patients with chronic CD; however, significantly more patients in the posaconazole group than in the BZN group had treatment failure during follow-up[151,167,169].
- From 2011 to 2017 (NCT0148228), the DND*i* and Eisai Co. were partnering in a phase II trial of a pro-drug of ravuconazole (E1224) in Bolivia. The results showed that ravuconazole displayed a transient, suppressive effect on parasite clearance, whereas BZN exhibited early and sustained efficacy until 12 months of follow-up[167,169,170].
- From 2011 to 2018 (STOPCHAGAS, NCT01377480), an international phase II clinical trial of oral posaconazole in the treatment of asymptomatic chronic CD was performed. The results showed that posaconazole demonstrated trypanostatic activity during the treatment, but it is ineffective long-term in asymptomatic CD. Again, BZN monotherapy resulted superior to posaconazole[150,169].

- From 2012 to 2018 (NCT01549236), the DND*i* performed a phase IV clinical trial in Argentina to study the population pharmacokinetics parameters of BZN in children with CD[169,171].
- From 2012 to 2018 (NCT01678599), the DND*i* performed a phase IV clinical trial in Bolivia to estimate the gain in sensitivity of several multiple-sample strategies of PCR samples with respect to the current standard to detect chronic CD[169,171].
- In 2015 (BENEFIT, NCT02444312), a multi-centre study evaluated the effects of BZN for interrupting cardiac CD. The results showed no delay in the clinical progression for the most severe forms of cardiomyopathy[169,171,172].
- In 2015 (NCT02498782), the DND*i* initiated a phase II clinical trial in Bolivia to evaluate if the treatment with fexinidazole lead to a better sustained clearance in adults patients with chronic CD[169,171].
- In 2017 (BENDITA, NCT03378661), the DND*i* initiated a phase II clinical trial in Bolivia to evaluate different oral BZN monotherapy and BZN/ravuconazole combination regimens for the treatment of adults patients with chronic CD[169,171].
- In 2018 (NCT03587766), the DND*i* initiated a phase II clinical trial in Spain to evaluate low doses and short treatment duration of fexinidazole to determine the minimal efficacious and safe dose for the treatment of adults patients with chronic CD[169,171].

To stablish a consensus on the desirable product profiles for CD, the Pan American Health Organization (PAHO), in collaboration with DND*i*, Médecins sans Frontières (MSF) and the Special Programme for Research and Training in Tropical Diseases (TDR, Tropical Diseases Research), convened a multidisciplinary group of experts in Brazil (2010) to establish the basis for the development of target product profile (TPP)[2] (**Table 2**).

Table 2. Target Product Profile for Chagas Disease. Taken from The Drugs for Neglected Diseases *initiative*[2].

	Acceptable	Ideal
Target population	Chronic	Chronic and Acute
Geographic Distribution	All regions	All regions
Efficacy	Non inferior to benznidazole standard dose* in all regions (parasitological)	Superiority to benznidazole standard dose to different phases of disease (acute and chronic) (parasitological)
Safety	Superiority to benznidazole* in the frequency of definitive treatment discontinuations for medical indication (clinical and laboratory)**	Superiority to benznidazole* in the frequency of definitive treatment discontinuations for medical indication (clinical and laboratory)**
Contraindications	Pregnancy	No contraindications
Precautions	No genotoxicity**; No pro-arrythmic potential	No genotoxicity; No teratogenicity; No pro-arrythmic potential
Interactions	No clinically significant interaction with anti-arrythmic and anticoagulants drugs	No clinically significant interaction
Presentation	Oral/Parenteral (short POC)*** Age-adapted	Oral Age-adapted
Stability	3 years, climatic zone IV	5 years, climatic zone IV
Dosing regimen	Oral – any duration Parenteral – <7 days	<30days
Cost	Current treatments	Lowest possible

* As per WHO recommendation
** No genotoxicity is a condition only for NCEs
*** Need for parenteral treatment for severe disease

2.5. Vaccines

The development of an effective human vaccine against CD has encountered many difficulties, and progress has been slow mainly because there is controversy about its autoimmune aetiology. The genetic complexity of *T. cruzi* and the limited set of efficient engineering techniques for genome manipulating contribute to the relative lack of progress in the understanding of this organism[173].

The immunological protection against *T. cruzi* has been studied since the second decade of the last century. In 1912, Blanchard showed that the animals that survived the acute-phase were resistant to reinfections. Since then, many types of immunogens vaccines have been evaluated: live attenuated parasites, non-pathogenic trypanosomes, non-infectious stages (epimastigotes), dead parasites, subcellular fractions, purified native proteins, recombinant proteins and DNA vaccines. These vaccines rarely resulted in sterile immunity that fully protects animals from becoming infected when challenged with virulent parasites[173,174]. Some examples are:

- Live or fixed *Ttypanosoma rangeli* epimastigotes[175,176] and live *Phytomonas serpens* parasites[177], which shares antigens with *T. cruzi* and are non-pathogenic trypanosomes, were used to immunize mice. These mice showed a significant reduction in parasitaemia and increased survival after *T. cruzi* infection[175,177].
- A variety of *T. cruzi* cell fractionation studies have been performed to identify the more immunogenic portion of the parasite that induces a protective immune response. Immunization with some fractions induced lesions similar to those in the control animals, suggesting that the fractions alone can produce damage, possibly by inducing an autoimmune response[178].
- Purified proteins from *T. cruzi* have also been used to identify those that provide a protective immune response. Studies that used surface glycoproteins as vaccines

indicated that selection of the immunogenic protein is important and must be present in the parasite stages that circulate in the mammal host[179]. Studies using 45 and 68 kDa antigens purified from the cell membrane of *T. cruzi*[180], purified antigenic preparations called TcY 72[181], and excretory-secretory antigens from trypomastigotes[181], among others, ranged from 100 % protection to a significant reduction in parasitaemia and increased survival when mice challenged with *T. cruzi*. These data suggested that despite the antigenic complexity, it is possible to generate similar protection using a macromolecule or a set of macromolecules[173].

- Mutant *T. cruzi* strains with reduced virulence have also been used to immunize mice. Mice challenged with virulent parasites one year after the original infection showed significant control over the secondary infection[182].
- In the recent years, recombinant proteins have begun to be used for immunization, which allow the amounts necessary to perform the studies. Some examples are the recombinant *T. cruzi* cytoplasmic repetitive antigen (CRA) and flagellar repetitive antigen (FRA)[183], the recombinant PFR proteins[184], the recombinant C-terminal domain of cruzipain[185], and the glycosylated mutant inactive trans-sialidase[186], among others. Mice immunized with these proteins showed significant protection after infection, with reduced parasite load and increased survival.
- Newest DNA vaccines provide an alternative for both prevention and treatment of a variety of infectious diseases[187–189], including CD. Several studies demonstrate that DNA immunization using plasmid or virus vectors induce a protective response in the experimental infection with *T. cruzi*. Some examples are the *T. cruzi* transsialidase superfamily (TcSP) gene[190,191] or the *T. cruzi* amastigote surface protein-2 (ASP-2) gen[192]. Furthermore, genes encoding molecules that

stimulate the immune system have been coadministered with some *T. cruzi* genes to enhance the immune response[173].

DNA vaccines could control *T. cruzi* infection and significantly reduce the progression in patients with chronic CD. However, the exploration of human vaccines has been widely avoided due to the fear that this prophylactic measure could exacerbate the disease that many consider to have an autoimmune aetiology, although later it became clear that autoimmune reaction is a consequence of parasite persistence in tissues[193].

Since 2012, a therapeutic Chagas vaccine is under development by a consortium of Mexican and Texan scientific institutions based on the evidence of therapeutic efficacy of Tc24 and trypomastigotes surface antigen 1 (TSA-1) vaccines in mice and dogs[194].

An ideal vaccine candidate should: I) be highly immunogenic; II) be expressed in all the parasite forms, mainly in those present in humans; and III) be conserved and expressed in different *T. cruzi* strains. During the last 20 years, it has been demonstrated that Cruzipain, Tc52 and Tc80 are excellent vaccine candidates since exhibits these attractive properties[195–197]. In the genomic and proteomic era, new tools for the discovery of vaccines have emerged. Omics data together with bioinformatics tools can be used to find new immunogens. This approach is currently known as Reverse Vaccinology[198], and has identified 8 putative new membrane anchored or secreted proteins (TcG1-TcG8). Some of them were able to confer protection in different vaccination strategies[199]. However, there is no vaccine currently available.

3. OBJECTIVES/OBJETIVOS

1. Develop more effective, safer and affordable compounds since the current therapeutic arsenal to combat Chagas Disease is inadequate and insufficient.
2. Elucidate the mechanism of action of trypanocidal drug candidates for the following preclinical phase.
3. Establish a precise and accurate, reproducible and as complete as possible methodology for the *in vitro* screening of compounds with activity against *Trypanosoma cruzi*.

/

1. Desarrollar compuestos más efectivos, seguros y asequibles ya que el arsenal terapéutico actual para combatir la Enfermedad de Chagas es inadecuado e insuficiente.
2. Dilucidar el mecanismo de acción de los potenciales compuestos tripanocidas para la siguiente fase preclínica.
3. Establecer una metodología precisa y exacta, reproducible y lo más completa posible para el cribado *in vitro* de compuestos con actividad frente a *Trypanosoma cruzi*.

4. METHODOLOGY

4.1. Development of a novel in vitro screening method based on the fluorescence of T. cruzi CL-Luc:Neon/Cas9 parasites

4.1.1. Fluorescence quantification using extra- and intracellular parasite forms: fluorescence vs. parasites

Genetically manipulated and fluorescent *T. cruzi* CL-Luciferase:NeonGreen (Luc:Neon)/CRISPR associated protein 9 (Cas9) epimastigotes[200] in Dr J. Kelly laboratory (LSHTM, UK) were cultured at 28º C in liquid Roswell Park Memorial Institute (RPMI)-1640 (Gibco®) medium with 10 % (v/v) heat-inactivated foetal bovine serum (FBS), 0.5 % (w/v) trypticase (BBL), 0.03 M hemin[201], and maintained on their selective agent (0.15 $mg \cdot mL^{-1}$ hygromycin)[200]. Epimastigote forms were collected by centrifugation at 400 g for 10 min and plated into dark 96-well microtiter flat-bottom plates in serial two-fold dilutions from 2.0×10^6 to 2.0×10^3 $well^{-1}$ in 200 µL volumes. Blanks were also included, and each parasite concentration was tested in octuplicate. Plates were immediately centrifuged and fixed using 100 $\mu L \cdot well^{-1}$ of 4 % cold-paraformaldehyde (PFA) for 20 min. Thereafter, plates were washed twice with cold-phosphate-buffered saline (PBS) and resuspended in 200 µL PBS $well^{-1}$. Finally, fluorescence units were measured at 497/520 nm (*ex/em*) using a fluorescence microplate reader. Mean and standard deviations were calculated for each concentration. For intracellular amastigote forms, BSR cells (mouse fibroblast cells, the mammalian cells used to perform this assay) were cultured in liquid Dulbecco's Modified Eagle Medium (DMEM) (Gibco®) with 10 % (v/v) heat-inactivated FBS at 37 ºC in humidified 95 % air and 5 % CO_2 atmosphere. First, BSR cells were collected by trypsinization and centrifugation at 400 g for 10 min, and then seeded into dark 96-well microtiter flat-bottom plates in serial two-fold dilutions from 1.0×10^4 to 6.3×10^2 $well^{-1}$. Plates were cultured in 100 $\mu L \cdot well^{-1}$ volumes in DMEM (Gibco®) medium with 1 %

(v/v) heat-inactivated FBS at 37 ºC in humidified 95 % air and 5 % CO_2 atmosphere for 16 h. After incubation, supernatants were removed, and each cell concentration was infected in serial two-dilutions from 5.0×10^4 to 3.1×10^3 culture-derived fluorescent trypomastigotes·well^{-1} in 200 µL DMEM (Gibco®) medium with 0.2 % (v/v) heat-inactivated FBS. Non-infected BSR cells were also included. After an infecting time of 16 h, non-phagocyted trypomastigotes were removed by washing with pre-warmed PBS, and plates were incubated for further 72 h. Then, plates were washed twice with cold-PBS, fixed using 4 % cold-PFA for 20 min, and washed again twice with cold-PBS. Finally, 200 µL PBS well^{-1} were added, and fluorescence units were measured at 497/520 nm (*ex/em*) using a fluorescence microplate reader.

4.1.2. Monitoring infection profile of intracellular amastigote forms

BSR cells were seeded into dark 96-well microtiter flat-bottom plates in serial two-fold dilutions from 1.0×10^4 to 1.3×10^3 well^{-1}. Plates were cultured in 100 µL·well^{-1} volumes in DMEM (Gibco®) medium with 1 % (v/v) heat-inactivated FBS at 37 ºC in humidified 95 % air and 5 % CO_2 atmosphere for 16 h. After incubation, supernatants were removed, and each cell concentration was infected in serial two-dilutions from 5.0×10^4 to 1.3×10^4 culture-derived fluorescent trypomastigotes·well^{-1} in 200 µL DMEM (Gibco®) medium with 0.2 % (v/v) heat-inactivated FBS. Non-infected cells were also included, and each condition was tested in triplicate. After an infecting time of 16 h, non-phagocyted trypomastigotes were washed out with pre-warmed PBS, and plates were again incubated in DMEM (Gibco®) medium with 0.2 % (v/v) heat-inactivated FBS. After that, fluorescence units were measured at each timepoint (every day from the 2nd to the 8th day post-infection (dpi)) after washing and fixing one plate at each time, as described above (see *section 4.1.1*). Mean and standard deviations were calculated for each condition. **Scheme 1** shows the timeline for this assay.

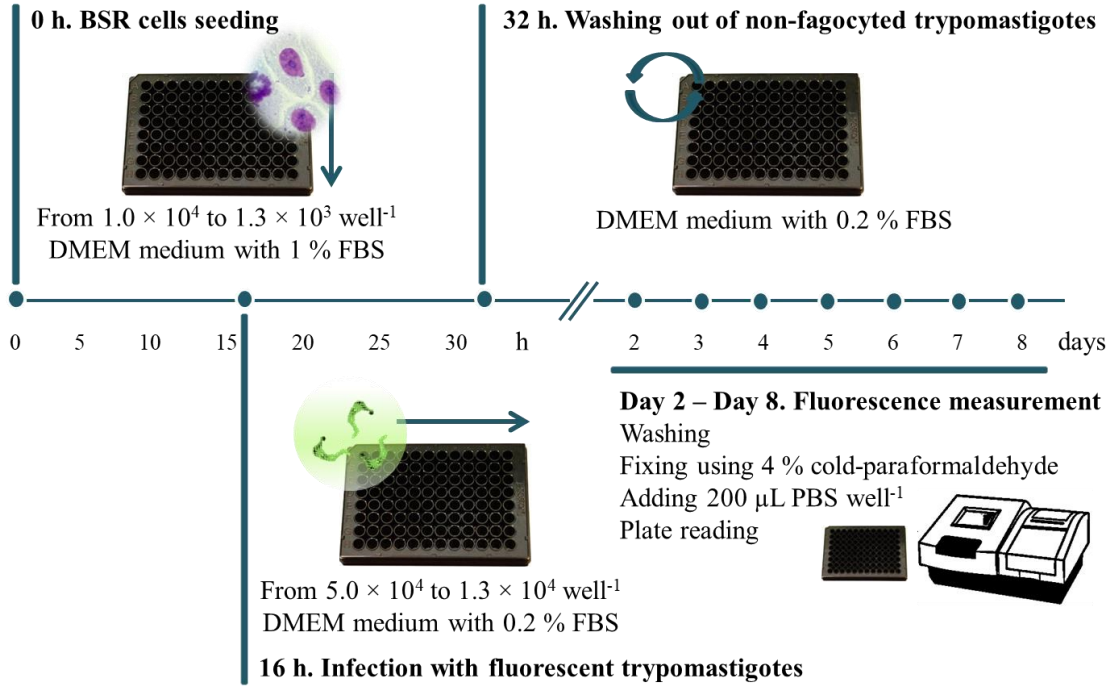

Scheme 1. Timeline to monitor the infection profile of intracellular amastigote forms by fluorescence.

The same methodology was followed using 24-well microtiter flat-bottom plates with rounded coverslips on the bottom. Then, images were obtained at each timepoint as follow: cultures on coverslips were fixed in 2 % cold-PFA in PBS and air-dried onto glass slides; cultures were washed once in cold-PBS, permeabilised in 0.1 % TritonX-100/PBS for 5 minutes and washed 3 times with cold-PBS; finally, slides were mounted with 4′,6-diamidino-2-phenylindole (DAPI, a fluorescent stain for labelling DNA) and imaged on a Zeiss LSM 510 confocal microscope.

4.1.3. Drug screening assay against extracellular epimastigote forms

Fluorescent epimastigotes were collected as described above (see *section 4.1.1*), and then plated into dark 96-well microtiter flat-bottom plates in in liquid RPMI-1640 (Gibco®) medium with 10 % (v/v) heat-inactivated FBS, 0.5 % (w/v) trypticase (BBL), 0.03 M hemin[201]. Parasites were seeded at 1.0×10^5 mL^{-1}, and after addition of BZN and NFX at dosages from 100 to 1.6 µM in 200 $\mu L \cdot well^{-1}$ volumes. Growth controls

were also included, and each concentration was tested in triplicate. After 72 h incubation at 28 ºC, plates were centrifuged, fixed, and washed as described above (see *section 4.1.1*). Finally, fluorescence units were measured at 497/520 nm (*ex/em*). Mean and standard deviations were calculated for each concentration. The trypanocidal effect was determined using GraphPad Prism 6 Software, and it is expressed as the inhibitoy concentration 50 (IC_{50}), i.e., the concentration required to result in 50% inhibition. **Scheme 2** shows the timeline for this assay.

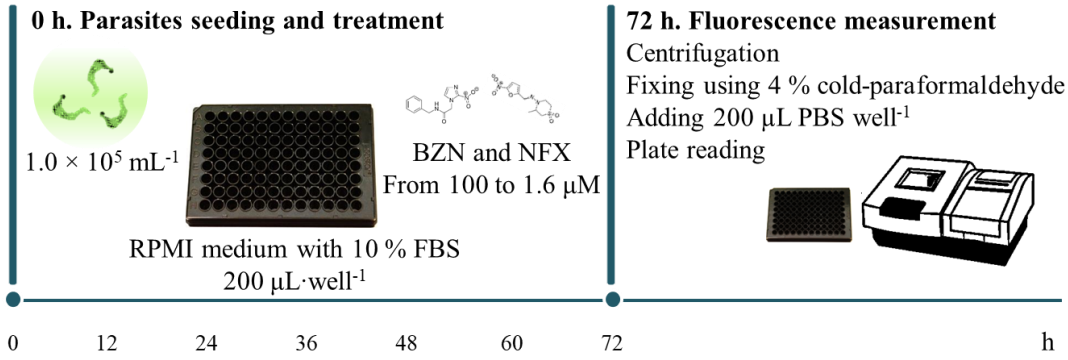

Scheme 2. Screening timeline against extracellular epimastigote forms by fluorescence. BZN, benznidazole; NFX, nifurtimox

4.1.4. Drug screening assay against intracellular amastigote forms

BSR cells were seeded into dark 96-well microtiter flat-bottom plates at 5.0×10^3 well^{-1} in liquid DMEM (Gibco®) medium with 1 % (v/v) heat-inactivated FBS, and incubated at 37 ºC in humidified 95 % air and 5 % CO_2 atmosphere for 16 h. Cells were then infected with culture-derived fluorescent trypomastigotes at a multiplicity of infection (MOI) ratio of 10, that is, 5.0×10^4 trypomastigotes·well^{-1} for 16 h. Non-phagocyted parasites were removed by washing, and after addition of the compound BZN and NFX at dosages from 100 to 1.6 µM in DMEM (Gibco®) medium with 0.2 % (v/v) heat-inactivated FBS in 200 µL·well^{-1} volumes. Non-infected BSR cells were also included, and each concentration was tested in triplicate. Plates were incubated for 72 h at 37 ºC

in humidified 95 % air and 5 % CO_2 atmosphere. Finally, plates were washed and fixed as described above (see *section 4.1.1*), 200 µL PBS well^{-1} were added, and fluorescence units were measured at 497/520 nm (*ex/em*). Mean and standard deviations were calculated for each concentration. The trypanocidal effect was determined using GraphPad Prism 6 Software, and it is expressed as the IC_{50}, i.e., the concentration required to result in 50% inhibition. **Scheme 3** shows the timeline for this assay.

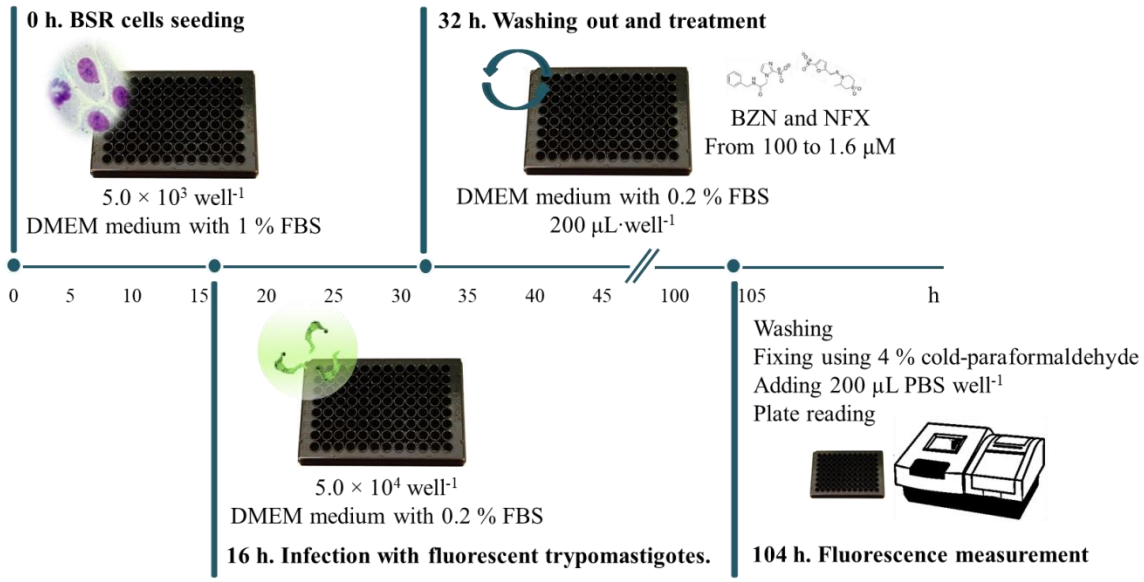

Scheme 3. Screening timeline against intracellular amastigote forms by fluorescence. BZN, benznidazole; NFX, nifurtimox

4.1.5. Drug screening assay against extracellular trypomastigote forms

Culture-derived fluorescent trypomastigotes were treated into 1.5-mL centrifuge tubes by adding BZN and NFX at dosages of 40. 20 and 1 µM for 3 h, 6 h, and 9 h. Non-treated trypomastigotes were also included. Trypomastigotes were then centrifuged at 400 g for 10 min, washed twice with pre-warned PBS, and used to infect BSR cells previously seeded into dark 96-well microtiter flat-bottom plates, as described above (see *section 4.1.4*). BSR cells were infected at a MOI ratio of 10, that is, 5.0 × 10^4 trypomastigotes·well^{-1}. Non-infected BSR cells were also included, and each concentration was tested in triplicate. After an infecting time of 16 h, non-phagocyted

trypomastigotes were washed out with pre-warned PBS, and plates were again incubated for 72 h. Finally, plates were washed and fixed as described above (see *section 4.1.1*), 200 µL PBS well^{-1} were added, and fluorescence units were measured at 497/520 nm (*ex/em*). Mean and standard deviations were calculated for each concentration. The trypanocidal effect was determined using GraphPad Prism 6 Software, and it is expressed as the IC_{50}, i.e., the concentration required to result in 50% inhibition. **Scheme 4** shows the timeline for this assay.

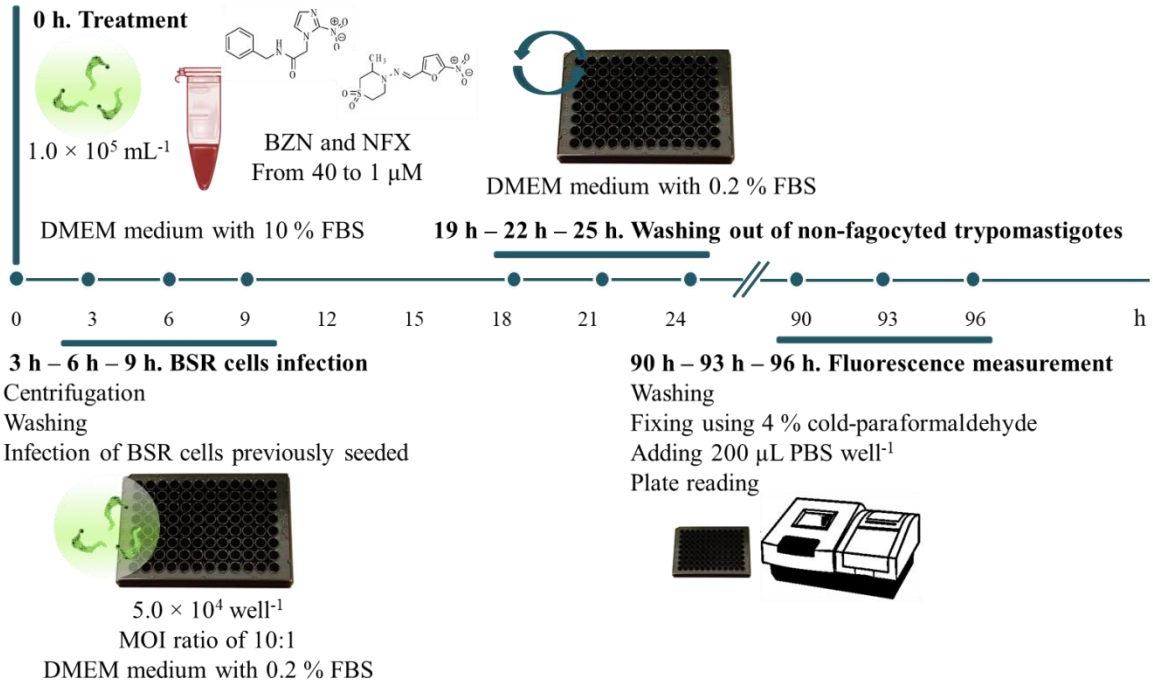

Scheme 4. Screening timeline against extracellular trypomastigote forms by fluorescence. BZN, benznidazole; NFX, nifurtimox

4.2. Setting up a new in vivo approach for Chagas Disease chemotherapy

Female BALB/c mice were infected by intraperitoneal inoculation of 5.0×10^5 BTs of *T. cruzi* Arequipa strain (MHOM/Pe/2011/Arequipa), belonging to the DTU V according to the literature[63]. These parasites were obtained from previously infected mice, and injected in 0.2 mL PBS.

On the one hand, 10 infected mice were used to determine the acute-phase parasitaemia load of this strain, obtaining peripheral blood from the mandibular vein. 5 µL blood was obtained each 2-3 days from the 3rd dpi until the day parasitaemia was not detected for 7 consecutive days. Blood was diluted 1:100 in PBS, and the number of BTs per mL was quantified using a Neubauer chamber[202] (**Scheme 5A**).

On the other hand, 15 infected mice were used to evaluate the chronic-phase tropism in a time-dependent manner, sacrificing 5 mice by cervical dislocation for each experimental time: 20th, 40th, and 60th dpi. 14 organs/tissues were harvested to reveal the tropism of this strain: adipose tissue, bone marrow, brain, oesophagus, heart, kidney, large intestine, liver, lung, mesenteric tissue, muscle, small intestine, spleen and stomach (**Scheme 5B**). These organs/tissues were immediately flushed free of blood by infusion of pre-warmed PBS to avoid contamination with BTs[203], and they were then thawed and ground up using a Potter-Elvehjem. Organs/tissues DNA was extracted using Wizard® Genomic DNA Purification Kit (Promega)[202]. The detection of *T. cruzi* DNA was achieved by PCR based on the sequence of the *T. cruzi* (CL Brener) *superoxide dismutase* (*SOD)* gene (GenBank accession No. XM_808937) using two primers designed in our laboratory (GenBank accession number DQ441589) and a Thermal Cycler™ MyCycler thermal cycler (Bio-Rad). The reaction mixture was as follows (total volume: 20 µL): 1 µL DMSO, 200 nM iSODd, 200 nM iSODr, 10 mM Tris·HCl (pH 9.0), 1.5 mM $MgCl_2$, 50 mM KCl, 0.01 % gelatin, 0.1 % Triton X-100, 100 mM of each dNTP, 0.5 U of Taq DNA polymerase, 1 µg of DNA, and HPLC water; and the following routine: 95 ºC/3 min, 30 cycles of 95 ºC/30 s, 55.5 ºC/45 s, 72 ºC/30 s, and 72 ºC/7 min[202]. Finally, the PCR products were visualised using UV illumination after a 2 % agarose gel electrophoresis for 90 min at 90 V, containing 1:10000 GelRed nucleic acid gel stain.

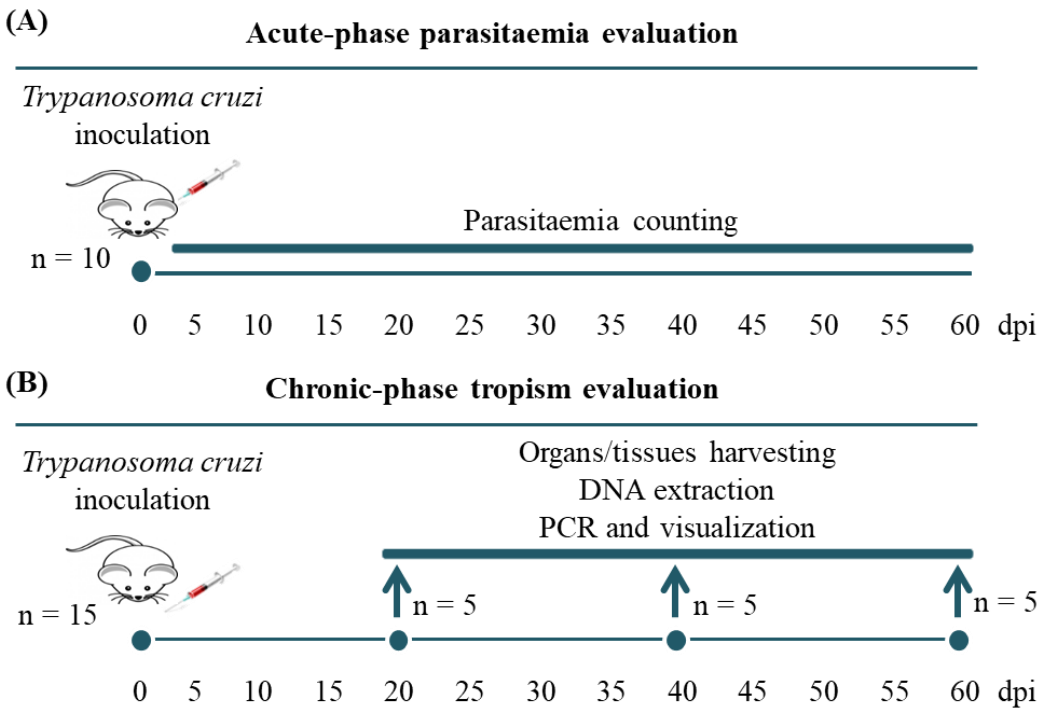

Scheme 5. Timeline for *in vivo* assays on BALB/c mice infected with 5.0×10^5 bloodstream trypomastigotes of *T. cruzi* Arequipa strain. dpi, days post-infection.

4.3. Synthesis of compounds

The compounds tested in this doctoral thesis were synthesized and provided by different groups of chemistry within collaborative projects. **Table 3** shows the groups, the families of the new synthesized compounds and the publication where the synthesis is detailed.

4.4. Published methods

All methodology performed in this doctoral thesis is detailed in the publications included: [1] (*section 5.3.1*), [2] (*section 5.3.2*), and [3] (*section 5.3.3*). This methodology is summarized in **Table 4**.

Table 3. Groups of chemistry, chemical families and publications of the synthesized compounds.

Group	Principal Investigator	Chemical family	Publication
Department of Chemistry, Universitat de les Illes Balears, Palma, Spain	Dr Antonio Costa Torres	Squaramides	[1] (*section 5.3.1*)
Departamento de Química Inorgánica, Universidad de Valencia, Spain*	Dr Enrique García-España Monsonis	Polyamines	[2] (*section 5.3.2*)
Instituto de Química Médica (IQM), Consejo Superior de Investigaciones Científicas (CSIC), Madrid, Spain	Dr Vicente J. Arán Redo	Nitroindazoles	[3] (*section 5.3.3*)

* Acid-base equilibrium studies were also performed by this group (Publication [2], *section 5.3.2*).

Table 4. Methods performed and publications where they are written in more detail.

Method	Publication
• Chemistry	
○ Synthesis of compounds	*Section 4.3*
○ Acid-base equilibrium studies	*Section 4.3*
• Cellular cultures	
○ Parasite strain culture	[2]
○ Mammalian VERO cell culture	[2]
• *In vitro* assays	
○ Obtaining parasite metacyclic forms	[3]
○ Screening tests against extracellular epimastigote forms	[2]
○ Screening tests against extracellular trypomastigote forms	[2]
○ Screening tests against intracellular amastigote forms	[2]

○ Cytotoxicity tests	[2]
• *In vivo* assays	
○ Mice infection and treatment	[3]
○ Parasitaemia counting	[1]
○ Cyclophosphamide-induced IS	[3]
○ Tissues harvesting	[3]
○ DNA extraction, PCR and electrophoresis	[3]
○ ELISA tests	[3]
○ Biochemical analyses	[3]
• Mechanism of action assays	
○ Metabolic excretion studies	[3]
○ Mitochondrial membrane potential tests	[2]
○ Nucleic acids levels tests	[2]
○ SOD enzyme inhibition tests	[3]

[1]: Publication 1 (*section 5.3.1*); [2]: Publication 2 (*section 5.3.2*); [3]: Publication 3 (*section 5.3.3*). IS, immunosuppression; PCR, polymerase chain reaction; SOD, superoxide dismutase.

5. RESULTS

5.1. Novel fluorescence-based in vitro screening method

The genetically manipulated and fluorescent *T. cruzi* CL-Luc:Neon/Cas9 strain[200], which express a fusion protein comprising red-shifted luciferase and green fluorescent protein domains, was used for the development of this novel method. Fluorescence allows us to follow the kinetics of infection within a single culture, to visualise individual parasites to study host-parasite interactions at a cellular level, and to perform improved screening assays against the three morphological forms of the parasite.

5.1.1. Fluorescence quantification

The main objective was to develop a single methodology capable of performing drug screening assays against intra- and extracellular parasite forms. Therefore, the first step was to quantify the fluorescence associated to genetically manipulated epimastigote and amastigote forms, and to determine whether different parasite concentrations and infection levels, respectively, were detectable. Fluorescence quantifications are shown in **Figure 14**. **Figure 14A** shows that the two quantitative variables, that is, fluorescence and concentration of epimastigote forms, have a strong positive linear correlation (Pearson correlation coefficient (r) = 0.9994; $p<0.05$, 95% confidence level). For fluorescence and concentration of intracellular amastigote forms (**Figure 14B**), this coefficient indicates a strong positive linear correlation for most of the analysed cases ($r > 0.9000$; $p<0.05$, 95% confidence level), except for tests using the two lowest number of trypomastigote forms for infection. Since this test requires a cellular support, the initial number of host cells and the MOI ratio, that is, the ratio between the number of infectious trypomastigote forms and mammalian cells available for infection, are really important. MOI ratios below 5 are not usually used for short *in vitro* infections using *T. cruzi*[204–207]. In summary, we can state that this method is able to detect different levels

of extracellular forms and intracellular infections, and it serves us to carry out screening of trypanocidal compounds against all three morphological forms of *T. cruzi*.

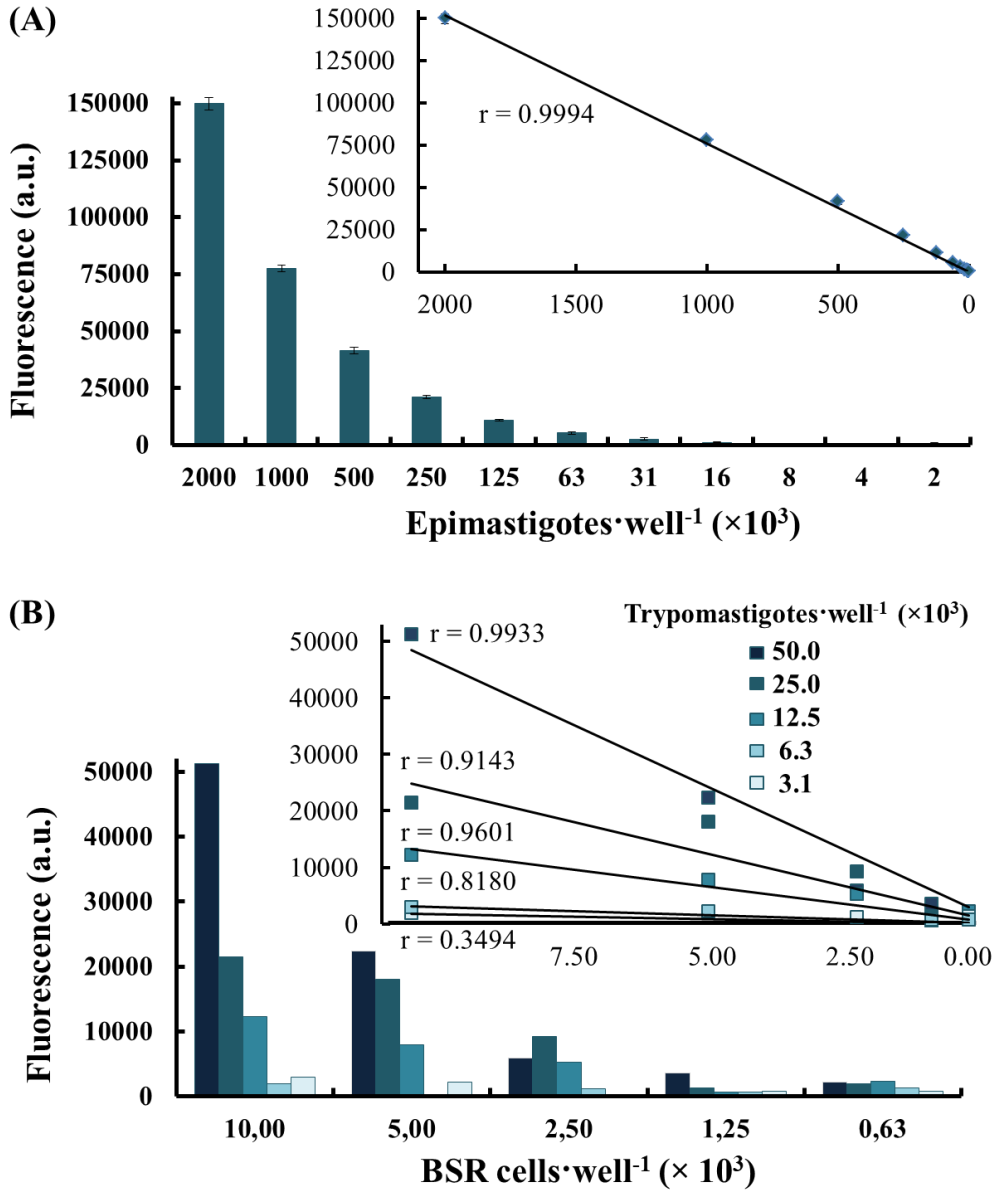

Figure 14. Fluorescence quantifications using extra- and intracellular fluorescent parasites in 96-well microtiter plates. (A) Fluorescence and lineal correlation of epimastigote forms, and (B) fluorescence and lineal correlation of amastigote forms after infection using trypomastigote forms. a.u., arbitrary units; r, Pearson correlation coefficient.

5.1.2. Infection profile monitoring

The kinetics of infection produced within an *in vitro* cell culture over time is an important aspect in the search of trypanocidal drugs: the intracellular life-cycle can be reproduced in cell cultures and it can be used as a model for the evaluation of trypanocidal drugs and to study host-parasite interactions. Hence, next step was to monitor the infection profile of intracellular amastigote forms by fluorescence in a quick and simple way.

Different MOI ratios were tested to determine the infection profiles resulting from each and to determine which generated a balanced kinetics for short and long times of infection. **Figure 15** shows the infection profile produced for 8 days at each MOI ratio. Firstly, it has to be highlighted that kinetics of infection not only depends on the MOI ratio, but also the number of host cells that form the culture is quite important. Secondly, it is interesting to consider two characteristics related to the kinetic of infection observed:

- The period of the infection profile, that is, the time elapsed between two infection peaks, is 3 days regardless of the MOI ratio.
- The reproducibility of this period depends to a large extent on the number of host cells available after the first infection period. This number should allow reproducibility, and not depletion caused by lack of cellular support, after the first infection peak.

In summary, the MOI ratio and the initial host cell culture must be those that allow the reproducibility, a quite interesting characteristic for long times of infection. Therefore, the best conditions for the *in vitro* evaluation of fast- and slow-acting trypanocidal drugs were as follow: MOI ratio of 10 and 5.0×10^3 BSR cells·well^{-1} as initial host cell culture.

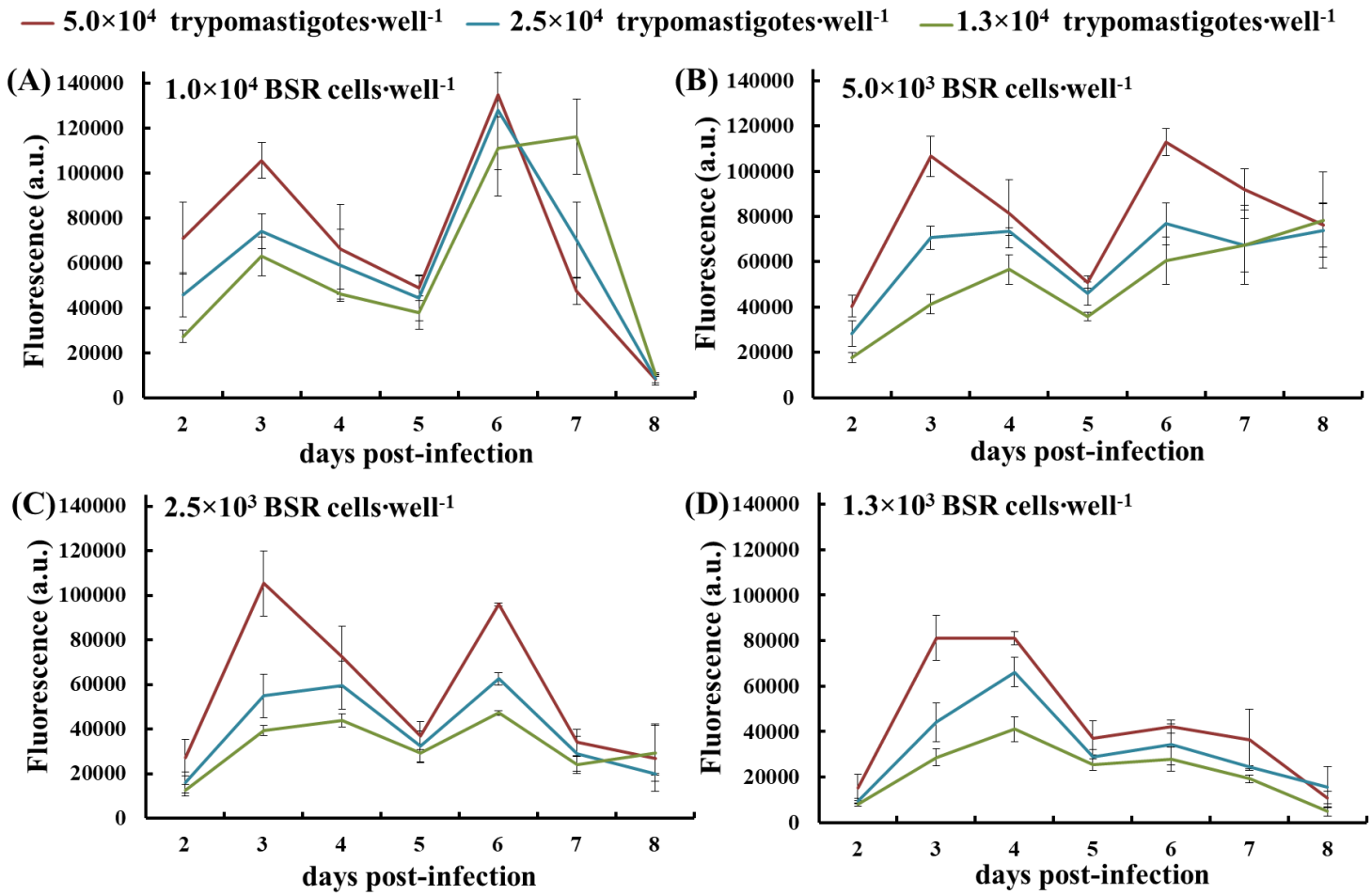

Figure 15. Infection profiles obtained by fluorescence measurement for 8 days at different multiplicities of infection using culture-derived fluorescent trypomastigotes. a.u., arbitrary units.

In order to obtain representative images from different dpi (**Figure 16**), the same methodology was followed using 24-well microtiter flat-bottom plates with rounded coverslips on the bottom and a Zeiss LSM 510 confocal microscope.

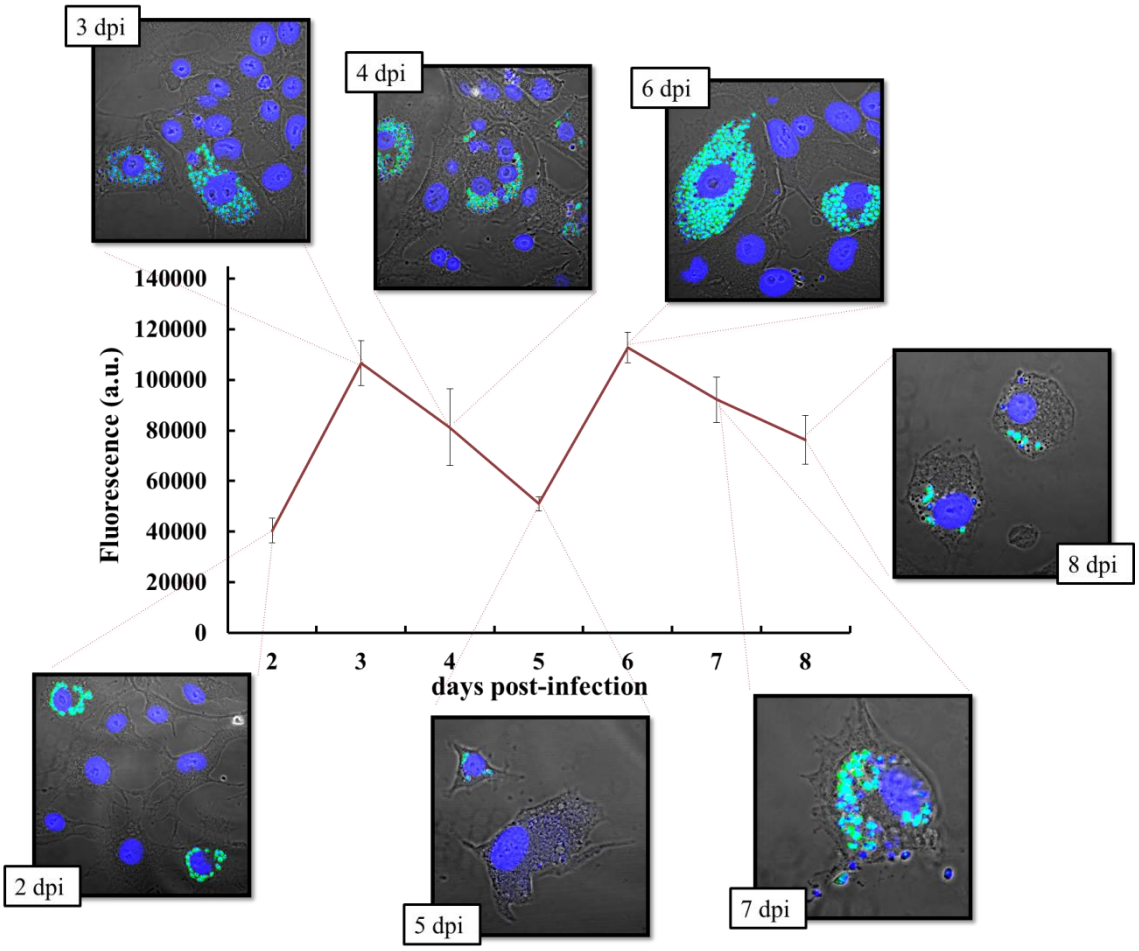

Figure 16. Infection profile obtained by fluorescence measurement for 8 days and representative images at a MOI ratio of 10 and 5.0×10^3 BSR cells·well^{-1} as initial host cell culture. Cultures were fixed in 2 % paraformaldehyde and imaged on a Zeiss LSM 510 confocal microscope. DNA is stained with DAPI (coloured blue on images); Fluorescent intracellular amastigotes expressing the fluorescent NeonGreen protein (coloured green on images); a.u., arbitrary units: dpi, days post-infection.

5.1.3. Drug screening assays

Once the detection of different extracellular parasite concentrations and different intracellular infection levels were confirmed, *in vitro* drug screening assays were performed using BZN and NFX to check this new methodology. These screening assays

were performed, as stated before, against the three morphological forms of *T. cruzi* (**Figures 17-19**). It should be noted that the development of innovative methodologies for drug evaluation against extra- and intracellular forms is an interesting point for the search of new trypanocidal agents.

Figures 17-19 show the fluorescence measurements, the dose-response inhibition curves, and the IC_{50} values against epimastigote, amastigote and trypomastigote forms of *T. cruzi*, respectively, treated with BZN and NFX. Assays were performed by treating parasites for 72 h for epimastigote and amastigote forms, since both drugs are considered fast-acting drugs[208]. Trypomastigotes were treated for 3 h, 6 h and 9 h before infection because of the half-life of these forms is about 48 h (data not shown).

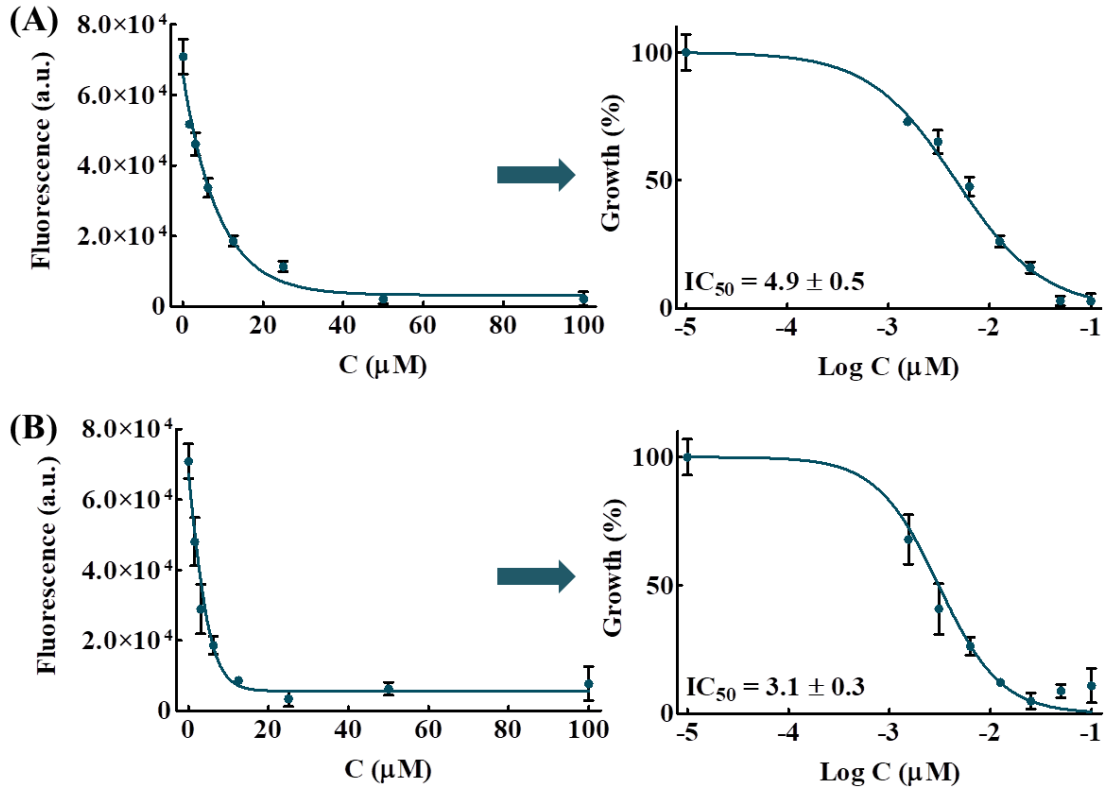

Figure 17. Fluorescence measurements, dose-response inhibition curves, and inhibitory concentrations 50 (IC_{50}) values (µM) obtained using GraphPad Prism 6 Software against epimastigote forms treated with (A) benznidazole and (B) nifurtimox for 72 h. a.u., arbitrary units; C, drug concentration.

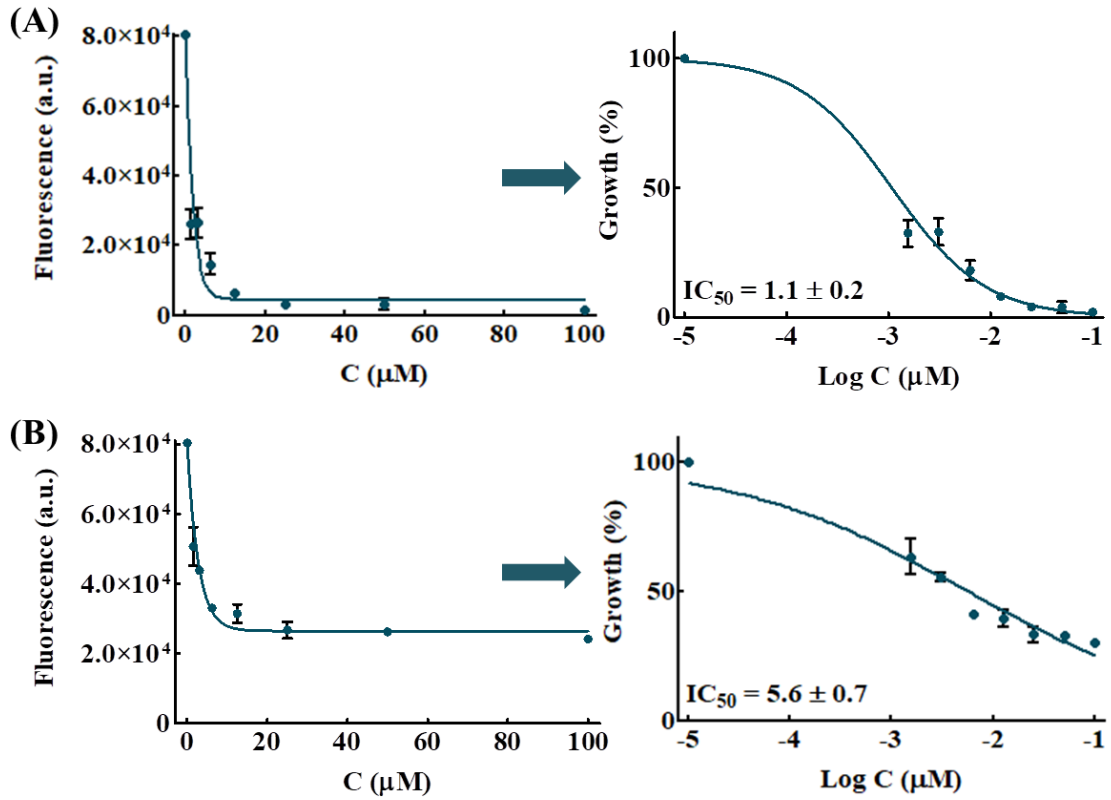

Figure 18. Fluorescence measurements, dose-response inhibition curves, and inhibitory concentrations 50 (IC_{50}) values (µM) obtained using GraphPad Prism 6 Software against amastigote forms treated with (A) benznidazole and (B) nifurtimox for 72 h. a.u., arbitrary units; C, drug concentration.

Finally, in order to compare the results obtained and to validate this novel fluorescence-based method, screening assays against epimastigote forms were performed using the resazurin-based method[209,210]. This method obtained IC_{50} values of 5.3 µM and 2.9 µM for BZN and NFX, respectively. These results were very similar to those obtained using this novel method (4.9 µM and 3.1 µM).

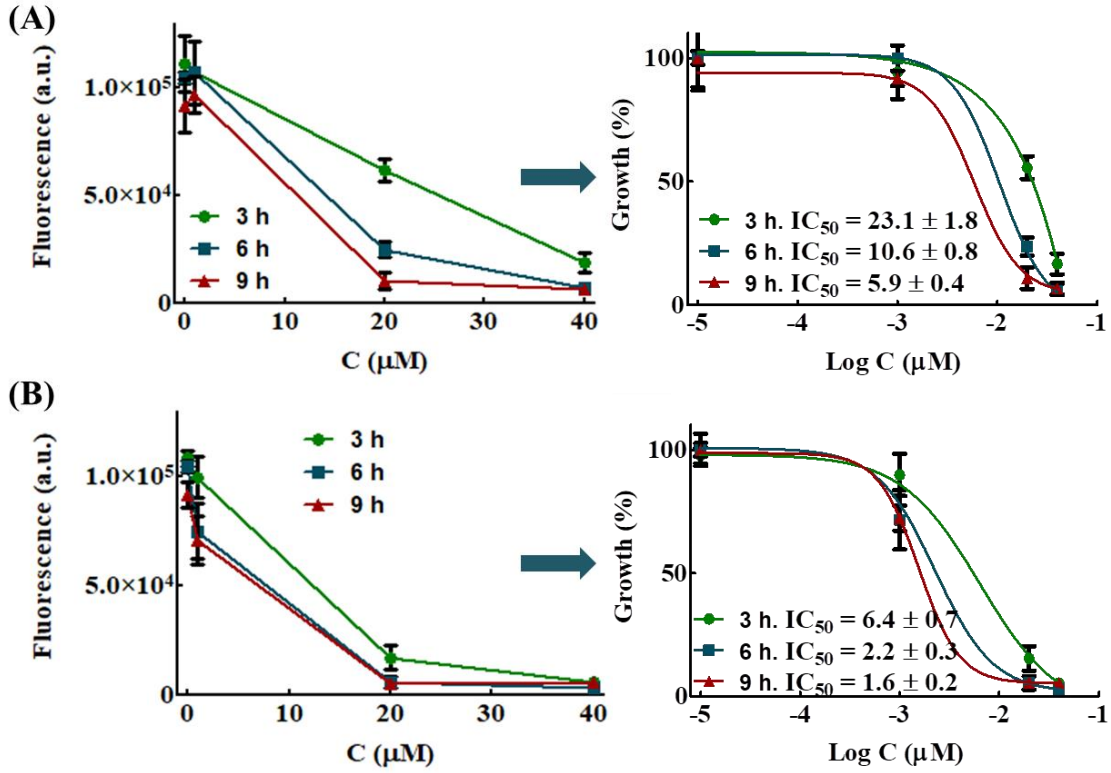

Figure 19. Fluorescence measurements, dose-response inhibition curves, and inhibitory concentrations 50 (IC_{50}) values (µM) obtained using GraphPad Prism 6 Software against trypomastigote forms treated with (A) benznidazole and (B) nifurtimox for 3 h, 6 h and 9 h before infection for 72 h. a.u., arbitrary units; C, drug concentration.

5.2. In vivo approach for Chagas Disease chemotherapy

It is widely known that the *T. cruzi* infection is dependent on the genetic composition of the infecting *T. cruzi* strain[211–213] and the genetic background of the animal model used as a host[214], that is, the host-parasite interactions[121]. On the one hand, *T. cruzi* Arequipa was the strain used for *in vivo* chemotherapy because it present moderate resistance to BZN and does not cause mortality[210,215], which is ultimately useful for comparing the *in vivo* trypanocidal efficacy of the tested compounds and the reference drug BZN. On the other hand, female BALB/c mice were the animals chosen as model since they are widely used for the study of human CD[216–218].

It is really important to know the infective capacity of the strain used, that is, virulence (quantitative) and tropism (qualitative) in BALB/c mice, before *in vivo* assays[211]. It is well known that *T. cruzi* is able to parasitize a large variety of cells[92,211,219,220] and its tissue homing ability has been reported to be strain-specific[221]. Hence, the acute-phase parasitaemia and the chronic-phase tropism of *T. cruzi* Arequipa strain were evaluated in BALB/c mice to screening the trypanocidal activity of new synthetic compounds with the aim of developing new drugs to treat CD.

First, the course of infection was monitored during the acute-phase (**Figure 20**). Parasitaemia was detected from the 9th dpi, it showed the highest levels between the 22nd and 24th dpi, reaching more than 5 million per mL of blood, and it was undetectable from the 45th dpi in all infected mice. Therefore, it can be established that the acute-phase ends on this day[14,31].

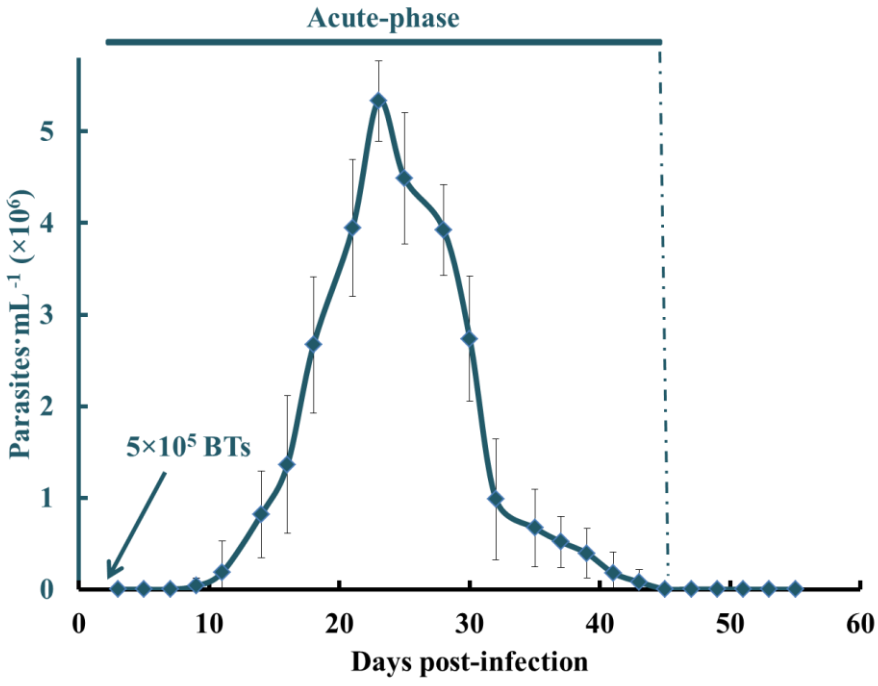

Figure 20. Acute-phase parasitaemia in murine model of *T. cruzi* Arequipa strain (MHOM/Pe/2011/Arequipa) after intraperitoneal inoculation of 5×10^5 bloodstream trypomastigotes (BTs). Values constitute means of 10 mice ± standard deviation.

However, parasites were detected at 20st dpi in 6 out of the 14 analysed organs/tissues, and 9 out of them were infected at the end of the acute-phase (40th dpi). The same organs/tissues were infected at 60th dpi. **Table 5** shows the PCR analysis of 14 organs/tissues for each experimental time. Therefore, this assay reveals the tropism of this strain for 9 target organs/tissues: adipose tissue, bone marrow, brain, oesophagus, heart, lung, muscle, spleen and stomach. Analysis of murine model has identified the gastrointestinal tract as a primary reservoir using different *T. cruzi* strains[220,222,223]; hence, the intestine may also be parasitized in some areas along its length using *T. cruzi* Arequipa strain, but we did not observe parasitization in the selected fragments for PCR. Other reason would be that the parasite load to be below the PCR limit detection (~1 parasite per 10 mg)[216], although three rounds of PCR were performed for all tissues/organs.

It should be noted that the chronic-phase begins when the amastigote forms are nested inside target organs/tissues[14,31,224]. Here, amastigote forms were already found nesting in 6 out of the 9 target organs/tissues at 20th dpi; hence, chronic-phase begins, at least, on this day (**Figure 21**).

It should be highlighted that the chronic-phase is characterized by a low and intermittent parasitaemia[14,31,225], but not detectable by counting BTs. In addition, sophisticated parasite-detection bioluminescence technologies are leading to a better appreciation of the spatiotemporal and quantitative dynamics of chronic infections[219,220,222,223], limited using the PCR method.

In summary, acute-phase treatment should be performed once the parasitaemia is confirmed, that is, ~9th dpi; and parasitaemia should be monitored until ~55th dpi, when parasitaemia is not detected. For chronic-phase treatment, it should be performed from 70th dpi, when this phase is established. Thereafter, assessment of cure should be

confirmed by PCR of the 9 target organs/tissues in late chronic-phase. It should be noted that most *in vivo* chemotherapy has focused on acute-phase infections, partially because it is simpler to monitor the course of parasitaemia[226–229]. However, the ability to cure chronic-phase infections is the main need from a clinical point of view[2], and it should be the main research focus in animal models.

Table 5. PCR analysis of 14 organs/tissues based on the sequence of the *T. cruzi SOD* gene for each experimental time (20^{th}, 40^{th}, and 60^{th} day post-infection).

Organs/tissues	Days post-infection*		
	20	40	60
Adipose tissue	2/5	3/5	3/5
Bone marrow	3/5	4/5	5/5
Brain	2/5	4/5	4/5
Oesophagus	0/5	3/5	4/5
Heart	4/5	5/5	5/5
Kidney	0/5	0/5	0/5
Large intestine	0/5	0/5	0/5
Liver	0/5	0/5	0/5
Lung	3/5	4/5	4/5
Mesenteric tissue	0/5	0/5	0/5
Muscle	3/5	5/5	5/5
Small intestine	0/5	0/5	0/5
Spleen	0/5	4/5	5/5
Stomach	0/5	3/5	4/5

*n = 5; mice used for each experimental time.

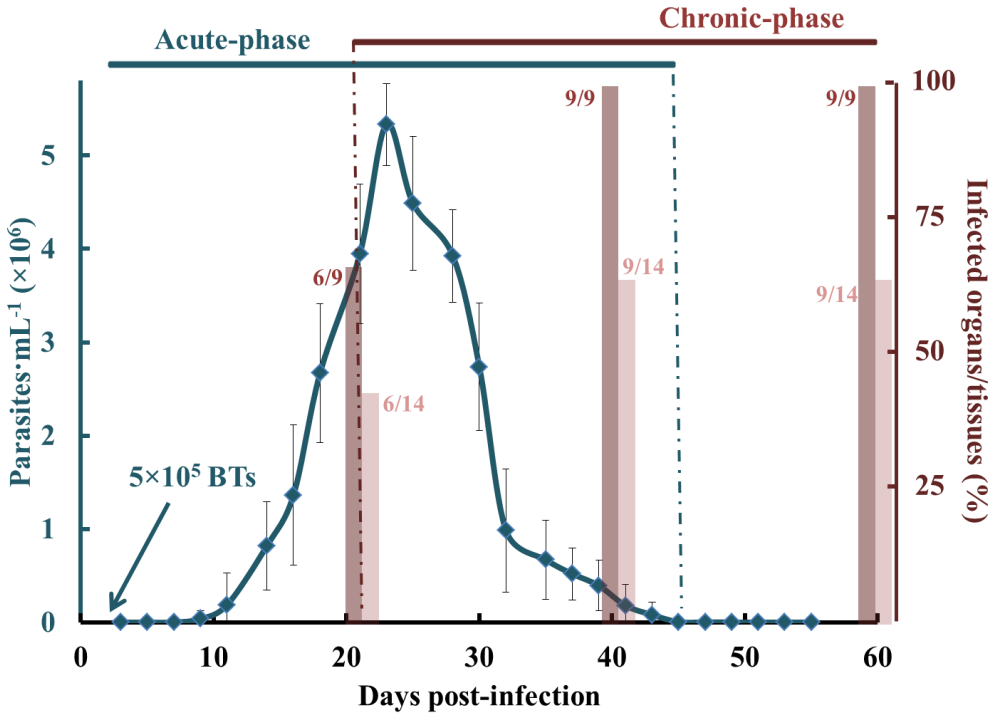

Figure 21. Acute-phase parasitaemia (blue) and chronic-phase tropism (red) in murine model of *T. cruzi* Arequipa strain (MHOM/Pe/2011/Arequipa) after intraperitoneal inoculation of 5×10^5 bloodstream trypomastigotes (BTs). Values constitute means of 10 mice ± standard deviation for parasitaemia curve. Tropism bars represent the percentage of organs/tissues with nested amastigote forms with respect to the target organs/tissues (9, dark red) and all the organs/tissues analysed (14, light red).

5.3. Published results

5.3.1. Publication 1

[1] Martín-Escolano, R., Marín, C., Vega, M., Martin-Montes, Á., Medina-Carmona, E., López, C., Rotger, C., Costa, A., Sánchez-Moreno, M., 2019. Synthesis and biological evaluation of new long-chain squaramides as anti-chagasic agents in the BALB/c mouse model. Bioorg. Med. Chem. 27, 865–879. https://doi.org/10.1016/j.bmc.2019.01.033.

Journal Citation Reports (JCR) Impact Factor (2018): **2.802**

Category name: **Chemistry, Medicinal**

Journal rank in Category & Quartile & Percentile: **28/61 & Q2 & 54.918**

Category name: **Chemistry, Organic**

Journal rank in Category & Quartile & Percentile: **19/57 & Q2 & 67.544**

Cites: **1**

5.3.2. Publication 2

[2] Martín-Escolano, R., Molina-Carreño, D., Delgado-Pinar, E., Martin-Montes, Á., Clares, M.P., Medina-Carmona, E., Pitarch-Jarque, J., Martín-Escolano, J., Rosales, M.J., García-España, E., Sánchez-Moreno, M., Marín, C., 2019. New polyamine drugs as more effective antichagas agents than benznidazole in both the acute and chronic phases. Eur. J. Med. Chem. 15, 27–46. https://doi.org/10.1016/j.ejmech.2018.12.034.

Journal Citation Reports (JCR) Impact Factor (2018): **4.833**

Category name: **Chemistry, Medicinal**

Journal rank in Category & Quartile & Percentile: **5/61 & Q1 & 92.623**

Cites: **0**

5.3.3. Publication 3

[3] Martín-Escolano, R., Aguilera-Venegas, B., Marín, C., Martín-Montes, Á., Martín-Escolano, J., Medina-Carmona, E., Arán, V.J., Sánchez-Moreno, M., 2018. Synthesis and biological in vitro and in vivo evaluation of 2-(5-Nitroindazol-1-yl)ethylamines and related compounds as potential therapeutic alternatives for Chagas Disease. ChemMedChem. 13, 2104–2118. https://doi.org/10.1002/cmdc.201800512.

Journal Citation Reports (JCR) Impact Factor (2018): **3.016**

Category name: **Pharmacology & Pharmacy**

Journal rank in Category & Quartile & Percentile: **100/267 & Q2 & 62.734**

Category name: **Chemistry, Medicinal**

Journal rank in Category & Quartile & Percentile: **26/61 & Q2 & 58.197**

Cites: **2**

[1] PUBLICATION 1

Bioorganic & Medicinal Chemistry 27 (2019) 865–879

Contents lists available at ScienceDirect

Bioorganic & Medicinal Chemistry

journal homepage: www.elsevier.com/locate/bmc

Synthesis and biological evaluation of new long-chain squaramides as anti-chagasic agents in the BALB/c mouse model

Rubén Martín-Escolano[a], Clotilde Marín[a,*], Manuel Vega[b], Álvaro Martin-Montes[a], Encarnación Medina-Carmona[c], Carlos López[b], Carmen Rotger[b], Antonio Costa[b], Manuel Sánchez-Moreno[a]

[a] Department of Parasitology, Instituto de Investigación Biosanitaria (ibs. Granada), Hospitales Universitarios de Granada/University of Granada, Severo Ochoa s/n, E-18071 Granada, Spain
[b] Department of Chemistry, Universitat de les Illes Balears, Ctra. Valldemossa, Km. 7.5, Palma 07122, Spain
[c] School of Biosciences, University of Kent, Stacey Building, Canterbury CT2 7NJ, UK

ARTICLE INFO

Keywords:
Chagas Disease
Chemotherapy
Murine model
Squaramides
Trypanosoma cruzi

ABSTRACT

Chagas Disease is caused by infection with the insect-transmitted protozoan *Trypanosoma cruzi* and affects more than 10 million people. It is a paradigmatic example of a chronic disease without an effective treatment in Latin America where the current therapies, based on Benznidazole and Nifurtimox, are characterised by limited efficacy, toxic side-effects and frequent failures in the treatment. We present a series of new long-chain squaramides, identified based on their ^{1}H and ^{13}C NMR spectra, and their trypanocidal activity and cytotoxicity were tested *in vitro* through the determination of IC_{50} values. Compounds **4** and **7** were more active and less toxic than the reference drug Benznidazole, and these results were the basis of promoting *in vivo* assays, where parasitaemia levels, assignment of cure, reactivation of parasitaemia and others parameters were determined in mice treated in both the acute and chronic phases. Finally, the mechanisms of action were elucidated at metabolic and mitochondrial levels and superoxide dismutase inhibition. The experiments allowed us to select compound **7** as a promising candidate for treating Chagas Disease, where the activity, stability and low cost make long-chain squaramides appropriate molecules for the development of an affordable anti-chagasic agent versus current treatments.

1. Introduction

Chagas Disease (CD), whose causative agent is the protozoan parasite *Trypanosoma cruzi* (*T. cruzi*), is the most important parasitic disease in Latin America, with 20–50 thousand deaths per year, more than 10 million infected people and more than 25 million people at risk of infection.[1–4] CD is the most prevalent of the poverty-caused and poverty-promoting neglected parasitic disease in 21 endemic Latin America countries.[5–7] Recently, the disease has become more widespread due to the increase mobility and migration, with large numbers of infected individuals, particularly in Europe (80,000) and North America (300,000).[8,9] Because of the complex pathology and the long-term nature of CD, there are no available vaccines for the prevention.[10,11] Currently, the only way to combat the infection is chemotherapy based on two nitroheterocyclic drugs developed more than 40 years ago. These drugs are Benznidazole (BZN) and Nifurtimox (NFX). However, long-term therapeutic schedules are required, the treatment have inconsistent efficacy, specially in the chronic phase, and serious side effects are frequently observed.[12–17] In addition, the efficacy of BZN and NFX change according to the geographical area because of a different susceptibility by the different strains of *T. cruzi*.[18] Moreover, both drugs are prodrugs activated by the same nitroreductase and this result in cross-resistance in several cases.[10,19]

Abbreviations: CD, Chagas Disease; BZN, Benznidazole; NFX, Nifurtimox; MILT, Miltefosine; Fe- SOD, iron superoxide dismutase; ppm, parts per million; DMSO, dimethyl sulfoxide; DTU, discrete typing unit; IC, inhibitory concentration; BTs, bloodstream trypomastigotes; pi, post-infection; CP, cyclophosphamide monohydrate; IS, immunosuppression; PCR, polymerase chain reaction; ELISA, enzyme-linked immunosorbent assay; ^{1}H NMR, proton nuclear magnetic resonance; Rho, rhodamine 123; AO, acridine orange; SI, selectivity index; IgG, immunoglobulin G; PEP, phosphoenolpyruvate; PK, pyruvate kinase; PPDK, pyruvate phosphate dikinase; TCA, tricarboxylic acid

* Corresponding author at: Department of Parasitology, Faculty of Sciences (Mecenas), Severo Ochoa s/n, 18001 Granada, Spain.
E-mail address: cmaris@ugr.es (C. Marín).

https://doi.org/10.1016/j.bmc.2019.01.033
Received 3 December 2018; Received in revised form 25 January 2019; Accepted 28 January 2019
Available online 29 January 2019
0968-0896/ © 2019 Elsevier Ltd. All rights reserved.

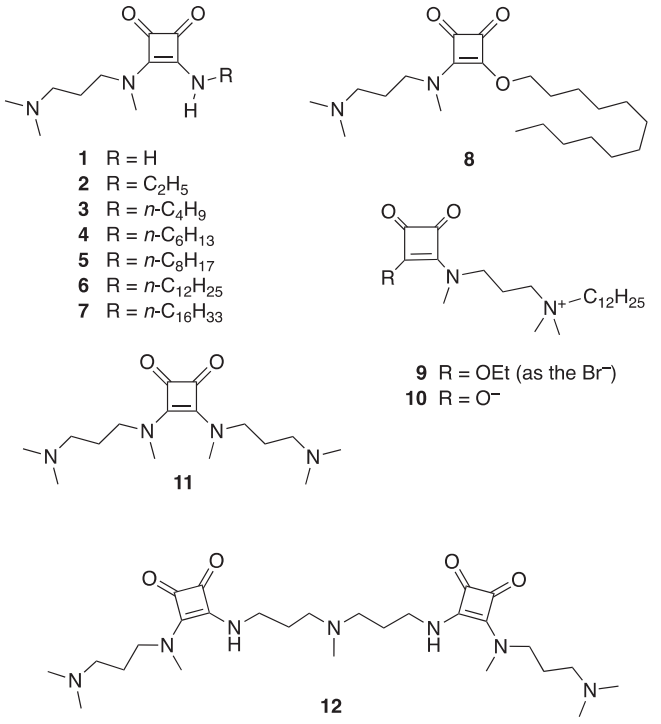

Chart 1. Chemical structures of the squaramides investigated in this work.

Therefore, this background, coupled with frequent reports of treatment failure, makes the development of new drugs, safer and more widely effective, an important need. In this way, the urgency to continue researching, in order to discover novel therapeutic alternatives, is justified. These new drugs should present an efficacy at least equal to the reference drug BZN and with better safety profile, active against most *T. cruzi* strains and administered orally.[20] Other strategy that has emerged is the drug repositioning, a fruitful strategy for improving the drug development process, but it has not obtained good results either.[21–23] Among the targets, those based on squaramides has attracted attention because of its activity against parasites such us, *Trypanosoma brucei*,[24] and as antimalarials.[25,26] In particular, simple model squaryl diamides (a.k.a. squaramides) bearing N^3-3-(dimethylamino)propyl and N^4-*n*-butyl substituents **3** has proven effective against *T. cruzi*.[27] However, the origin of the antiparasitic activity of these squaramides remains unknown. Based on our previous results, and continuing with our efforts in this line, herein we describe the antiparasitic activity of a series of related squaramides (Chart 1). Thus, compounds **1** to **7** constitute a series with increasing length of the linear aliphatic chain from C0 to C16. The aim of this series was to study the effect of the increasing lipophilicity on the antiparasitic activity. Compound **8** (C12), allows us to compare its activity with that of **6**, to inform regarding the effect of the squaramide nitrogen. Compound **9** and **10**, can be considered as squaryl analogues of Miltefosine (MILT). Given the antileishmanial activity of MILT we considered the bioisosteric substitution of the phosphate group of MILT by the squaryl moiety.[28,29] Compounds **11** and **12** containing two and three basic nitrogens, respectively, were included to check the effect of the increasing basicity of these compounds on the antiparasitic activity.

Herein, we report the synthesis, *in vitro* and *in vivo* trypanocidal activity of a new series of squaramides. Furthermore, we analyse the possible mechanisms of action of these compounds in terms of the variation in the excreted metabolites, the alteration on the mitochondrial membrane potential and the inhibition over the iron superoxide dismutase (Fe-SOD), which represent one of the many mechanisms of antioxidant defence in trypanosomatids.

2. Materials and methods

2.1. Chemistry

The various chemicals were of commercial origin (Aldrich or Across) and used as received. Melting points were obtained in open capillary tubes with a Büchi melting point apparatus (Dr. Tottoli) and are uncorrected. ^{1}H, ^{13}C spectra (at 300 and 600 MHz) and ^{13}C (at 75 and 150 MHz) spectra were recorded on a 300 MHz (Bruker Avance) and 600 MHz (Bruker Avance III) spectrometers in CDCl3 or *d6*-dimethyl sulfoxide (DMSO) solutions at room temperature. The residual proton signal was used as reference at 7.26/77.16 parts per million (ppm) for chloroform or 2.50/39.52 for DMSO. Chemical shifts (δ) are given in ppm and coupling constants (J) in Hz. ESI-HRMS mass spectra were recorded on a magnetic sector (Micromass Autospec) or on a Thermo Scientific (Orbitrap Q Exactive) mass spectrometers. Elemental analyses (C, H, N) were conducted by the "Centro de Microanálisis Elemental" of the "Universidad Complutense de Madrid" (Spain). Squaramides **3** and **11**, were prepared according to reported procedures.[27,30]

2.2. Preparation of squaramides.

A conventional method for the synthesis of unsymmetrical squaramides involves the sequential two-step condensation of dialkyl esters of squaric acid, usually diethyl squarate, with the appropriates amines dissolved in ethanol or methanol.[31,32] In this work, we report a one-step procedure for the synthesis of the unsymmetrical squaramides **1–7**, **9**, **10** and **12**. In our method, the amines were introduced as neat liquids or in dissolution, for NH_3 and solid amines (C_{12} and C_{16}), using a minimum volume of solvent. In parallel, we took advantage of the inherent increase of the reaction rate of solventless methods to avoid the use of triethylamine or any added catalyst, thus facilitating the isolation and purification of the final products.

2.2.1. Procedure for the preparation of the squaramides 1–7, 9, 10, 12. Part (A)

Common to squaramides **1–7, 9, 10** and **12**. A mixture of neat diethyl squarate (1.0 g, 5.88 mmol) and neat N^1,N^1,N^3-trimethyl-1,3-propanediamine (890 µL, 5.89 mmol) was magnetically stirred at room temperature for 90 min. The appropriate amine was then added to the above mixture as described in part (B).

2.2.2. 3-amino-4-{[3-(dimethylamino)propyl](methyl)amino}cyclobut-3-ene-1,2-dione (1). Part (B)

After addition of a 7 N NH_3 solution in MeOH (1 mL, 7 mmol), the mixture was stirred at 40 °C for 5 h. The crude was purified by CC (SiO_2, CH_2Cl_2-MeOH 3%; CH_2Cl_2-NH_3 7 N in MeOH 5%, Rf: 0.20). The squaramide **1** was obtained as a yellow solid, 1.02 g, yield 82%. Mp: 154–156 °C. ^{1}H NMR ($CDCl_3$) δ: 7.34 (br, 2H), 3.40 (t, J = 5.7 Hz, 2H), 3.35 (s, 3H), 2.36 (t, J = 5.7 Hz, 2H), 2.21 (s, 6H), 1.76 (m, 2H). ^{13}C NMR ($CDCl_3$, 75 MHz) δ: 183.9, 183.4, 170.5, 169.3, 54.3, 49.0, 44.8, 36.1, 23.8. ESI(+)-HRMS: *m/z* calcd for $C_{20}H_{34}N_6O_4Na$ $[2M + Na]^+$ 445.2539, found 445.2536.

2.2.3. 3-{[(3-(dimethylamino)propyl](methyl)amino}-4-(ethylamino) cyclobut-3-ene-1,2-dione (2). Part (B)

After addition of a 2 N ethylamine solution in MeOH (3 mL, 6 mmol), the mixture was stirred a room temperature for 15 h. The crude mixture was purified by CC (SiO_2, CH_2Cl_2-MeOH 3%; CH_2Cl_2-NH_3 7 N in MeOH 5%, Rf: 0.38). The squaramide **2** was obtained as a white solid, 1.32 g, yield 94%. Mp: 64–66 °C. ^{1}H NMR ($CDCl_3$) δ: 8.41 (br, 1H), 3.67 (m, 2H), 3.34–3.30 (br, 5H), 2.36 (m, 2H), 2.22 (s, 6H), 1.73 (m, 2H), 1.22 (t, J = 7.2 Hz, 3H). ^{13}C NMR ($CDCl_3$, 75 MHz) δ: 183.4, 183.3, 169.2, 168.4, 54.2, 48.4, 44.9, 39.7, 36.2, 23.8, 22.7, 17.0 ESI(+)-HRMS: *m/z* calcd for $C_{12}H_{22}N_3O_2$ $[M + H]^+$ 240.1712, found 240.1716.

*2.2.4. 3-{[3-(dimethylamino)propyl)](methyl)amino}-4-(butylamino) cyclobut-3-ene-1,2-dione (**3**). Part (B)*

After addition of neat *n*-butylamine (590 μL, 5.94 mmol) the mixture was stirred at 100 °C for 2 h. The crude was purified by CC (neutral Al_2O_3, act. I, CH_2Cl_2; CH_2Cl_2-EtOH 5%, Rf: 0.69). The squaramide **3** was obtained as a thick oil which solidifies on standing, 1.54 g, yield 98%. Mp: 56–58 °C.[27,30]

*2.2.5. 3-{[3-(dimethylamino)propyl](methyl)amino}-4-(hexylamino) cyclobut-3-ene-1,2-dione (**4**). Part (B)*

After addition of neat *n*-hexylamine (942 μL, 7.06 mmol) the mixture was stirred at 100 °C for 2 h. The crude was purified by CC (neutral Al_2O_3, act. I, CH_2Cl_2; CH_2Cl_2-EtOH 5%, Rf: 0.69). The squaramide **4** was obtained as a white solid, 1.60 g, yield 92%. Mp: 44–46 °C. ^{1}H NMR ($CDCl_3$) *δ*: 8.39 (br, 1H), 3.63 (q, *J* = 7.2 Hz, 2H), 3.33–3.30 (br, 5H), 2.35 (t, *J* = 5.7 Hz, 2H), 2.21 (s, 6H), 1.73 (m, 2H), 1.54 (m, 2H), 1.49–1.27 (br, 6H), 0.86 (t, *J* = 7.2 Hz, 3H). ^{13}C NMR ($CDCl_3$, 75 MHz) *δ*: 183.4, 183.3, 169.1, 168.5, 54.3, 48.4, 44.9, 36.2, 31.6, 26.5, 23.8, 22.7, 14.2. ESI(+)-HRMS *m/z* calcd for $C_{16}H_{29}N_3O_2Na$ $[M + Na]^+$ 318.2157, found 318.2169.

*2.2.6. 3-{[3-(dimethylamino)propyl](methyl)amino}-4-(octylamino) cyclobut-3-ene-1,2-dione (**5**). Part (B)*

After addition of neat *n*-octylamine (1.47 mL, 8.8 mmol), the mixture was stirred at 100 °C for 2 h. The crude was purified by CC (SiO_2, CH_2Cl_2-MeOH 3%; CH_2Cl_2-NH_3 7 N in MeOH 5%, Rf: 0.39). The squaramide **5** was obtained as a white solid, 1.62 g, yield 85%. Mp: 40–44 °C. ^{1}H NMR ($CDCl_3$) *δ*: 8.39 (br, 1H), 3.62 (q, *J* = 6.9 Hz, 2H), 3.31 (br, 5H), 2.35 (t, *J* = 2.4 Hz, 2H), 2.21 (s, 6H), 1.73 (m, 2H), 1.54 (m, 2H), 1.24 (br, 10*H*), 0.85 (t, *J* = 6.9 Hz, 3H). ^{13}C NMR ($CDCl_3$, 75 MHz) *δ*: 183.5, 183.4, 169.1, 168.6, 54.3, 48.4, 45.0, 36.3, 32.0, 31.7, 29.5, 29.4, 26.8, 23.8, 22.8, 14.3. ESI(+)-HRMS *m/z* calcd. for $C_{18}H_{34}N_3O_2$ *m/z* $[M + H]^+$ 324.2646, found 324.2644.

*2.2.7. 3-{[3-(dimethylamino)propyl](methyl)amino}-4-(dodecylamino) cyclobut-3-ene-1,2-dione (**6**). Part (B)*

After addition of a solution of *n*-dodecylamine (1.2 g, 6.47 mmol) in 20 mL of EtOH, the mixture was stirred at room temperature for 24 h. Once concentrated at reduced pressure, the residue was purified by CC (SiO_2, CH_2Cl_2-MeOH 3%; CH_2Cl_2-NH_3 7 N in MeOH 5%, Rf: 0.44). The squaramide **6** was isolated as a white solid, 1.78 g, yield 80%. Mp: 36–38 °C. ^{1}H NMR ($CDCl_3$) *δ*: 8.40 (br, 1H), 3.62 (q, *J* = 6.9 Hz, 2H), 3.30 (br, 5H), 2.33 (t, *J* = 5.7 Hz, 2H), 2.20 (s, 6H), 1.72 (m, 2H), 1.53 (m, 2H), 1.22 (br, 18H), 0.84 (t, *J* = 6.3 Hz, 3H). ^{13}C NMR ($CDCl_3$, 75 MHz) *δ*: 183.29, 183.18, 169.0, 168.4, 54.3, 48.4, 44.9, 36.2, 32.0, 31.6, 29.7, 29.4, 26.7, 23.8, 22.8, 14.2. ESI(+)-HRMS *m/z* calcd for $C_{22}H_{42}N_3O_2$ $[M + H]^+$ 380.3272, found 380.3271.

*2.2.8. 3-{[3-(dimethylamino)propyl](methyl)amino}-4-(hexadecylamino) cyclobut-3-ene-1,2-dione (**7**). Part (B)*

After addition of a hot solution of *n*-hexadecylamine (2.4 g, 8.94 mmol) in 15 mL of EtOH, the mixture was stirred at room temperature for 15 h. Once concentrated at reduced pressure, the residue was purified by CC (neutral Al_2O_3, act. I, CH_2Cl_2-EtOH 2%, Rf: 0.43). The squaramide **7** was obtained as a white solid, 2.25 g, yield 88%. Mp: 55–57 °C. ^{1}H NMR ($CDCl_3$) *δ*: 8.33 (br, 1H), 3.65 (q, *J* = 6.3, 2H), 3.37 (br, 2H), 3.31 (br, 3H), 2.42 (br, 2H), 2.28 (s, 6H), 1.78 (br, 2H), 1.54 (m, 2H), 1.29–1.23 (br, 26H), 0.57 (t, *J* = 6.3, 3H). ^{13}C NMR ($CDCl_3$, 75 MHz) *δ*: 183.5, 183.4, 169.1, 168.5, 54.3, 48.4, 44.9, 36.2, 32.1, 31.7, 26.8, 29.5, 26.8, 23.8, 22.8, 14.3. ESI(+)-HRMS *m/z* calcd for $C_{26}H_{50}N_3O_2$ $[M + H]^+$ 436.3898, found 436.3897.

*2.2.9. N-{3-[(2-ethoxy-3,4-dioxocyclobut-1-en-1-yl)(methyl)amino] propyl}-N,N-dimethyldodecan-1-aminium Bromide (**9**). Part (B)*

The mixture was diluted with 5 mL of dry acetonitrile and *n*-bromododecane (2.92 mL, 11.8 mmol) was added under stirring at room temperature. The mixture was then stirred at 80 °C for 20 h. After allowing to cool to room temperature, the reaction flask was treated with 20 mL of diethyl ether to induce the separation of the crude product as a thick oil. The solvent was discharged, and the oily residue was redissolved in CH_2Cl_2 (5 mL) and reprecipitated with diethyl ether (20 mL) for three times. The synthesis was outlined in Scheme 1. The squaramide was obtained as a thick oil, 2.53 g, yield 88%. ^{1}H NMR (DMSO-d_6) *δ*: 4.67 (q, *J* = 6.9 Hz, 2H), 3.66 (t, *J* = 6.3 Hz, 1H), 3.42 (t, *J* = 6 Hz, 1H), 3.26 (m, 5.5H), 3.12 (s, 1.5H), 3.01 (s, 6H), 2.02 (m, 2H), 1.63 (m, 2H), 1.38 (t, *J* = 6.9 Hz, 3H), 1.24 (m, 18H), 0.85 (t, *J* = 5.7 Hz, 3H). ^{13}C NMR (DMSO-d_6, 75 MHz) *δ*: 188.7, 181.4, 176.3, 175.9, 171.7, 69.2, 63.0, 60.0, 50.0, 48.5, 47.6, 36.3, 35.8, 31.3, 29.0, 28.8, 28.7, 28.5, 25.8, 22.1, 21.7, 20.4, 20.1, 15.6, 13.9. ESI(+)-HRMS *m/z* calcd for $C_{24}H_{45}N_2O_3$ $[M-Br]^+$ 409.34247, found 409.3425.

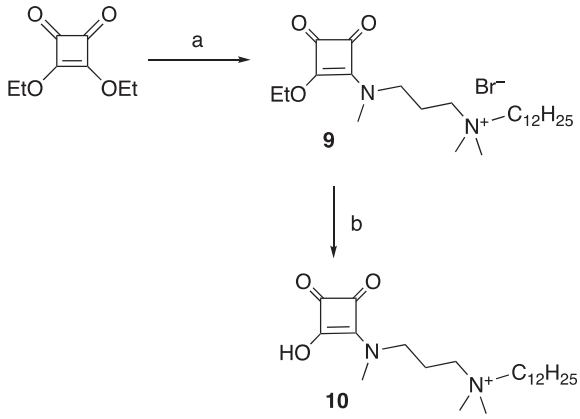

Scheme 1. Procedure for the synthesis of squaramides **9** and **10.** (a) 1. neat $Me_2N(CH_2)_3NHMe$, rt. 2. $C_{12}H_{25}Br$, Δ. (b) H_2O, Δ.

*2.2.10. N-{3-[(2-hydroxy-3,4-dioxocyclobut-1-en-1-yl)(methyl)amino] propyl}-N,N-dimethyldodecan-1-aminium bromide (**10**)*

The squaramide **9** (0.5 g, 1.02 mmol) was dissolved in water (30 mL) and refluxed for 17 h. The solution was concentrated at reduced pressure and the resulting residue dried at reduced pressure (Scheme 1**)**. The squaramic acid **10** was obtained as an hygroscopic amber-like solid, 0.47 g, yield 99%. Mp: 83–85 °C. ^{1}H NMR (DMSO-d_6) *δ*: 3.58 (t, *J* = 6.3 Hz, 2H), 3.25 (m, 4H), 3.18 (s, 3H), 3.00 (s, 6H), 2. (m, 2H), 1.63 (m, 2H), 1.25 (m, 18H), 0.85 (t, *J* = 6.3 Hz, 3H). ^{13}C NMR (DMSO-d_6, 75 MHz) *δ*: 189.4, 185.2, 175.9, 63.0, 60.3, 50, 47.3, 35.3, 31.3, 29.0, 28.9, 28.8, 28.7, 28.5, 25.82. ESI(+)-HRMS *m/z* calcd for $C_{22}H_{40}N_2O_3$ $[M-Br]^+$ 403.2931, found 403.2931.

*2.2.11. 4,4′-{[(methylazanediyl)bis(propane-3,1-diyl)]bis(azanediyl)}bis {3-[(3-(dimethylamino)propyl](methyl)amino}cyclobut-3-ene-1,2-dione (**12**). Part (B)*

After addition of 3,3′-diamino-*N*-methyldipropylamine, the mixture was stirred at room temperature for 15 h. The crude reaction mixture was purified by CC (Al_2O_3, neutral act. I, EtOH-TEA 10%, Rf: 0.72). The squaramide **12** was obtained as a white solid, 1.40 g, 89%. Mp: 97–99 °C. ^{1}H NMR ($CDCl_3$) *δ*: 8.51 (br, 2H), 3.66 (q, *J* = 6.3, 4H), 3.35 (br, 4H), 3.29 (s, 6H), 2.39 (t, 4H), 2.32 (t, 4H), 2.21 (s, 12H), 2.18 (s, 3H), 1.72 (m, 8H). ^{13}C NMR ($CDCl_3$, 75 MHz) *δ*: 183.3, 183.2, 169.2, 168.4, 55.0, 54.5, 48.7, 45.1, 43.2, 42.7, 36.3, 29.4, 24.1. ESI-HRMS *m/z* calcd for $C_{27}H_{47}N_7O_4Na$ *m/z* $[M + Na]^+$ 556.3582, found 556.3584.

*2.2.12. 3-{[(3-(dimethylamino)propyl](methyl)amino}-4-(dodecyloxy) cyclobut-3-ene-1,2-dione (**8**)*

A mixture of squaric acid (0.5 g, 4.38 mmol), anhydrous KF (1.02 g, 17.5 mmol), and 1-bromododecane (4.34 mL, 17.5 mmol) was heated at 200 °C under stirring for 20 h. After cooling at room temperature, the residue was diluted with hexane (20 mL), filtered and purified by CC

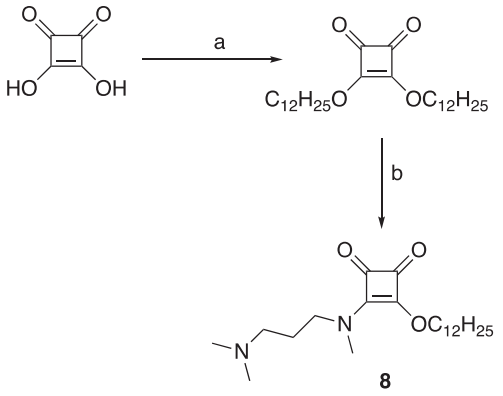

Scheme 2. Procedure for the synthesis of squaramide **8**. (a) anhydrous KF, $C_{12}H_{25}Br$, 200 °C, 20 h. (b) $Me_2N(CH_2)_3NHMe$, rt 12 h.

(SiO_2; eluting with CCl_4, hexane and finally with hexane-ether 30%, Rf: 0.6). The dodecyl squarate was obtained as a white solid, 1.34 g, 68%. Mp: 40–41 °C. ^{1}H NMR ($CDCl_3$) δ: 4.64 (t, J = 6.6, 4H), 1.78 (m, 4H), 1.41–1.24 (br, 36H), 0.86 (t, J = 6.3, 6H). ^{13}C NMR ($CDCl_3$, 75 MHz) δ: 189.6, 184.5, 74.8, 32.1, 30.0, 29.8, 29.7, 29.6, 29.5, 29.3, 25.4, 22.9, 14.3. ESI(+)-HRMS calcd. for $C_{28}H_{50}O_4Na$ m/z $[M + Na]^+$ 473.3601, found 473.3603; $C_{28}H_{50}O_4K$ m/z $[M + K]^+$ 489.3341, found 489.3342. Anal. Calcd. for $C_{28}H_{50}O_4$: C, 74.62; H, 11.18, Found: C, 74.58; H, 10.42.

A solution of dodecyl squarate (1.2 g, 6.47 mmol) in MeCN (10 mL) and N^1,N^1,N^3-trimethyl-1,3-propanediamine was stirred at room temperature for 12 h. The synthesis was outlined in Scheme 2. The mixture was concentrated and the residue purified by CC (SiO_2, CH_2Cl_2-EtOH 10% Rf: 0.1). The squaramide **8** was obtained as an oil, 2.29 g, 93%. ^{1}H NMR ($CDCl_3$) δ: 4.68 (br, 2H), 3.70 (t, J = 7.2 Hz, 1H), 3.42 (t, J = 7.8 Hz, 1H), 3.32 (s, 1.5H), 3.13 (s, 1.5H), 2.26 (m, 2H), 2.22 (s, 3H), 2.19 (s, 3H), 1.76 (br, 4H), 1.4–1.2 (br, 18H), 0.85 (br, 3H). ^{13}C NMR ($CDCl_3$, 75 MHz) δ: 189.2, 188.8, 182.64, 182.57, 176.6, 172.4, 172.0, 73.8, 56.4, 56.3, 50.6, 49.8, 45.5, 45.4, 36.7, 36.5, 32.0, 30.15, 30.1, 29.7, 29.7, 29.4, 29.3, 26.1, 25.9, 25.5, 22.8, 14.2. ESI(+)-HRMS m/z calcd for $C_{22}H_{41}N_3O_2$ $[M + H]^+$ 381.3112, found 381.3111. Anal. Calcd for $C_{22}H_{40}N_2O_3$: C, 69.43; H, 10.59; N, 7.36; O, found: C, 69.38; H, 10.29; N, 7.14.

The synthesised compounds had their structures confirmed through the usual analytical techniques [^{1}H NMR and ^{13}C NMR spectra] are available in Supplementary Data.

2.3. In vitro trypanocidal activity assays.

2.3.1. Extracellular epimastigotes culture and in vitro trypanocidal activity assays.

Three different *T. cruzi* strains were evaluated: *T. cruzi* SN3 (IRHOD/CO/2008/SN3) isolated from *Rhodnius prolixus* from Colombia[33]; *T. cruzi* Arequipa (MHOM/Pe/2011/Arequipa) isolated from human from Peru; *T. cruzi* Tulahuen (TINF/CH/1956/Tulahuen) isolated from *Triatoma infestans* from Chile. These strains belong to discrete typing units (DTUs) I, V and VI, respectively. Epimastigote forms were grown at 28 °C in RPMI (Gibco®) with 10% (v/v) FBS heat-inactivated, 0.03 M hemin and 0.5% (w/v) trypticase (BBL).[34]

Epimastigote forms were centrifuged in the exponential growth phase at 400 g for 10 min. The compounds to be tested were dissolved in 0.01% (v/v) DMSO (Panreac, Barcelona, Spain), and assayed as nontoxic DMSO concentrations on parasite growth. Trypanocidal activity was determined by centrifugation and seeding the parasites at 5×10^5 mL^{-1} in 96-well microtiter plates, and after addition of the compounds at dosages of 100 to 0.2 µM, using Resazurin sodium salt (Sigma-Aldrich) following the method described by Martín-Escolano et al.[35] Growth controls, BZN and MILT were also included. The trypanocidal effect, using GraphPad Prism 6, was expressed as the half-maximal inhibitory concentrations (IC_{50}/72 h), i.e., the concentration required to result in 50% inhibition. Each drug concentration was tested in triplicate in three separate determinations.

2.3.2. Vero cells and cytotoxicity tests.

Vero cells (EACC number 84113001) were cultured in RPMI (Gibco®) with 10% (v/v) FBS heat-inactivated at 37 °C in humidified 95% air, 5% CO_2 atmosphere.[36] Cytotoxicity tests were performed by trypsinization, centrifugation and seeding the Vero cells at 1.25×10^4 mL^{-1} in 96-well microtiter plates, and after addition of the compounds at dosages of 2000 to 1 µM, using Resazurin sodium salt (Sigma-Aldrich) following the method described by Martín-Escolano et al.[35]. Growth controls, BZN and MILT were also included. The same procedure as detailed in 2.3.1. section was carried out.

2.3.3. In vitro assays against intracellular amastigote forms.

Trypanocidal activity against amastigote forms and the infectivity index were determined according to the method described Martín-Escolano et al.[35] at dosages of 50 to 0.02 µM. Briefly, tests were performed in 24-well microtiter plates with rounded coverslips by seeding the Vero cells at 1×10^4 well^{-1} in RPMI (Gibco®) with 10% (v/v) FBS heat-inactivated, at 37 °C in humidified 95% air and 5% CO2 atmosphere. After 24 h of incubation, the cells were infected with Vero cell-derived trypomastigotes at a multiplicity of infection (MOI) ratio of 1:10. After 24 h, non-phagocyted parasites were washed away, and after adding the compounds and BZN in 500 µL volumes in RPMI (Gibco®) with 1% (v/v) FBS heat-inactivated. After 72 h of incubation, the trypanocidal activity was assessed by analysing 500 host cells in methanol-fixed and Giemsa-stained preparations. The trypanocidal effect was determined using GraphPad Prism 6, as mentioned in 2.3.1. section.

2.3.4. In vitro assays against extracellular trypomastigote forms

Metacyclic trypomastigotes were induced by culturing according to the method described by Martín-Escolano et al.[35] Subsequently, the metacyclic trypomastigotes were used to infect Vero cells for 5 to 7 days.[37] Finally, the culture-derived trypomastigotes were used to infect BALB/c mice, and *T. cruzi* bloodstream trypomastigotes (BTs) were obtain by cardiac puncture during the parasitaemia peak after infection and dissolved in RPMI (Gibco®) with 10% (v/v) FBS heat-inactivated.

Trypanocidal activity was determined by seeding the parasites at 2×10^6 mL^{-1} in 96-well microtiter plates, and after addition of the compounds at dosages of 100 to 0.2 µM, using Resazurin sodium salt (Sigma-Aldrich) following the method described by Martín-Escolano et al.,[35]. Growth controls, BZN and MILT were also included. The same procedure as detailed in 2.3.1. section was carried out.

2.4. In vivo trypanocidal activity assays.

2.4.1. Mice infection and treatment.

BALB/c mice (female, 8–10 weeks old, 20–25 g) maintained under standard conditions and standard chow *ad libitum* were used for *in vivo* assays, conformed to relevant ethical standars. The experiments were performed under the rules and principles of the international guide for biochemical research in experimental animals, involving the use of the minimum number of animals necessary to produce statistically reproducible results.

The mice were intraperitoneally infected with 5×10^5 BTs of *T. cruzi* Arequipa strain in 0.2 mL PBS, and gruoped in the acute and chronic phases as follows: 0, uninfected and untreated mice (negative control group); I, infected and untreated mice (positive control group); II, BZN-treated mice; III, Compound 4-treated mice; IV, Compound 7-treated mice.

BZN and compounds **4** and **7** were prepared at 2 mg/mL in an aqueous suspension vehicle containing 5% (v/v) DMSO and 0.5% (w/v)

hydroxypropyl methylcellulose.[38] Drugs were orally administered at a dose of 20 mg/kg per day (~200 μL) for five consecutive days, and vehicle only was administered in the negative and positive control groups. The treatment was initiated once the infection was confirmed (10th day post-infection (pi)) in mice treated in the acute phase, and once the chronic phase was established (75th day pi) in the mice treated in the chronic phase.

2.4.2. Parasitaemia levels in the acute phase treatment.

Peripheral bloods from mice treated in the acute phase were obtained from the mandibular vein and diluted 1:100 in PBS. The parasitaemia levels (number of BTs) were quantified every two or three days from the 7th day pi until the day parasitaemia was not detected. This counting was performed using a Neubauer chamber, and the number of BTs was expressed as parasites/mL.[27]

2.4.3. Cyclophosphamide-induced Immunosuppression.

After 100th dpi, established mice in the chronic phase, regardless of the treatment, were immunosuppressed with cyclophosphamide monohydrate (CP) (ISOPAC®) using the method previously described by Francisco et al.[38] Within 1 week after the last CP injection, parasitaemia reactivation rate was evaluated according the procedure described in 2.4.2. section.

2.4.4. Organs/tissues DNA extraction, polymerase chain reaction (PCR) and electrophoresis.

Our previous *in vivo* studies using the *T. cruzi* Arequipa strain revealed its tropism for the following organs/tissues: adipose tissue, bone marrow, brain, oesophagus, heart, lung, muscle, spleen and stomach. Therefore, after CP-induced IS, mice were bled out under gaseous anaesthesia (CO2) via heart puncture, blood was collected, and these 9 organs/tissues were harvested and flushed free of blood by infusion of pre-warmed PBS to avoid contamination with BTs.[39] In addition, spleens were weighed to evaluate its inflammation in the different groups of mice. Finally, the target organs/tissues were thawed and ground up as described by Martín-Escolano et al.[35]

PCR was performed based on the published sequence of the enzyme SOD *T. cruzi* CL Brenner (GenBank accession No. XM_808937) using two primers designed in our laboratory (GenBank accession number DQ441589) that allow the detection of *T. cruzi* DNA in different biological samples. These primers amplify a fragment belonging to SOD gene b of *T. cruzi* consisting of approximately 300 base pairs (bp). The amplifications were performed using a Thermal Cycler TM MyCycler thermal cycler (Bio-Rad) as described by Olmo et al.[40] Finally, the amplification products were subjected to electrophoresis on a 2% agarose gel for 90 min at 90 V, containing 1:10000 GelRed nucleic acid gel stain.

2.4.5. Enzyme-linked immunosorbent assay (ELISA).

Serum samples were obtained two days after treatment, one day before IS and on the day of necropsy for the mice treated in the acute phase, and two days after treatment and on the day of necropsy (sera post-IS) for the mice treated in the chronic phase.

SODe from *T. cruzi* Arequipa strain (extracted and purified as described in 2.5.3. section) was used as the antigen fraction. Circulating antibodies in serum against *T. cruzi* Arequipa strain were qualitatively and quantitatively evaluated in triplicate by ELISA as described by Olmo et al.[27]

2.4.6. Biochemical analysis.

Serum samples were obtained at two days after treatment and on the day of necropsy (sera post-IS) for mice treated in both phases. These sera were sent to the Scientific Instrumentation service at University of Granada to measure a series of parameters using commercial kits from Cromakit® with the BS-200 Chemistry Analyzer Shenzhen Mindray (Bio-medical Electronics Co., LTD). Means and standard deviations were calculated for different populations of sera (n = 6, n = 3), and the confidence interval for the mean normal populations were also calculated based on a confidence level of 95% (100 × (1-α) = 100 × (1–0.05)).

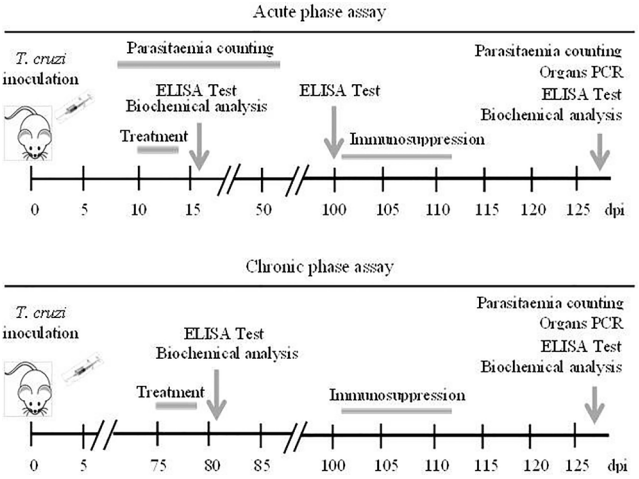

Figure 1. Timeline for all *in vivo* experiments in the acute and chronic phases. dpi = day pi.

The timeline for all *in vivo* experiments is shown in Figure 1.

2.5. Studies of the action mechanism.

2.5.1. Metabolite excretion.

T. cruzi Arequipa epimastigotes (5×10^5 mL^{-1}) in cell culture flasks were added of compounds **4** and **7** at IC_{25} concentrations and then maintained at 28 °C for 72 h.[41] Non-treated parasites (controls) were also included. The supernatants were then collected by centrifugation at 800 g for 10 min to determine the excreted metabolites by ^{1}H NMR using a VARIAN DIRECT DRIVE 400 MHz Bruker spectrometer with an AutoX probe using D2O as described by Fernández-Becerra et al.[42] The binning, normalisations and analyses were obtained using Mestrenova 9.0 software.

2.5.2. Rhodamine 123 (Rho) and acridine orange (AO) assays.

The treated *T. cruzi* Arequipa epimastigotes described in 2.5.1. section were centrifuged, washed 3 times with PBS, and then resuspended in 0.5 mL PBS at 10 μg/mL Rho or AO (Sigma-Aldrich) for 20 min.[43] Thereafter, the samples were prepared and the data were captured and analysed as previously described by Martín-Escolano et al.[35] The fluorescence intensity for Rho (mitochondrial membrane potential) and AO (nucleic acids) were measured as described Sandes et al.[43]

2.5.3. SOD inhibition studies.

Epimastigotes of *T. cruzi* Arequipa strain were grown as detailed in 2.3.1. section, collected by centrifugation and resuspended at 5×10^9 mL^{-1} in medium without FBS in cell culture flasks (surface area, 75 cm^2). After 28 h of incubation at 28 °C, the culture was centrifuged, the supernatant was treated following the procedure described by Martín-Escolano et al.,[35] the protein was precipitated using the method described by López-Céspedes et al.,[44] and the protein concentration was determined using the Bradford method (Sigma Immunochemical, St. Louis) with bovine serum albumin as a standard.[45] Finally, Fe-SODe and commercial CuZn-SOD from erythrocytes (Sigma-Aldrich) activities were determined using the method described by Beyer and Fridovich.[46]

2.6. Statistical analyses.

Data were recorded on an Excel spreadsheet (Microsoft), and

statistical analyses were performed by using SPSS software (v. 21, IBM). The *t*-test for paired samples was used to verify whether there were differences between the assays used, with p-0.05 considered statistically significant and with a 95% confidence level. Also statistical studies based on contingency tables (prevalence) were conducted, together with the × 2 test of the relationship between variables.

3. Results

3.1. In vitro biological activity.

The extracellular epimastigote form is the most frequently used owing to its simple culture in the laboratory. However, assays against the forms developed in mammalian hosts, BTs and intracellular amastigotes are more appropriate.[47] Therefore, the trypanocidal activities of compounds **1–12** and BZN were evaluated after 72 h of exposure with the aim of obtaining the IC_{50} values. Moreover, given that the squaryl group mimics the phosphate group in a number of bioisosteres of oligodeoxynucleotides [48] and amphiphilic lipids,[28] it is worth comparing their activities with that of MILT, a known antileishmanial agent. We have also compared the results with those obtained for squaramide **3**, a compound that belong to the series of lipophilic squaramides and whose anti-chagasic activity was previously reported by Olmo et al.[27] The data are shown in Table 1.

Simultaneously, the cytotoxicities of compounds **1–12**, BZN and MILT were tested using Vero cells with the objectives of determining their toxicities in mammalian cells (Table 1) and selectivity indexes (SI = IC_{50} Vero cells/IC_{50} extra- and intracellular forms), and comparing with BZN (Table 2). Interestingly, all the compounds were substantially less toxic than the reference drug BZN. The cytotoxicity IC_{50}/72 h values ranged from 159.8 to 2169.7 μM in contrast to BZN (23.2 μM), with SI values ten-fold higher than for most of them.

As summarised, compounds **4** and **7** showed low toxicity and a promising trypanocidal activity, independent of the parasite forms, and were chosen for further *in vivo* (murine model) and *in vitro* assays.

Finally, to obtain accurate information regarding the trypanocidal activity of the most active compounds, the *in vitro* infection in host Vero cells were measured by counting infected cells after 72 h of exposure at different concentrations. The data are shown in Figure 2, together with the data of amastigotes and trypomastigotes. It was found that the rates of infected cells gradually decreased in all cases. In particular, the effect of compound **7** should be highlighted, since it practically reduces the number of infected cells to 0 at a concentration of 50 μM and with an IC_{50}/72 h value of 5.6 μM.

Likewise, the average number of amastigotes per cell, shown in Figure 3, decreased for all tested compounds.

In summary, compound **7** showed a higher efficiency than BZN, acting like a fast acting drug: compound **7** not only inhibits the parasite multiplication (static), but also produces its death (cidal).[49] For compound **4**, it is observed that there was no reduction in the number of infected cells at a concentration equal to or less than 12 μM, which did occur for the total number of amastigotes. In view of the results, we can suggest that it is a slow killing drug, like the ergosterol biosynthesis inhibitors, such as posoconazole,[50] inhibiting the replication of the amastigote form but not killing the parasite. A decrease in the number of amastigotes and trypomastigotes was also observed for all compounds.

3.2. In vivo trypanocidal evaluation.

Compounds **4** and **7** were evaluated on BALB/c mice since these squarmides exhibited remarkable *in vitro* results against trypomastigotes and amastigotes, with IC_{50} and SI values close to the criteria established by Nwaka et al.[51]

As mentioned above, and because of the different effectiveness of current drugs in the treatment against CD, especially during the chronic phase (it is not as effective as it should be),[52] the effect of these squaramides was tested by treating mice in each phase. Drugs were administered orally since oral therapy leads to better patient compliance, it has a low cost (critical aspects of human treatment in developing countries)[53] and it is the preferred route for the treatment of parasitic diseases.

First, Figure 4 shows the parasitaemia in the different groups of mice untreated and treated in the acute phase. Little differences were observed in the mice treated with compound **4**. A significant reduction of parasitaemia in compound **7**-treated mice was observed, even exhibiting higher *in vivo* trypanocidal activity than BZN.

The activity of compound **7** was manifest from the beginning of the treatment, and it was extended until the end of the acute phase. The parasitaemia was undetected 10 and 7 days before (40th day pi) with respect to the control mice and mice treated with BZN, respectively. The same activity at the beginning of treatment was observed for compound **4**, but an increase in the parasitaemia was observed after treatment, perhaps due to rapid metabolism, which would require long-term treatment that can be achieved as a result of its low toxicity (as mentioned below). Alternatively, the peak of parasitaemia (23rd day pi) in mice treated with compound **7** caused a reduction of ~ 80%, with this reduction also being higher than BZN (70%).

Table 1
In vitro activity and toxicity for compounds on extra- and intracellular forms of *T. cruzi* strains.

Compound	Activity IC_{50} (μM)[a] *T. cruzi* Arequipa strain			Activity IC_{50} (μM)[a] *T. cruzi* SN3 strain			Activity IC_{50} (μM)[a] *T. cruzi* Tulahuen strain			Toxicity IC_{50}/72 h (μM) Vero cell
	E/72 h	A/72 h	T/24 h	E/72 h	A/72 h	T/24 h	E/72 h	A/72 h	T/24 h	
BZN	16.9 ± 1.8	8.3 ± 0.7	12.4 ± 1.1	36.2 ± 2.4	16.6 ± 1.4	36.1 ± 3.1	19.7 ± 1.7	10.0 ± 0.8	15.1 ± 1.3	23.2 ± 2.1
MILT	20.8 ± 1.8	29.6 ± 2.1	18.8 ± 1.4	55.9 ± 4.5	39.7 ± 2.9	34.8 ± 2.7	22.9 ± 1.8	31.8 ± 3.0	20.1 ± 2.3	21.6 ± 1.8
1	42.3 ± 3.8	39.6 ± 3.0	33.2 ± 2.7	33.7 ± 2.1	62.6 ± 5.8	30.2 ± 2.7	42.6 ± 3.4	51.3 ± 4.6	33.6 ± 3.8	1069.6 ± 84.3
2	41.3 ± 4.0	27.8 ± 2.5	29.1 ± 2.1	41.0 ± 3.8	54.5 ± 4.8	28.0 ± 2.1	27.8 ± 2.1	31.6 ± 2.9	26.6 ± 1.9	899.5 ± 59.4
3	12.4 ± 1.1	14.7 ± 1.2	10.4 ± 0.8	15.2 ± 1.1	13.1 ± 1.5	7.5 ± 0.7	9.1 ± 0.7	11.7 ± 1.4	8.9 ± 1.0	439.2 ± 31.0
4	20.3 ± 1.6	17.3 ± 1.2	6.5 ± 0.6	14.3 ± 1.0	50.0 ± 4.5	15.8 ± 1.3	14.7 ± 1.1	38.3 ± 3.1	17.2 ± 1.3	899.6 ± 74.6
5	101.6 ± 15.3	nd	nd	87.8 ± 7.8	nd	nd	82.0 ± 9.0	nd	nd	1148.9 ± 121.3
6	64.6 ± 4.8	nd	nd	37.5 ± 2.9	nd	nd	49.5 ± 5.2	nd	nd	127.9 ± 15.8
7	7.3 ± 0.9	0.2 ± 0.0	4.4 ± 0.3	16.0 ± 1.2	18.9 ± 1.4	5.4 ± 0.4	9.5 ± 0.8	6.4 ± 0.5	4.7 ± 0.3	678.7 ± 49.7
8	36.2 ± 2.4	nd	nd	19.4 ± 1.5	28.4 ± 2.1	24.1 ± 1.9	14.6 ± 1.0	25.5 ± 1.6	19.1 ± 1.4	291.0 ± 31.5
9	63.3 ± 8.4	nd	nd	74.5 ± 6.8	nd	nd	89.1 ± 7.1	nd	nd	352.7 ± 45.9
10	22.1 ± 1.5	nd	nd	33.1 ± 2.4	nd	nd	66.1 ± 5.9	nd	nd	159.8 ± 12.5
11	107.0 ± 11.5	nd	nd	403.5 ± 31.8	nd	nd	359.7 ± 38.5	nd	nd	1137.3 ± 109.7
12	177.2 ± 12.8	nd	nd	310.8 ± 34.2	nd	nd	241.2 ± 21.2	nd	nd	2169.7 ± 174.8

[a] IC_{50} = the concentration required to give 50% inhibition, calculated using GraphPad Prism 6. Results are averages of three separate determinations ± standard deviation. nd, not determined. E, epimastigote forms. A, amastigote forms. T, trypomastigote forms.

Table 2
Selectivity indexes for compounds on extra- and intracellular forms of *T. cruzi* strains.

Comp.	Selectivity index[a] *T. cruzi* Arequipa strain			Selectivity index[a] *T. cruzi* SN3 strain			Selectivity index[a] *T. cruzi* Tulahuen strain		
	Epim. forms	Amast. forms	Trypom. forms	Epim. forms	Amast. forms	Trypom. forms	Epim. Forms	Amast. Forms	Trypom. forms
BZN	1.4	2.8	1.9	0.6	1.4	0.6	1.2	2.3	1.5
MILT	1.0	0.7	1.2	0.4	0.5	0.6	0.9	0.7	1.1
1	25.3 (18)	27.0 (10)	32.2 (17)	31.8 (53)	17.1 (12)	35.4 (59)	25.1 (21)	20.8 (9)	31.8 (21)
2	21.8 (16)	32.3 (11)	30.9 (16)	22.0 (37)	16.5 (12)	32.1 (54)	32.4 (27)	28.5 (12)	33.8 (23)
3	35.4 (25)	29.9 (11)	42.2 (22)	28.9 (48)	33.5 (24)	58.6 (98)	48.3 (40)	37.5 (16)	49.3 (33)
4	44.3 (32)	52.1 (19)	138.6 (73)	63.0 (1 0 5)	18.0 (13)	57.0 (95)	61.3 (51)	23.5 (10)	52.2 (35)
5	11.4 (8)	nd	nd	13.2 (22)	nd	nd	14.2 (12)	nd	nd
6	2.0 (1)	nd	nd	3.4 (6)	nd	nd	2.6 (2)	nd	nd
7	93.1 (67)	3085.1 (1102)	153.9 (81)	42.5 (71)	35.9 (26)	126.4 (2 1 1)	71.1 (59)	106.5 (46)	143.8 (96)
8	8.0 (6)	nd	nd	15.0 (25)	10.3 (7)	12.1 (20)	19.9 (8)	11.4 (5)	15.3 (10)
9	5.6 (4)	nd	nd	4.7 (8)	nd	nd	4.0 (3)	nd	nd
10	7.2 (5)	nd	nd	4.8 (8)	nd	nd	2.4 (2)	nd	nd
11	10.6 (8)	nd	nd	2.8 (5)	nd	nd	3.2 (3)	nd	nd
12	12.2 (9)	nd	nd	7.0 (12)	nd	nd	9.0 (8)	nd	nd

[a] Selectivity index (SI) = IC50 Vero cells//IC50 extracellular and intracellular form of parasite. In brackets: number of times that compound excedes the reference drug SI (on extracellular and intracellular forms of *T. cruzi*). nd, not determined.

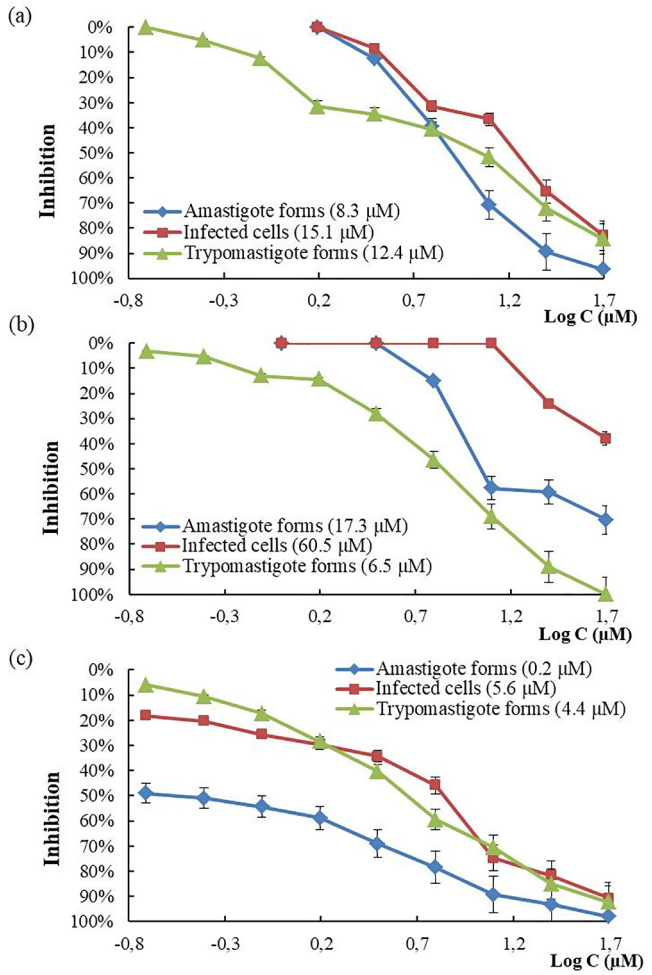

Figure 2. Infection of *T. cruzi* Arequipa strain regarding the decrease of amastigote and trypomastigote forms and infected cells treated with (a) BZN, (b) **4** and (c) **7**. Values are the means of three separate experiments ± standard deviation. In brackets: IC_{50} value, calculated using GraphPad Prism 6.

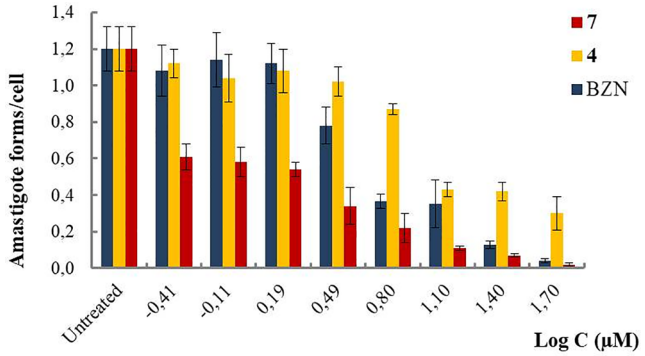

Figure 3. Number of amastigote forms of *Trypanosoma cruzi* Arequipa strain per Vero cell treated with BZN, **4** and **7**. Values are the means of the three separate determinations ± standard deviation. Significant differences between the parasites treated with BZN, **4** and **7** for α = 0.05.

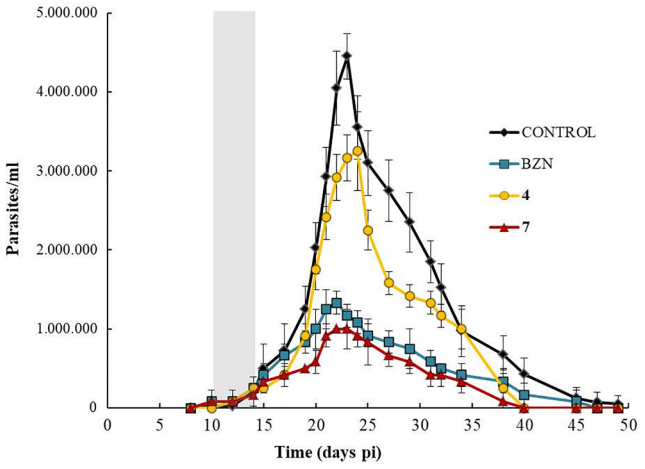

Figure 4. Parasitaemia of acute CD for mice untreated (control) and treated with BZN, **4** and **7**. Compounds were orally administered using 100 mg/kg of body mass. Treatment days are represented in grey. Values constitute means of three mice ± standard deviation. Significant differences between the control group and groups treated with BZN, **4** and **7**.

Second, mice were immunosuppressed using CP with the objective of reactivating the parasitaemia under the control of the immunological system and evaluating the effectiveness of the treatment, the survival rate of the parasites and the disease extent in the chronic phase. To do this, the parasitaemia reactivation was ascertained after IS until the 120th day pi (late chronic phase, when the amastigotes are nested inside target organs). This is an important matter because apparently

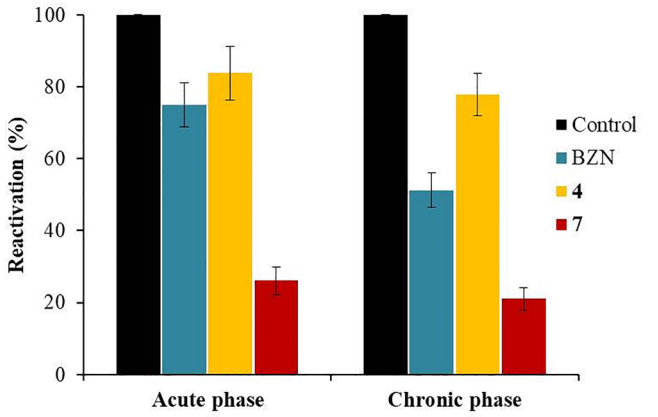

Figure 5. Reactivation of parasitaemia after the immunosuppression cycles by fresh blood for mice untreated (control) and treated with BZN, **4** and **7**. Values constitute means of three mice ± standard deviation. Significant differences between the control group and groups treated with BZN, **4** and **7** for $\alpha = 0.05$.

cured immunocompromised individuals and cured patients submitted to transplantation (diagnosed with AIDS or treated with anticancer chemotherapy) present clinically aggressive parasitaemia reactivation. Therefore, IS is carried out as a first cure confirmation technique, with the second being PCR of the organs/tissues, as mentioned below. The mice infected and treated with parasitaemia that does not reappear and negative PCR results for organs/tissues after IS are considered cured.[54] The percentages of parasitaemia reactivation compared to untreated (control) mice are shown in Figure 5. A reduction in the parasitaemia reactivation was observed in both phases for all treated mice. The reactivation was lower for the compound 7-treated mice (26% and 21% for those treated in the acute and chronic phases, respectively) than for mice treated with BZN (75% and 51%, respectively). A significant decrease in parasitaemia was presumed in compound **7**-treated mice during the acute phase because of the observed parasitaemia levels (as mentioned above), but even a lower reactivation was observed for compound **7**-treated mice in the chronic phase (as discussed below, the presence of parasites was negative for most of the analysed organs/tissues). In contrast, higher percentages were obtained for compound **4**-treated mice.

Finally, the presence of parasites in the target organs/tissues was determined by PCR (127th day pi) to assess the curative effect of these squaramides as a second technique of confirmation of cure. Figure 6 shows the PCR results for the target organs/tissues in the different groups of mice, including mice treated in the acute and chronic phases. The PCR of the untreated (control) groups was positive for these nine organs and tissues (defined as target organs/tissues): adipose, bone marrow, brain, oesophagus, heart, lung, muscle, spleen and stomach. Percentages of 33% and 55% of parasite-free organs/tissues were observed for BZN-treated mice in the acute and chronic phases, respectively. A lower percentage was observed for compound **4**-treated mice, but the *in vivo* trypanocidal activity for compound **7** is noteworthy, with 67% and 78% of parasite-free organs/tissues for the acute and chronic phases, respectively.

For the purpose of assessing the immune status of the mice during infection, IgG levels were measured by ELISA using the isolated Fe-SOD enzyme such as antigen.[55] The detection of total IgG verifies the level of protection (effectiveness) ascribed to the tested squaramides since the titre of immunoglobulins is linked with the parasite load and reflects the infection rates.[56] Figure 7 shows the titre of anti-*T. cruzi* IgG. The IgG levels decreased for all treated mice and all analysed samples except for those of day 81 pi in the chronic phase, which is logical since its samples from mice have previously suffered an untreated acute phase. Non-significant differences were observed in compound **4**-treated mice with respect to the untreated mice. A significant reduction in the IgG levels occurred for mice treated with compound **7**, principally due to the high *in vivo* trypanocidal activity that this squaramide presents, as demonstrated with parasitaemia and organ PCR assays. Despite the parasitaemia reactivation, no increase in the IgG levels after IS was observed, which is logical due to the IS itself suffered by these mice. Therefore, these are not data that indicate levels of infection, but that help us to verify that immunosuppression has been suffered by the mice.

Another aspect linked with the parasite load is splenomegaly, since the spleen is an organ involved in the fight against infections. Therefore, Figure 8 shows the weight percentage of spleens from different groups of mice. Splenomegaly occurs in experimentally infected mice, whose spleens are approximately twice the mass of those from uninfected mice [57] (as the figure shows). Moreover, treatment with BZN significantly reduces infection-induced splenomegaly, even in treatment with subcurative doses, since it is linked with a reduction in parasite load [57] (as the figure also shows). Regarding the tested compounds, the mice treated with compounds **4** and **7** exhibited a lower weight percentage in both phases with respect to the untreated mice. This means that both squaramides reduced splenomegaly and, therefore, infection rates (as noted above). Compound **7**-treated mice showed lower splenomegaly, with reductions of splenomegaly of 66% and 55% in the acute and chronic phases, respectively, compared with untreated mice. The higherst splenomegalies observed in the mice treated in the chronic phase are not due to lower activities in this phase; it is just that an acute phase without treatment was suffered by these mice.

The splenomegaly studies are in agreement with the studies shown above in terms of the parasitaemia in the acute phase, the reactivation of parasitaemia after IS, the presence or absence of parasites in target organs/tissues and the ELISA test. All these studies showed that the compound **7**-treated mice exhibited the greatest reduction in parasitaemia, indicating that compound **7** exhibits a high *in vivo* trypanocidal activity. As stated above, in order to reach a total cure and thanks to the low toxicity at the dose tested (shown in Table 3), the *in vivo* activity of compound **7** can be studied at higher doses. Furthermore, a modification in the structure of the compound and in the schedule of treatment for a better exposure of the compound in the bloodstream and adipose tissue can be carried out.

In order to prove the metabolic disturbances associated with the treatment, biochemical measurements were performed, as discussed in 2.4.6. section. Table 3 shows the biochemical clinical parameters obtained in untreated and treated mice in both phases, including values for uninfected and untreated mice. For the mice treated with the squaramides, almost all the biochemical parameters were not altered after compound administration, and those alterations returned to normal levels in the samples obtained on the day of necropsy of the mice. Therefore, the tested compounds showed less toxicity than BZN. This lack of toxicity added to the high activity of compound **7** led us to consider this compound as a promising candidate to treat CD.

3.3. Studies of the mechanism of action.

3.3.1. Metabolite excretion.

The ^{1}H NMR spectra of the medium of treated *T. cruzi* Arequipa epimastigotes were qualitatively and quantitatively registered in order to obtain information regarding the effects of compounds **4** and **7**, at IC_{25} concentrations, on the glucose metabolism. The final excretions were analysed and compared with those found for the untreated (control) *T. cruzi* epimastigotes. Figure 9 shows the results obtained in comparison with respect to this control. The excretion of all metabolites was disturbed in both treatments. An increase in the excretion of glycerol and succinate metabolites and a decrease in the rest of the metabolites were observed for compound **4**-treated parasites. Alternatively, all metabolites increased for the parasites treated with compound **7**.

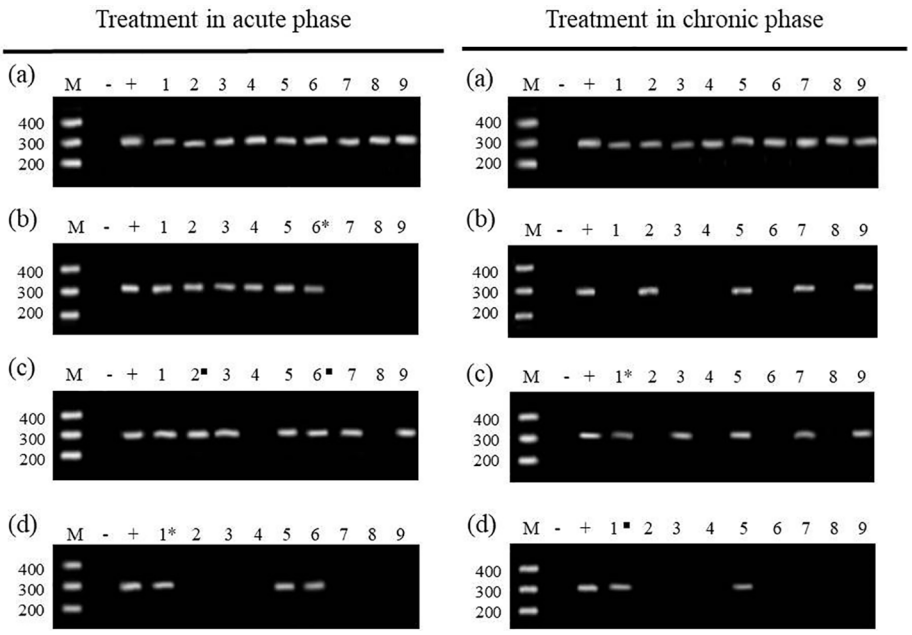

Figure 6. PCR analysis of nine organs/tissues with the *T. cruzi* SOD gene primers at the final day of experiment in mice treated with 100 mg/kg body mass. (a) Untreated (control) mice group, (b) Group of mice treated with BZN, (c) Group of mice treated with **4**, (d) Group of mice treated with **7**. Lanes: M, base pair marker; -, PCR negative control; +, PCR positive control; 1–9, organs/tissues PCR: 1, adipose; 2, bone marrow; 3, brain; 4, oesophagus; 5, heart; 6, lung; 7, muscle; 8, spleen; 9, stomach. *, 1/3 of the corresponding organ/tissue PCR products showed 300 bp band on electrophoresis; ■, 2/3 of the corresponding organ/tissue PCR products showed 300 bp band on electrophoresis; no *■, 3/3 or 0/3 of the corresponding organ/tissue PCR products showed 300 bp band on electrophoresis.

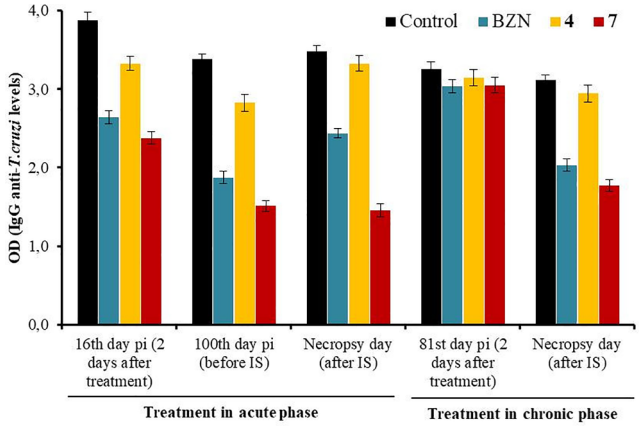

Figure 7. IgG levels of anti-*T. cruzi* antibodies, expressed in absorbance units (optical densities (OD) at 490 nm), for mice untreated (control) and treated at different days post-infection (pi). Values constitute means of three mice ± standard deviation. IS, immunosuppression. Significant differences between the control group and groups treated with BZN and **7** for $\alpha = 0.05$. Non-significat differences between the control group and group treated with **4**. IS, immunosuppression.

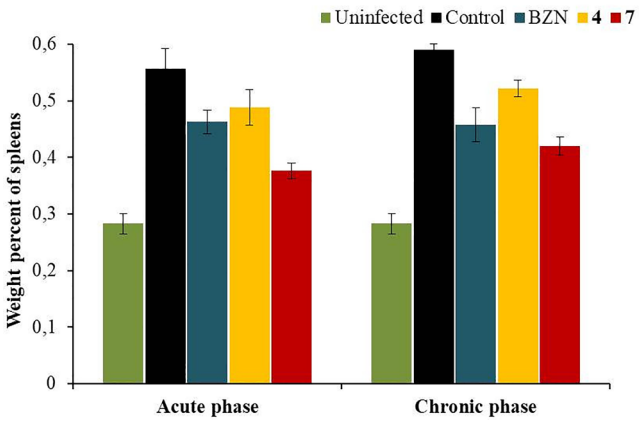

Figure 8. Weight percentage of spleens for different groups of mice at the final day of experiment. Values constitute means of three mice ± standard deviation. Significant differences between the uninfected group, control group and groups treated with BZN, **4** and **7** for $\alpha = 0.05$.

3.3.2. *Mitochondrial membrane potential and on DNA and RNA levels.*

In order to evaluate and relate the effect of compounds **4** and **7** with the previous *in vitro* trypanocidal activity on the mitochondrial membrane potential and on the DNA and RNA levels, the fluorescence intensity of Rho 123 and AO, respectively, was quantified by cytometry flow. Figure 10 shows the flow cytometry analysis of the mitochondrial membrane potential. It is well-known that BZN kills through its transformation to highly reactive metabolites after reduction by type I nitroreductase activity,[58] causing, among others, respiratory chain inhibition. Thus, we observed a decrease in the mitochondrial membrane potential when treating *T. cruzi* with BZN. The compound **4**-treated parasites showed no depolarisation in the mitochondrial membrane, suggesting that the trypanocidal activity is due to its glycosomal effect, as discussed in 4.2. section. The parasites treated with compound **7**, in contrast, showed a depolarisation of 80.6% in the mitochondrial membrane potential.

The fluorescence intensities of AO, shown in Figure 11, were registered in order to determine whether the compounds also produced a reduction in DNA and RNA levels. BZN-treated parasites showed a decrease of AO fluorescence, with a value of 22.4%. Higher reductions were observed for the parasites treated with compounds **4** and **7** (31.1% and 49.1%, respectively).

3.3.3. *Inhibition of the T. Cruzi Fe-SOD enzyme.*

Fe-SODe and CuZn-SOD inhibitions were determined using the method described by Beyer and Fridovich.[46] Figure 12 shows the inhibition data by compounds **4** and **7**, with the corresponding calculated IC_{50}, for Fe-SOD from *T. cruzi* and Cu/Zn-SOD from human erythrocytes. Higher inhibitions were observed on the Fe-SOD of the parasite for both compounds: the IC_{50} values were 25 μM for compound **4** and 70 μM for compound **7**.

4. Discussion

4.1. *Trypanocidal activity*

The genetic diversity of *T. cruzi* is extensively known and divided into seven DTUs, with different evolutionary relationships, epidemiological and ecological associations, tropism, pathogenesis, genotype,

Table 3
Biochemical clinical parameters measured at different experimental situations in groups of BALB/c mice infected with *T. cruzi*.

		Kidney marker profile		Heart marker profile		Liver marker profile			
		Urea (mg/dL)	Uric acid (mg/dL)	CK-MB[a] (U/L)	LDH[b] (U/L)	AST/GOT[c] (U/L)	ALT/GPT[d] (U/L)	Total bilirubin (mg/dL)	Alkaline phosphatase (U/L)
Uninfected mice (n = 6)		35 [32–40]	4.5 [4.0 –5.1]	372 [150–630]	3180 [2505–3851]	153 [132–177]	55 [46–62]	0.28 [0.22 –0.31]	169 [141–192]
Treatment in acute phase	16th day pi (Control) (n = 3)	31	4.3	535	3275	167	60	0.23	180
	16th day pi and BZN (2 days after treatment) (n = 3)	—	——	=	=	++++	++++	++	++
	16th day pi and 4 (2 days after treatment) (n = 3)	–	——	=	=	+++	=	=	+
	16th day pi and 7 (2 days after treatment) (n = 3)	–	——	=	=	+	=	=	=
	Necropsy day of mice (Control) (n = 3)	34	4.0	496	2761	179	49	0.21	161
	Necropsy day of mice and BZN (n = 3)	—	=	=	=	++++	=	+	=
	Necropsy day of mice and 4 (n = 3)	–	–	=	=	++	=	=	=
	Necropsy day of mice and 7 (n = 3)	–	=	=	=	=	=	=	=
Treatment in chronic phase	81th day pi (Control) (n = 3)	45	5.7	751	5951	260	57	0.25	167
	81th day pi and BZN (2 days after treatment) (n = 3)	—	——	–	—	++	++	+++	++++
	81th day pi and 4 (2 days after treatment) (n = 3)	–	–	=	=	+	++	+	=
	81th day pi and 7 (2 days after treatment) (n = 3)	–	—	=	=	+	++	++	+
	Necropsy day of mice (Control) (n = 3)	37	4.8	538	6679	286	64	0.20	149
	Necropsy day of mice and BZN (n = 3)	—	–	=	–	+	=	++	++
	Necropsy day of mice and 4 (n = 3)	–	–	=	=	=	=	=	=
	Necropsy day of mice and 7 (n = 3)	–	=	=	=	=	=	+	=

Key: =, variation ≤ 10%; +, 10–20% increase over the range; ++, 20–30% increase over the range; +++, 30–40% increase over the range; ++++, >40% increase over the range; −, 10–20% decrease over the range; − −, 20–30% decrease over the range; − − −, 30–40% decrease over the range; − − − −, >40% decrease over the range.

[a] CK-MB, creatine kinase-muscle/brain. [b]LDH, lactate dehydrogenase. [c]AST/GOT, aspartate aminotransferase. [d]ALT/GPT, alanine aminotransferase. pi = post-infection.

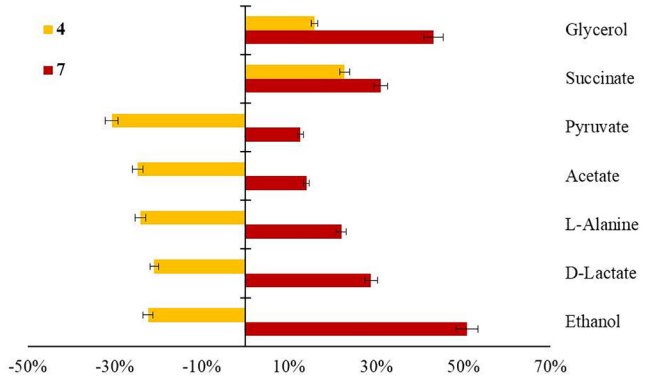

Figure 9. Variation (%) among catabolites excreted by epimastigotes of *T. cruzi* Arequipa strain treated with **4** and **7** at IC_{25} concentrations in comparison to untreated (control) parasites incubated 72 h. Each drug was tested in three separate determinations ± standard deviation. Significant differences between the control, **4** and **7** for $\alpha = 0.05$.

phenotype, and drug resistance.[59] Accordingly, three different DTUs (I, V and VI), from different location, host and tropism, were used in order to determine and select those compounds with a good performance.

According to some authors, potential anti-chagasic agents have to meet certain criteria: $IC_{50} \leq 10\,\mu M$, and SI greater than 10,[60] $IC_{50} \leq 1\,\mu g/ml$, and SI greater than 50.[51] Therefore, the trypanocidal activities were evaluated in the epimastigote forms, and the potential compounds were then tested against the forms developed in vertebrate hosts (amastigotes and trypomastigotes) (Table 1). Compounds **1**, **2**, **3**, **4** and **7** were selected to test against these forms in vertebrate hosts due to their high SI values in epimastigote forms, with SI values at least 18 times higher than BZN (Table 2). Compounds **4** and **7** were selected for the subsequent *in vivo* tests because of the IC_{50} values obtained against the amastigote and trypomastigote forms, which met IC_{50} and SI requirements in parasite forms in the vertebrate host. In general, it was found that these compounds were more active against the trypomastigote forms of *T. cruzi*, reaching an effectiveness between 35 and 211 times higher than the one corresponding to BZN. The *in vitro* activity of compound **7** should be highlighted, with IC_{50} values lower than 6.5 µM for all parasite forms and strains of *T. cruzi*.

Moreover, Figure 3 shows us that compound **7** acts like a fast acting drug since it not only inhibits the parasite multiplication (static), but also produces its death (cidal). For compound **4**, it is observed that there was no reduction in the number of infected cells at a concentration equal to or less than 12 µM, which did occur for the total number of amastigotes. In view of the results, we can suggest that it is a slow killing drug, like the ergosterol biosynthesis inhibitors, such as posoconazole, inhibiting the replication of the amastigote form but not killing the parasite.

Regarding the *in vivo* tests, these were performed for the evaluation of: I) Parasitaemia as an indicator of the effectiveness of treatment during the acute phase; II) Parasitaemia reactivation in the chronic phase after IS as an indicator of the effectiveness of treatment in both phases; III) Parasites in organs in the chronic phase after IS as an indicator of the effectiveness of treatment in both phases; IV) Levels of immunoglobulin G (IgG) and the splenomegaly as indicators of immune response in both phases; V) Serum biochemical parameters as an indicator of metabolic disturbances associated with the treatment.

The treatment for compounds **4** and **7** and the reference drug BZN was performed at subcurative doses for BZN (20 mg/kg per day for five days) in order to evaluate whether the compounds under study showed higher *in vivo* effectiveness than the previous one. It should be noted that none of the mice treated died, lose more than 10% their body mass or presented altered biochemical parameters (Table 3). Therefore, these compounds can be tested at higher doses, establishing a new treatment guideline based on pharmacokinetic studies, with the aim of achieving

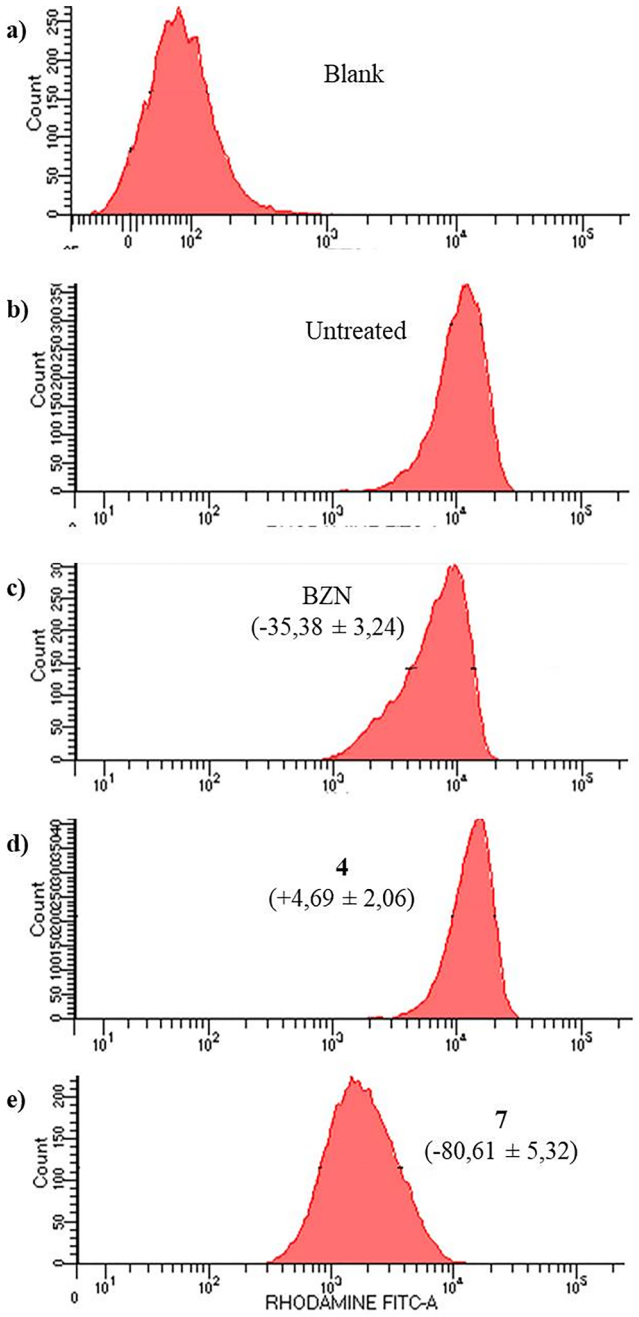

Figure 10. Mitochondrial membrane potential from epimastigotes of *T. cruzi* Arequipa strain treated with BZN and **4** and **7** at IC_{25} concentrations incubated 72 h: (a) blank, (b) untreated (control), (c) BZN, (d) **4** and (e) **7**. In brackets: variation ± standard deviation, in percentage, on mitochondrial membrane potential with respect to untreated parasites. Significant differences between the control, BZN and **7** for $\alpha = 0.05$. Non-significant differences between the control and compound **4**. Each drug was tested in three separate determinations.

a total cure. It is noteworthy that compound **7** meets the majority of the *in vivo* criteria of the target product profile (TPP).[49] It is proposed that the different effectiveness in both phases is associated to inadequate pharmacokinetics between the compounds and the location of the amastigotes in the tissues during the chronic phase.[61] Moreover, the reason of the presence of parasites observed in adipose tissue in both treatments for compound **7** (Figure 6) could be the differential drug accessibility, due to the peculiarity of this tissue, or the higher parasite load (reservoir sites).[62]

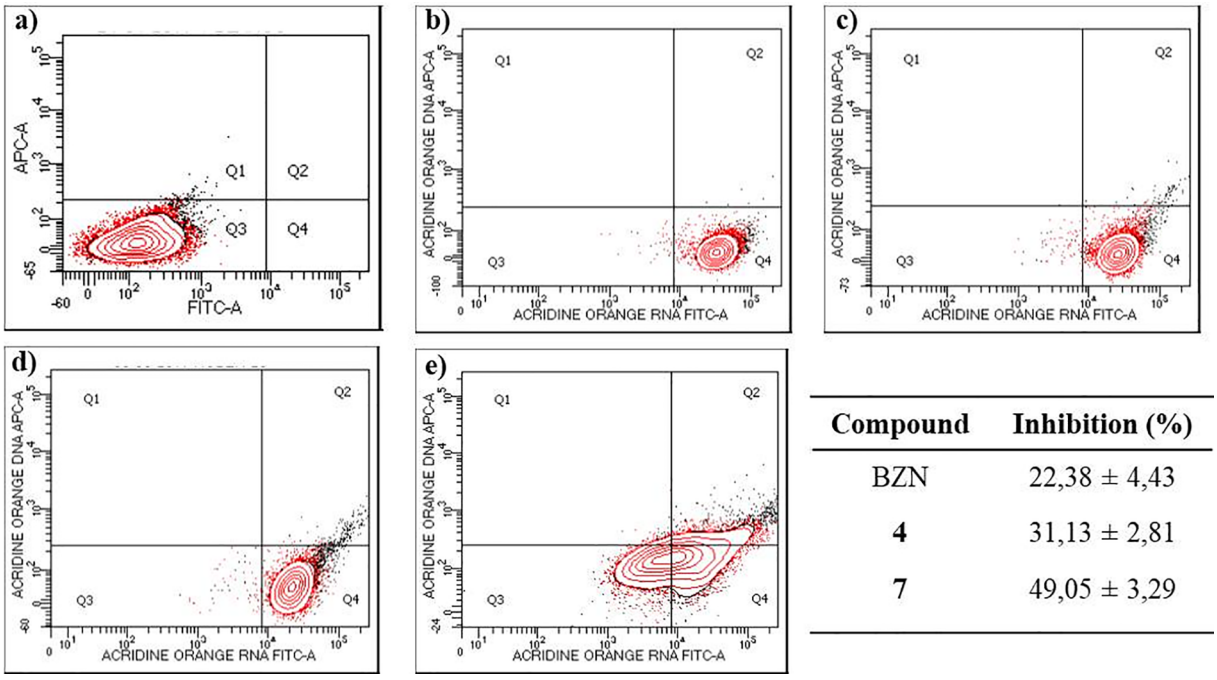

Compound	Inhibition (%)
BZN	22,38 ± 4,43
4	31,13 ± 2,81
7	49,05 ± 3,29

Figure 11. DNA and RNA levels of epimastigotes of *T. cruzi* Arequipa strain treated with BZN and **4** and **7** at IC_{25} concentrations incubated 72 h: (a) blank, (b) untreated (control), (c) BZN, (d) **4** and (e) **7**. Significant differences between the control, BZN, **4** and **7** for $\alpha = 0.05$. Each drug was tested in three separate determinations ± standard deviation.

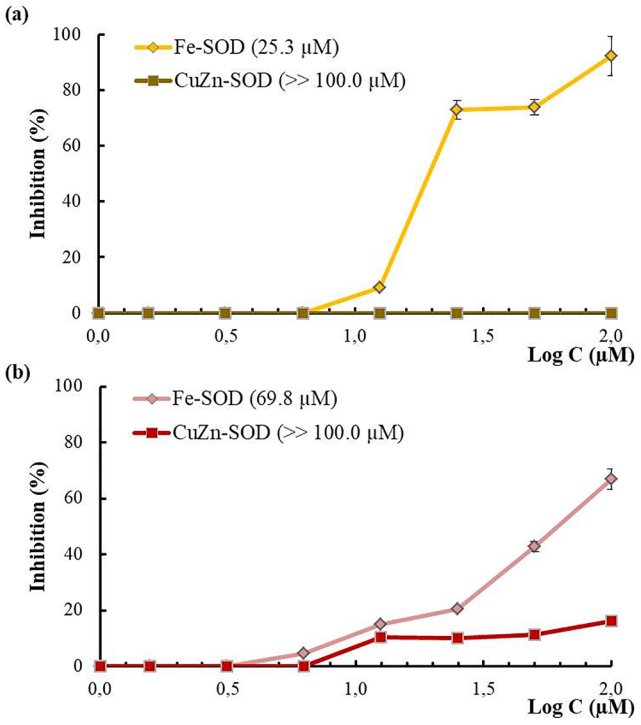

Figure 12. Inhibition *in vitro* (%) of Fe-SOD from epimastigotes of *T. cruzi* Arequipa strain (activity 42.0 ± 3.8 U/mg) and of CuZn-SOD from human erythrocytes (activity 47.3 ± 4.1 U/mg) for (a) **4** and (b) **7**. In brackets: IC_{50} value, calculated by linear regression analysis. Activity differences in the control vs. the sample incubated using compounds were identified by the Newman-Keuls test. Values are the average of three separate rate determinations ± standard deviation.

It should be noted that the assessment of clinical cure in *T. cruzi* infections is questionable due to the lack of a reliable test to assure the complete parasite elimination.[63] The main utility of the PCR technique is to verify the failure of clinical cure because even consistently negative results in blood (where the PCR is able to detect a single parasite in 5 mL) are not enough to secure the whole removal of tissue parasites.[7,64] Regarding experimental cure in animal models, IS is the formula employed to demonstrate cure.[38] We evaluate the establishment of cure, as mentioned in 3.2. section, using a double confirmation based on the IS and the PCR of the target organs. Therefore, we assess the presence (or not) of parasites in both blood and tissue. Currently, bioluminescence imaging model techniques are used to demonstrate cure, producing data with superior accuracy to other methods, including PCR.[57] However, we can state evidence of curation (or, at least, a considerable reduction in the parasitic load) found on the results of three independent samples using the double confirmation of cure.

4.2. Action mechanism.

It is well-known that *T. cruzi* catabolizes glucose at a high rate, acidifying the medium owing to incomplete oxidation to acids.[65,66] The final products in this catabolism are mainly pyruvate, acetate, succinate, L-alanine, D-lactate and ethanol.[67] Consistently, the ^1H NMR spectra were registered in order to obtain information regarding the effects of the compounds on the glucose metabolism. Regarding the data obtained for compound **4**, we suggest an inhibition in some of the glycolytic pathway enzymes involved in the catabolism of phosphoenolpyruvate (PEP) to pyruvate, such as cytosolic pyruvate kinase (PK) or pyruvate phosphate dikinase (PPDK) of the glycosome. This would cause an accumulation of PEP, both at the cytosolic and glycosomal levels, and a reduction of pyruvate, which would reduce its excretion, as observed in Figure 9, with a reduction in excretion of 30%. This deficit of pyruvate would obviously cause a deficit of catabolites in catabolic pathways that require pyruvate (such as ethanol), and metabolites that require pyruvate for synthesis (such as lactate and alanine).[68] These disturbances were also observed, with reductions close to that observed for pyruvate. In addition, this would involve an energy deficit, so the parasite would accelerate other ways to compensate for this deficit. One of them could be the glycolytic pathway with glycerol as a final product, generating high levels of glycerol in the cell and

excreting it to the outside; a disturbance that was also observed. The fact that there was a blockade in the pyruvate pathway would also make it easier for the entire carbon skeleton of glucose to go to this pathway. Another route that the parasite could use to obtain energy is the anaplerotic route that supplies malate to the tricarboxylic acid (TCA) cycle, whose final product is succinate, and an increase in the excretion of this metabolite was also observed.

For compound **7**, it is interesting to note that an increase in succinate metabolite indicates catabolic changes that could be related to a mitochondrial dysfunction.[69] Moreover, the highest alterations were shown by the metabolites glycerol and ethanol (with increases of 43% and 51%, respectively), which are the final products of catabolic routes (glycosomal for glycerol and citoplasmatic for ethanol) that the parasite can use in energy deficient conditions.[66] These results suggest that an alteration at the mitochondrial level may be the ultimate reason for the alterations observed in the excreted products of *T. cruzi*. Therefore, mitochondrial studies were conducted.

It is well-known that mitochondria play an imperative role in cell death decisions, and disturbances in the electrochemical gradients lead to a decrease in ATP production and a reduction in DNA and RNA levels, causing apoptosis and/or necrosis.[70,71] Therefore, the alteration in the metabolite excretion could be the result of this membrane depolarisation, which produces an accumulation of succinate, pyruvate and malate, causing a blockade of the glycolytic pathway. Thus, energy is obtained through other catabolic routes, with glycerol and ethanol as the final products that are excreted. In addition, the mitochondrial membrane potential reduction produces an imbalance in the NADH/NAD^+ and ATP/ADP ratios,[66] which may compromise the DNA and RNA levels. The ATP deficit produced by the mitochondrial depolarisation in compound **7**-treated parasites could involve a considerable reduction in the cellular levels of DNA and RNA. It must be noted that the decrease in nucleic acids levels is also due to random nucleic acids degradation as commonly attributed feature to cell necrosis, and not only because of ATP deficit.[72]

In summary, we suggest that compound **7** induces *T. cruzi* cell death via necrosis in a mitochondrion-dependent manner. Lastly, enzyme inhibition studies of the mitochondrion-resident Fe-SOD, as a key enzyme in the defence of these parasites, were performed with the aim of evaluating whether death in a mitochondrion-dependent manner is ultimately due to the redox stress produced by inhibition of this enzyme.[69]

Enzymes are one of the most interesting therapeutic targets, and the trypanosomatid exclusive Fe-SOD presents structural and biochemical differences with respect to other homologue eukaryote enzimes, including the human Cu/Zn-SOD.[73,74] This enzyme has been given special importance because it plays the crucial role of eliminating reactive oxygen species (ROS), allowing trypanosomatids to protect themselves from the damage produced by oxidative stress.[75,76] Trypanosomatids have other alternative mechanism to avoid oxidative damage, such as trypanothione and glutathione. The IC_{50} values obtained (Figure 12) are too high to ascribe the trypanocidal effect on the inhibition of Fe-SOD of the parasite, even the inhibition produced by compound **4** does not cause a mitochondrial dysfunction. For compound **7**, the mitochondrial dysfunction cannot be attributed to the enzymatic inhibition of Fe-SOD and, in order to know the final cause of the mitochondrial dysfunction caused by this compound, inhibition studies will be carried out on tripanotione reductase and at the level of the electron transport chain, since these are possible targets.

Lastly, it should be noted that compound **7** is a long-chain squaramide and bioisostere of MILT, so the mechanism of action could be similar as an inhibitor of lipid biosynthesis of the parasite. MILT acts as an inhibitor at the level of phosphatidylethanolamine *N*-methyltransferase, inhibiting the biosynthesis of phosphatidylcholine in *T. cruzi* [77] with 10 to 20 times more potency compared to that of mammalian cells.[78] Others reports demonstrate that MILT inhibits the mitochondrial cytochrome *c* oxidase of *L. donovani* causing decreases in the oxygen consumption rate and ATP levels,[79] in addition to producing an apoptosis-like death,[80] which may be related to the mitochondrial dysfunction observed in *T. cruzi* for compound **7**.

5. Conclusions

In summary, we identified that compounds **4** and **7** showed better trypanocidal properties *in vitro* than BZN, with higher activity, a larger spectrum of action and lower toxicity. With respect to *in vivo* activity, the treatment with compound **7** obtained promising results to fight CD, both in the acute and chronic phases, as indicated by the different assays, such as PCR or IS. Studies conducted in parallel to try to determine the mechanism of action suggest that compound **4** can carry out its effect by inhibiting the enzymes PK or PPDK of the glycosome. As for compound **7**, we suggest that its trypanocidal effect is due to the significant depolarisation of the mitochondrial membrane, which causes an energetic deficit and induces *T. cruzi* cell death by necrosis in a mitochondrion-dependent manner, without forgetting its possible effect as an inhibitor of lipid biosynthesis of the parasite. It is worth considering higher doses and combined therapies (due to their different mechanisms of action) to obtain better efficacy, even improving the pharmacokinetics of both compounds. Therefore, we present candidate molecules for the development of an easy-to-synthesise anti-Chagas agent to be implemented in a further step within the preclinical phase.

Funding

This work was supported by the Spanish Ministry of Economy and Competitiveness (MINECO) [grant number CTQ2014-57393-C2-1P and CSD2010-00065, FEDER funds]; the Spanish Ministry of Economy, Innovation and Science [grant number P11-CTS-7651]; the Junta de Andalucia [grant number P11-CTS-07187]; the Spanish Ministry of Education [R.M-E., grant number FPU14/01537]; the Junta de Andalucia [E.M-C., postdoctoral fellowship]; and the Govern de les Illes Balears [C. L., predoctoral fellowship, FSE funds].

Declaration of interest

None

Appendix A. Supplementary data

Supplementary data to this article can be found online at https://doi.org/10.1016/j.bmc.2019.01.033.

References

1. Moncayo Á, Silveira AC. Current epidemiological trends of Chagas disease in Latin America and future challenges in epidemiology, surveillance, and health policy. *Mem Inst Oswaldo Cruz.* 2009;104:17–30. https://doi.org/10.1016/B978-0-12-801029-7.00004-6.
2. Tarleton RL, Curran JW. Is Chagas disease really the "new HIV/AIDS of the Americas"? *PLoS Negl Trop Dis.* 2012;6:e1861https://doi.org/10.1371/journal.pntd.0001861.
3. Bern C, Kjos S, Yabsley MJ, Montgomery SP. *Trypanosoma cruzi* and chagas' disease in the United States. *Clin Microbiol Rev.* 2011;24:655–681. https://doi.org/10.1128/CMR.00005-11.
4. Gascon J, Bern C, Pinazo MJ. Chagas disease in Spain, the United States and other non-endemic countries. *Acta Trop.* 2010;115:22–27. https://doi.org/10.1016/j.actatropica.2009.07.019.
5. Montgomery SP, Starr MC, Cantey PT, Edwards MS, Meymandi SK. Neglected parasitic infections in the United States: Chagas Disease. *Am J Trop Med Hyg.* 2014;90:814–818. https://doi.org/10.4269/ajtmh.13-0726.
6. Jackson Y, Herrera MV, Gascon J. Economic crisis and increased immigrant mobility: new challenges in managing Chagas disease in Europe. *Bull World Health Organ.* 2014;92:771–772. https://doi.org/10.2471/BLT.13.134072.
7. Requena-Méndez A, Aldasoro E, de Lazzari E, et al. Prevalence of Chagas disease in Latin-American migrants living in Europe: a systematic review and meta-analysis. *PLoS Negl Trop Dis.* 2015;9:e0003540https://doi.org/10.1371/journal.pntd.0003540.
8. Pérez-Molina JA, Norman F, López-Vélez R. Chagas disease in non-endemic

countries: epidemiology, clinical presentation and treatment. *Curr Infect Dis Rep.* 2012;14:263–274. https://doi.org/10.1007/s11908-012-0259-3.
9. DNDi - Drugs for Neglected Diseases initiative. Diseases & Projects - Chagas Disease. https://www.dndi.org/diseases-projects/chagas/. Accessed 5 October 2018.
10. Wilkinson SR, Taylor MC, Horn D, Kelly JM, Cheeseman I. A mechanism for cross-resistance to nifurtimox and benznidazole in trypanosomes. *Proc Natl Acad Sci USA.* 2008;105:5022–5027. https://doi.org/10.1073/pnas.0711014105.
11. Marin-Neto JA, Rassi Jr A, Avezum Jr A, et al. The BENEFIT trial: testing the hypothesis that trypanocidal therapy is beneficial for patients with chronic Chagas heart disease. *Mem Inst Oswaldo Cruz.* 2009;104:319–324. https://doi.org/10.1590/S0074-02762009000900042.
12. Urbina JA. Specific chemotherapy of Chagas disease: relevance, current limitations and new approaches. *Acta Trop.* 2010;115:55–68. https://doi.org/10.1016/j.actatropica.2009.10.023.
13. Rodrigues Coura J, de Castro SL. A critical review on Chagas disease chemotherapy. *Mem Inst Oswaldo Cruz.* 2002;97:3–24. https://doi.org/10.1590/S0074-02762002000100001.
14. Viotti R, Vigliano C, Lococo B, et al. Side effects of benznidazole as treatment in chronic Chagas disease: fears and realities. *Expert Rev Anti Infect Ther.* 2009;7:157–163. https://doi.org/10.1586/14787210.7.2.157.
15. de Andrade AL, Zicker F, de Oliveira RM, et al. Randomised trial of efficacy of benznidazole in treatment of early *Trypanosoma cruzi* infection. *Lancet.* 1996;348:1407–1413. https://doi.org/10.1016/S0140-6736(96)04128-1.
16. Prata A. Clinical and epidemiological aspects of Chagas disease. *Lancet Infect Dis.* 2001;1:92–100. https://doi.org/10.1016/S1473-3099(01)00065-2.
17. Aldasoro E, Posada E, Requena-Méndez A, et al. What to expect and when: Benznidazole toxicity in chronic Chagas' disease treatment. *J Antimicrob Chemother.* 2018;73:1060–1067. https://doi.org/10.1093/jac/dkx516.
18. Bermudez J, Davies C, Simonazzi A, Real JP, Palma S. Current drug therapy and pharmaceutical challenges for Chagas disease. *Acta Trop.* 2015;156:1–16. https://doi.org/10.1016/j.actatropica.2015.12.017.
19. Mejia AM, Hall BS, Taylor MC, et al. Benznidazole-resistance in *Trypanosoma cruzi* is a readily acquired trait that can arise independently in a single population. *J Infect Dis.* 2012;206:220–228. https://doi.org/10.1093/infdis/jis331.
20. Hotez PJ, Bottazzi ME, Franco-Paredes C, Ault SK, Periago MR. The eglected tropical diseases of Latin America and the Caribbean: a review of disease burden and distribution and a roadmap for control and elimination. *PLoS Negl Trop Dis.* 2008;2:e300https://doi.org/10.1371/journal.pntd.0000300.
21. Swinney DC, Anthony J. How were new medicines discovered? *Nat Rev Drug Discov.* 2011;10:507–519. https://doi.org/10.1038/nrd3480.
22. Jin G, Wong ST. Toward better drug repositioning: prioritizing and integrating existing methods into efficient pipelines. *Drug Discov Today.* 2014;19:637–644. https://doi.org/10.1016/j.drudis.2013.11.005.
23. Mendoza A, Pérez-Silanes S, Quiliano M, et al. Aryl piperazine and pyrrolidine as antimalarial agents. Synthesis and investigation of structure-activity relationships. *Exp Parasitol.* 2011;128:97–103. https://doi.org/10.1016/j.exppara.2011.02.025.
24. Niewiadomski S, Beebeejaun Z, Denton H, Smith TK, Morris RJ, Wagner GK. Rationally designed squaryldiamides - a novel class of sugar-nucleotide mimics? *Org Biomol Chem.* 2010;8:3488. https://doi.org/10.1039/c004165c.
25. Kumar SP, Glória PM, Gonçalves LM, et al. Squaric acid: a valuable scaffold for developing antimalarials? *Medchemcomm.* 2012;3:489–493. https://doi.org/10.1039/c2md20011b.
26. Ribeiro CJ, Espadinha M, Machado M, et al. Novel squaramides with *in vitro* liver stage antiplasmodial activity. *Bioorganic Med Chem.* 2016;24:1786–1792. https://doi.org/10.1016/j.bmc.2016.03.005.
27. Olmo F, Rotger C, Ramírez-Macías I, et al. Synthesis and biological evaluation of *N*, N′-squaramides with high *in vivo* efficacy and low toxicity: toward a low-cost drug against Chagas disease. *J Med Chem.* 2014;57:987–999. https://doi.org/10.1021/jm4017015.
28. Saha A, Panda S, Paul S, Manna D. Phosphate bioisostere containing amphiphiles: a novel class of squaramide-based lipids. *Chem Commun.* 2016;52:9438–9441. https://doi.org/10.1039/C6CC04089F.
29. Sato K, Seio K, Sekine M. SquarylgGroup as a new mimic of phosphate group in modified oligodeoxynucleotides: synthesis and properties of new oligodeoxynucleotide analogues containing an internucleotidic squaryldiamide linkage. *J Am Chem Soc.* 2002;124:12715–12724. https://doi.org/10.1021/ja027131f.
30. Ximenis M, Bustelo E, Algarra AG, et al. Kinetic analysis and mechanism of the hydrolytic degradation of squaramides and squaramic acids. *J Org Chem.* 2017;82:2160–2170. https://doi.org/10.1021/acs.joc.6b02963.
31. Tietze LF, Arlt M, Beller M, Glüsenkamp KH, Jähde E, Rajewsky MF. Anticancer Agents, 15. Squaric acid diethyl ester: a new coupling reagent for the formation of drug biopolymer conjugates. Synthesis of squaric acid ester amides and diamides. *Chem Ber.* 1991;124:1215–1221. https://doi.org/10.1002/cber.19911240539.
32. Rotger MC, Piña MN, Frontera A, et al. Conformational preferences and self-template macrocyclization of squaramide-based foldable modules. *J Org Chem.* 2004;69:2302–2308. https://doi.org/10.1021/jo035546t.
33. Téllez-Meneses J, Mejía-Jaramillo AM, Triana-Chávez O. Biological characterization of *Trypanosoma cruzi* stocks from domestic and sylvatic vectors in Sierra Nevada of Santa Marta, Colombia. *Acta Trop.* 2008;108:26–34. https://doi.org/10.1016/j.actatropica.2008.08.006.
34. Kendall G, Wilderspin AF, Ashall F, Miles MA, Kelly JM. *Trypanosoma cruzi* glycosomal glyceraldehyde-3-phosphate dehydrogenase does not conform to the "hotspot" topogenic signal model. *EMBO J.* 1990;9:2751–2758. https://doi.org/10.1002/j.1460-2075.1990.tb07462.x.
35. Martín-Escolano R, Moreno-Viguri E, Santivañez-Veliz M, et al. Second generation of Mannich base type derivatives with *in vivo* activity against *Trypanosoma cruzi*. *J Med Chem.* 2018;61:5643–5663. https://doi.org/10.1021/acs.jmedchem.8b00468.
36. Pless-Petig G, Metzenmacher M, Türk TR, Rauen U. Aggravation of cold-induced injury in Vero-B4 cells by RPMI 1640 medium - identification of the responsible medium components. *BMC Biotechnol.* 2012;12:73. https://doi.org/10.1186/1472-6750-12-73.
37. Contreras VT, Salles JM, Thomas N, Morel CM, Goldenberg S. *In vitro* differentiation of *Trypanosoma cruzi* under chemically defined conditions. *Mol Biochem Parasitol.* 1985;16:315–327. https://doi.org/10.1016/0166-6851(85)90073-8.
38. Francisco AF, Jayawardhana S, Lewis MD, et al. Nitroheterocyclic drugs cure experimental *Trypanosoma cruzi* infections more effectively in the chronic stage than in the acute stage. *Sci Rep.* 2016;6:35351. https://doi.org/10.1038/srep35351.
39. Ye X, Ding J, Zhou X, Chen G, Liu SF. Divergent roles of endothelial NF-κB in multiple organ injury and bacterial clearance in mouse models of sepsis. *J Exp Med.* 2008;205:1303–1315. https://doi.org/10.1084/jem.20071393.
40. Olmo F, Gómez-Contreras F, Navarro P, et al. Synthesis and evaluation of *in vitro* and *in vivo* trypanocidal properties of a new imidazole-containing nitrophthalazine derivative. *Eur J Med Chem.* 2015;106:106–119. https://doi.org/10.1016/j.ejmech.2015.10.034.
41. Bahia MT, de Andrade IM, Martins TA, do Nascimento ÁF, Diniz Lde F, Caldas IS, Talvani A, Trunz BB, Torreele E, Ribeiro I. Fexinidazole: a potential new drug candidate for Chagas disease. PLoS Negl Trop Dis. 2012;6:e1870. https://doi.org/10.1371/journal.pntd.0001870.
42. Fernández-Becerra C, Sanchez-Moreno M, Osuna A, Opperdoes FR. *Comparative aspects of energy metabolism in plant trypanosomatids.* 1997;44:523–529.
43. Sandes JM, Fontes A, Regis-da-Silva CG, et al. *Trypanosoma cruzi* cell death induced by the Morita-Baylis-Hillman adduct 3-Hydroxy-2-methylene-3-(4-nitrophenylpropanenitrile). *PLoS ONE.* 2014;9:e93936https://doi.org/10.1371/journal.pone.0093936.
44. López-Céspedes Á, Villagrán E, Briceño Álvarez K, et al. *Trypanosoma cruzi*: Seroprevalence detection in suburban population of Santiago de Querétaro (Mexico). *Sci World J.* 2011;2012:914129https://doi.org/10.1100/2012/914129.
45. Bradford MM. A rapid and sensitive method for the quantitation of microgram quantities of protein utilizing the principle of protein-dye binding. *Anal Biochem.* 1976;72:248–254. https://doi.org/10.1016/0003-2697(76)90527-3.
46. Beyer WF, Fridovich I. Assaying for superoxide dismutase activity: some large consequences of minor changes in conditions. *Anal Biochem.* 1987;161:559–566. https://doi.org/10.1016/0003-2697(87)90489-1.
47. González P, Marín C, Rodríguez-González I, et al. *In vitro* activity of C20-diterpenoid alkaloid derivatives in promastigotes and intracellular amastigotes of *Leishmania infantum*. *Int J Antimicrob Agents.* 2005;25:136–141. https://doi.org/10.1016/j.ijantimicag.2004.08.010.
48. Sato K, Seio K, Sekine M. Squaryl group as a new mimic of phosphate group in modified oligodeoxynucleotides: synthesis and properties of new oligodeoxynucleotide analogues containing an internucleotidic squaryldiamide linkage. *J Am Chem Soc.* 2002;124:12715–12724. https://doi.org/10.1021/ja027131f.
49. Chatelain E. Chagas disease drug discovery: toward a new era. *J Biomol Screen.* 2014;20:22–35. https://doi.org/10.1177/1087057114550585.
50. Moraes CB, Giardini MA, Kim H, et al. Nitroheterocyclic compounds are more efficacious than CYP51inhibitors against *Trypanosoma cruzi*: implications for Chagas disease drug discovery and development. *Eur J Med Chem.* 2016;109:107–113. https://doi.org/10.1038/srep04703.
51. Nwaka S, Besson D, Ramirez B, et al. Integrated dataset of screening hits against multiple neglected disease pathogens. *PLoS Negl Trop Dis.* 2011;5:e1412https://doi.org/10.1371/journal.pntd.0001412.
52. Fabbro De Suasnábar D, Arias E, Streiger M, et al. Evolutive behavior towards cardiomyopathy of treated (nifurtimox or benznidazole) and untreated chronic chagasic patients. *Rev Inst Med Trop Sao Paulo.* 2000;42:99–109.
53. Espuelas S, Plano D, Nguewa P, et al. Innovative lead compounds and formulation strategies as newer kinetoplastid therapies. *Curr Med Chem.* 2012;19:4259–4288. https://doi.org/10.2174/092986712802884222.
54. Santos DM, Martins TA, Caldas IS, et al. Benznidazole alters the pattern of Cyclophosphamide-induced reactivation in experimental *Trypanosoma cruzi*-dependent lineage infection. *Acta Trop.* 2010;113:134–138. https://doi.org/10.1016/j.actatropica.2009.10.007.
55. El Bouhdidi A, Truyens C, Rivera M-T, Bazin H, Carlier Y. *Trypanosoma cruzi* infection in mice induces a polyisotypic hypergammaglobulinaemia and parasite-specific response involving high lgG2a concentrations and highly avid lgG1 antibodies. *Parasite Immunol.* 1994;16:69–76. https://doi.org/10.1111/j.1365-3024.1994.tb00325.x.
56. Kayama H, Takeda K. The innate immune response to *Trypanosoma cruzi* infection. *Microbes Infect.* 2010;12:511–517. https://doi.org/10.1016/j.micinf.2010.03.005.
57. Francisco AF, Lewis MD, Jayawardhana S, Taylor MC, Chatelain E, Kelly JM. Limited ability of Posaconazole to cure both acute and chronic *Trypanosoma cruzi* infections revealed by highly sensitive *in vivo* imaging. *Antimicrob Agents Chemother.* 2015;59:4653–4661. https://doi.org/10.1128/AAC.00520-15.
58. Hall BS, Wilkinson SR. Activation of benznidazole by trypanosomal type I nitroreductases results in glyoxal formation. *Antimicrob Agents Chemother.* 2012;56:115–123. https://doi.org/10.1128/AAC.05135-11.
59. Zingales B. *Trypanosoma cruzi* genetic diversity: Something new for something known about Chagas disease manifestations, serodiagnosis and drug sensitivity. *Acta Trop.* 2017;S0001–706X(17):30426–30436. https://doi.org/10.1016/j.actatropica.2017.09.017.
60. Don R, Ioset JR. Screening strategies to identify new chemical diversity for drug development to treat kinetoplastid infections. *Parasitology.* 2014;141:140–146. https://doi.org/10.1017/S003118201300142X.
61. Urbina JA. Chemotherapy of Chagas Disease. *Curr Pharm Des.* 2002;8:287–295. https://doi.org/10.2174/1381612023396177.

62. Lewis MD, Fortes Francisco A, Taylor MC, et al. Bioluminescence imaging of chronic *Trypanosoma cruzi* infections reveals tissue-specific parasite dynamics and heart disease in the absence of locally persistent infection. *Cell Microbiol.* 2014;16:1285–1300. https://doi.org/10.1111/cmi.12297.
63. Murcia L, Carrilero B, Ferrer F, Roig M, Franco F, Segovia M. Success of benznidazole chemotherapy in chronic *Trypanosoma cruzi*-infected patients with a sustained negative PCR result. *Eur J Clin Microbiol Infect Dis.* 2016;35:1819–1827. https://doi.org/10.1007/s10096-016-2733-6.
64. Basquiera AL, Sembaj A, Aguerri AM, et al. Risk progression to chronic Chagas cardiomyopathy: influence of male sex and of parasitaemia detected by polymerase chain reaction. *Heart.* 2003;89:1186–1190. https://doi.org/10.1136/heart.89.10.1186.
65. Ginger ML. Trypanosomatid biology and euglenozoan evolution: new insights and shifting paradigms revealed through genome sequencing. *Protist.* 2005;156:377–392. https://doi.org/10.1016/j.protis.2005.10.001.
66. Bringaud F, Rivière L, Coustou V. Energy metabolism of trypanosomatids: Adaptation to available carbon sources. *Mol Biochem Parasitol.* 2006;149:1–9. https://doi.org/10.1016/j.molbiopara.2006.03.017.
67. Cazzulo JJ. Aerobic fermentation of glucose by trypanosomatids. *FASEB J.* 1992;6:3153–3161. https://doi.org/10.1096/fasebj.6.13.1397837.
68. Michels PAM, Bringaud F, Herman M, Hannaert V. Metabolic functions of glycosomes in trypanosomatids. *Biochim Biophys Acta - Mol Cell Res.* 2006;1763:1463–1477. https://doi.org/10.1016/j.bbamcr.2006.08.019.
69. Kirkinezos IG, Moraes CT. Reactive oxygen species and mitochondrial diseases. *Semin Cell Dev Biol.* 2001;12:449–457. https://doi.org/10.1006/scdb.2001.0282.
70. Shang XJ, Yao G, Ge JP, Sun Y, Teng WH, Huang YF. Procyanidin induces apoptosis and necrosis of prostate cancer cell line PC-3 in a mitochondrion-dependent manner. *J Androl.* 2009;30:122–126. https://doi.org/10.2164/jandrol.108.005629.
71. Lee W, Thévenod F. A role for mitochondrial aquaporins in cellular life-and-death decisions? *AJP Cell Physiol.* 2006;291:C195–C202. https://doi.org/10.1152/ajpcell.00641.2005.
72. Verma NK, Singh G, Dey CS. Miltefosine induces apoptosis in arsenite-resistant *Leishmania donovani* promastigotes through mitochondrial dysfunction. *Exp Parasitol.* 2007;116:1–13. https://doi.org/10.1016/j.exppara.2006.10.007.
73. Hunter WN, Alphey MS, Bond CS, Schüttelkopf AW. Targeting metabolic pathways in microbial pathogens: oxidative stress and anti-folate drug resistance in trypanosomatids. *Biochem Soc Trans.* 2003;31:607–610. https://doi.org/10.1042/.
74. Piacenza L, Zago MP, Peluffo G, Alvarez MN, Basombrio MA, Radi R. Enzymes of the antioxidant network as novel determiners of *Trypanosoma cruzi* virulence. *Int J Parasitol.* 2009;39:1455–1464. https://doi.org/10.1016/j.ijpara.2009.05.010.
75. Maes L, Vanden Berghe D, Germonprez N, et al. *In vitro* and *In vivo* activities of a triterpenoid saponin extract (PX-6518) from the plant *Maesa balansae* against visceral *Leishmania* species. *Antimicrob Agents Chemother.* 2004;48:130–136. https://doi.org/10.1128/AAC.48.1.130-136.2004.
76. Germonprez N, Maes L, Van Puyvelde L, Van Tri M, Tuan DA, De Kimpe N. *In vitro* and *in vivo* anti-leishmanial activity of triterpenoid saponins isolated from *Maesa balansae* and some chemical derivatives. *J Med Chem.* 2005;48:32–37. https://doi.org/10.1021/jm031150y.
77. Lira R, Contreras LM, Santa Rita RM, Urbina JA. Mechanism of action of anti-proliferative lysophospholipid analogues against the protozoan parasite *Trypanosoma cruzi*: potentiation of *in vitro* activity by the sterol biosynthesis inhibitor ketoconazole. *J Antimicrob Chemother.* 2001;47:537–546. https://doi.org/10.1093/jac/47.5.537.
78. Wieder T, Orfanos CE, Geilen CC. Induction of ceramide-mediated apoptosis by the anticancer phospholipid analog, hexadecylphosphocholine. *J Biol Chem.* 1998;273:11025–11031. https://doi.org/10.1074/jbc.273.18.11025.
79. Luque-Ortega JR, Rivas L. Miltefosine (hexadecylphosphocholine) inhibits cytochrome c oxidase in *Leishmania donovani* promastigotes. *Antimicrob Agents Chemother.* 2007;51:1327–1332. https://doi.org/10.1128/AAC.01415-06.
80. Paris C, Loiseau PM, Bories C, Bréard J. Miltefosine induces apoptosis-like death in *Leishmania donovani* promastigotes. *Antimicrob Agents Chemother.* 2004;48:852–859. https://doi.org/10.1128/AAC.48.3.852-859.2004.

[2] PUBLICATION 2

European Journal of Medicinal Chemistry 164 (2019) 27–46

Contents lists available at ScienceDirect

European Journal of Medicinal Chemistry

journal homepage: http://www.elsevier.com/locate/ejmech

Research paper

New polyamine drugs as more effective antichagas agents than benznidazole in both the acute and chronic phases

Rubén Martín-Escolano [a], Daniel Molina-Carreño [a], Estefanía Delgado-Pinar [b], Álvaro Martin-Montes [a], M. Paz Clares [b], Encarnación Medina-Carmona [c, 1], Javier Pitarch-Jarque [b], Javier Martín-Escolano [a], María José Rosales [a], Enrique García-España [b, *], Manuel Sánchez-Moreno [a, **], Clotilde Marín [a, ***]

[a] Department of Parasitology, Instituto de Investigación Biosanitaria (ibs. Granada), Hospitales Universitarios de Granada/University of Granada, Severo Ochoa s/n, E-18071, Granada, Spain
[b] ICMol, Departamento de Química Inorgánica, Universidad de Valencia, C/Catedrático José Beltrán 2, 46980, Paterna, Spain
[c] Department of Physical Chemistry, Faculty of Sciences, University of Granada, Av. Fuentenueva s/n, 18071, Granada, Spain

ARTICLE INFO

Article history:
Received 27 July 2018
Received in revised form
10 December 2018
Accepted 14 December 2018
Available online 15 December 2018

Keywords:
Antichagas agents
Chemotherapy
In vivo
Polyamines
Trypanosoma cruzi

ABSTRACT

Despite the continuous research effort that has been made in recent years to find ways to treat the potentially life threatening Chagas disease (CD), this remains the third most important infectious disease in Latin America. CD is an important public health problem affecting 6–7 million people. Since the need to search for new drugs for the treatment of DC persists, in this article we present a panel of new polyamines based on the tripodal structure of tris(2-aminomethyl)amine (*tren*) that can be prepared at low cost with high yields. Moreover, these polyamines present the characteristic of being water-soluble and resistant to the acidic pH values of stomach, which would allow their potential oral administration. *In vitro* and *in vivo* assays permitted to identify the compound with the *tren* moiety functionalized with one fluorene unit (**7**) as a potential antichagas agent. Compound **7** has broader spectrum of action, improved efficacy in acute and chronic phases of the disease and lower toxicity than the reference drug benznidazole. Finally, the action mechanisms studied at metabolic and mitochondrial levels shows that the trypanocidal activity of compound **7** could be related to its effect at the glycosomal level. Therefore, this work allowed us to select compound **7** as a promising candidate to perform preclinical evaluation studies.

© 2018 Elsevier Masson SAS. All rights reserved.

1. Introduction

Chagas Disease (CD), classified as a neglected tropical disease according to World Health Organization (WHO), is the most important parasitic disease in Latin America and, after AIDS and tuberculosis, the third most spread infectious disease in the region where about 6–7 million people are infected. Moreover, CD is the most prevalent of the poverty-caused/poverty-promoting neglected parasitic diseases in the America continent [1–6]. CD is a life-long and potentially life-threatening parasitic disease [2], which develops debilitating and chronic stages in around 40% of the infected people and produces about 7500 deaths per year [3]. CD is not only endemic in 21 Latin America countries but, due to the high mobility and migration produced in the last years, it has also spread to other continents including North America and Europe that present 300,000 and 80,000 infected individuals, respectively [7,8]. The protozoan parasite *Trypanosoma cruzi* (etiological agent of CD) is naturally transmitted by blood-sucking triatomine bugs, although the congenital route, blood transfusión, organ transplantation and contamined food are other ways of transmission [7,8].

CD can be divided into distinct phases. The initial acute phase (4–6 weeks post-infection) is relatively mild (transient low-level

* Corresponding author. Current address: Departamento de Química Inorgánica, Universidad de Valencia, C/Catedrático José Beltrán 2, 46980, Paterna, Spain.
** Corresponding author. Current address: Department of Parasitology, Faculty of Sciences (Mecenas), Severo Ochoa s/n, 18001, Granada, Spain.
*** Corresponding author. Current address: Department of Parasitology, Faculty of Sciences (Mecenas), Severo Ochoa s/n, 18001, Granada, Spain.
E-mail addresses: Enrique.Garcia-Es@uv.es (E. García-España), msanchem@ugr.es (M. Sánchez-Moreno), cmaris@ugr.es (C. Marín).
[1] Current address: School of Biosciences, University of Kent, Stacey Building, Canterbury, CT2 7NJ, UK.

https://doi.org/10.1016/j.ejmech.2018.12.034
0223-5234/© 2018 Elsevier Masson SAS. All rights reserved.

febrile condition) and often undiagnosed. However, the acute phase can be more severe in children, causing myocarditis or meningoencephalitis and even death in some cases [9,10]. This phase is generally well controlled by a robust adaptive immune response, and the disease proceeds to a long-lasting and low parasitaemia asymptomatic chronic phase [11]. However, about a third of infected individuals go through an asymptomatic chronic phase whose manifestation may take several decades to occur. Most of these individuals will develop cardiomyopathy due to the persistence of the inflammatory response elicited by the infected host cells [12,13], and more rarely damage in the digestive tract (megaoesophagus and megacolon) as well as lesions in the peripheral nervous system. It has be remarked that for this symptomatic chronic phase there exist very few therapeutic options [10].

Currently, there are no vaccines for the prevention of CD because of its complex pathology [14]. The only way to fight against this disease is the chemotherapy treatment based on two nitroheterocyclic compounds developed more than 40 years ago [4,15,16]: benznidazole (BZN, *N*-benzyl-2-nitroimidazolylacetamide) and nifurtimox (NFX, (R,S)-3-methyl-*N*-[(1E)-(5-nitro-2-furyl)methylene]thiomorpholin-4-amine-1,1-dioxide) [14,17,18]. In general, BZN is the first option in most endemic countries for its better tolerability [19]. However, both treatments are not optimal because they show toxic side effects, require long-term therapeutic schedules, and have inconsistent efficacy. These drugs reduce parasitism during the acute phase, but their efficacy during the chronic phase is limited [4,15,16]. Moreover, NFX and BZN are both prodrugs activated by the same mitochondrial nitroreductase [20,21], which can result in cross-resistance. Finally, the treatment efficacy could change according to the geographical area as a consequence of a different drug susceptibility by the different *T. cruzi* strains [22].

Thus, the development of safer and more effective anti-trypanosomal agents is needed, especially for the treatment of the chronic phase. Recently there has been a significant increase in development towards this goal with several clinical trials to test candidate compounds. Sadly, the new candidates have not demonstrated enough efficacies [4,23]. Therefore, the search for new chemotherapeutic targets is an important goal. In this respect, the parasite antioxidant system is an appealing target due to its uniqueness in the trypanosomatids. The new anti-trypanosomal drugs should present an efficacy at least equal to those drugs currently in use, a better safety profile, possibility of oral administration, and activity against most *T. cruzi* strains [24]. In this scenario, here we present a study of the *in vivo* and *in vitro* efficacy of a panel of novel compounds based on the well-known tripodal polyamine tris(2-amimoethyl)amine (tren) which can be readily prepared in procedures involving two or three synthetic steps in high yields. Moreover, the compounds are water-soluble and resist the acid pH of the stomach allowing for a potential oral administration. Improved *in vitro* trypanocidal activity and lower toxicity than the reference drug BZN were the reasons for further *in vivo* assays. The possible action mechanisms of these new compounds have been studied at the glycosomal and mitochondrial levels, including Fe-SOD inhibition studies. The results obtained led us to consider these compounds as potential candidate for the development of new anti-Chagas treatment with *in vitro* and *in vivo* trypanocidal activity and lower toxicity than BZN in both the acute and chronic phases of CD.

2. Materials and methods

2.1. Chemistry

2.1.1. Synthesis

Compound **1** was prepared following a multi-step synthetic procedure already described by Albelda et al. [25].

*2.1.1.1. N,N′-{2-bis[2-(3-aminopropylamino)ethyl]aminoethyl}-1,3-propanediamine hexahydrobromide (**1**).* ^{1}H NMR (300 MHz, D_2O): δ (ppm), 3.20–3.31 (m, 4H), 3.12 (t, $J = 8$ Hz, 2H), 2.95 (t, $J = 7$ Hz, 2H), 2.10–2.20 (m, 2H).^{13}C NMR (75 MHz, D_2O): 49.1, 45.3, 44.9, 36.9, 24.1. Yield: 52%; $C_{15}H_{39}N_7 \cdot 6HBr$, MW: 796 g/mol. Elemental analysis: Calculated: C, 22.44; H, 5.65; N, 12.21; Experimental: C, 22.5; H, 5.4; N, 12.4. ESI-MS (*m*/*z*): Calculated for $C_{15}H_{39}N_7$, 317.53.; Found: 318.35 $[L + H]^+$.

Monofunctionalized derivatives were synthesised by the reaction of the appropriate carboxaldehyde with a 4-fold excess of tris(2-aminoethyl)amine (*tren*) in dry EtOH [26,27]. The resulting mixture was stirred for 2 h at room temperature under argon, and then, a 4-fold excess of sodium borohydride was added portion wise. For **6**, the reaction was carried out in THF, after 12 h, the solvent was removed and the crude was solved in ethanol before adding the sodium borohydride. After 2 h, the solvent was evaporated to dryness. The residue was treated with water and repeatedly extracted with CH_2Cl_2 (3×40 mL). The organic phase was collected and was dried with anhydrous $MgSO_4$ and the solvent evaporated to dryness to give the amines as oils. The oil was then taken in a minimum amount of EtOH and precipitated with HCl in dioxane to obtain the compounds as their hydrochloride salt.

*2.1.1.2. N^1,N^1-bis-(2-aminoethyl)-N′-(9-anthracenylmethyl)-ethane-1,2-diamine trihydrochloride salt (**2**) [27].* ^{1}H NMR (300 MHz, D_2O): δ (ppm), 7.79 (d, $J = 6.61$ Hz, 2H), 7.76 (s, 1H), 7.55 (d, $J = 8.35$ Hz, 2H), 7.44 (t, $J = 7.45$ Hz, 2H), 7.31 (t, $J = 7.06$ Hz, 2H), 4.55 (s, 2H), 3.06 (t, $J = 6.95$ Hz, 2H), 2.89 (t, $J = 6.27$ Hz, 4H), 2.66–2.59 (m, 6H). ^{13}C NMR (75 MHz, D_2O): Yield: 67%; $C_{21}H_{28}N_4 \cdot 3HCl \cdot (C_2H_5OH) \cdot 2H_2O$: MW: 526.20 g/mol; Elemental analysis: Calculated: C, 49.37; H, 7.49; N, 13.54; Experimental: C, 49.41; H, 7.04; N, 13.98. ESI-MS (*m*/*z*): Calculated for $C_{21}H_{28}N_4$, 336.23; Found: 337.42 $[L + H]^+$.

*2.1.1.3. N^1,N^1-bis-(2-aminoethyl)-N′-(2-nafthilmethyl)-ethane-1,2-diamine trihydrochloride salt (**3**) [26].* ^{1}H NMR (300 MHz, D_2O): δ (ppm), 8.06–8.16 (m, 3H), 7.59–7.76 (m, 4H), 4.82 (s, 2H), 3.32 (t, $J = 7$ Hz, 2H), 3.09 (t, $J = 6$ Hz, 4H), 2.93 (t, $J = 7$ Hz, 2H), 2.85 (t, $J = 6$ Hz, 4H). ^{13}C NMR (75 MHz, D_2O): 131.05, 130.14, 129.54, 127.89, 127.10, 125.99, 122.85, 50.12, 48.83, 48.52, 44.24, 36.70. Yield: 93%; $C_{17}H_{26}N_4 \cdot 3HCl$, MW: 395.56 g/mol; Elemental analysis: Calculated: C, 49.37; H, 7.49; N, 13.54; Experimental: C, 49.41; H, 7.04; N, 13.98. ESI-MS (*m*/*z*): Calculated for $C_{17}H_{26}N_4$, 286.22; Found: 287.22 $[L + H]^+$.

*2.1.1.4. N^1,N^1-bis-(2-aminoethyl)-N′-(pyren-1-ylmethyl)ethane-1,2-diamine trihydrochloride salt (**4**) [28].* ^{1}H NMR (300 MHz, D_2O): δ (ppm), 8.26 (d, $J = 7.39$ Hz, 1H), 8.20 (d, $J = 6.95$ Hz, 1H), 8.09 (t, $J = 7.67$ Hz, 1H), 8.06 (d, $J = 9.06$ Hz, 1H), 8.02 (d, $J = 7.83$ Hz, 1H), 7.99 (d, $J = 7.88$ Hz, 1H), 7.95 (d, $J = 9.10$ Hz, 1H), 7.91 (d, $J = 9.36$ Hz, 1H), 7.82 (d, $J = 7.97$ Hz, 1H), 4.74 (s, 2H), 3.25 (t, $J = 6.77$ Hz, 2H), 3.05 (t, J = 6.62, 4H), 2.86 (t, $J = 6.92$ Hz, 2H), 2.81 (t, $J = 6.59$ Hz, 4H). ^{13}C NMR (75 MHz, D_2O): δ (ppm), 132.10, 130.95, 130.21, 129.23, 129.05, 128.90, 128.63, 127.43, 126.95, 126.36, 126.20, 125.13, 123.88, 123.57, 123.02, 121.66, 50.08, 48.82, 48.53, 44.03, 36.68. Yield: 78%; $C_{23}H_{28}N_4 \cdot 3HCl$, MW: 468.16 g/mol; Elemental analysis: Calculated: C, 58.79; H, 6.64; N, 11.92; Experimental: C, 58.60; H, 6.80; N, 11.50 ESI-MS (*m*/*z*): Calculated for $C_{23}H_{28}N_4$, 360.23; Found: 361.32 $[L + H]^+$.

*2.1.1.5. N^1,N^1-bis-(2-aminoethyl)-N′-(5-(Dimethylamino)naphthalene-1-sulfonyl)ethane-1,2-diamine tetrahydrochloride sal. (**5**) [29].* ^{1}H NMR (300 MHz, D_2O): δ (ppm), 8.82 (d, $J = 8.8$ Hz, 1H), 8.50 (d, $J = 8.7$ Hz, 1H), 8.44 (d, $J = 7.6$ Hz, 1H), 8.15 (d, $J = 7.8$ Hz, 1H), 7.96

(dd, 2H), 3.20 (t, $J = 6.5$ Hz, 4H), 3.12 (t, $J = 6.1$ Hz, 2H), 3.00 (t, $J = 6.5$ Hz, 4H), 2.85 (t, $J = 6.1$ Hz, 2H). ^{13}C-DEPT NMR (75 MHz, D_2O): δ (ppm), 131.14, 128.61, 127.30, 126.67, 126.37, 119.98, 53.00, 50.44, 47.13, 38.86, 35.35. Yield: 72%; $C_{18}H_{29}N_5O_2S$ 3HCl·2H_2O, MW: 523,16 g/mol; Elemental analysis: Calculated: C, 41.33; H, 6.94; N, 13.39; Experimental: C, 41.53; H, 7,20; N, 13.16, ESI-MS (*m/z*): Calculated for $C_{18}H_{29}N_5O_2S$, 377.75; Found: 378.77 $[L + H]^+$.

*2.1.1.6. N^1,N^1-bis-(2-aminoethyl)-$N^{'}$-(Ferrocenylmethyl)ethane-1,2-diamine trihydrochloride salt (**6**).* ^{1}H NMR (300 MHz, D_2O): δ (ppm), 4.47 (s, 2H), 4.38 (s, 2H), 4.30 (s, 5H), 4.13 (s, 2H), 3.14–3.04 (m, 6H), 2.85–2.79 (m, 6H). ^{13}C NMR (75 MHz, D_2O): δ (ppm), 75.83, 70.99, 70.46, 69.63, 50.16, 49.15, 47.77, 43.24, 36.75. Yield: 70%; $C_{17}H_{28}FeN_4 \cdot 3HCl \cdot 1.5H_2O$ MW: 479.11 g/mol; Elemental analysis: Calculated: C, 42.57; H, 7.15; N, 11.69; Experimental: C, 42.20; H, 6.73; N, 11.37. ESI-MS (*m/z*): Calculated for $C_{17}H_{28}FeN_4$ 344.17; Found: 344.98 $[L + H]^+$.

*2.1.1.7. N^1,N^1-bis-(2-aminoethyl)-$N^{'}$-(2-fluorenilmethyl) ethane-1,2-diamine trihydrochloride salt (**7**).* ^{1}H NMR (300 MHz, D_2O): δ (ppm), 7.95–7.99 (m, 2H), 7.72 (s, 1H), 7.69 (d, $J = 7.5$ Hz, 1H), 7.41–7.53 (m, 3H), 4.35 (s, 2H), 4.01 (s, 2H), 3.23 (t, $J = 7$ Hz, 2H), 3.10 (t, $J = 6.4$ Hz, 4H), 2.91 (t, $J = 7$ Hz, 2H), 2.85 (t, $J = 6.4$ Hz, 4H). ^{13}C NMR (75 MHz, D_2O): δ (ppm), 36.96, 44.20, 50.62, 51.50, 120.38, 120.66, 125.57, 127.17, 127.47, 127.57, 129.58, 130.78, 140.87, 141,94, 143.50, 143,60. Yield: 66%; $C_{20}H_{28}N_4Cl_3 \cdot NaCl \cdot C_2H_5OH$, MW: 538.36 g/mol; Melting point: 254.6 °C; Elemental analysis: $C_{20}H_{28}N_4 \cdot 3HCl \cdot NaCl \cdot C_2H_5OH$ Calculated: C, 49.08; H, 6.93; N, 10.14; Experimental: C, 49.04; H, 6.39; N, 10.39. ESI-MS (*m/z*): Calculated for $C_{20}H_{28}N_4$; 324.50 Found: 325.63 $[L + H]^+$.

Tri-functionalized ligands were synthesised by the reaction of a 3-fold excess of the appropriated carboxaldehyde with tris(2-aminoethyl)amine (*tren*) in dry EtOH [30]. The resulting mixture was stirred for 2 h at room temperature under argon, and then, a 3-fold excess of sodium borohydride was added portion wise (except for **10**, where the reaction was carried out in THF. After 12 h, the solvent was removed and ethanol was added to the crude obtained. Finally, the sodium borohydride was added). After 2 h, the solvent was evaporated to dryness. The residue was treated with water and repeatedly extracted with CH_2Cl_2 (3 × 40 mL). The organic phase was collected and dried with anhydrous $MgSO_4$ and the solvent evaporated to dryness to give an oil. The oil was then taken in a minimum amount of EtOH and precipitated with HCl in dioxane to obtain its hydrochloride salt.

*2.1.1.8. {Bis-2-[(5-indazolulmethyl)amino]ethyl-2-[(2-naphthylmethyl)amino]ethyl}amine trihydrochloride salt (**8**).* ^{1}H NMR (300 MHz, D_2O): δ (ppm), 8.21 (d, 1H), 8.05 (m, 2H), 8.04 (m, 1H), 7.94 (t, 2H), 7.80 (d, H), 7.57 (m, 8H), 4.74 (s, 2H), 4.35 (s, 4H), 3.30 (m, 2H), 3.19 (m, 4H), 2.82 (m, 6H). ^{13}C NMR (75 MHz, D_2O): δ (ppm), 141.94, 135.61, 135.43, 133.04, 131.86, 131.35, 130.30, 130.04, 128.68, 128.18, 127.75, 126.63, 125.14, 124.63, 124.53, 124.30, 112.17, 52.87, 51.71, 46.39, 45.76. Yield: 51%; $C_{33}H_{38}N_8 \cdot 2CH_3OH \cdot 3H_2O \cdot 3HCl$ MW: 774.22 g/mol; Elemental analysis: Calculated: C, 54.29; H, 6.77; N, 14.47; Experimental: C, 54.43; H, 6.51; N, 14.32 ESI-MS (*m/z*): Calculated for $C_{33}H_{38}N_8$ 546.7; Found: 547.3 $[L + H]^+$.

*2.1.1.9. Tris{2-[(3-phenyl-1H-4-Pyrazolylmethyl)amino]ethyl}amine hexahydrochloride salt (**9**).* ^{1}H NMR (300 MHz, D_2O): δ (ppm), 8.67 (s, 3H), 7.74–7.70 (m, 6H), 7.62–7.57 (m, 12H), 4.41 (s, 6H), 3.20–3.15 (m, 6H), 2.93–2.77 (m, 12H).^{13}C NMR (75 MHz, D_2O): δ (ppm), 1.7.56, 130.15, 130.69, 42.12, 38.25, 52.53, 51.66. Yield: 54%; $C_{36}H_{42}N_{10} \cdot 6HCl$, MW: 830,219 g/mol; Elemental analysis: Calculated: C, 52,03; H, 5,82; N, 16,86; Experimental: C, 51.50; H, 6.39; N, 16.59 ESI-MS (*m/z*): Calculated for $C_{36}H_{42}N_{10}$ 614.80; Found: 615.99 $[L + H]^+$.

*2.1.1.10. Tris{2-[(Ferrocenylmethyl)amino]ethyl}amine hexahydrochloride salt (**10**).* ^{1}H NMR (300 MHz, D_2O): δ (ppm), 4.72–4.22 (m, 33H), 3.23–2.98 (m, 6H), 2.93–2.71 (m, 6H). ^{13}C NMR (75 MHz, D_2O): δ (ppm), 86.42, 68.62, 68.2, 66.01, 52.10, 45.86, 47. Yield: 62%; $C_{39}H_{48}Fe_3N_4 \cdot 3HCl \cdot 3H_2O$ · MW = 903.79 g/mol; Elemental analysis: Calculated: C, 51.82; H, 6.35; N, 6.20; Experimental: C, 51.71; H, 6.39; N, 6.28. ESI-MS (*m/z*): Calculated for $C_{39}H_{48}Fe_3N_4$ 740.36; Found: 741.09 $[L + H]^+$.

*2.1.1.11. Tris{2-[(4-quinolylmethyl)amino]ethyl}amine hexahydrochloride salt (**11**).* ^{1}H NMR (300 MHz, D_2O): δ (ppm), 8.50 (d, $J = 6.94$ Hz, 3H), 7.88 (d, $J = 8.09$ Hz, 3H), 7.72–7.70, (m, 6H), 7.63–7.58 (m, 6H), 4.60 (s, 6H), 3.39 (t, $J = 6.06$ Hz, 6H), 3.02 (t, $J = 5.82$ Hz, 6H).^{13}C-DEPT NMR (75 MHz, D_2O): δ (ppm), 144.87, 135.35, 132.11, 124.55, 122.55, 122.91, 49.15, 45.73. Yield: 79%; $C_{36}H_{39}N_7 \cdot 6HCl \cdot 3H_2O$, MW = 842.55; Elemental analysis: Calculated: C, 51.31; H, 6.10; N, 11.64; Experimental: C, 51.615; H, 5805; N, 11.685. ESI-MS (*m/z*): Calculated for $C_{36}H_{39}N_7$ 569.76; Found: 570.28 $[L + H]^+$.

*2.1.1.12. Tris{2-[(2-quinolylmethyl)amino]ethyl}amine hexahydrochloride salt (**12**).* ^{1}H NMR (300 MHz, D_2O): δ (ppm), 8.54 (d, $J = 8.48$ Hz, 3H), 7.98 (d, $J = 8.14$ Hz, 3H), 7.81–7.80, (m, 6H), 7.73–7.71 (m, 3H), 7.64 (d, $J = 8.50$ Hz, 3H), 4.70 (s, 6H), 3.51 (t, $J = 6.25$ Hz, 6H), 3.15 (t, $J = 6.32$ Hz, 6H). ^{13}C-DEPT NMR (75 MHz, D_2O): δ (ppm), 143.09, 133.39, 129.27, 129.01, 124.54, 121.24, 49.94, 49.67, 45.56. Yield: 68%; $C_{36}H_{39}N_7 \cdot 6HCl \cdot 4H_2O$, MW: 860.57 Elemental analysis: Calculated: C, 50.24; H, 6.21; N, 11.39; Experimental: C, 50.55; H, 5.46; N, 10.89. ESI-MS (*m/z*): Calculated for $C_{36}H_{39}N_7$ 569.33; Found: 570.31 $[L + H]^+$.

2.1.2. Proton nuclear magnetic resonance (^{1}H NMR) measurements

The ^{1}H NMR spectra were recorded on a Bruker DPX-300 or a Bruker 400 AV spectrometers operating at 299.95 MHz or 399.91 for ^{1}H NMR, the solvent signal was used as reference. Adjustments to the desired pH were made using drops of DCl or NaOD solutions. The pD was calculated from the measured pH values using the correlation, pH = pD - 0.4 [31].

2.1.3. Equilibrium studies

The potentiometric titrations were carried out at 298.1 ± 0.1 K using 0.15 M NaCl as supporting electrolyte. The experimental procedure (burette, potentiometer, cell, stirrer, microcomputer, etc.) has been fully described elsewhere [32]. The reference electrode was an Ag/AgCl electrode in saturated KCl solution. The glass electrode was calibrated as a hydrogen-ion concentration probe by titration of previously standardized amounts of HCl with CO_2-free NaOH solutions and the equivalent point determined by Gran's method [33,34], which gives the standard potential, E°', and the ionic product of water (pKw = 13.73 (1)). The acquisition of the emf data was performed with the computer program PASAT [35]. The computer program HYPERQUAD was used to calculate the protonation and stability constants and the logician HYSS was employed ton derive the distribution diagrams [36,37].

The pH range investigated was 2.5–11.0. The different titration curves (at least two) were treated either as a single set or as separated curves without significant variations in the values of the stability constants. Finally, the sets of data were merged together and treated simultaneously to give the final stability constants.

2.2. Biology

2.2.1. In vitro activity assays

2.2.1.1. Parasite culture. Three different *Trypanosoma cruzi* strains were evaluated in this work: *Trypanosoma cruzi* SN3 strain (IRHOD/CO/2008/SN3, discrete typing unit (DTU) I) isolated from domestic *Rhodnius prolixus* from Guajira, Colombia [38]; *Trypanosoma cruzi* Arequipa strain (MHOM/Pe/2011/Arequipa, DTU V) isolated from a human from Arequipa, Peru [39]; *Trypanosoma cruzi* Tulahuen strain (TINF/CH/1956/Tulahuen, DTU VI) isolated from Tulahuen, Chile [39]. Epimastigote culture forms were grown at 28 °C in RPMI (Gibco®) with 10% (v/v) foetal bovine serum (FBS) (heat-inactivated), 0.5% (w/v) trypticase (BBL) and 0.03 M hemin [40].

2.2.1.2. In vitro activity screening assays against extracellular epimastigote forms. T. cruzi epimastigotes (strains SN3, Arequipa and Tulahuen) were collected in the exponential growth phase by centrifugation at 400*g* for 10 min. The compounds to be tested and BZN were dissolved in DMSO, and assayed as nontoxic or inhibitory DMSO concentrations on parasite growth. Trypanocidal activity was determined using the method described by Rolón et al. [41] with some modifications. Assays were performed in microtiter plates (96-well plates) by seeding the parasites at 5×10^5 mL^{-1}, and after addition of the compounds at dosages of 100 to 0.2 μM and cultured in 200 μL/well volumes at 28 °C. Growth controls and BZN were also included. After a 48-h incubation, 20 μL (0.125 mg/mL) of resazurin sodium salt (Sigma-Aldrich) was added, and the plates were incubated for a further 24 h. Finally, 5 μL (10% w/v) of sodium dodecyl sulphate (SDS) was added, and after 10 min, the trypanocidal activity of the compounds on the plates was assessed by absorbance measurements (Sunrise, TECAN) at 570 and 600 nm [42]. The trypanocidal effect was determined using GraphPad Prism 6 and is expressed as the IC_{50}, i.e., the concentration required to result in 50% inhibition. Each drug concentration was tested in triplicate in four separate determinations.

2.2.1.3. Vero cells culture and cytotoxicity tests. Vero cells (EACC number 84113001) from monkey kidney were grown in humidified 95% air, 5% CO_2 atmosphere at 37 °C in RPMI (Gibco®) with 10% (v/v) FBS (heat-inactivated) [43]. Vero cells were collected first by trypsinization and then by centrifugation at 400*g* for 10 min. Cytotoxicity against Vero cells was assessed using microtiter plates (96-well plates) by seeding the cells at 1.25×104 mL^{-1}, and after addition of the compounds at dosages of 2000 to 1 μM and cultured in 200 μL/well volumes in RPMI (Gibco®) with 1% (v/v) foetal bovine serum (heat-inactivated). Growth controls and BZN were also included. After a 48-h incubation, 20 μL (0.125 mg/mL) of resazurin sodium salt (Sigma-Aldrich) was added, and the plates were incubated for a further 24 h. Finally, 5 μL (10% w/v) of SDS was added, and after 10 min, the cytotoxicity of the compounds on the plates was assessed by absorbance measurement (Sunrise, TECAN) at 570 and 600 nm [42]. Cytotoxicity was determined using GraphPad Prism 6 and it is expressed as the IC_{50}, i.e., the concentration required to result in 50% inhibition. Each drug concentration was tested in triplicate in four separate determinations.

2.2.1.4. In vitro activity screening assays against intracellular amastigote forms and infected cells. Assays were performed in microtiter plates (24-well plates) by seeding the Vero cells at 1×10^4 well^{-1} with rounded coverslips on the bottom. 24 h later the cells were infected with culture-derived trypomastigotes of *T. cruzi* (strains SN3, Arequipa and Tulahuen) at a multiplicity of infection (MOI) ratio of 1:10 during 24 h. Non-phagocyted parasites were removed by washing, and after addition of the compounds at dosages of 100 to 0.2 μM, cultured in 500 μL/well volumes in RPMI (Gibco®) with 1% (v/v) foetal bovine serum (heat-inactivated) in a humidified 95% air, 5% CO_2 atmosphere at 37 °C. Growth controls and BZN were also included. After a 72-h incubation, the trypanocidal effect was assessed based on the number of amastigotes and infected cells in treated and untreated cultures in methanol-fixed and Giemsa-stained preparations by analysing 500 host cells distributed in randomly chosen microscopic fields. The infectivity index was defined as the average number of amastigote forms in infected cells multiplied by the percentage of infected cells. The trypanocidal effect was determined using GraphPad Prism 6 and it is expressed as the IC_{50}, i.e., the concentration required to result in 50% inhibition. Each drug concentration was tested in triplicate in four separate determinations.

2.2.1.5. Obtaining metacyclic forms. Metacyclic trypomastigotes (aged epimastigote cultures) were induced with the method described by Martín-Escolano et al. [39]. Subsequently, the metacyclic trypomastigotes were used to infect Vero cells in humidified 95% air, 5% CO_2 atmosphere at 37 °C in RPMI (Gibco®) with 10% (v/v) FBS (heat-inactivated) for 5–7 days [44]. Finally, the culture-derived trypomastigotes were collected by centrifugation at 3000*g* for 5 min and used to infect BALB/c albino mice.

2.2.1.6. In vitro activity screening assays against extracellular trypomastigote forms. T. cruzi blood trypomastigotes (strain SN3, Arequipa and Tulahuen) were obtain by cardiac puncture from BALB/c mice during the parasitaemia peak after infection and diluted in RPMI (Gibco®) with 10% (v/v) FBS (heat-inactivated). Trypanocidal activity was determined according to the method described by Faundez et al. [45] with certain modifications. Assays were performed in microtiter plates (96-well plates) by seeding the parasites at 2×10^6 mL^{-1}, and after addition of the compounds at dosages of 50 to 0.2 μM, cultured in 200 μL/well volumes in humidified 95% air, 5% CO_2 atmosphere at 37 °C. Growth controls and BZN were also included. After a 24-h incubation, 20 μL (0.125 mg/mL) of resazurin sodium salt (Sigma-Aldrich) was added, and the plates were incubated for 4 h. Finally, the same procedure as described to assess the trypanocidal activity in the epimastigote forms was carried out.

2.2.2. In vivo activity assays

2.2.2.1. Mice. Female BALB/c mice (8–10 weeks old and 20–25 g) were used to perform the experiments, provided with water and standard chow *ad libitum* and maintained under standard conditions.

These experiments were approved by the Ethics Committee on Animal Experimentation of the University of Granada (RD53/2013) and performed under the rules and principles of the international guide for biomedical research in experimental animals.

2.2.2.2. Infection and treatment. Groups of three mice were infected via intraperitoneal inoculation with 5×10^5 bloodstream trypomastigotes (BTs) of *T. cruzi* Arequipa strain in 0.2 mL PBS.

The mice were divided as follows: 0, negative control group (uninfected and untreated); I, positive control group (infected and untreated); II, BZN group (infected and treated with BZN); III, study group (infected and treated with the compounds under study). BZN and the compounds under study were prepared at 2 mg/mL in an aqueous suspension vehicle containing 5% (v/v) DMSO and 0.5% (w/v) hydroxypropyl methylcellulose [46]. Drugs were administered by the oral route (~200 μL) once daily for 5 consecutive days, and vehicle only was administered in the negative and positive control groups. Therefore, doses of 20 mg/kg per day were administered for 5 consecutive days. Administration of the tested compounds was initiated on the 10th day post-infection (dpi) (once the infection

was confirmed) in mice treated in the acute phase and on the 75th dpi (it is established that the animals had entered the chronic phase of the experiment) in the mice treated in the chronic phase.

2.2.2.3. Parasitaemia levels during the acute phase treatment. Peripheral blood from each mouse treated in the acute phase was obtained from the mandibular vein, and the number of BTs was quantified using the method described by Olmo et al. [47] until the day parasitaemia was not detected. The number of BTs was expressed as parasites/mL.

2.2.2.4. Immunosuppression. After 100^{th} dpi, the mice were immunosuppressed with cyclophosphamide monohydrate (CP) (ISOPAC®) as follow: 1 intraperitoneal injection every 4 days with a dose of 200 mg/kg, for a maximum of three doses [46]. The efficacy of such an immunosuppression (IS) procedure for assessing cryptic infection was verified by the high parasitaemia in chronically untreated mice. Within 1 week after the last CP injection, the reactivation rate was evaluated according the procedure described for parasitaemia levels in the acute phase.

2.2.2.5. Tissues DNA extraction, PCR and electrophoresis. After CP-induced IS, mice were bled out under gaseous anaesthesia (CO_2) via heart puncture, and blood was collected.

Our previous *in vivo* studies using the *T. cruzi* Arequipa strain revealed its tropism for the following tissues: adipose tissue, bone marrow, brain, oesophagus, heart, lung, muscle, spleen and stomach. Therefore, these 9 tissues were harvested and immediately perfused with pre-warmed PBS to avoid contamination of the tissue with BTs [48]. In addition, spleen was weighed to evaluate inflammation of this organ in the different groups of mice. Finally, the target tissues were thawed and ground up using the method described by Olmo et al. [47], and DNA extraction was performed using Wizard® Genomic DNA Purification Kit (Promega).

PCR was performed out based on the published sequence of the enzyme superoxide dismutase (SOD) *T. cruzi* CL Brenner (GenBank accession No. XM_808937) using two primers designed in our laboratory (GenBank accession number DQ441589), as described by Olmo et al. [49], that allow the detection of *T. cruzi* DNA in different biological samples. Finally, the amplification products were subjected to electrophoresis on a 2% agarose gel for 90 min at 90 V, containing 1:10,000 GelRed nucleic acid gel stain.

2.2.2.6. ELISA tests. Serum samples were obtained 2 days after treatment, 1 day before IS and on the day of necropsy for the mice treated in the acute phase, and 2 days after treatment and on the day of necropsy (sera post-IS) for the mice treated in the chronic phase. To obtain serum, the method described by Moreno-Viguri [50] was followed.

Circulating antibodies in serum against *T. cruzi* Arequipa strain were qualitatively and quantitatively evaluated by ELISA. The serum from whole blood was diluted 1:80 in PBS, and all serum samples were analysed in triplicate in polystyrene 96-well microtiter plates. The absorbance was read at 492 nm using a microplate reader (Sunrise, TECAN). Mean and standard deviations of the optical densities of the negative control sera were used to calculate the cut-off value (mean plus three times the standard deviation) [47].

2.2.2.7. Toxicity tests. Serum samples were obtained at 2 days after treatment and on the day of necropsy (sera post-IS) both for mice treated in the acute and chronic phases.

A series of parameters of these sera were measured in the Biochemical Service (University of Granada) using the commercial Cromakit® with the BS-200 Chemistry Analyzer Shenzhen Mindray (Bio-medical Electronics Co., LTD). Mean values and standard deviations were calculated using the levels obtained for different populations of sera ($n = 15$, $n = 6$), and the confidence interval for the mean normal populations were also calculated based on a confidence level of 95% ($100 \times (1\text{-}\alpha) = 100 \times (1-0.05)$).

2.2.3. Studies of the action mechanism

2.2.3.1. Metabolite excretion. The assays were performed in cell culture flasks (surface area, 25 cm^2) by seeding epimastigote forms from *T. cruzi* Arequipa strain at 5×10^5 mL^{-1} and after the addition of the compounds at IC_{25} concentrations at 28 °C. Non-treated parasites were also included. After a 72-h incubation, treated and non-treated parasites were centrifugated at 800 g for 10 min to collect the supernatants to determine the excreted metabolites by ^1H NMR using a VARIAN DIRECT DRIVE 400 MHz Bruker spectrometer with an AutoX probe using D_2O as described by Fernández-Becerra et al. [51]. The binning and normalisations were achieved using Mestrenova 9.0 software. The matrix obtained in Mestrenova was imported into Microsoft Excel for further data analyses.

2.2.3.2. Mitochondrial membrane potential and DNA and RNA levels. The treated epimastigote forms from *T. cruzi* Arequipa strain described above and collected by centrifugation were washed 3 times with PBS. Subsequently, the parasites were resuspended in 0.5 mL PBS with 10 μg/mL Rho (Sigma-Aldrich) or 10 μg/mL AO (Sigma-Aldrich) for 20 min [52]. Finally, the samples were washed twice with ice-cold PBS, dispersed in 1 mL of PBS and immediately analysed by flow cytometry (BECTON DICKINSON FACSAria III). The data were captured and analysed using BD FACSDiva v8.01 software (Becton Dickinson Biosciences, 2350 Qume Drive, San Jose, Palo-Alto, California). The fluorescence intensities for Rho (mitochondrial membrane potential) and AO (nucleic acids) were quantified based on the forward (FSC) and side (SSC) scatter, for which a total of 10,000 events were acquired in the previously established region corresponding to epimastigote forms [53]. Alterations in the fluorescence intensities of AO (APC-A) or Rho (FITC-A) were quantified as described elsewhere [52].

2.2.3.3. SOD inhibition studies. Epimastigote forms from *T. cruzi* Arequipa strain were grown and collected in the exponential growth phase by centrifugation at 400*g* for 10 min. The pellet was resuspended at 5×10^9 mL^{-1} in the growth medium without FBS in cell culture flasks (surface area, 75 cm^2). After a 28-h incubation at 28 °C, the culture was centrifugated at 800 g for 10 min at 4 °C, and the supernatant was processed using the method previously described by López-Céspedes et al. [54]. The protein concentration was determined using the Bradford method (Sigma Immunochemical, St. Louis) with bovine serum albumin as a standard [55].

Iron and commercial copperezinc (Sigma-Aldrich) superoxide dismutases (Fe-SODe and CuZn-SOD) activities were determined using the method described by Beyer and Fridovich [56].

3. Results and discussion

3.1. Chemistry

3.1.1. Synthesis

Compounds **2**–**12** were obtained in high yield by easy synthetic routes involving the reaction of tris(2-aminoethyl)amine (*tren*) with the corresponding commercially available aldehydes either in mole ratio amine:aldehyde mole ratio 4:1 for **2**–**7** or 1:3 for compounds **8**–**12** (Scheme 1). Then, sodium borohydride was added and the corresponding amines separated by extraction in CH_2Cl_2. The compounds are finally isolated as their hydrochloride salts. A

few examples of this procedure can be found in Refs. [25–30].

Compound **1** requires however the extension of the tren moiety with aminopropyl chains as previously reported [25]:

Both procedures permit the ready preparation of the compounds with high yields at relatively low costs.

3.1.2. Acid-base behaviour

Polyamines bear protonation equilibria and at the physiological pH of 7.4 they are present in solution as charged species. Therefore, the protonation constants have to be calculated previously to perform any other study. Tables 1 and 2 show the protonation constants of the compounds determined in water at 298.1 K. Due to its low solubility at the milimolar concentrations required for the potentiometric studies, the protonation constants of compounds **7**, **8** and **9** were measured in hydroalcoholic water:ethanol 70:30 mixtures. The solubility of **10** was very low even in this solvent mixture preventing the calculation of the stability constans.

All the monosubstituted compounds have three protonation constants involving the primary and secondary ammine groups. This makes the protonation degree (mean number of charged

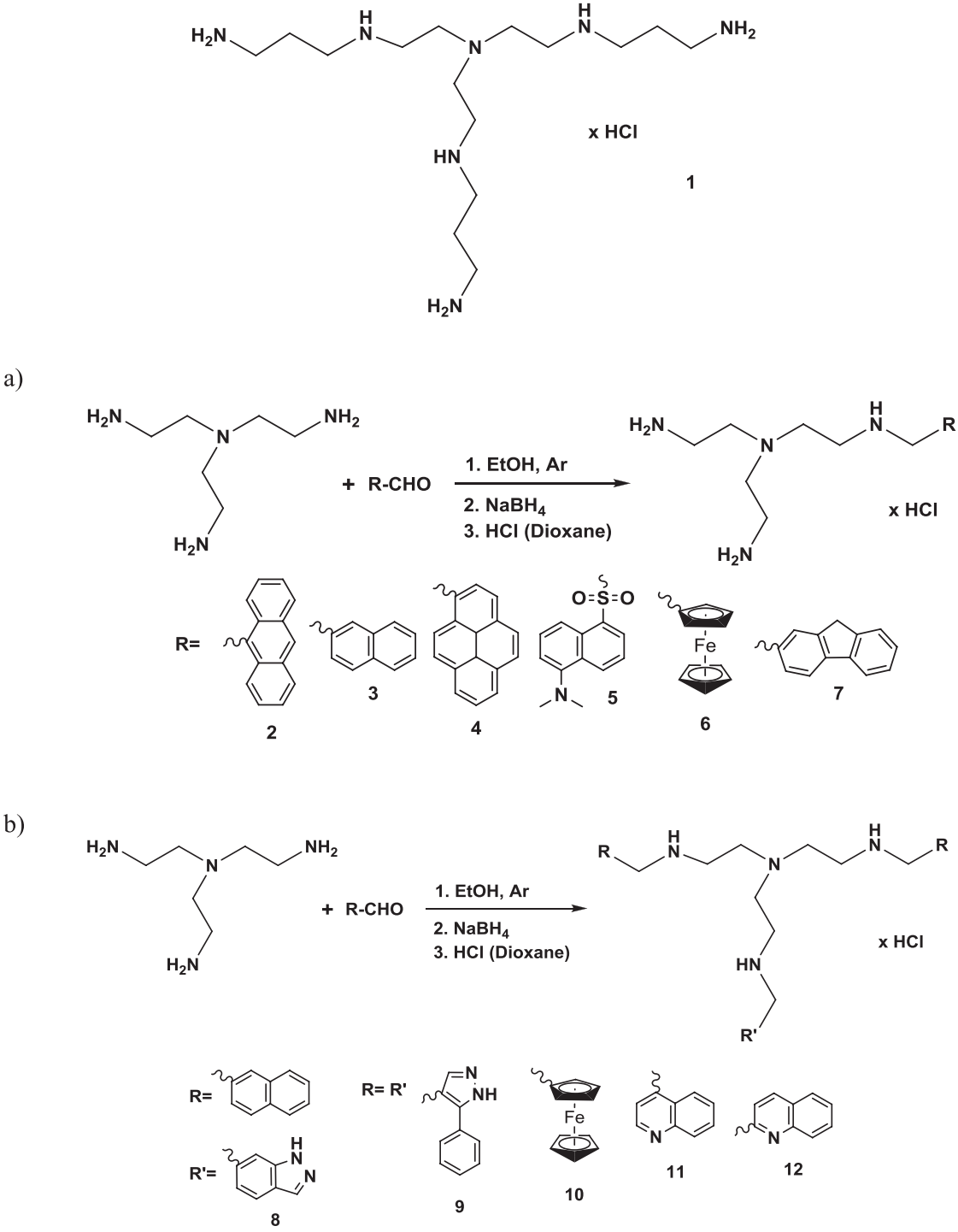

Scheme 1. Compound **1** and experimental procedure for the preparation of a) compounds **2**–**7** and b) compounds **8**–**12**.

Table 1
Protonation constants for the monofunctionalized tren derivatives **2**–**7** determined at 25 °C.

Reaction	2 [a]	3 [b]	4 [a]	5 [b]	6 [a]	7 [c]
$H + L \leftrightarrows HL$[d]	9.81 (1)[e]	9.72 (2)	9.90 (1)	10.19 (2)	10.03 (2)	9.58 (1)
$H + HL \leftrightarrows H_2L$	8.88 (1)	9.10 (1)	8.66 (1)	9.44 (1)	9.35 (1)	8.85 (1)
$H + H_2L \leftrightarrows H_3L$	7.15 (2)	7.45 (1)	6.62 (2)	4.16 (3)	8.1 (1)	7.46 (1)
$H + H_3L \leftrightarrows H_4L$				2.21 (2)		
log β[f]	25.84	26.27	25.18	26	27.48	25.89
Mean No. Prot. pH = 7.4	2.3	2.8	2.1	2.0	2.8	2.5

[a] 0.15 M NaCl, logK of 2 ref. 27, 4 ref. 28, and 6 this work.
[b] 0.15 M $NaClO_4$, logK of 3 ref. 26, 5. ref. 29,
[c] 0. 15 M NaCl in EtOH:H_2O (30:70), logK of 7, this work.
[d] Charges omitted.
[e] Values in parentheses are standard deviations in the last significant figure.
[f] log β = Σ Log K.

Table 2
Protonation constants for the tri-functionalized tren derivatives **1, 8**–**12** determined at 25 °C.

Reaction	1 [a]	8 [c]	9 [c]	10	11 [b]	12 [b]
$H + L \leftrightarrows HL$[d]	10.34 (7)[e]	9.27 (1)	8.70 (2)	nd	10.76 (2)	10.60 (2)
$H + HL \leftrightarrows H_2L$	10.26 (2)	8.07 (1)	7.59 (1)	nd	8.13 (4)	9.61 (1)
$H + H_2L \leftrightarrows H_3L$	9.52 (4)	6.77 (1)	6.38 (1)	nd	5.67 (3)	6.79 (2)
$H + H_3L \leftrightarrows H_4L$	8.68 (4)				3.95 (2)	2.99 (3)
$H + H_4L \leftrightarrows H_5L$	7.91 (5)					
$H + H_5L \leftrightarrows H_6L$	7.37 (4)					
$H + H_6L \leftrightarrows H_7L$	2.2 (1)					
$2H + H_4L \leftrightarrows H_6L$					6.89 (2)	
log β[f]	56.3	24.1	22.68	nd	35.4	29.99
Mean No. Prot. pH = 7.4	5.3	2.0	1.7	–	1.9	2.2

[a] 0.15 M NaCl, log K of **1** ref. 25.
[b] 0.15 M $NaClO_4$.
[c] 0. 15 M NaCl in EtOH:H_2O (30:70).
[d] Charges omitted.
[e] Values in parentheses are standard deviations in the last significant figure.
[f] log β = Σ Log K.

ammonium groups) at the physiological pH of 7.4 to be rather constant for all the compounds varying from 2 for **5** to 2.8 for **3**. Even if dansyl has an additional step, such a protonation occurs at a much lower pH since it affects the tertiary amine groups of the dansyl moiety.

All the three-substituted compounds show three relatively high constants that can be ascribed to the protonation of the secondary amine groups, while **11** and **12** show additional protonation steps attributable to the nitrogen atoms of the quinoline moieties. However, in spite of having additional protonable heterocycles, all the tri-substituted compounds show, analogously to the mono-substituted derivatives, protonation degrees at physiological pH around 2.0.

In a first approach and taking into account the behaviour of related ligands, all these compounds should be able to interiorize within the parasite cells [59,60]. The only difference in this respect is compound **1**, derivative functionalized with aminopropyl moieties, which presents a protonation degree of 5.2 which might be too high for permitting an effective capture within the cells.

3.2. Biology

3.2.1. In vitro biological activity

The genetic diversity of *T. cruzi* is widely recognized. Currently, *T. cruzi* is divided into seven DTUs, with different genotype, phenotype, evolutionary relationships, ecological and epidemiological associations, tropism, pathogenesis and drug resistance [57]. Accordingly, three different *T. cruzi* strains (TcI, TcV and TcVI), with different locations, hosts and tropisms, were used to determine the compounds with good performance.

The extracellular epimastigote form is the most frequently used owing to its simple culture in the laboratory. However, tests against the developed forms in vertebrate hosts, BT and intracellular amastigote form (responsible for the chronic phase of CD), are more interesting [58]. Moreover, according to some authors, potential antichagas agents must meet certain criteria: a) $IC_{50} \leq 10$ μM, and SI > 10 [61]; b) $IC_{50} < 5$ μM, SI > 10 [62]; c) SI > 50 [63]. Therefore, the *in vitro* trypanocidal activities of polyamines **1**–**12** and the reference drug BZN were evaluated, after a 72-h exposure, in epimastigote forms as a primary screening. The potential polyamines were then tested against the amastigote and trypomastigote forms as relevant forms from the clinic with the aim of obtaining the inhibition concentrations 50 (IC_{50} values) (Table 3).

Alternatively, the cytotoxicity of polyamines **1**–**12** was tested using mammalian Vero cells to determine the toxicity and the selectivity index (SI) (Table 4). Interestingly, almost all these polyamines, after a 72-h exposure, were substantially less toxic than BZN. The cytotoxicity IC_{50} values ranged from 20.5 to 1765.4 μM (most of them with a value higher than 200 μM) in contrast to BZN (23.2 μM). In brackets it has been added the number of times that the compound SI exceeded the reference drug BZN SI.

Four polyamines (**3**, **7**, **11** and **12**) showed SI values that were between 12 and 186-fold higher than BZN at least for one of the strains. Subsequently, these 4 polyamines were tested against amastigote and trypomastigote forms. Thereafter, polyamines **7** and **12** met the most stringent requirements mentioned above about the IC_{50} values at least for one of the parasite forms in vertebrate hosts for the three *T. cruzi* strains. Regarding the SI, it should be noted that both compounds fullfiled the requirement of having values over 50 for the 3 parasite forms and the 3 *T. cruzi*

Table 3
In vitro activity and toxicity for compounds on extra- and intracellular forms of *Trypanosoma cruzi* strains.

Comp.	Activity IC_{50} (μM)[a]			Activity IC_{50} (μM)[a]			Activity IC_{50} (μM)[a]			Toxicity IC_{50} Vero cell (μM)[b]
	T. cruzi Arequipa strain			*T. cruzi* SN3 strain			*T. cruzi* Tulahuen strain			
	Epim. forms	Amast. forms	Trypom. forms	Epim. forms	Amast. forms	Trypom. forms	Epim. Forms	Amast. Forms	Trypom. forms	
BZN	16.9 ± 1.8	8.3 ± 0.7	12.4 ± 1.1	36.2 ± 2.4	16.6 ± 1.4	36.1 ± 3.1	19.7 ± 1.7	10.0 ± 0.8	15.1 ± 1.3	23.2 ± 2.1
1	127.6 ± 11.7	nd	nd	123.6 ± 11.8	nd	nd	202.0 ± 19.2	nd	nd	1176.0 ± 110.4
2	29.6 ± 2.7	nd	nd	16.2 ± 1.4	nd	nd	54.7 ± 5.1	nd	nd	20.5 ± 1.9
3	42.5 ± 4.0	nd	nd	8.0 ± 0.7	21.1 ± 2.2	18.4 ± 2.0	13.6 ± 1.1	26.4 ± 2.8	19.0 ± 2.1	202.1 ± 25.7
4	22.7 ± 2.2	nd	nd	71.0 ± 6.9	nd	nd	21.9 ± 2.3	nd	nd	33.4 ± 3.1
5	65.9 ± 6.6	nd	nd	101.2 ± 11.4	nd	nd	87.4 ± 8.9	nd	nd	136.7 ± 15.1
6	132.4 ± 15.4	nd	nd	90.4 ± 8.8	nd	nd	84.9 ± 9.0	nd	nd	842.5 ± 75.1
7	26.6 ± 2.4	4.8 ± 0.4	14.7 ± 1.2	19.3 ± 1.4	19.7 ± 2.7	12.4 ± 1.1	30.7 ± 2.8	15.1 ± 1.3	17.6 ± 1.4	1765.4 ± 158.4
8	24.0 ± 2.0	nd	nd	15.8 ± 1.7	nd	nd	14.7 ± 0.5	nd	nd	22.3 ± 2.4
9	72.4 ± 7.0	nd	nd	185.5 ± 19.9	nd	nd	88.2 ± 9.1	nd	nd	678.1 ± 74.2
10	15.3 ± 1.4	nd	nd	9.4 ± 0.8	nd	nd	7.2 ± 0.8	nd	nd	36.6 ± 4.1
11	11.9 ± 12.4	20.1 ± 1.8	14.3 ± 1.2	25.1 ± 2.1	nd	nd	23.5 ± 2.5	nd	nd	198.7 ± 21.0
12	15.1 ± 1.4	2.4 ± 2.3	1.2 ± 0.1	14.0 ± 2.2	1.6 ± 0.2	1.1 ± 0.1	19.5 ± 1.7	2.3 ± 0.2	1.9 ± 0.2	1564.6 ± 180.1

[a] IC_{50} = the concentration required to give 50% inhibition, calculated using GraphPad Prism 6. Results are averages of three separate determinations ± standard deviation.
[b] Towards Vero cells after a 72-h culture. nd, not determined.

Table 4
Selectivity index for compounds on extra- and intracellular forms of *T. cruzi* strains.

Comp.	Selectivity index			Selectivity index			Selectivity index		
	T. cruzi Arequipa strain[a]			*T. cruzi* SN3 strain[a]			*T. cruzi* Tulahuen strain[a]		
	Epim. forms	Amast. forms	Trypom. forms	Epim. forms	Amast. forms	Trypom. forms	Epim. Forms	Amast. Forms	Trypom. forms
BZN	1.4	2.8	1.9	0.6	1.4	0.6	1.2	2.3	1.5
3	4.8 (3)	nd	nd	25.4 (42)	9.6 (7)	11.0 (18)	14.8 (12)	7.7 (3)	10.6 (7)
7	66.3 (48)	364.8 (130)	120.0 (63)	91.3 (152)	89.6 (64)	142.3 (236)	57.5 (48)	117.1 (51)	100.4 (67)
11	16.7 (12)	9.9 (4)	13.9 (7)	7.9 (12)	nd	nd	8.5 (7)	nd	nd
12	109.7 (78)	692.3 (247)	1356.3 (713)	111.8 (186)	1015.1 (725)	1561.0 (2601)	84.8 (70)	707.1 (307)	889.6 (593)

[a] Selectivity index = IC_{50} Vero cells/IC_{50} extracellular and intracellular form of parasite. In brackets: number of times that compound exceeds the reference drug SI (on extracellular and intracellular forms of *Ttypanosoma cruzi*). nd, not determined.

strains. Moreover, they met the majority of the *in vitro* criteria of the target product profile (TPP) [62]. It was found that these polyamines were more active against the amastigote and trypomastigote forms of *T. cruzi*, reaching effectiveness between 51 and 2601-fold higher than BZN.

As summarised, these 2 polyamines showed a low toxicity and an excellent trypanocidal activity independent of the parasite forms. These compounds were chosen for further *in vivo* (see Fig. 1) and *in vitro* assays that were performed only with the *T. cruzi* Arequipa strain to reduce the number of animal testing, as there were no significant differences between the performances of the selected compounds for the other evaluated strains.

Ultimately, to obtain more accurate information regarding the most active polyamines, including BZN, the rates of infection in host Vero cells were measured by counting the number of infected cells after a 72-h exposure (Fig. 2), together with the amastigote and trypomastigote forms data. The rates of infected cells gradually decreased in all cases. Compound **12** should be highlighted, showing 0% of infected cells at 25 μM. In summary, polyamines **7** and **12** showed a higher efficiency than BZN. A decrease in the total number of amastigote and trypomastigote forms was also observed.

Likewise, to give an idea of the kill rate for the compounds, the average number of amastigote forms per cell was also determined (Fig. 3). The number of amastigotes per cell (and the rate of infected cells) decreased for all tested compounds, showing that compounds **7** and **12** are trypanocidal drugs because they cause the parasite death, and not only inhibit the multiplication (trypanostatic drug action), an important feature to avoid any relapse after chemotherapeutic treatment [62].

3.2.2. *In vivo* trypanocidal evaluation in BALB/c mice

Since polyamines **7** and **12** showed striking *in vitro* activities against the developed forms in vertebrate hosts, those compounds were evaluated in BALB/c mice. The experimental tests during the *in vivo* evaluation were carried out to determine the effectiveness of treatment in the acute and chronic phases because of the different effectiveness levels of current drugs in both phases; the performance of drugs during the chronic phase has not the desired effect [64]. Therefore, the compounds were evaluated by treating mice during 5 consecutive days from the 10th dpi for the mice treated in the acute phase, and from 75th dpi (there are no parasites in the bloodstream and it is established that the mice entered the chronic phase) for the mice treated in the chronic phase. Drugs were administered orally because the oral therapeutic route leads to better patient compliance, has a low cost (critical aspects in developing countries), and it is the preferred route for the treatment of parasitic diseases [65].

The treatment for both polyamines and the reference drug BZN was performed at subcurative doses for BZN (20 mg/kg per day for 5 days) to evaluate whether the polyamines showed higher *in vivo* activity than the reference drug. Signally, none of the mice died nor did they lose more than 10% body mass during or after treatment. Thereafter, the *in vivo* assays were performed to evaluate the following: a) Parasitaemia levels by counting BTs; b) Parasitaemia reactivation by counting BTs after IS; c) Parasites in tissues by PCR; d) Levels of immunoglobulin G (Ig G) by ELISA and splenomegaly as indicators of the immune response. Moreover, serum biochemical parameters by clinical chemistry measurements were performed as an indicator of metabolic abnormalities associated with the treatment.

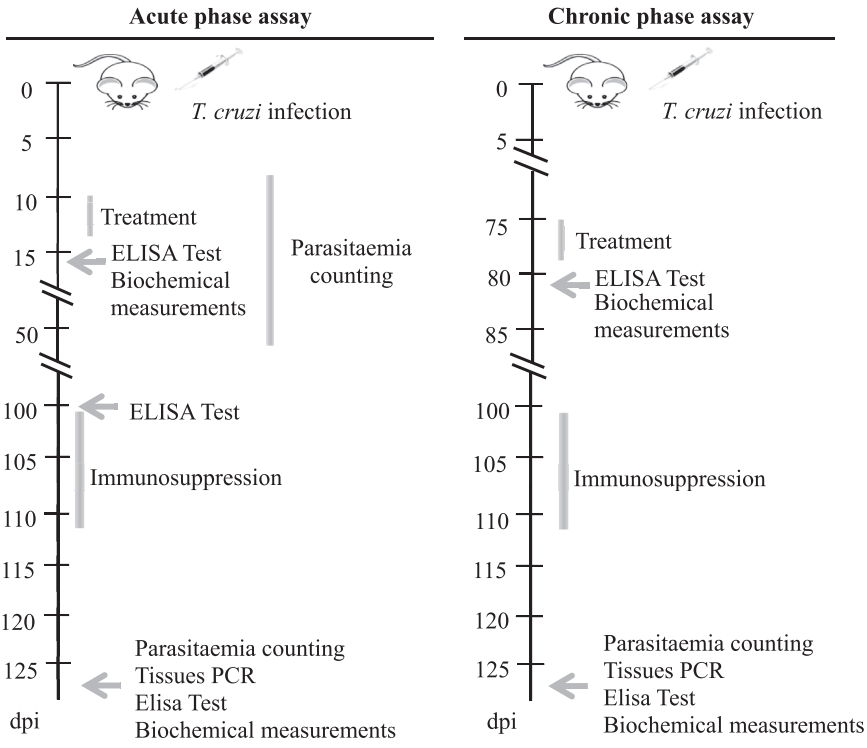

Fig. 1. Shows the timeline for all *in vivo* experiments in the acute and chronic phases.

First, parasitaemia levels in the different groups of untreated and treated mice in the acute phase were determined (Fig. 4). No significant differences were observed for mice treated with compound **12** compared with untreated (control) mice. However, a reduction of parasitaemia in compound **7**-treated mice with respect to the untreated mice was observed. This activity was evident since the beginning of the treatment (10th dpi) and it was maintained until the end of the acute phase. The peak of parasitaemia (23rd dpi) caused a reduction of 72% for compound **7** compared with the control group, being similar to BZN. Furthermore, parasitaemia was undetected on the 40th dpi for compound **7**, while it was observed until 50th and 47th dpi in the group of untreated- and BZN-treated mice, respectively. This finding appears to indicate that parasites were eliminated or depleted to non-detectable levels for counting, no longer detected in blood.

Second, to evaluate the effectiveness of the treatment and the disease extent in the chronic phase, the parasitaemia reactivation was determined after IS until 120th dpi (late chronic phase), when the amastigote forms are nested inside target tissues under the control of the immunological system of the mice. This matter is important since apparently cured immunocompromised individuals and patients submitted to liver or kidney transplantation (diagnosed with AIDS or treated with anticancer chemotherapy) present clinically aggressive parasitaemia reactivation. Therefore, IS is carried out as a first cure confirmation technique, with the second being PCR of the tissues: the infected and treated animals whose parasitaemia does not reappear and show negative PCR results for tissues are considered cured [66]. The percentage of parasitaemia reactivation after IS in comparison with the control groups, proportional to the survival rate of the parasites, is shown in Fig. 5. A reduction in the parasitaemia reactivation was observed for all mice treated in both the acute and chronic phases. In addition, both polyamines and BZN showed greater activity in the chronic phase treatment, since a lower parasitaemia reactivations were observed with respect to the control. As expected, the same subcurative dose of BZN was more active in the chronic than in the acute phase treatment (51.2% and 75.0%, respectively). The highest activity was observed for compound **7** since compound **7**-treated mice showed a parasitaemia reactivation with a value of 16.3% and 5.9% in the acute and chronic phases, respectively.

Finally, PCR was performed on the necropsy day (127th dpi) as a second technique of confirmation of cure to determine the presence of parasites in the target tissues and the curative effect of the compounds. Fig. 6 shows the PCR results for the target tissues in the different groups of mice. The PCR of the control groups in both the acute and chronic phases was positive for these 9 tissues (defined as target tissues): adipose, bone marrow, brain, oesophagus, heart, lung, muscle, spleen and stomach. As expected, the same subcurative dose of BZN was more active in the chronic (4 out of 9 target tissues were infected) than in the acute phase treatment (6 out of 9 target tissues were infected). Same results were observed for the mice treated with the tested compounds, according to the previous IS results. Compound 7-treated mice only showed 2 out of 9 tissues infected after treatment in the acute phase, and 1 out of 9 tissues infected after treatment in the chronic phase. The adipose tissue was the only tissue infected after the chronic phase treatment with compound **7**. Many of the current candidates to be antichagas agents show parasites located in adipose tissue after treatment in the chronic phase [67]. There are several reasons why these compounds could be less effective at eliminating parasites from this tissue, for instance, lesser drug accessibility or susceptibility to the parasite in a lipid/sterol rich environment [68,69]. It is proposed that the different effectiveness in the different phases is related to inadequate pharmacokinetics between the compounds and the tissue localization of parasites during the chronic phase [70]. Compound **7** can be studied at higher doses (since it do not present toxicity) establishing a new treatment guideline (based on pharmacokinetic studies) to achieve total cure.

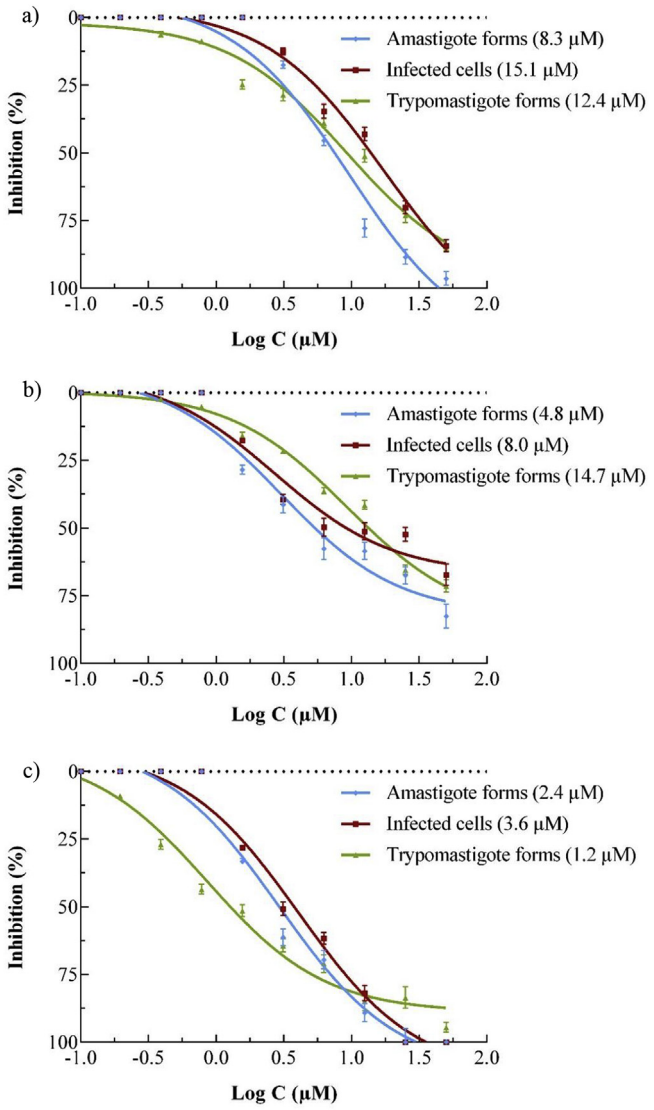

Fig. 2. Evaluation of the antitrypanosomal activity against amastigote and trypomastigote forms and infected cells treated with a) benznidazole, b) **7** and c) **12**. Values are the means of three separate experiments ± standard deviation. In brackets: IC_{50} value, calculated using GraphPad Prism 6.

Clinical cure in *T. cruzi* infections is a questionable assessment due to the lack of a reliable test to assure parasite elimination [71]. The main utility of the PCR technique is to verify the failure of clinical cure since even consistently negative results (using blood) are not enough to confirm the complete removal of tissue parasites [72,73]. For animal testing models, IS is the formula employed to demonstrate cure [46], and we assess the establishment of cure using a double confirmation based on the presence (or not) of parasites in blood (by IS) and in tissues (by PCR). Currently, highly sensitive techniques based on bioluminescence imaging are used to demonstrate cure, generating data with superior accuracy to PCR [74]. However, we can state evidence of curation (or, at least, a considerable reduction in the parasitic load) substantiated on the results of three independent samples by a double checking of cure (PCR and IS).

Since the titre of immunoglobulins is linked to the parasite load [75], the levels of total Ig G reflect the infection rate and verify the effectiveness ascribed to the tested compounds. Therefore, the immune status of the different groups of mice during infection were measured using the enzyme-linked immunosorbent assay (ELISA) [76], and the titre of anti-*T. cruzi* Ig G are shown in Fig. 7. All analysed samples from treated mice showed Ig G levels that decreased with respect to samples from untreated (control) mice, excluding the samples obtained 2 days after the treatment in the chronic phase. This is logical since those samples were retrieved from mice that suffered an acute phase without treatment, with the characteristic Ig G levels caused by the hypergammaglobulinemia of the infection by *T. cruzi*. Compound **12**-treated mice almost maintained the same levels as the untreated (control) mice, according to the PCR and IS assays. It should be noted that the Ig G levels of both groups of compound **7**-treated mice did not increase after IS due to the very low parasitaemia reactivation mentioned above. It has to be mentioned that, although the level of Ig G after IS do not provide relevant information about the treatment efficacy due to the depletion of T and B cells, these data verify the blockade of the immunological system of the mice.

Since the spleen is an involved organ in defence against infection, splenomegaly is another characteristic linked to the parasite load. Splenomegaly happens in experimentally infected mice during which the chronic mice spleen is often approximately twice the mass of uninfected mice spleen [74]. Therefore, the spleens from different groups of mice were weighed, and the data are shown in Fig. 8. Significantly, treatment even at subcurative doses of BZN decreases infection-induced splenomegaly since it is linked to a reduction of the parasite load [74]. Results obtained fom the ELISA assay were confirmed by splenomegaly tests since all polyamines and BZN reduced splenomegaly, and likewise infection rates. Compound 7-treated mice showed lesser splenomegaly than BZN-treated mice, exhibiting values very close to those of uninfected mice.

Kidney, heart and liver marker profiles were performed in untreated and treated mice in both phases of the disease to confirm the metabolic abnormalities associated with the treatment. The values for uninfected and untreated mice were also included. The data are shown in Table 5. All tested biochemical parameters for the evaluated compounds were no more altered than those obtained with BZN. Moreover, almost all those alterations were nonexistent or insignificant (less than 10%) the necropsy day of mice. Therefore, higher doses (since they do not present toxicity) and a new treatment guideline (to achieve better exposure in the bloodstream) could be studied to improve the effectiveness of compound 7 after studies based on pharmacokinetic (absorption, distribution, bioavailability and/or excretion). Likewise, these studies could be performed for compound **12** in order to know if its low *in vivo* activity, in contrast to the *in vitro* results, is due to poor treatment guideline.

3.2.3. Action mechanism studies

3.2.3.1. Metabolite excretion study. It is well-known that trypanosomatids, *T. cruzi* among them, are unable to completely degrade glucose to CO_2 in the presence of oxygen (so-called aerobic fermentation). Consistently, the parasites excrete into the medium a considerable portion of their hexose skeleton as partially oxidized end products in the form of fermented metabolites [77]. Focusing on *T. cruzi*, this parasite catabolizes glucose at a high rate, acidifying the medium owing to incomplete oxidation to acids [78]. The final products in this catabolism are mainly pyruvate, acetate, succinate, L-alanine, D-lactate and ethanol [79].

^{1}H NMR spectra of untreated and treated *T. cruzi* Arequipa epimastigotes were registered, qualitatively and quantitatively analysed and compared with those found for the control (untreated parasites) to know the effects of polyamines **7** and **12**, at IC_{25} concentrations, on glucose metabolism (spectra not shown). The data are shown in Fig. 9. The excretion of all metabolites (except

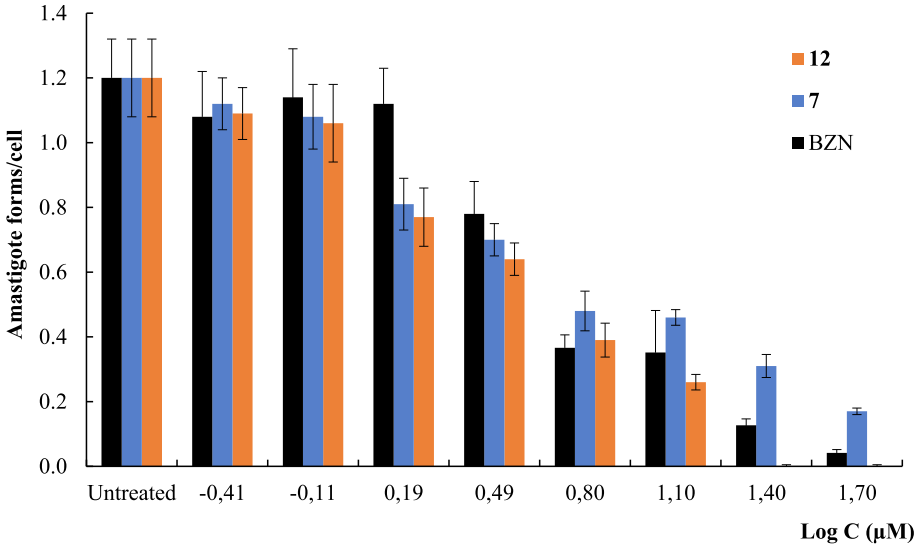

Fig. 3. Number of amastigote forms of *Trypanosoma cruzi* Arequipa strain per Vero cell treated with BZN, **7** and **9**. Values are the means of the three separate determinations ± standard deviation.

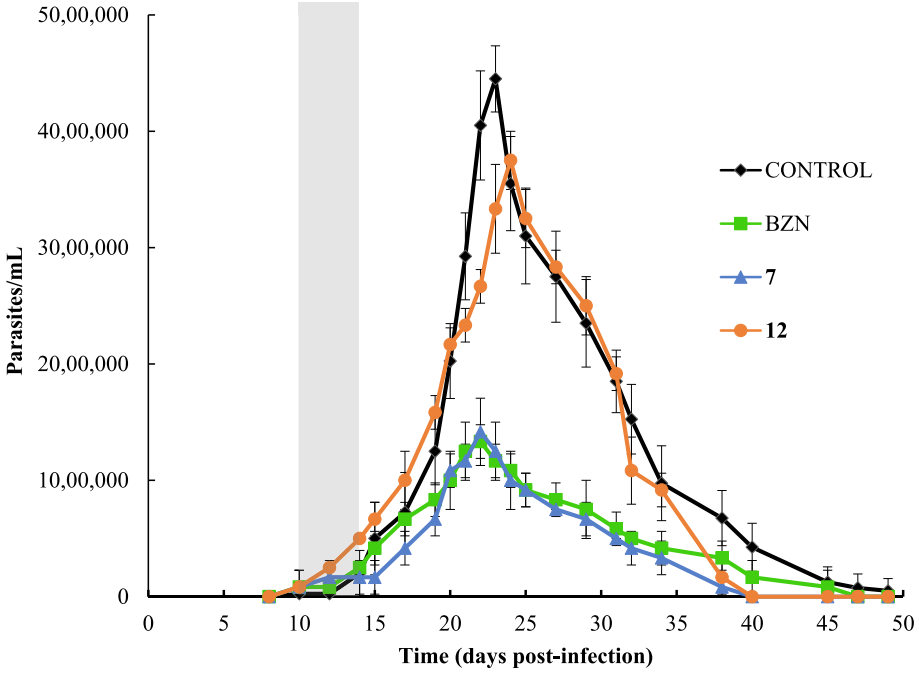

Fig. 4. Parasitaemia in murine model of acute Chagas Disease: (-◆-) untreated (control), (-■-) benznidazole, (-▲-) compound **7** and (- × -) compound **12**. In all cases, compounds were orally administered using 100 mg/kg of body mass. Treatment days are represented in grey. Values constitute means of three mice ± standard deviation.

glycerol) decreased after treatment with polyamines **7** and **12**, and the most remarkable decreases were for succinate and ethanol metabolites: 34% and 31% for compound 7, and 49% and 38% for compound 12, respectively. These alterations indicated a reduction on the catabolic glucose metabolism, and they can be a consequence of an inhibition in the first enzymes involved in this pathway (glycosomal level) or a consequence of a mitochondrial dysfunction: *T. cruzi* catabolizes glucose at a high rate through the pentose phosphate pathway (PPP), acidifying the glycosome medium owing to incomplete oxidation of the acid end products, such as pyruvate or succinate [78,79]. Subsequently, these metabolites are directed to the tricarboxylic acid (TCA) cycle in the mitochondria (succinate via malate) for ATP synthesis, along with the electron-transport chain [80]. In order to evaluate whether the alterations were a consequence of a mitochondrial dysfunction, studies were performed using Rho.

3.2.3.2. Effects on mitochondrial membrane potential and on DNA and RNA levels. To know wheter the glucose metabolism effects of polyamines **7** and **12** were a consequence of a dysfunction on the mitochondrial membrane potential, the fluorescence intensity of Rho was quantified by cytometry flow. The data are shown in Fig. 10. Currently, it is accepted that the BZN trypanocidal activity is produced through its reduction by type I nitroreductases, leading

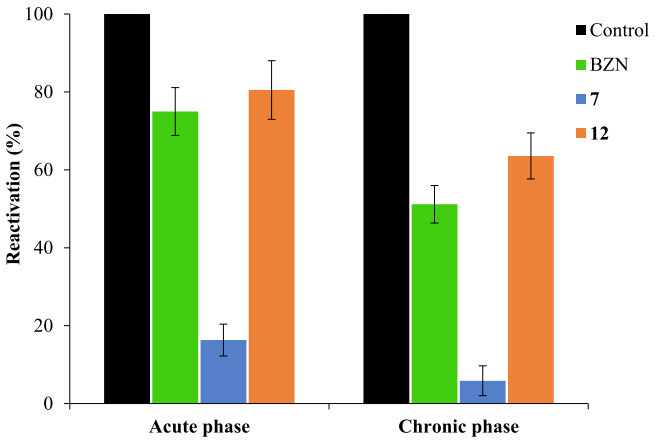

Fig. 5. Parasitaemia reactivation after the immunosuppression cycles for mice untreated (control) and treated with benznidazole, **7** and **12**. Values constitute means of three mice ± standard deviation.

its metabolization into glyoxal and other highly reactive metabolites [81]. This causes respiratory chain inhibition and the decrease observed in the mitochondrial membrane potential. On the one hand, compound **7**-treated cells labelled with Rho showed no depolarisation in the mitochondrial membrane, suggesting that the alteration observed on the catabolic glucose metabolism could be a consequence of an inhibition of the first enzymes involved in this pathway. On the other hand, analysis of compound **12**-treated cells indicated a considerable loss of the mitochondrial membrane potential (73.6%). This membrane depolarisation produces an imbalance in the ATP/ADP and NADH/NAD^+ ratios, in addition to a cellular accumulation of pyruvate, malate and succinate, causing a blockage of the glycolytic pathway [78]. Therefore, the alteration observed by compound **12** in catabolic glucose metabolism could be a consequence of its action at the mitochondrial level, and not by a direct effect on the glycosomal or cytoplasmic level.

In normal cells, active pumping of H^+ is produced in the mitochondrial membrane to maintain the electrochemical gradient, the integrity and the function of mitochondria. Since mitochondria play an imperative role in cell death decisions [82], alterations produced in this potential cause a decrease in ATP production that could affect DNA and RNA levels, causing necrosis and/or apoptosis. Therefore, the fluorescence intensities of AO of untreated and treated parasites were registered, and the data are shown in Fig. 11. Compound **7**-treated cells labelled with AO showed a decrease in AO fluoresence intensity, with an inhibition value of 18.3% with respect to the untreated cells, probably due to the ATP deficit produced by the alteration observed on the catabolic glucose metabolism. As expected, a higher decrease in the AO fluorescence intensity was observed for compound **12**-treated cells (56.7%). This considerable decrease in DNA and RNA levels could be due to the high ATP deficit caused by mitochondrial membrane depolarisation. It is interesting to note that the decrease in nucleic acids is not only due to an ATP deficit, but also random nucleic acid degradation as a feature commonly attributed to cell necrosis [83].

In conclusion, our findings suggest that compound **12** induces alterations in the mitochondrial membrane potential, which precedes *T. cruzi* cell death. Finally, to evaluate whether death of a mitochondrion-dependent manner is ultimately due to the redox

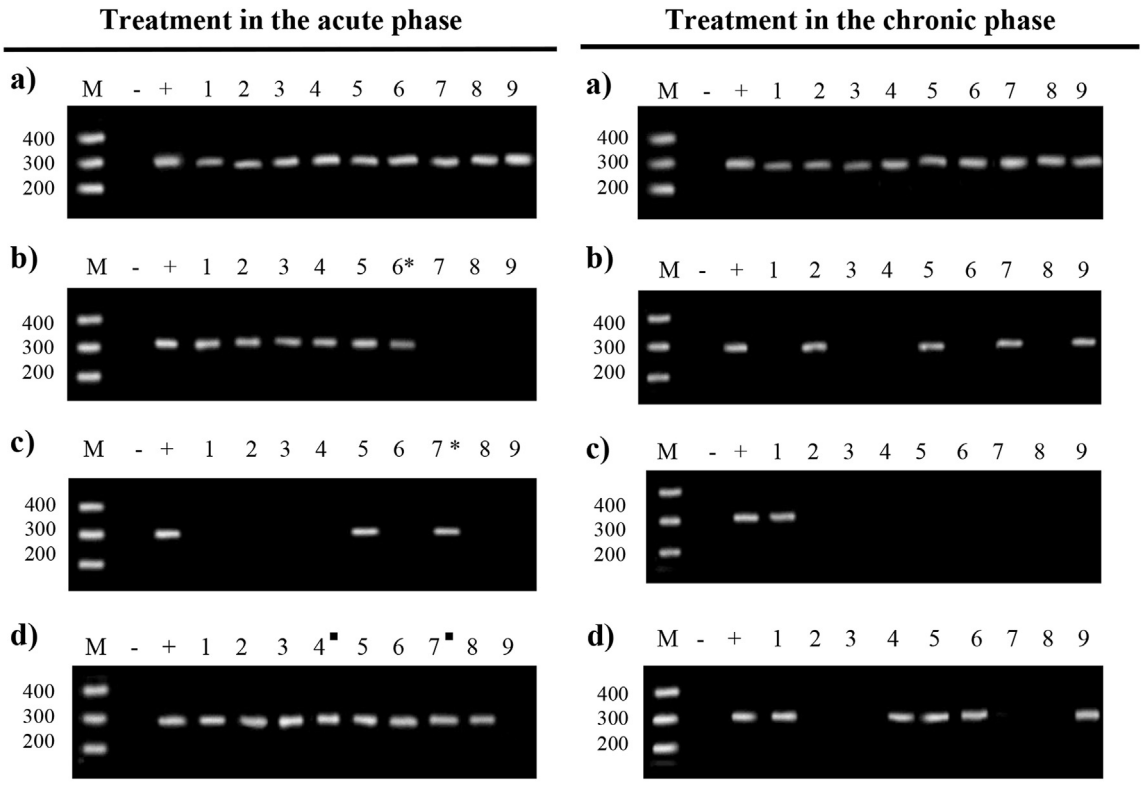

Fig. 6. PCR analysis of nine tissues at the final day of experiment in untreated (control) and treated mice. a) Shows untreated mice group, b) Shows the group of mice treated with Benznidazole, c) Shows the group of mice treated with **7**, d) Shows the group of mice treated with **12**. Lanes: M, base pair marker; -, PCR negative control; +, PCR positive control; 1, PCR adipose tissue; 2, PCR bone marrow tissue; 3, PCR brain tissue; 4, PCR opesophagus tissue; 5, PCR heart tissue; 6, PCR lung tissue; 7, PCR muscle tissue; 8, PCR spleen tissue; 9, PCR stomach tissue. *, It means that 2/6 of the corresponding tissue PCR products showed 300 bp band on electrophoresis; ■, It means that 1/3 of the corresponding tissue PCR products showed 300 bp band on electrophoresis; no *■, it means that 3/3 or 0/3 of the corresponding tissue PCR products showed 300 bp band on electrophoresis.

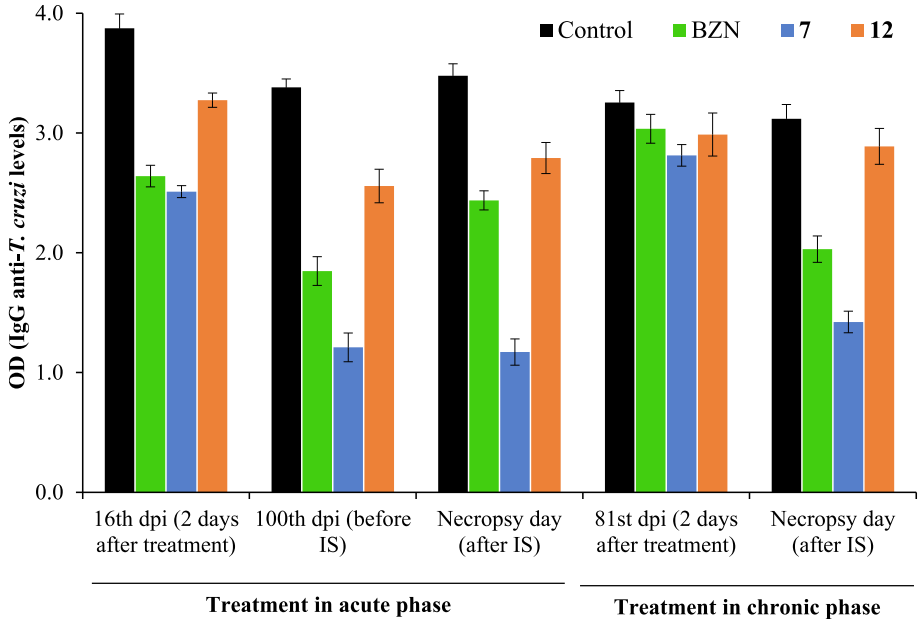

Fig. 7. Differences in the Ig G levels of anti-*T. cruzi* antibodies, expressed in absorbance units (optical density (OD) at 490 nm), between untreated (control) and treated groups of mice at different days post-infection (dpi). Values constitute means of three mice ± standard deviation. IS, immunosuppression.

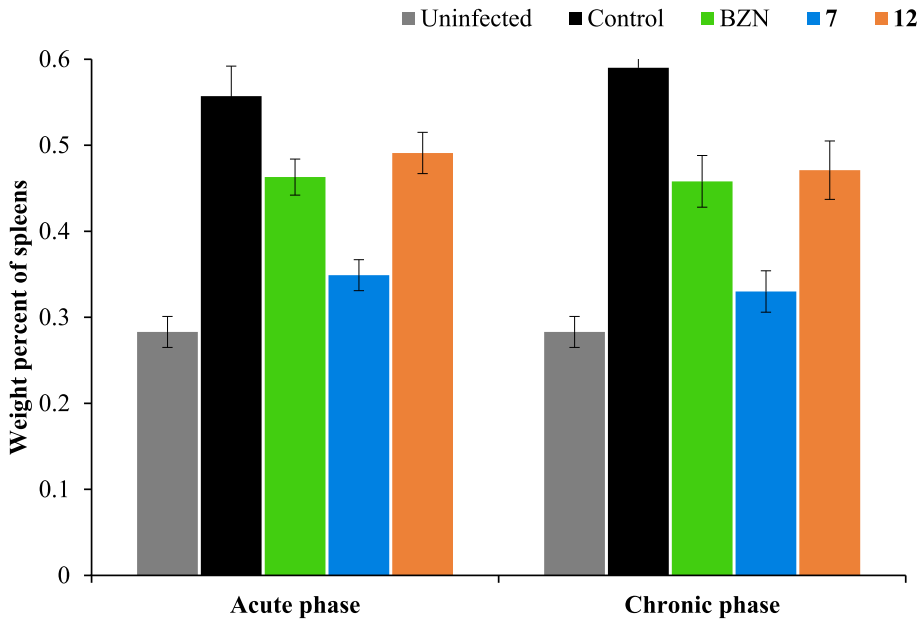

Fig. 8. Weight percentage of spleens of different groups of mice at the final day of experiment. Values constitute means of three mice ± standard deviation.

stress produced by inhibition of the mitochondrion-resident Fe-SOD enzyme [84], enzyme inhibition studies were performed using the method described by Beyer and Fridovich [56].

3.2.3.3. Inhibitory effect on the SOD enzyme. The trypanosomatid Fe-SOD enzyme has been given special importance for several reasons, including: it is absent in other eukaryotic cells [85,86], presents structural and biochemical differences with respect to its human homologue Cu/Zn-SOD, and its crucial role performed is the elimination of reactive oxygen species (ROS), allowing trypanosomatids to protect themselves from the damage produced by oxidative stress [87,88]. The design of an effective drug that is able to inhibit parasite Fe-SOD without inhibiting CuZn-SOD is an interesting goal. Therefore, iron and copperezinc superoxide dismutases (Fe-SODe and CuZn-SOD) activities were determined using the method described by Beyer and Fridovich [56]. The data are shown in Fig. 12, together with the corresponding calculated IC_{50} for both enzymes. For CuZn-SOD, IC_{50} values were over 100 μM for both polyamines **7** and **12**. For Fe-SOD, compound **7** was the least efficient, with an IC_{50} value (56.86 μM) too high to attribute the trypanocidal effect on the inhibition of this enzyme. Significant inhibitory values were found for compound **12**, with 82 and 100% inhibition at 50 and 100 μM, respectively, and an IC_{50} value of 29.01 μM. We suggest that this Fe-SOD enzyme be considered one of the targets of this compound, and modelling studies will be performed to further investigate this point. Because SOD enzyme is

Table 5
Biochemical clinical parameters measured at different experimental situations and days post-infection (dpi) in groups of mice infected with *Trypanosoma cruzi*.

		Kidney marker profile		Heart marker profile		Liver marker profile			
		Urea (mg/DL)	Uric acid (mg/DL)	CK-MB[a] (U/L)	LDH[b] (U/L)	AST/GOT[c] (U/L)	ALT/GPT[d] (U/L)	Total bilirubin (mg/DL)	Alkaline phosphatase (U/L)
Uninfected mice (n = 6)		36 [32–40]	4.7 [4.0–5.1]	420 [150–630]	3218 [2505–3851]	161 [132–177]	58 [46–62]	0.29 [0.22–0.31]	173 [141–192]
Treatment in the acute phase	16th dpi and untreated	31	4.3	535	3275	167	60	0.23	180
	16th dpi and BZN*	−	−	=	=	++++	++++	++	++
	16th dpi and **7***	−	−	−	−	++++	−	+++	++
	16th dpi and **12***	−	−	=	=	−	++++	+++	+
	Necropsy day of mice and untreated	34	4.0	496	2761	179	49	0.21	161
	Necropsy day of mice and BZN	−	=	=	=	++++	=	+	=
	Necropsy day of mice and **7**	=	=	=	=	+++	=	+	−
	Necropsy day of mice and **12**	=	=	=	=	+	+++	+	=
Treatment in the chronic phase	81st dpi and untreated	45	5.7	751	5951	260	57	0.25	167
	81st dpi and BZN*	−	−	−	−	++	++	+++	++++
	81st dpi and **7***	−	−	−	−	−	−	=	=
	81st dpi and **12***	−	−	=	=	−	−	+++	++
	Necropsy day of mice and untreated	37	4.8	538	6679	286	64	0.20	149
	Necropsy day of mice and BZN	−	−	=	−	+	=	++	++
	Necropsy day of mice and **7**	−	−	=	−	−	=	=	=
	Necropsy day of mice and **12**	−	+	=	=	+	+	−	=

Key: = , variation no larger than 10%; +, up to 10% increase over the range; ++, up to 20% increase over the range; +++, up to 30% increase over the range; ++++, more than 40% increase over the range; −, up to 10% decrease over the range; − −, up to 20% decrease over the range; − − −, up to 30% decrease over the range; − − − −, more than 40% decrease over the range.

[a] CK-MB, creatine kinase-muscle/brain.
[b] LDH, lactate dehydrogenase.
[c] AST/GOT, aspartate aminotransferase.
[d] ALT/GPT, alanine aminotransferase.
* 2 days after treatment.

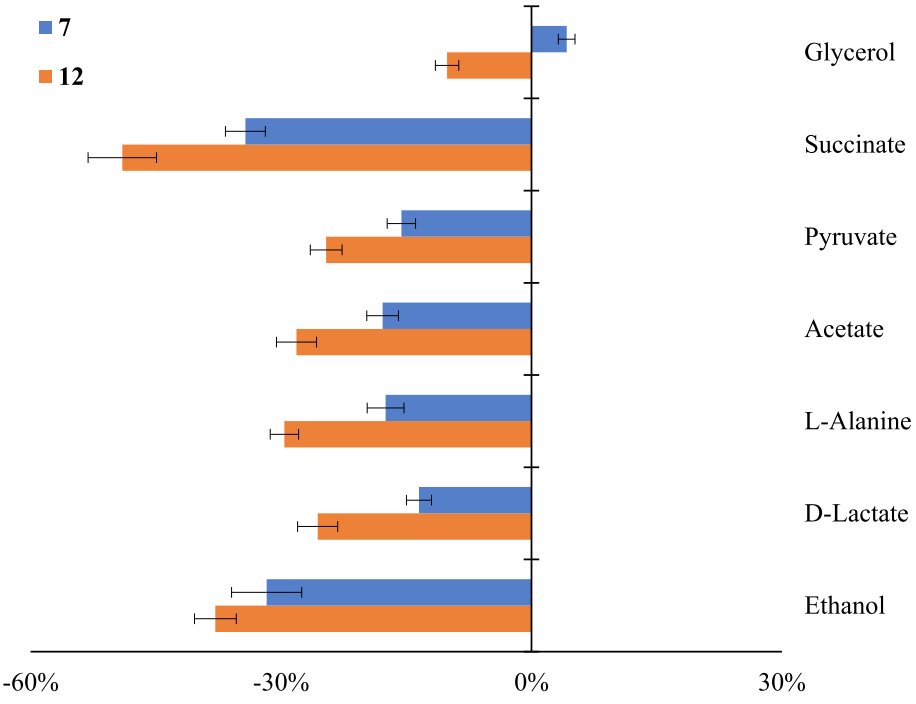

Fig. 9. Percentages of variation among peaks of catabolites excreted by epimastigotes of *Trypanosoma cruzi* Arequipa strain exposed to compounds **7** and **12** at their IC_{25} in comparison to a control (untreated) incubated 72 h. Values are the means of three separate determinations ± standard deviation.

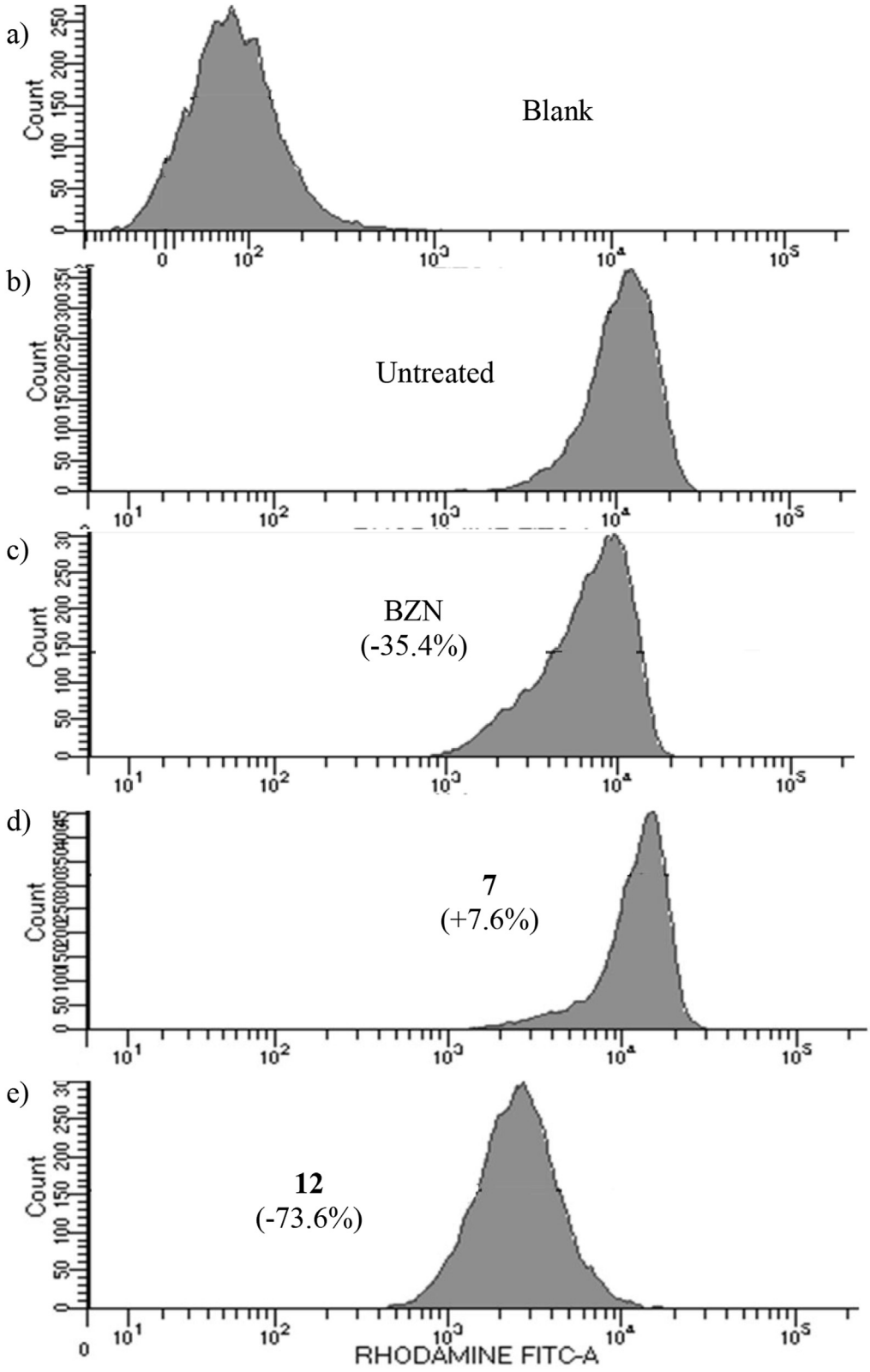

Fig. 10. Cytometry analysis of the mitochondrial membrane potential from epimastigotes of *Trypanosoma cruzi* Arequipa strain exposed to benznidazole and compounds **7** and **12** at their IC_{25} in comparison to a control (untreated) incubated 72 h: a) blank, b) control (untreated), c) benznidazole, d) **7** and e) **12**. In brackets: variation, in percentage, on mitochondrial membrane potential with respect to untreated parasites. Values are the means of three separate determinations.

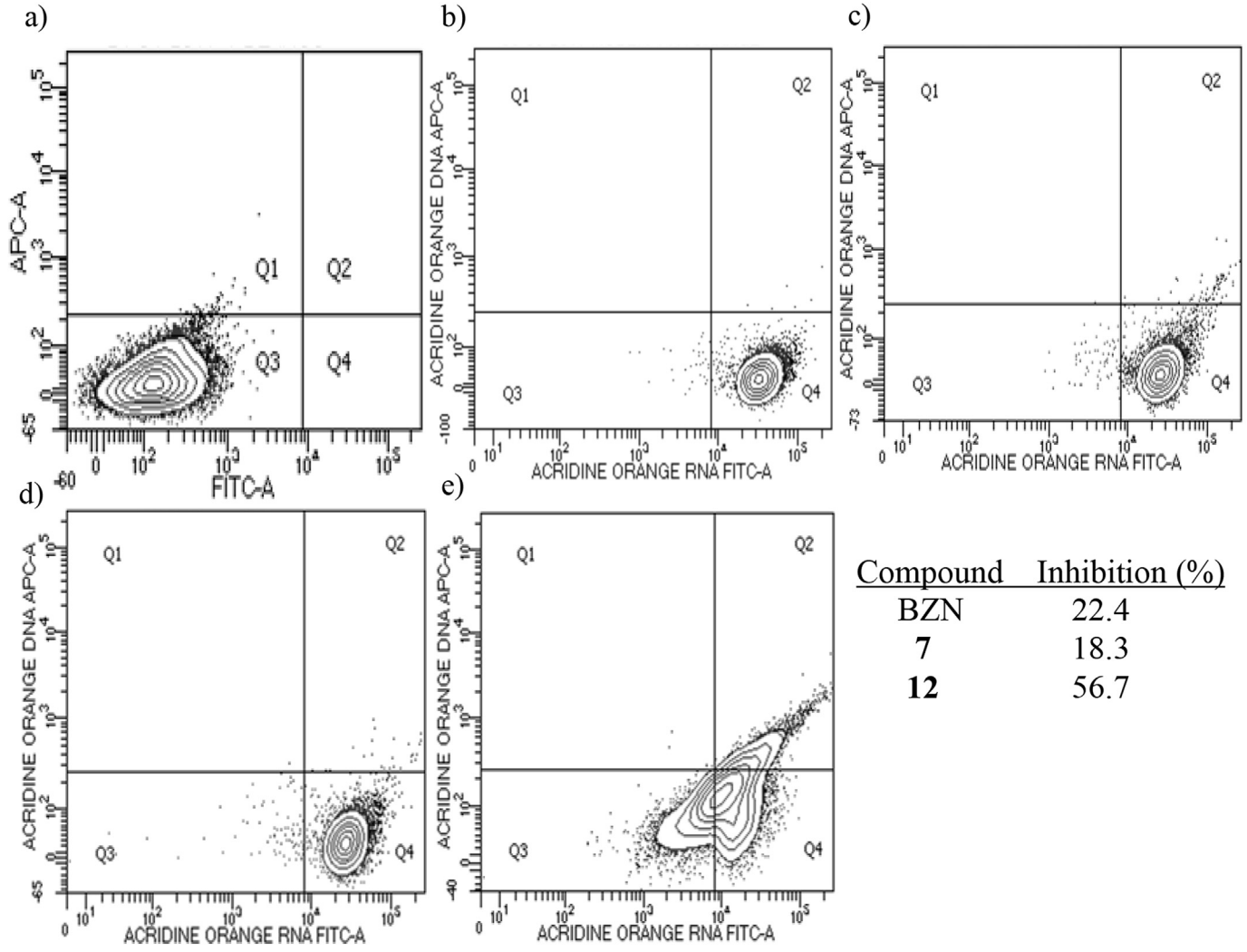

Compound	Inhibition (%)
BZN	22.4
7	18.3
12	56.7

Fig. 11. Cytometry analysis of the inhibition in DNA and RNA levels of epimastigotes of *Trypanosoma cruzi* Arequipa strain exposed to benznidazole and compounds **7** and **12** at their IC_{25} in comparison to a control (untreated) incubated 72 h: a) blank, b) control (untreated), c) benznidazole, d) **7** and e) **12**. Values are the means of three separate determinations.

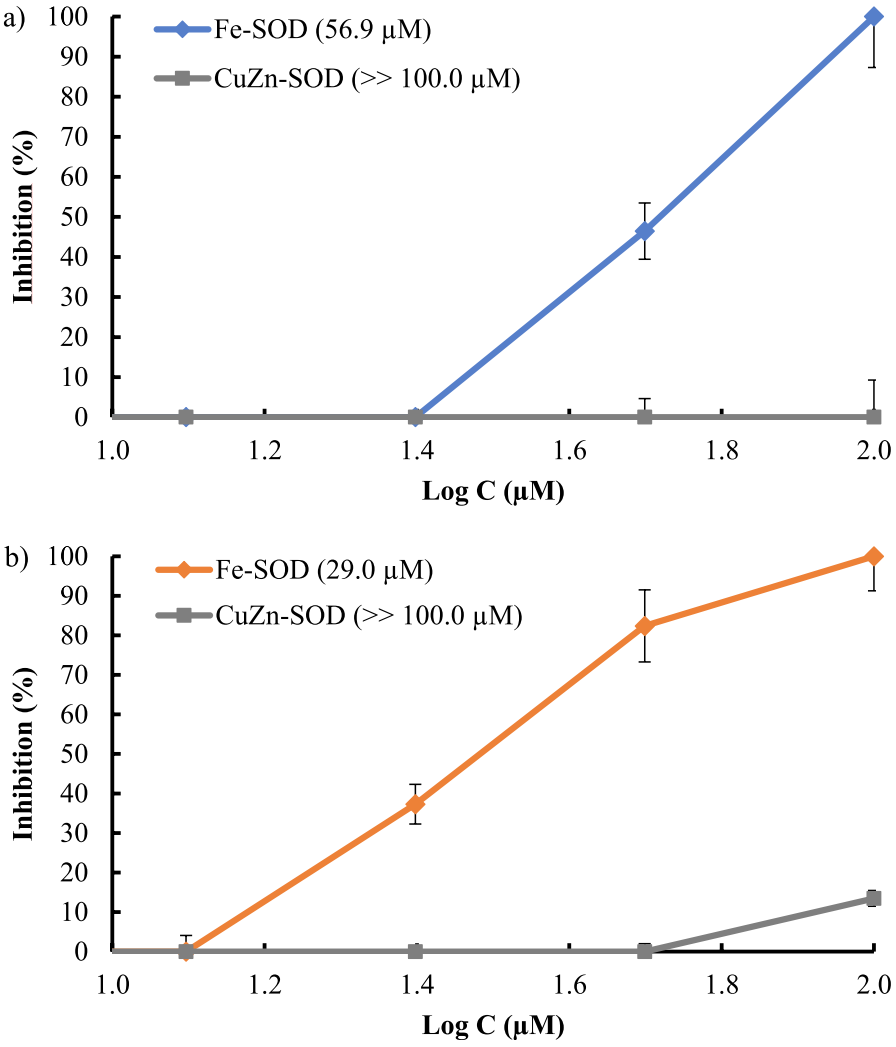

Fig. 12. Fe-SOD *in vitro* inhibition (%) from epimastigotes of *Trypanosoma cruzi* Arequipa strain (activity 42.0 ± 3.8 U/mg) and of CuZn-SOD from human erythrocytes (activity 47.3 ± 4.1 U/mg) for compounds a) **7** and b) **12**. Activity differences in the control vs. the sample incubated using compounds were identified by the Newman-Keuls test. Values are the average of three separate rate determinations ± standard deviation. In brackets: IC_{50} value, calculated by linear regression analysis.

an essential component of the mitochondrial redox stress response [89], this inhibition could be the final cause of both mitochondrial dysfunction and blockage in the glycolytic pathway. The possibility of a multitarget compounds should not be discarded.

4. Conclusions

In conclusion, the trypanocidal properties of these compounds have been examined both *in vitro* and *in vivo*. These assays allowed us to identify 2 polyamines (**7** and **12**) which exhibited improved *in vitro* trypanocidal properties: higher activity, larger spectrum of action and less toxicity than the reference drug BZN. In regard to *in vivo* activity, compound **7** showed greater activity than BZN for treating CD in both the acute and chronic phases, as indicated by the tissues PCR. Parallel studies have been performed to establish the mechanisms of action at the glycosomal and mitochondrial levels, showing that the trypanocidal activity of compound **7** could be related to a glycosomal effect. Owing to their promising activity, others high-level studies should be considered to obtain an improved efficiency. Moreover, it deserves mention that higher doses and combined therapies should be considered due to their different mechanisms of action (after improving the pharmacokinetics of both compounds). Therefore, we present candidate molecules that are easy to synthesise as a promising therapeutic alternative for the development of a new antichagas agent.

Conflicts of interest

The authors have no competing interests to declare and have no conflicts of interest.

Acknowledgments

Financial support by the Spanish Ministry of Economy and Competitiveness, MINECO (CONSOLIDER-INGENIO 2010 CSD2010-00065). R.M.-E. is grateful for a FPU Grant (FPU14/01537) from the Ministry of Education of Spain. Dr. E.M.-C.. acknowledges a post-doctoral fellowship from Junta de Andalucia.

Appendix A. Supplementary data

Supplementary data to this article can be found online at https://doi.org/10.1016/j.ejmech.2018.12.034.

References

[1] Á. Moncayo, A.C. Silveira, Current epidemiological trends of Chagas disease in Latin America and future challenges in epidemiology, surveillance, and health policies, in: second ed.Am. Trypanos. Chagas Dis. One Hundred Years Res, vol. 104, 2009, pp. 17–30, https://doi.org/10.1016/B978-0-12-801029-7.00004-6.

[2] C. Bern, Chagas' Disease, N. Engl. J. Med. 373 (2015) 456–466, https://doi.org/10.1056/NEJMra1410150.

[3] DNDi (Drugs for Neglected Diseases initiative), Diseases & projects – Chagas disease. https://www.dndi.org/diseases-projects/chagas/, 2018 accessed September 10, 2018.

[4] J.A. Urbina, Specific chemotherapy of Chagas disease: relevance, current limitations and new approaches, Acta Trop. 115 (2010) 55–68, https://doi.org/10.1016/j.actatropica.2009.10.023.

[5] A.J. Romanha, S.L. de Castro, M.N. Correia Soeiro, J. Lannes-Vieira, I. Ribeiro, A. Talvani, B. Bourdin, B. Blum, B. Olivieri, C. Zani, C. Spadafora, E. Chiari, E. Chatelain, G. Chaves, J.E. Calzada, J.M. Bustamante, L.H. Freitas-junior, L.I. Romero, M.T. Bahia, M. Lotrowska, M. Soares, S.G. Andrade, T. Armstrong, W. Degrave, Z.D.A. Andrade, *In vitro* and *in vivo* experimental models for drug screening and development for Chagas disease, Mem. Inst. Oswaldo Cruz 105 (2010) 233–238.

[6] A. Rassi Jr., A. Rassi, J.A. Marin-Neto, Chagas disease, Lancet 375 (2010) 1388–1402, https://doi.org/10.1016/S0140-6736(10)60061-X.

[7] S.P. Montgomery, M.C. Starr, P.T. Cantey, M.S. Edwards, S.K. Meymandi, Neglected parasitic infections in the United States: Chagas disease, Am. J. Trop. Med. Hyg. 90 (2014) 814–818, https://doi.org/10.4269/ajtmh.13-0726.

[8] Y. Jackson, M.V. Herrera, J. Gascon, Economic crisis and increased immigrant mobility: new challenges in managing Chagas disease in Europe, Bull. World Health Organ. 92 (2014) 771–772, https://doi.org/10.2471/BLT.13.134072.

[9] R.L. Tarleton, CD8+ T cells in *Trypanosoma cruzi* infection, Semin. Immunopathol. 37 (2015) 233–238, https://doi.org/10.1007/s00281-015-0481-9.

[10] A.F. Henao-Martínez, D.A. Schwartz, I.V. Yang, Chagasic cardiomyopathy, from acute to chronic: is this mediated by host susceptibility factors? Trans. R. Soc. Trop. Med. Hyg. 106 (2012) 521–527, https://doi.org/10.1016/j.trstmh.2012.06.006.

[11] E. Cunha-Neto, C. Chevillard, Chagas disease cardiomyopathy: immunopathology and genetics, Mediat. Inflamm. 2014 (2014) 683230, https://doi.org/10.1155/2014/683230.

[12] A. Rassi, A. Rassi Jr., J.A. Marin-Neto, Posaconazole versus benznidazole for chronic Chagas' disease, N. Engl. J. Med. 371 (2014) 965–966, https://doi.org/10.1056/NEJMc1407914.

[13] R. Reithinger, R.L. Tarleton, J.A. Urbina, U. Kitron, R.E. Gürtler, Eliminating Chagas disease: challenges and a roadmap, Br. Med. J. 338 (2009) b1283, https://doi.org/10.1136/bmj.b1283.

[14] S.R. Wilkinson, J.M. Kelly, Trypanocidal drugs: mechanisms, resistance and new targets, Expert Rev. Mol. Med. 11 (2009) e31, https://doi.org/10.1017/S1462399409001252.

[15] J.R. Coura, S.L. De Castro, A critical review on Chagas disease chemotherapy, Mem. Inst. Oswaldo Cruz 97 (2002) 3–24, https://doi.org/10.1590/S0074-02762002000100001.

[16] R. Viotti, C. Vigliano, B. Lococo, M.G. Alvarez, M. Petti, G. Bertocchi, A. Armenti, Side effects of benznidazole as treatment in chronic Chagas disease: fears and realities, Expert Rev. Anti Infect. Ther. 7 (2009) 157–163, https://doi.org/10.1586/14787210.7.2.157.

[17] A.L.S. Sgambatti de Andrade, F. Zicker, R.M. de Oliveira, S. Almeida Silva, A. Luquetti, L.R. Travassos, I.C. Almeida, S.S. de Andrade, J.G. de Andrade, C.M.T. Martelli, Randomised trial of efficacy of benznidazole in treatment of early *Trypanosoma cruzi* infection, Lancet 348 (1996) 1407–1413, https://doi.org/10.1016/S0140-6736(96)04128-1.

[18] A. Prata, Clinical and epidemiological aspects of Chagas disease, Lancet. Inf. Disp. 1 (2001) 92–100, https://doi.org/10.1016/S1473-3099(01)00065-2.

[19] G. Rojo, C. Castillo, J. Duaso, A. Liempi, D. Droguett, N. Galanti, J.D. Maya, R. López-Muñoz, U. Kemmerling, Toxic and therapeutic effects of Nifurtimox and Benznidazol on *Trypanosoma cruzi* ex vivo infection of human placental chorionic villi explants, Acta Trop. 132 (2014) 112–118, https://doi.org/10.1016/j.actatropica.2014.01.002.

[20] S.R. Wilkinson, M.C. Taylor, D. Horn, J.M. Kelly, I. Cheeseman, A mechanism for cross-resistance to nifurtimox and benznidazole in trypanosomes, Proc. Natl. Acad. Sci. U.S.A. 105 (2008) 5022–5027, https://doi.org/10.1073/pnas.0711014105.

[21] A.M. Mejia, B.S. Hall, M.C. Taylor, A. Gómez-Palacio, S.R. Wilkinson, O. Triana-Chávez, J.M. Kelly, Benznidazole-resistance in *Trypanosoma cruzi* is a readily acquired trait that can arise independently in a single population, J. Infect. Dis. 206 (2012) 220–228, https://doi.org/10.1093/infdis/jis331.

[22] J. Bermudez, C. Davies, A. Simonazzi, J. Pablo Real, S. Palma, Current drug therapy and pharmaceutical challenges for Chagas disease, Acta Trop. 156 (2015) 1–16, https://doi.org/10.1016/j.actatropica.2015.12.017.

[23] D.A. Nicoll-Griffith, Use of cysteine-reactive small molecules in drug discovery for trypanosomal disease, Expert Opin. Drug Discov. 7 (2012) 353–366, https://doi.org/10.1517/17460441.2012.668520.

[24] P.J. Hotez, M.E. Bottazzi, C. Franco-Paredes, S.K. Ault, M.R. Periago, The neglected tropical diseases of Latin America and the caribbean: a review of disease burden and distribution and a roadmap for control and elimination, PLoS Neglected Trop. Dis. 2 (2008) e300, https://doi.org/10.1371/journal.pntd.0000300.

[25] M.T. Albelda, E. García-España, H.R. Jiménez, J.M. Llinares, C. Soriano, A. Sornosa-Ten, B. Verdejo, Cu^{2+} and AMP complexation of enlarged tripodal polyamines, Dalton Trans. (2006) 4474–4481, https://doi.org/10.1039/b605639c.

[26] M.P. Clares, J. Aguilar, R. Aucejo, C. Lodeiro, M.T. Albelda, F. Pina, J.C. Lima, A. Parola, J. Pina, J. Seixas de Melo, C. Soriano, E. García-España, Synthesis and H^{+}, Cu^{2+} and Zn^{2+} coordination behaviour of a bis(fluorophoric) bibracchial lariat aza-crown, Inorg. Chem. 43 (2004) 6114–6122, https://doi.org/10.1021/ic049694t.

[27] G. De Santis, L. Fabrizzi, M. Licchelli, A. Poggi, A. Taglietti, Molecular recognition of carboxilate ions based on the metal-ligand interaction and signaled through fluorescence quenching, Angew. Chem., Int. Ed. Engl. 35 (1996) 202–204, https://doi.org/10.1002/anie.199602021.

[28] E. Carbonell, E. Delgado-Pinar, J. Pitarch-Jarque, J. Alarcón, E. García-España, Boehmite supported pyrene polyamine systems as probes for iodide recognition, J. Phys. Chem. C 117 (2013) 14325–14331, https://doi.org/10.1021/jp4032546.

[29] L. Prodi, M. Montalti, N. Zaccheroni, F. Dallavalle, G. Folesani, M. Lanfranchi, R. Corradini, S. Pagliari, R. Marchelli, Dansylated polyamines as fluorescent sensors for metal ions photophysical properties and stability of copper(II) complexes in solution, Helv. Chim. Acta 84 (2001) 690–706, https://doi.org/10.1002/1522-2675(20010321)84:3<690::AID-HLCA690>3.0.CO;2-L.

[30] B. Biswal, A. Pal, A.B. Bag, Two-step FRET Mediated metal-ion induced signalling responses in a probe appended with three fluorophores, Dalton Trans. 46 (2017) 8975–8991, https://doi.org/10.1039/c7dt01592e.

[31] A.K. Covington, M. Paabo, R.A. Robinson, R.G. Bates, Use of the glass electrode in deuterium oxide and the relation between the standardized pD (paD) scale and the operational pH in heavy water, Anal. Chem. 40 (1968) 700–706, https://doi.org/10.1021/ac60260a013.

[32] E. Garcia-Espafia, M. Ballester, F. Lloret, J.M. Moratal, J. Faus, A. Bianchi, Low-spin six-co-ordinate cobalt(II) complexes, in: A Solution Study of Tris(violurato)cobaltate(II) Ions, 1988, pp. 101–104.

[33] G. Gran, H. Dahlenborg, S. Laurell, M. Rottenberg, Determination of the equivalent point in potentiometric titrations, Acta Chem. Scand. 4 (1950) 559–577, https://doi.org/10.3891/acta.chem.scand.04-0559.

[34] F.J.C. Rossotti, H. Rossotti, Potentiometric titrations using Gran plots: a textbook omission, J. Chem. Educ. 42 (1965) 375, https://doi.org/10.1021/ed042p375.

[35] M. Fontanelli, M. Micheloni, in: Procedings of the I Spanish-Italian Congress of Thermodinamics of Metal Complexes, 1990.

[36] P. Gans, A. Sabatini, A. Vacca, Investigation of equilibria in solution. Determination of equilibrium constants with the HYPERQUAD suite of programs, Talanta 43 (1996) 1739–1753, https://doi.org/10.1016/0039-9140(96)01958-3.

[37] P. Gans, Program to Determine the Distribution of Species in Multiequilibra Systems from the Stability Constants and Mass Balance Equations.

[38] J. Téllez-Meneses, A.M. Mejía-Jaramillo, O. Triana-Chávez, Biological characterization of *Trypanosoma cruzi* stocks from domestic and sylvatic vectors in Sierra Nevada of Santa Marta, Colombia, Acta Trop. 108 (2008) 26–34, https://doi.org/10.1016/j.actatropica.2008.08.006.

[39] R. Martín-Escolano, E. Moreno-viguri, M. Santivañez-Veliz, Á. Martín-Montes, E. Medina-carmona, R. Paucar, C. Marín, A. Azqueta, N. Cirauqui, A.L. Pey, S. Pérez-silanes, M. Sánchez-moreno, Second generation of Mannich base type derivatives with *in vivo* activity against *Trypanosoma cruzi*, J. Med. Chem. 61 (2018) 5643–5663, https://doi.org/10.1021/acs.jmedchem.8b00468.

[40] G. Kendall, A.F. Wilderspin, F. Ashall, M.A. Miles, J.M. Kelly, *Trypanosoma cruzi* glycosomal glyceraldehyde-3-phosphate dehydrogenase does not conform to the "hotspot" topogenic signal model, EMBO J. 9 (1990) 2751–2758, https://doi.org/10.1002/j.1460-2075.1990.tb07462.x.

[41] M. Rolón, C. Vega, J.A. Escario, A. Gómez-Barrio, Development of resazurin microtiter assay for drug sensibility testing of *Trypanosoma cruzi* epimastigotes, Parasitol. Res. 99 (2006) 103–107, https://doi.org/10.1007/s00436-006-0126-y.

[42] S.N. Rampersad, Multiple applications of alamar blue as an indicator of metabolic function and cellular health in cell viability bioassays, Sensors 12 (2012) 12347–12360, https://doi.org/10.3390/s120912347.

[43] G. Pless-Petig, M. Metzenmacher, T.R. Türk, U. Rauen, Aggravation of cold-induced injury in Vero-B4 cells by RPMI 1640 medium - identification of the responsible medium components, BMC Biotechnol. 12 (2012) 73, https://doi.org/10.1186/1472-6750-12-73.

[44] V.T. Contreras, J.M. Salles, N. Thomas, C.M. Morel, S. Goldenberg, *In vitro* differentiation of *Trypanosoma cruzi* under chemically defined conditions, Mol. Biochem. Parasitol. 16 (1985) 315–327, https://doi.org/10.1016/0166-6851(85)90073-8.

[45] M. Faundez, L. Pino, P. Letelier, C. Ortiz, R. López, C. Seguel, J. Ferreira, M. Pavani, A. Morello, J.D. Maya, Buthionine sulfoximine increases the toxicity of nifurtimox and benznidazole to *Trypanosoma cruzi*, Antimicrob. Agents Chemother. 49 (2005) 126–130, https://doi.org/10.1128/AAC.49.1.126-130.2005.

[46] A.F. Francisco, S. Jayawardhana, M.D. Lewis, K.L. White, D.M. Shackleford, G. Chen, J. Saunders, M. Osuna-Cabello, K.D. Read, S.A. Charman, E. Chatelain, J.M. Kelly, Nitroheterocyclic drugs cure experimental *Trypanosoma cruzi* infections more effectively in the chronic stage than in the acute stage, Sci. Rep. 6 (2016) 35351, https://doi.org/10.1038/srep35351.

[47] F. Olmo, C. Rotger, I. Ramírez-Macías, L. Martínez, C. Marín, L. Carreras, K. Urbanová, M. Vega, G. Chaves-Lemaur, A. Sampedro, M.J. Rosales, M. Sánchez-Moreno, A. Costa, Synthesis and biological evaluation of *N,N'*-Squaramides with high *in vivo* efficacy and low toxicity: toward a low-cost drug against Chagas disease, J. Med. Chem. 57 (2014) 987–999, https://doi.org/10.1021/jm4017015.

[48] X. Ye, J. Ding, X. Zhou, G. Chen, S.F. Liu, Divergent roles of endothelial NF-κB in multiple organ injury and bacterial clearance in mouse models of sepsis, J. Exp. Med. 205 (2008) 1303–1315, https://doi.org/10.1084/jem.20071393.

[49] F. Olmo, F. Gómez-Contreras, P. Navarro, C. Marín, M.J.R. Yunta, C. Cano, L. Campayo, D. Martín-Oliva, M.J. Rosales, M. Sánchez-Moreno, Synthesis and evaluation of *in vitro* and *in vivo* trypanocidal properties of a new imidazole-containing nitrophthalazine derivative, Eur. J. Med. Chem. 106 (2015) 106–119, https://doi.org/10.1016/j.ejmech.2015.10.034.

[50] E. Moreno-Viguri, C. Jiménez-Montes, R. Martín-Escolano, M. Santivañez-Veliz, A. Martin-Montes, A. Azqueta, M. Jimenez-Lopez, S. Zamora Ledesma, N. Cirauqui, A. López De Ceráin, C. Marín, M. Sánchez-Moreno, S. Pérez-Silanes, *In vitro* and *in vivo* anti-*Trypanosoma cruzi* activity of new arylamine Mannich base-type derivatives, J. Med. Chem. 59 (2016) 10929–10945, https://doi.org/10.1021/acs.jmedchem.6b00784.

[51] C. Fernández-Becerra, M. Sanchez-moreno, A. Osuna, F.R. Opperdoes, Comparative Aspects of Energy Metabolism in Plant Trypanosomatids, vol. 44, 1997, pp. 523–529.

[52] J.M. Sandes, A. Fontes, C.G. Regis-da-Silva, M.C.A. Brelaz De Castro, C.G. Lima-Junior, F.P.L. Silva, M.L.A.A. Vasconcellos, R.C.B.Q. Figueiredo, *Trypanosoma cruzi* cell death induced by the morita-baylis-hillman adduct 3-hydroxy-2-methylene-3-(4-nitrophenylpropanenitrile), PLoS One 9 (2014), e93936, https://doi.org/10.1371/journal.pone.0093936.

[53] N. Hussein, H. Amawi, C. Karthikeyan, F.S. Hall, R. Mittal, P. Trivedi, C.R. Ashby, A.K. Tiwari, The dopamine D3 receptor antagonists PG01037, NGB2904, SB277011A, and U99194 reverse ABCG2 transporter-mediated drug resistance in cancer cell lines, Cancer Lett. 396 (2017) 1–14, https://doi.org/10.1016/j.canlet.2017.03.015.

[54] Á. López-Céspedes, E. Villagrán, K. Briceño Álvarez, J.A. de Diego, H.L. Hernández-Montiel, C. Saldaña, M. Sánchez-Moreno, C. Marín, *Trypanosoma cruzi*: seroprevalence detection in suburban population of santiago de Querétaro (Mexico), Sci. World J. 2012 (2011) 914129, https://doi.org/10.1100/2012/914129.

[55] M.M. Bradford, A rapid and sensitive method for the quantitation of microgram quantities of protein utilizing the principle of protein-dye binding, Anal. Biochem. 72 (1976) 248–254, https://doi.org/10.1016/0003-2697(76)90527-3.

[56] W.F. Beyer, I. Fridovich, Assaying for superoxide dismutase activity: some large consequences of minor changes in conditions, Anal. Biochem. 161 (1987) 559–566, https://doi.org/10.1016/0003-2697(87)90489-1.

[57] B. Zingales, *Trypanosoma cruzi* genetic diversity: something new for something known about Chagas disease manifestations, serodiagnosis and drug sensitivity, Acta Trop. (2017), https://doi.org/10.1016/j.actatropica.2017.09.017. S0001-706–6.

[58] P. González, C. Marín, I. Rodríguez-González, A.B. Hitos, M.J. Rosales, M. Reina, J.G. Díaz, A. González-Coloma, M. Sánchez-Moreno, *In vitro* activity of C_{20}-diterpenoid alkaloid derivatives in promastigotes and intracellular amastigotes of *Leishmania infantum*, Int. J. Antimicrob. Agents 25 (2005) 136–141, https://doi.org/10.1016/j.ijantimicag.2004.08.010.

[59] F. Olmo, C. Marín, M.P. Clares, S. Blasco, M.T. Albelda, C. Soriano, R. Gutiérrez-Sánchez, F. Arrebola-Vargas, E. García-España, M. Sánchez-Moreno, Scorpiand-like azamacrocycles prevent the chronic establishment of *Trypanosoma cruzi* in a murine model, Eur. J. Med. Chem. 70 (2013) 189–198, https://doi.org/10.1016/j.ejmech.2013.09.048.

[60] F. Olmo, M.P. Clares, C. Marín, J. González, M. Inclán, C. Soriano, K. Urbanová, R. Tejero, M.J. Rosales, R.L. Krauth-Siegel, M. Sánchez-Moreno, E. García-España, Synthetic single and double aza-scorpiand macrocycles acting as inhibitors of the antioxidant enzymes iron superoxide dismutase and trypanothione reductase in *Trypanosoma cruzi* with promising results in a murine model, RSC Adv. 4 (2014) 65108–65120, https://doi.org/10.1039/C4RA09866H.

[61] R. Don, J.R. Ioset, Screening strategies to identify new chemical diversity for drug development to treat kinetoplastid infections, Parasitology 141 (2014) 140–146, https://doi.org/10.1017/S003118201300142X.

[62] E. Chatelain, Chagas disease drug discovery: toward a new era, J. Biomol. Screen 20 (2014) 22–35, https://doi.org/10.1177/1087057114550585.

[63] S. Nwaka, D. Besson, B. Ramirez, L. Maes, A. Matheeussen, Q. Bickle, N.R. Mansour, F. Yousif, S. Townson, S. Gokool, F. Cho-Ngwa, M. Samje, S. Misra-Bhattacharya, P.K. Murthy, F. Fakorede, J.-M. Paris, C. Yeates, R. Ridley, W.C. van Voorhis, T. Geary, Integrated dataset of screening hits against multiple neglected disease pathogens, PLoS Neglected Trop. Dis. 5 (2011) e1412, https://doi.org/10.1371/journal.pntd.0001412.

[64] D.F. De Suasnábar, E. Arias, M. Streiger, M. Piacenza, M. Ingaramo, M. Del Barco, N. Amicone, Evolutive behavior towards cardiomyopathy of treated (nifurtimox or benznidazole) and untreated chronic chagasic patients, Rev. Inst. Med. Trop. Sao Paulo 42 (2000) 99–109. S0036-46652000000200007.

[65] S. Espuelas, D. Plano, P. Nguewa, M. Font, J.A. Palop, J.M. Irache, C. Sanmartín, Innovative lead compounds and formulation strategies as newer kinetoplastid therapies, Curr. Med. Chem. 19 (2012) 4259–4288, https://doi.org/10.2174/092986712802884222.

[66] D.M. Santos, T.A.F. Martins, I.S. Caldas, L.F. Diniz, G.L.L. Machado-Coelho, C.M. Carneiro, R. de P. Oliveira, A. Talvani, M. Lana, M.T. Bahia, Benznidazole alters the pattern of Cyclophosphamide-induced reactivation in experimental *Trypanosoma cruzi*-dependent lineage infection, Acta Trop. 113 (2010) 134–138, https://doi.org/10.1016/j.actatropica.2009.10.007.

[67] A.V.M. Ferreira, M. Segatto, Z. Menezes, A.M. Macedo, C. Gelape, L. de Oliveira Andrade, F. Nagajyothi, P.E. Scherer, M.M. Teixeira, H.B. Tanowitz, Evidence for *Trypanosoma cruzi* in adipose tissue in human chronic Chagas disease, Microb. Infect. 13 (2011) 1002–1005, https://doi.org/10.1016/j.micinf.2011.06.002.

[68] D.A. Galloway, L.A. Laimins, B. Division, F. Hutchinson, Adipose tissue - a safe haven for parasites? Trends Parasitol. 33 (2016) 276–284, https://doi.org/10.1016/j.coviro.2015.09.001.Human.

[69] F. Nagajyothi, F.S. Machado, B.A. Burleigh, L.A. Jelicks, E. Scherer, S. Mukherjee, M.P. Lisanti, L.M. Weiss, N.J. Garg, H.B. Tanowitz, Mechanisms of *Trypanosoma cruzi* persistence in Chagas disease, Cell Microbiol. 14 (2013) 634–643, https://doi.org/10.1111/j.1462-5822.2012.01764.x.

[70] J.A. Urbina, Chemotherapy of Chagas disease, Curr. Pharmaceut. Des. 8 (2002) 287–295, https://doi.org/10.2174/1381612023396177.

[71] L. Murcia, B. Carrilero, F. Ferrer, M. Roig, F. Franco, M. Segovia, Success of benznidazole chemotherapy in chronic *Trypanosoma cruzi*-infected patients with a sustained negative PCR result, Eur. J. Clin. Microbiol. Infect. Dis. 35 (2016) 1819–1827, https://doi.org/10.1007/s10096-016-2733-6.

[72] A.L. Basquiera, A. Sembaj, A.M. Aguerri, M. Omelianiuk, S. Guzmán, J. Moreno Barral, T.F. Caeiro, R.J. Madoery, O.A. Salomone, Risk progression to chronic Chagas cardiomyopathy: influence of male sex and of parasitaemia detected by polymerase chain reaction, Heart 89 (2003) 1186–1190, https://doi.org/10.1136/heart.89.10.1186.

[73] J.T. Williams, J.N. Mubiru, N.E. Schlabritz-loutsevitch, R.C. Rubicz, L. Vandeberg, E.J.D. Jr, G.B. Hubbard, Polymerase Chain Reaction Detection of *Trypanosoma cruzi* in *Macaca fascicularis* Using Archived Tissues, vol. 81, 2010, pp. 228–234.

[74] A.F. Francisco, M.D. Lewis, S. Jayawardhana, M.C. Taylor, E. Chatelain, J.M. Kelly, Limited ability of posaconazole to cure both acute and chronic *Trypanosoma cruzi* infections revealed by highly sensitive *in vivo* imaging, Antimicrob. Agents Chemother. 59 (2015) 4653–4661, https://doi.org/10.1128/AAC.00520-15.

[75] H. Kayama, K. Takeda, The innate immune response to *Trypanosoma cruzi* infection, Microb. Infect. 12 (2010) 511–517, https://doi.org/10.1016/j.micinf.2010.03.005.

[76] A. El Bouhdidi, C. Truyens, M.-T. Rivera, H. Bazin, Y. Carlier, *Trypanosoma cruzi* infection in mice induces a polyisotypic hypergammaglobulinaemia and parasite-specific response involving high lgG2a concentrations and highly avid lgG1 antibodies, Parasite Immunol. 16 (1994) 69–76, https://doi.org/10.1111/j.1365-3024.1994.tb00325.x.

[77] M.L. Ginger, Trypanosomatid biology and euglenozoan evolution: new insights and shifting paradigms revealed through genome sequencing, Protist 156 (2005) 377–392, https://doi.org/10.1016/j.protis.2005.10.001.

[78] F. Bringaud, L. Rivière, V. Coustou, Energy metabolism of trypanosomatids: adaptation to available carbon sources, Mol. Biochem. Parasitol. 149 (2006) 1–9, https://doi.org/10.1016/j.molbiopara.2006.03.017.

[79] J.J. Cazzulo, Aerobic fermentation of glucose by trypanosomatids, Faseb. J. 6 (1992) 3153–3161, https://doi.org/10.1096/fasebj.6.13.1397837.

[80] J.-J. Wen, S. Gupta, Z. Guan, M. Dhiman, D. Condon, C. Lui, N.J. Garg, Phenyl-α-tert-butyl-nitrone and benzonidazole treatment controlled the mitochondrial oxidative stress and evolution of cardiomyopathy in chronic chagasic rats, J. Am. Coll. Cardiol. 55 (2010) 2499–2508, https://doi.org/10.1016/j.jacc.2010.02.030.

[81] B.S. Hall, S.R. Wilkinson, Activation of benznidazole by trypanosomal type I nitroreductases results in glyoxal formation, Antimicrob. Agents Chemother. 56 (2012) 115–123, https://doi.org/10.1128/AAC.05135-11.

[82] W. Lee, F. Thévenod, A role for mitochondrial aquaporins in cellular life-and-death decisions? AJP Cell Physiol. 291 (2006) C195–C202, https://doi.org/10.1152/ajpcell.00641.2005.

[83] N.K. Verma, G. Singh, C.S. Dey, Miltefosine induces apoptosis in arsenite-resistant *Leishmania donovani* promastigotes through mitochondrial dysfunction, Exp. Parasitol. 116 (2007) 1–13, https://doi.org/10.1016/j.exppara.2006.10.007.

[84] I.G. Kirkinezos, C.T. Moraes, Reactive oxygen species and mitochondrial diseases, Semin. Cell Dev. Biol. 12 (2001) 449–457, https://doi.org/10.1006/scdb.2001.0282.

[85] W.N. Hunter, M.S. Alphey, C.S. Bond, A.W. Schüttelkopf, Targeting metabolic pathways in microbial pathogens: oxidative stress and anti-folate drug resistance in trypanosomatids, Biochem. Soc. Trans. 31 (2003) 607–610, https://doi.org/10.1042/.

[86] L. Piacenza, M.P. Zago, G. Peluffo, M.N. Alvarez, M.A. Basombrio, R. Radi, Enzymes of the antioxidant network as novel determiners of *Trypanosoma cruzi*

virulence, Int. J. Parasitol. 39 (2009) 1455–1464, https://doi.org/10.1016/j.ijpara.2009.05.010.
[87] L. Maes, D. Vanden Berghe, N. Germonprez, L. Quirijnen, P. Cos, N. De Kimpe, L. Van Puyvelde, *Vitro* and *in vivo* activities of a triterpenoid saponin extract (PX-6518) from the plant *Maesa balansae* against visceral *leishmania* species, Antimicrob. Agents Chemother. 48 (2004) 130–136, https://doi.org/10.1128/AAC.48.1.130-136.2004.
[88] N. Germonprez, L. Maes, L. Van Puyvelde, M. Van Tri, D.A. Tuan, N. De Kimpe, *Vitro* and *in vivo* anti-leishmanial activity of triterpenoid saponins isolated from *Maesa balansae* and some chemical derivatives, J. Med. Chem. 48 (2005) 32–37, https://doi.org/10.1021/jm031150y.
[89] R. Docampo, Sensitivity of parasites to free radical damage by antiparasitic drugs, Chem. Biol. Interact. 73 (1990) 1–27, https://doi.org/10.1016/0009-2797(90)90106-W.

[3] PUBLICATION 3

ChemPubSoc Europe

DOI: 10.1002/cmdc.201800512

CHEMMEDCHEM Full Papers

Synthesis and Biological in vitro and in vivo Evaluation of 2-(5-Nitroindazol-1-yl)ethylamines and Related Compounds as Potential Therapeutic Alternatives for Chagas Disease

Rubén Martín-Escolano[+],[a] Benjamín Aguilera-Venegas[+],[b] Clotilde Marín,*[a] Álvaro Martín-Montes,[a] Javier Martín-Escolano,[a] Encarnación Medina-Carmona,[c] Vicente J. Arán,*[d] and Manuel Sánchez-Moreno*[a]

Chagas disease, a neglected tropical disease caused by infection with the protozoan parasite *Trypanosoma cruzi*, is a potentially life-threatening illness that affects 5–8 million people in Latin America, and more than 10 million people worldwide. It is characterized by an acute phase, which is partly resolved by the immune system, but then develops as a chronic disease without an effective treatment. There is an urgent need for new antiprotozoal agents, as the current standard therapeutic options based on benznidazole and nifurtimox are characterized by limited efficacy, toxicity, and frequent failures in treatment. In vitro and in vivo assays were used to identify some new low-cost 5-nitroindazoles as a potential antichagasic therapeutic alternative. Compound **16** (3-benzyloxy-5-nitro-1-vinyl-1*H*-indazole) showed improved efficiency and lower toxicity than benznidazole in both in vitro and in vivo experiments, and its trypanocidal activity seems to be related to its effect at the mitochondrial level. Therefore, compound **16** is a promising candidate for the development of a new anti-Chagas agent, and further preclinical evaluation should be considered.

Introduction

American trypanosomiasis, commonly known as Chagas disease (CD), is one of the most prevalent parasitic neglected tropical diseases (NTD)[1] and a major cause of morbidity and mortality in many areas of Latin America[2] according to the World Health Organization (WHO). Although the disease has its greatest impact on Latin America, its spread to the eastern hemisphere and first-world countries[3–5] has converted CD into a global problem,[6] infecting more than 10 million people worldwide and more than 25 million are at risk of contracting CD.[7]

The protozoan parasite *Trypanosoma cruzi* is the causative agent of CD, the most important parasite in Latin America[8] and the leading cause of premature heart disease.[9] *T. cruzi* is naturally transmitted by hematophagus insects, is strongly linked to low socioeconomic factors, although other means of transmission include the congenital route, contaminated food and drink, organ transplantation, and blood transfusion.[9–11]

CD can be divided into distinct stages. The acute stage is usually relatively mild and often undiagnosed; 20–30% of infected individuals proceed to the "chronic" stage, sometimes decades later.[12] This phase is characterized by clinical manifestations, including cardiomyopathy and, more rarely, damage to the digestive tract (mainly megacolon and megaesophagus) and/or lesions in the peripheral nervous system.[9]

The lack of public policies, the missing interest of the pharmaceutical industry, the long-term nature of CD and its complex pathology have resulted in a lack of drugs suited for effective treatments, and no vaccine has been developed.[13] A major example of this is that over a century after discovery of the disease by Carlos Chagas in 1909, only two old nitroheterocyclic drugs—nifurtimox (NFX) and benznidazole (BZN) (Figure 1)—are currently available.[14] Unfortunately, the efficacy of these two antiprotozoal agents is not higher than 70%, being worst during the chronic phase of the disease,[15] not to mention the wide range of adverse side effects which may lead, in several cases, to stop therapy abruptly.[16,17] This, cou-

[a] *R. Martín-Escolano,[+] Prof. Dr. C. Marín, Á. Martín-Montes, J. Martín-Escolano, Prof. Dr. M. Sánchez-Moreno*
Department of Parasitology, Instituto de Investigación Biosanitaria (ibs.Granada), Hospitales Universitarios de Granada, University of Granada, c/ Severo Ochoa s/n, 18071 Granada (Spain)
E-mail: cmaris@ugr.es
msanchem@ugr.es

[b] *Dr. B. Aguilera-Venegas[+]*
Department of Inorganic and Analytical Chemistry, Faculty of Chemical and Pharmaceutical Sciences, University of Chile, Box 233, Santiago 8380492 (Chile)

[c] *Dr. E. Medina-Carmona*
Department of Physical Chemistry, Faculty of Sciences, University of Granada, Av. Fuentenueva s/n, 18071 Granada (Spain)

[d] *Dr. V. J. Arán*
Instituto de Química Médica (IQM), Consejo Superior de Investigaciones Científicas (CSIC), c/ Juan de la Cierva 3, 28006 Madrid (Spain)
E-mail: vjaran@iqm.csic.es

[+] *These authors contributed equally to this work.*

The ORCID identification number(s) for the author(s) of this article can be found under: https://doi.org/10.1002/cmdc.201800512.

© 2018 Wiley-VCH Verlag GmbH & Co. KGaA, Weinheim

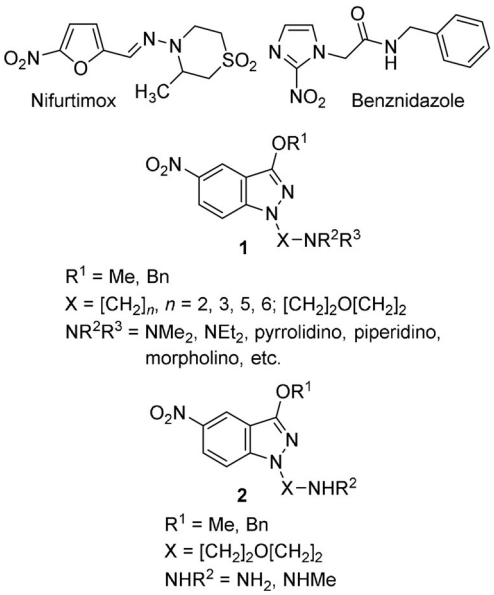

Figure 1. Chemical structure of the antichagasic nitroheterocyclic reference drugs and the previously studied 3-alkoxy-1-alkyl-5-nitro-1*H*-indazole derivatives **1** and **2**.

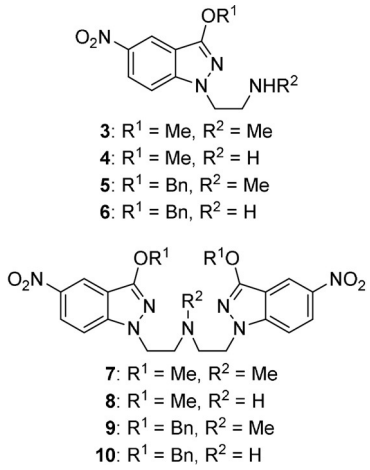

Figure 2. Chemical structure of 3-alkoxy-5-nitroindazole-derived amines **3**–**10** designed, prepared, and studied in the present work.

pled with that both drugs are prodrugs that require to be activated by the same mitochondrial nitroreductase[18,19]—a phenomenon with potential to result in cross-resistance—makes the development of safer and more widely effective antiprotozoal agents a major priority. Briefly, the ideal drug defined by the Target Product Profile (TPP) should present better safety profile and an efficacy at least equal to BZN.[20] Moreover, the search for new targets for chemotherapy is a major challenge. Among them, the parasite antioxidant system has attracted attention due to its uniqueness in the trypanosomatids.

With the aim of obtaining novel compounds as potential agents against CD, we have studied in the last years the antiprotozoal properties of many 5-nitroindazole derivatives, prepared by simple and inexpensive synthetic routes. In relation to the present work, we can mention the antichagasic activity reported for some 3-alkoxy-1-alkyl-5-nitro-1*H*-indazoles. The initially studied compounds were tertiary amines containing ω-(dialkylamino)alkyl or -oxaalkyl chains at position 1 of the heterocyclic ring (Figure 1, compounds **1**);[21–24] recently, we have also reported the trypanosomicidal properties of some primary and secondary 5-(indazol-1-yl)-3-oxapentylamines (Figure 1, compounds **2**) and related bis[5-(indazol-1-yl)-3-oxapentyl]amines.[25]

To explore the tolerance to structural changes of the mentioned 1,3-disubstituted 5-nitroindazole system, we describe here the synthesis, cytotoxicity, in vitro and in vivo trypanocidal activity and the possible mechanisms of action—the excreted metabolites, the mitochondrial membrane potential and the inhibition of iron superoxide dismutase (Fe-SOD)—of some new 5-nitroindazole-derived primary (**4**, **6**), secondary (**3**, **5**, **8**, **10**) and tertiary (**7**, **9**) amines supporting a substituted ethyl chain at position 1 of the heterocyclic ring (Figure 2). The required synthetic intermediates (**13**, **14**) as well as some reaction byproducts (**15**, **16**) (Scheme 1) were also studied. The compounds were tested in epimastigote, amastigote and trypomastigote forms in three different *T. cruzi* strains (Arequipa, SN3 and Tulahuen), the cytotoxicity was determined in Vero cells, and the in vivo trypanocidal activity was evaluated in both acute and chronic phases.

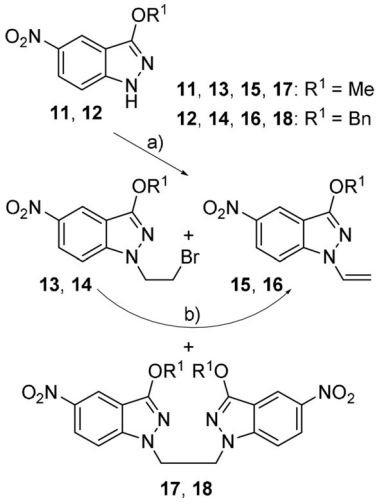

Scheme 1. Preparation of synthetic intermediates **13**, **14** and byproducts **15**–**18**: a) $BrCH_2CH_2Br$, K_2CO_3, acetone, reflux overnight; yields: 75% (**13**), 67% (**14**), 5% (**15**), 4% (**16**), 9% (**17**), 17% (**18**); b) K_2CO_3, 1-propanol, reflux, 3 h, 100% yield.

Results

Chemistry

The desired 3-alkoxy-1-(2-aminoethyl)indazoles **3**–**10** (Figure 2) were obtained from 2-bromoethyl derivatives **13**, **14** which were, in turn, prepared (Scheme 1) by *N*-1 alkylation of 3-alkoxyindazoles **11**, **12** with 1,2-dibromoethane; although an excess of the latter was used in order to minimize the formation of bisindazole derivatives,[26] 1,1′-ethylenebis(3-alkoxyindazoles) **17**,

© 2018 Wiley-VCH Verlag GmbH & Co. KGaA, Weinheim

18 were obtained as byproducts in these reactions. 3-Alkoxy-1-vinylindazoles **15**, **16**, arising from 2-bromoethyl derivatives **13**, **14** through hydrogen bromide elimination, could also be isolated in low yield from these processes. From a preparative point of view, 1-vinylindazoles **15**, **16** could also be obtained in quantitative yield from **13**, **14** by dehydrobromination with K_2CO_3/1-propanol at reflux.

Treatment of 2-bromoethyl derivatives **13**, **14** with methylamine or ammonia afforded *N*-methyl-2-(indazol-1-yl)ethylamines **3**, **5** or the corresponding primary amines **4**, **6**. Finally, alkylation of amines **3**–**6** with the required bromides **13**, **14** yielded the desired tertiary (**7**, **9**) and secondary (**8**, **10**) indazole-derived amines (Scheme 2).

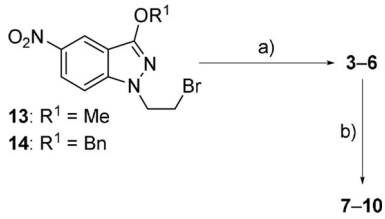

Scheme 2. Preparation of 3-alkoxy-5-nitroindazole-derived amines **3**–**6** and **7**–**10** designed in the present work: a) for **3**, **5**: 33% $MeNH_2$/EtOH, RT, 24 h, 90% yield; for **4**, **6**: sat. NH_3/MeOH, 70 °C (autoclave), 3 days, 79 and 81% yields, respectively; b) **13** or **14**, K_2CO_3, CH_3CN, reflux, 3 days (for **7**, **9**) or 7 days (for **8**, **10**), 75–91% yield.

Biology

In vitro trypanocidal evaluation

The extracellular epimastigote-like form is the most commonly used because of its simple culture and maintenance in vitro. However, tests against the developed forms in vertebrate hosts, bloodstream trypomastigotes (BTs) and intracellular amastigote-like forms (responsible for the chronic phase of CD) are more appropriate.[27]

On the one hand, the in vitro trypanocidal activity of compounds **3**–**10**, **13**–**16** and the reference drug BZN was evaluated on epimastigote forms with the objective of obtaining the half-maximal inhibitory concentrations (IC_{50} values; Table 1). On the other hand, the cytotoxicity was tested using Vero cells to determine the toxicity in mammalian cells (Table 1) and the selectivity index (SI = IC_{50} Vero cells/IC_{50} extra- and intracellular forms; Table 2). Interestingly, BZN was substantially more toxic than the tested compounds: 23.2 μM in contrast to values ranged from 34.9 to 493.9 μM, respectively. The compounds with IC_{50} values lower than 50 μM and SI higher than 10 were then evaluated in amastigote and trypomastigote forms (Tables 1 and 2). Compounds **3** and **16** showed the best trypanocidal activities, which were even better than those of BZN in epimastigote, amastigote and trypomastigote forms in the three *T. cruzi* strains.

In vivo trypanocidal evaluation in BALB/c mice

In vivo tests were performed for the evaluation of: a) Parasitemia levels by counting BTs as an indicator of the effectiveness of acute phase treatment; b) Parasitemia reactivation in the chronic phase by counting BTs after immunosuppression (IS) as an indicator of the effectiveness in both the acute and chronic phase treatments; c) Infected target organs in the chronic phase by PCR after IS as an indicator of the effectiveness in both the acute and chronic phase treatments; d) Levels of immunoglobulin G (IgG) by enzyme-linked immunosorbent assay (ELISA); e) Splenomegaly as indicators of immune response in both the acute and chronic phases; f) Serum parameters by biochemical measurements as an indicator of metabolic disturbances associated with the treatment.

The treatment was performed from the 10th to the 14th day post-infection (dpi) for the acute phase and from the 75th to the 79th dpi (it is established that the animals entered the chronic phase, in which there are no parasites remaining in the bloodstream) for the chronic phase. Oral therapy leads to

Table 1. In vitro activity of compounds **3**–**10** and **13**–**16** on extra- and intracellular forms of *T. cruzi* strains and toxicity toward Vero cells.

Compd	IC_{50} [μM][a]									
	Arequipa			SN3			Tulahuen			Toxicity
	Epi[b]	Ama[c]	Try[d]	Epi[b]	Ama[c]	Try[d]	Epi[b]	Ama[c]	Try[d]	Vero
BZN	16.9 ± 1.8	8.3 ± 0.7	12.4 ± 1.1	36.2 ± 2.4	16.6 ± 1.4	36.1 ± 3.1	19.7 ± 1.7	10.0 ± 0.8	15.1 ± 1.3	23.2 ± 2.1
3	0.1 ± 0.0	1.2 ± 0.2	1.1 ± 0.2	2.9 ± 0.2	1.9 ± 0.2	1.8 ± 0.2	1.9 ± 0.1	2.2 ± 0.2	1.6 ± 0.2	456.9 ± 28.9
4	24.4 ± 1.7	22.5 ± 1.0	19.0 ± 1.4	45.5 ± 4.8	46.5 ± 3.5	29.2 ± 2.0	46.6 ± 5.0	49.8 ± 3.3	31.1 ± 2.1	493.9 ± 41.7
5	17.7 ± 0.6	nd	nd	44.2 ± 6.1	nd	nd	14.5 ± 1.2	nd	nd	87.9 ± 2.7
6	34.1 ± 1.9	nd	nd	76.7 ± 5.8	nd	nd	25.0 ± 2.5	nd	nd	34.9 ± 1.6
7	29.3 ± 2.0	nd	nd	45.6 ± 5.2	nd	nd	73.2 ± 5.3	nd	nd	134.8 ± 5.3
8	11.7 ± 1.1	nd	nd	40.0 ± 3.4	nd	nd	14.5 ± 2.0	nd	nd	100.8 ± 3.2
9	53.2 ± 3.2	nd	nd	60.1 ± 5.1	nd	nd	78.5 ± 5.6	nd	nd	178.9 ± 10.6
10	4.2 ± 0.2	9.7 ± 0.4	8.2 ± 0.9	13.5 ± 2.0	nd	nd	27.1 ± 2.1	nd	nd	72.3 ± 2.7
13	10.2 ± 0.9	31.9 ± 1.2	25.1 ± 2.1	26.2 ± 2.1	36.9 ± 2.5	31.8 ± 2.9	16.5 ± 2.0	78.4 ± 8.1	31.0 ± 3.8	355.2 ± 6.1
14	57.5 ± 1.8	nd	nd	156.7 ± 12.4	nd	nd	215.4 ± 16.8	nd	nd	382.9 ± 7.9
15	82.2 ± 2.1	nd	nd	107.6 ± 9.8	nd	nd	78.2 ± 8.1	nd	nd	240.0 ± 8.4
16	4.7 ± 0.3	7.4 ± 0.4	5.4 ± 0.6	2.3 ± 0.3	5.8 ± 0.6	4.6 ± 0.5	1.5 ± 0.1	12.4 ± 1.3	6.1 ± 0.6	266.5 ± 10.7

[a] Compound concentration required to give 50% growth inhibition, calculated using GraphPad Prism; each compound was tested in triplicate in four separate determinations; nd: not determined. [b] Epimastigote forms. [c] Amastigote forms. [d] Trypomastigote forms.

© 2018 Wiley-VCH Verlag GmbH & Co. KGaA, Weinheim

Table 2. Selectivity index for compounds **3**–**10** and **13**–**16** on extra- and intracellular forms of *T. cruzi* strains.

Compd	Selectivity index[a]								
	Arequipa			SN3			Tulahuen		
	Epi[b]	Ama[c]	Try[d]	Epi[b]	Ama[c]	Try[d]	Epi[b]	Ama[c]	Try[d]
BZN	1.4	2.8	1.9	0.6	1.4	0.6	1.2	2.3	1.5
3	4569.0	380.7	415.4	157.6	240.5	253.8	240.5	207.7	285.6
	(3263)	(136)	(219)	(263)	(172)	(393)	(200)	(90)	(190)
4	20.2	22.0	26.0	10.9	10.3	16.9	10.6	9.9	15.9
	(14)	(8)	(14)	(18)	(7)	(28)	(9)	(4)	(11)
5	5.0	nd	nd	2.0	nd	nd	6.0	nd	nd
	(4)			(3)			(5)		
6	1.0	nd	nd	0.5	nd	nd	1.4	nd	nd
	(1)			(1)			(1)		
7	4.6	nd	nd	3.0	nd	nd	1.8	nd	nd
	(3)			(5)			(2)		
8	8.6	nd	nd	2.5	nd	nd	7.0	nd	nd
	(6)			(4)			(6)		
9	3.4	nd	nd	3.0	nd	nd	2.3	nd	nd
	(24)			(5)			(2)		
10	17.2	7.5	8.8	5.4	nd	nd	2.7	nd	nd
	(12)	(3)	(5)	(9)			(2)		
13	34.8	11.1	14.2	13.6	9.6	11.2	21.5	4.5	11.5
	(25)	(4)	(7)	(23)	(7)	(18)	(18)	(2)	(8)
14	6.7	nd	nd	2.4	nd	nd	1.8	nd	nd
	(5)			(4)			(2)		
15	2.9	nd	nd	2.2	nd	nd	3.1	nd	nd
	(2)			(4)			(3)		
16	56.7	36.0	49.4	115.9	45.9	57.9	177.7	21.5	43.7
	(41)	(13)	(26)	(193)	(33)	(97)	(148)	(9)	(29)

[a] Selectivity index (SI) = IC_{50} Vero cells/IC_{50} extracellular and intracellular forms of the parasite. In brackets: number of times that the compound SI exceeds the reference drug SI on extracellular and intracellular forms of *T. cruzi*; nd: not determined. [b] Epimastigote forms. [c] Amastigote forms. [d] Trypomastigote forms.

better patient compliance and has a low cost (critical aspects of human treatment in developing countries).[28] Moreover, oral administration is the preferred route for the treatment of parasitic diseases.

First, parasitemia levels were determined in the different groups of mice in the acute phase (Figure 3). Nonsignificant differences were observed in mice treated with compound **3** with respect to the untreated mice, but a decrease in parasitemia was observed in mice treated with compound **16**, which exhibited even better in vivo trypanocidal activity than BZN. The trypanocidal activity of compound **16** was evident from the beginning of the treatment, and the parasitemia was undetected 11 and 9 days before (38th dpi) with respect to the control and BZN-treated mice, respectively. Alternatively, the peak of parasitemia (23rd dpi) in mice treated with compound **16** caused a decrease of ≈70% with respect to the control mice.

Second, to evaluate the effectiveness of the treatment and the disease extent in the chronic phase, the parasitemia reactivation was determined after IS until the 120th dpi (late chronic phase, when the amastigote form is nested inside target organs/tissues) with the objective of reactivating the parasitemia under the control of the immunological system of the mice. The percentages of reactivation of parasitemia after IS (Figure 4) were proportional to the survival rate of the parasites in the acute phase treatment, and the effectiveness of treatments in the chronic phase were shown (as confirmed below with the results of infected organs). A significant decrease in the reactivation of parasitemia was observed in both phases for mice treated with compound **16** (30% for acute phase and 35% for chronic phase), which were higher than

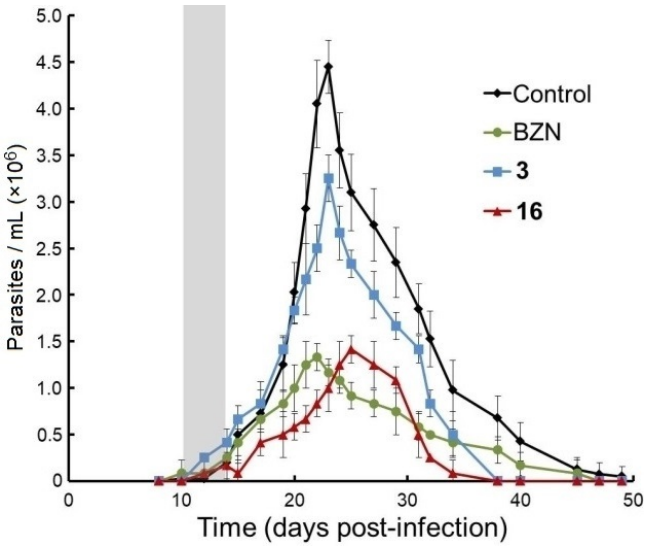

Figure 3. Parasitemia in murine model of acute CD: control (untreated), BZN, compound **3**, and compound **16**. In all cases, compounds were orally administered using, for each compound, 100 mg kg^{-1} of body mass. Treatment days are represented in grey. Values constitute means of three mice ± standard deviation.

© 2018 Wiley-VCH Verlag GmbH & Co. KGaA, Weinheim

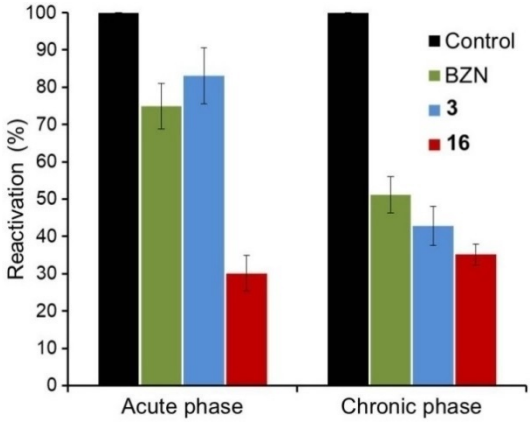

Figure 4. Immunosuppression in vivo assay for mice untreated (control) and treated with BZN, **3** and **16**. The figure shows the reactivation of parasitemia after the immunosuppression cycles by fresh blood in comparison with untreated mice (control). Values constitute means of three mice ± standard deviation.

those of the reference drug BZN (75 and 51%, respectively). In contrast, these results showed that the effectiveness of compound **3** was better in chronic than in acute phase (as mentioned below).

Finally, the presence of parasites in the defined as target organs/tissues (positive for control groups: adipose, bone marrow, brain, esophagus, heart, lung, muscle, spleen and stomach) was determined by PCR after necropsy (127th dpi) to evaluate the curative effect of these nitroindazoles as a second technique of confirmation of cure (Figure 5).

BZN-treated mice were shown to have 33 and 55% parasite-free organs/tissues in the acute and chronic phases, respectively. Interestingly, a notable in vivo trypanocidal activity was observed for mice treated with compound **16**, with 67% of parasite-free organs/tissues for mice treated in the acute and chronic phases.

It is well known that IgG levels (anti-*T. cruzi* IgG) are linked with the parasite load[29] such that the detection of total IgG reflects the infection rates, and verifies the effectiveness ascribed to the tested nitroindazoles together with the innate protection of mice. Because of that, aiming at evaluating the immune status of the mice during infection, the titer of anti-*T. cruzi* IgG was determined by ELISA (Figure 6), and the isolated Fe-SOD enzyme such as antigen.[30] The titer of anti-*T. cruzi* IgG decreased for mice treated with BZN and compound **16** in all analyzed samples except for those of 81st dpi in the chronic

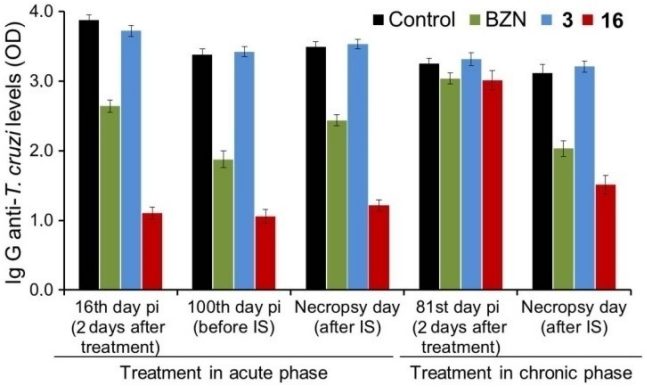

Figure 6. Differences in the IgG levels of anti-*T. cruzi* antibodies, expressed in absorbance units [optical densities (OD) at 490 nm], between control (untreated) and treated groups of mice at different days post-infection (pi). Values constitute means of three mice ± standard deviation.

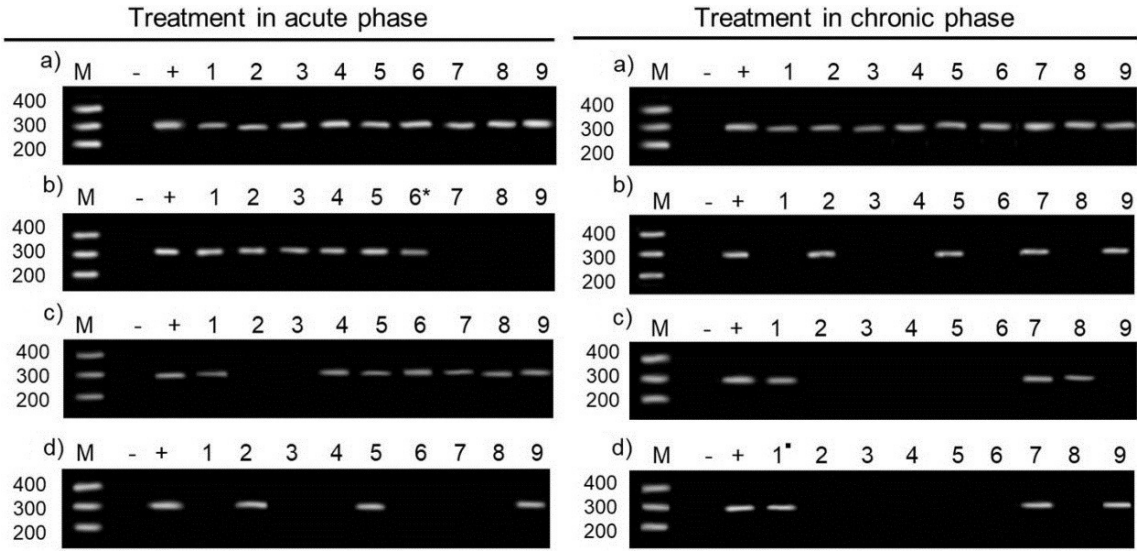

Figure 5. PCR analysis of nine organs/tissues with the *T. cruzi* SOD gene primers at the final day of experiment in mice treated with 100 mg kg^{-1} body mass. a) Untreated mice, b) mice treated with BZN, c) mice treated with **3**, d) mice treated with **16**. Lanes: M, base pair marker; -, PCR negative control; +, PCR positive control; 1, PCR adipose tissue; 2, PCR bone marrow tissue; 3, PCR brain tissue; 4, PCR esophagus tissue; 5, PCR heart tissue; 6, PCR lung tissue; 7, PCR muscle tissue; 8, PCR spleen tissue; 9, PCR stomach tissue. *: 1/3 of the corresponding organ PCR products showed 300 bp band on electrophoresis; ■: 2/3 of the corresponding organ PCR products showed 300 bp band on electrophoresis; no *■: 3/3 or 0/3 of the corresponding organ PCR products showed 300 bp band on electrophoresis.

© 2018 Wiley-VCH Verlag GmbH & Co. KGaA, Weinheim

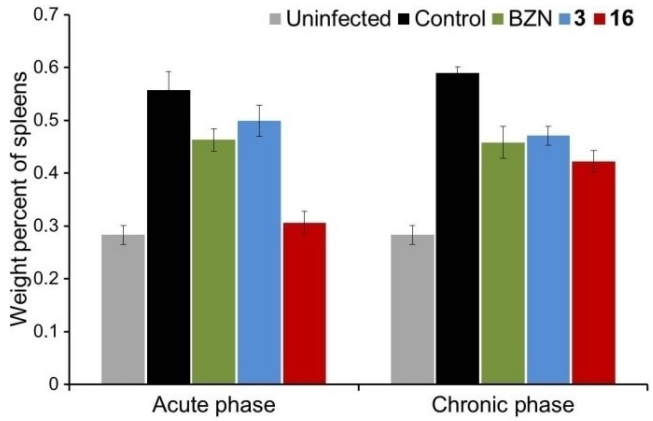

Figure 7. Weight percent of spleens of different groups of mice at the final day of experiment. Values constitute means of three mice ± standard deviation.

phase, which is logical, as its samples from mice are only from 2 days after treatment and have previously suffered an untreated acute phase.

Nonsignificant differences were observed for mice treated with compound **3**. In contrast, a notable decrease in the IgG levels occurred in mice treated with compound **16**, suggesting a formidable in vivo trypanocidal activity consistent with the previous studies.

Splenomegaly is another feature linked to the parasite load because the spleen is an organ that is implicated in immune defense against infection. Splenomegaly occurs in experimentally infected mice in which the spleen of chronic mice is approximately twice the mass of those from uninfected mice.[31] Accordingly, weight percentage of spleens was determined from different groups of mice (Figure 7). According to that mentioned above, uninfected mice showed a weight percentage of spleen of 0.28%, and untreated (control) mice exhibited values that were twice the value corresponding to uninfected mice: 0.56 and 0.59% in the acute and chronic phase experiments, respectively.

Because infection-induced splenomegaly is linked to the parasite load,[31] BZN-treated mice showed a decrease in splenomegaly, even at subcurative doses and in the absence of parasitological cure. Interestingly, mice treated with compound **16** showed a weight percentage of 0.30% for mice treated in the acute phase and 0.42% for mice treated in chronic phase, which means a decrease in splenomegaly of 93 and 55% compared with untreated mice, respectively. It should be remarked that the higher splenomegaly observed in the mice treated in the chronic phase should not be related to a lower activity, but rather to the fact that these mice suffered an acute phase without treatment, i.e., high levels of parasitemia.

Finally, biochemical clinical parameters were measured to confirm the possible metabolic abnormalities associated with treatment (Table 3). Most of the biochemical parameters for the mice treated with the two nitroindazoles were not altered more than for mice treated with BZN after administration, and ≈50% returned to normal levels on the day of mice necropsy.

Table 3. Biochemical clinical parameters measured at different experimental situations and daya post-infection (dpi) in groups of Balb/c mice infected with *T. cruzi*.

	Kidney marker profile		Heart marker profile		Liver marker profile			
	Urea [mg dL^{-1}]	Uric acid [mg dL^{-1}]	CK-MB [U L^{-1}][a]	LDH [U L^{-1}][b]	AST/GOT [U L^{-1}][c]	ALT/GPT [U L^{-1}][d]	Total bilirubin [mg dL^{-1}]	Alkaline phosphatase [U L^{-1}]
Uninfected mice ($n=6$):	35 [32-40]	4.5 [4.0–5.1]	372 [150–630]	3180 [2505–3851]	153 [132–177]	55 [46–62]	0.28 [0.22–0.31]	169 [141–192]
Treatment in acute phase								
16th dpi (control) ($n=3$)	31	4.3	535	3275	167	60	0.23	180
16th dpi and BZN (2 days after treatment) ($n=3$)	−−−	−−−−	=	=	++++	++++	++	++
16th dpi and **3** (2 days after treatment) ($n=3$)	−−	−−	−	=	++	++++	+	=
16th dpi and **16** (2 days after treatment) ($n=3$)	−−	−−−	−	=	++	++	=	=
Necropsy day of mice (control) ($n=3$)	34	4.0	496	2761	179	49	0.21	161
Necropsy day of mice and BZN ($n=3$)	−−−	=	=	=	++++	=	+	=
Necropsy day of mice and **3** (n=3)	−	=	−	=	+	++	=	=
Necropsy day of mice and **16** ($n=3$)	−	=	−	=	++	+	=	=
Treatment in chronic phase								
81st dpi (control) ($n=3$)	45	5.7	751	5951	260	57	0.25	167
81st dpi and BZN (2 days after treatment) ($n=3$)	−−−	−−−−	−−	−−−	++	++	+++	++++
81st dpi and **3** (2 days after treatment) ($n=3$)	−−−	−−−	−−	−	+	+	=	++
81st dpi and **16** (2 days after treatment) ($n=3$)	−−	−−−	−−	=	+	+	=	+
Necropsy day of mice (control) (n=3)	37	4.8	538	6679	286	64	0.20	149
Necropsy day of mice and BZN ($n=3$)	−−−	−−	=	−−	+	=	++	++
Necropsy day of mice and **3** ($n=3$)	−	=	=	−	+	=	=	+
Necropsy day of mice and **16** ($n=3$)	−	−	−	=	+	=	=	+

[a] CK-MB, creatine kinase-muscle/brain. [b] LDH, lactate dehydrogenase. [c] AST/GOT, aspartate aminotransferase. [d] ALT/GPT, alanine aminotransferase. dpi = day post-infection. Key: =, variation no larger than 10%; +, up to 10% increase over the range; ++, up to 20% increase over the range; +++, up to 30% increase over the range; ++++, more than 40% increase over the range; −, up to 10% decrease over the range; −−, up to 20% decrease over the range; −−−, up to 30% decrease over the range; −−−−, more than 40% decrease over the range.

© 2018 Wiley-VCH Verlag GmbH & Co. KGaA, Weinheim

Studies of the action mechanism

Metabolite excretion study

It is well known that *T. cruzi* is unable to totally degrade glucose to CO_2 in the presence of oxygen, and excretes into the medium a considerable portion of the hexose skeleton as incompletely oxidized final products in the form of fermented metabolites (so-called aerobic fermentation): pyruvate, acetate, succinate, L-alanine, D-lactate, and ethanol.[32–34]

The ^{1}H NMR spectra of culture media were registered in order to obtain information regarding the effects of compounds **3** and **16** on the glucose metabolism of *T. cruzi* (spectra not shown). The final excretions were qualitatively and quantitatively analyzed and compared with those found for untreated (control) *T. cruzi* epimastigotes (Figure 8). Compound

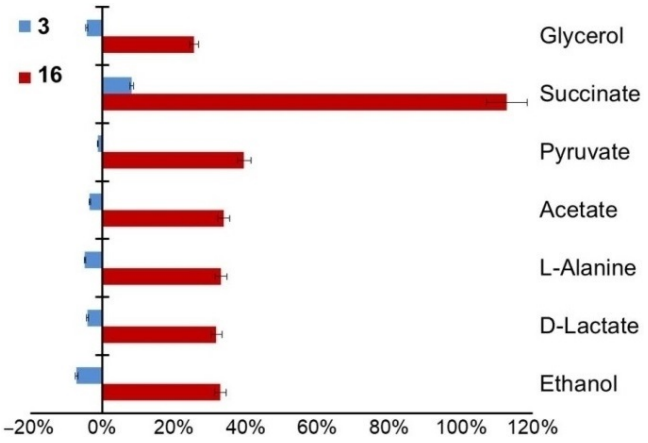

Figure 8. Percentages of variation among peaks of catabolites excreted by epimastigotes of *T. cruzi* Arequipa strain exposed to compounds **3** and **16** at their IC_{25} in comparison with a control (untreated) incubated 72 h. Each drug was tested in three separate determinations.

3 showed no significant disturbances on glucose metabolism; however, the excretion of all metabolites was increased in epimastigotes treated with compound **16**, especially succinate (113%). It is interesting to mention that an increase in succinate excretion indicates catabolic alterations that could be related to a mitochondrial dysfunction.[35]

Effects on mitochondrial membrane potential and on DNA and RNA levels in T. cruzi

In normal cells, to sustain the electrochemical potential and function of mitochondria, an active pumping of H^+ is produced during the electron transport chain. It is well-known that mitochondria play an imperative role in cell death,[36] and disturbances in the mitochondrial membrane potential lead to a decrease in ATP production and a reduction in DNA and RNA levels, causing necrosis and/or apoptosis.[37] Therefore, the fluorescence intensity of rhodamine 123 (Rho 123) and acridine orange (AO) was quantified by cytometry flow to evaluate and relate the effect of compounds **3** and **16** on the membrane potential and on the DNA and RNA levels, respectively.

We suggest that the trypanocidal activities of compound **3** and **16** could be partially associated with its mitochondrial effect (Figure 9), although the parasites treated with com-

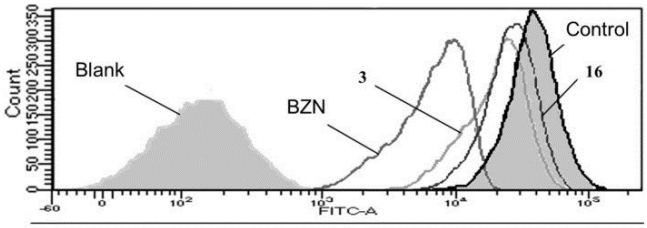

Compound	Inhibition (%)
BZN	45.8
3	35.6
16	23.5

Figure 9. Cytometry analysis of the mitochondrial membrane potential from epimastigotes of *T. cruzi* Arequipa strain exposed to BZN and compounds **3** and **16** at their IC_{25} in comparison with a control (untreated) incubated 72 h. Each drug was tested in three separate determinations.

pounds **3** and **16** showed lower depolarizations in the mitochondrial membrane than BZN (35.6 and 23.5%, respectively).

Nonspecific nucleic acid degradation is a feature intimately connected to cell necrosis,[38] accordingly, DNA and RNA levels were determined (Figure 10). The parasites treated with BZN exhibited a decrease of nucleic acid levels, with a value of 22.4% with respect to the untreated parasites. Higher reductions showed the parasites treated with compounds **3** and **16**, with values of 58.1 and 58.2%, respectively.

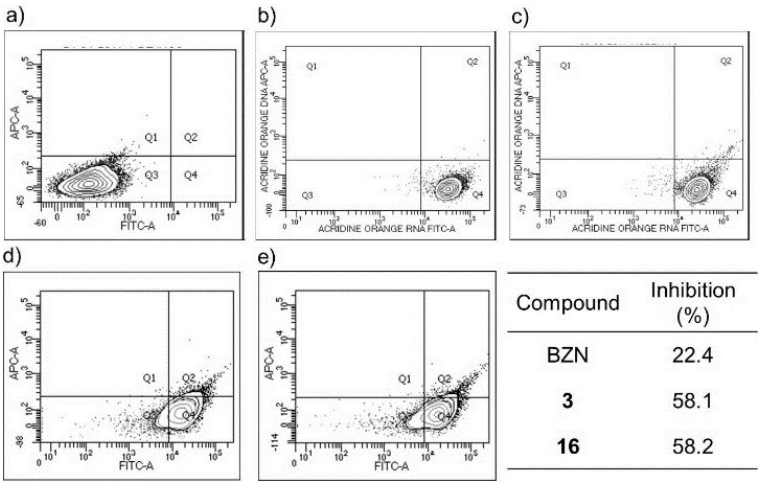

Compound	Inhibition (%)
BZN	22.4
3	58.1
16	58.2

Figure 10. Cytometry analysis on DNA and RNA levels of epimastigotes of *T. cruzi* Arequipa strain exposed to BZN and compounds **3** and **16** at their IC_{25} in comparison with a control (untreated) incubated 72 h: a) blank, b) control (untreated), c) BZN, d) **3**, and e) **16**. Each drug was tested in three separate determinations.

© 2018 Wiley-VCH Verlag GmbH & Co. KGaA, Weinheim

Inhibitory effect on* T. cruzi *Fe-SOD enzyme

Enzymes are one of the most studied therapeutic targets, and the Fe-SOD is a trypanosomatid exclusive enzyme and absent in other eukaryotic cells.[39,40] It presents biochemical and structural differences with respect to its human homologue Cu/Zn-SOD enzyme. The crucial role performed by this enzyme is the elimination of reactive oxygen species (ROS), allowing trypanosomatids to protect themselves from the damage produced by oxidative stress.[41,42] Therefore, the inhibitory effects of compounds **3** and **16** on these enzymes were determined using the method described by Beyer and Fridovich[43] (Figure 11).

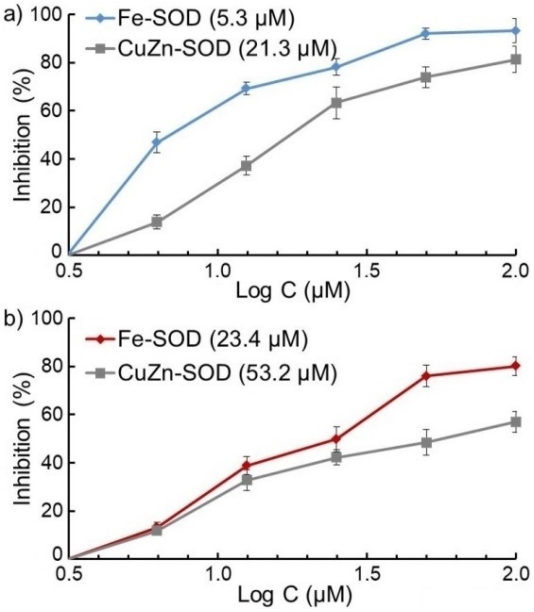

Figure 11. Percent inhibition in vitro of Fe-SOD from epimastigotes of *T. cruzi* Arequipa strain (activity 42.0 ± 3.8 U mg^{-1}) and of CuZn-SOD from human erythrocytes (activity 47.3 ± 4.1 U mg^{-1}) for compounds a) **3** and b) **16**. Activity differences in the control versus the sample incubated using compounds were identified by the Newman–Keuls test. Values are the average of three separate rate determinations. In brackets: IC_{50} value, calculated by linear regression analysis.

Higher inhibitions were observed on the parasite enzyme than on the human SOD for both compounds. Significant inhibition values were found for the Fe-SOD enzyme for compound **3**, with an IC_{50} value of 5.3 μM. Therefore, we suggest that this inhibitory effect on the Fe-SOD enzyme be considered one of the causes of the in vitro trypanocidal activity of compound **3**. For compound **16**, the IC_{50} value (23.4 μM) is too high to attribute the trypanocidal effect on the inhibition of the parasite enzyme.

Discussion

At present, the genetic diversity of *T. cruzi* is widely recognized, and the parasite is classified into seven discrete typing units (DTUs), with different evolutionary relationships, ecological and epidemiological associations, tropism, pathogenesis, genotypes, phenotypes and drug resistance.[43] Accordingly, three different *T. cruzi* strains (TcI, TcV, and TcVI), with different tropisms, hosts and locations, were used to evaluate the synthesized compounds, to determine the compounds with a good performance, and to select those compounds that avoid the natural resistance of the three strains. Moreover, according to some authors, it must be kept in mind that potential anticha-gasic agents have to meet certain in vitro criteria: the IC_{50} value must not exceed 10 μM, and the SI must be 10-fold higher.[44] We tested initially against epimastigotes of the three strains of *T. cruzi* all new 5-nitroindazole derivatives (**3**–**10**, **13**–**16**), and only the few compounds with $IC_{50} < 50$ μM and SI > 10 were evaluated against the corresponding amastigotes and trypomastigotes. Considering only the complete results obtained against epimastigotes, we have not been able to find a clear structure–activity relationship for these compounds. Among amines, 3-methoxy-*N*-methyl derivative **3** was much more active and selective than the remaining compounds against epimastigotes of the different studied strains ($IC_{50} < 2.9$ μM; SI > 158), and this high activity was also displayed against the corresponding amastigotes ($IC_{50} < 2.2$ μM; SI > 208) and trypomastigotes ($IC_{50} < 1.8$ μM; SI > 254). Compound **3** was also more efficient than the related indazole-derived amines **1**, **2** (Figure 1), previously studied against SN3[25] and CL Brener[21,23,24] strains of the parasite. On the other hand, 3-benzyloxy-1-vinylindazole **16**, a reaction byproduct which was not included in our initial design (Figure 2), showed also good trypanocidal properties and selectivities ($IC_{50} = 1.5$–12.4 μM; SI = 21–178). Thus, the commented 5-nitroindazoles **3** and **16**, showing better trypanocidal activities than the reference drug BZN and good selectivities in the three forms of the three *T. cruzi* strains, were selected for further in vivo evaluation.

The in vivo assays on BALB/c mice were only performed with *T. cruzi* Arequipa strain with the object to limit as much as possible animal testing, and as there were no significant differences between the performances of the selected compounds for the other evaluated strains. Moreover, and because of the performance of drugs during the acute and chronic phases is not as effective as it should be,[45] the impact of these 5-nitroindazole derivatives was evaluated by treating mice in each phase.

The treatment was 20 mg kg^{-1} per day for five consecutive days, that is, subcurative doses for the BZN, to evaluate whether the compounds **3** and **16** demonstrated higher in vivo effectiveness than the reference drug. Noticeably, none of the treated mice died during the treatment or lost more than 10% body mass. The fact that mice treated with compound **16** lack of toxicity, together with this treatment guideline significantly decreased parasitemia (especially during the days of treatment), higher doses and/or a new treatment guideline based on pharmacokinetic studies could be administered to achieve a total cure. We must highlight that inadequate pharmacokinetics between the compounds and the locations of the parasites in the tissues during the chronic phase of infection are related to different effectiveness levels in the acute and chronic phases.[46]

© 2018 Wiley-VCH Verlag GmbH & Co. KGaA, Weinheim

Furthermore, the formidable in vivo trypanocidal activity of compound **16** was confirmed with two techniques of cure confirmation[47] in both acute and chronic phase treatments. First, IS was performed because of the fact that apparently cured immunocompromised individuals present clinically aggressive reactivation of the parasitemia. Second, the PCR technique was carried out to determine the presence or absence of parasites in the target organs. The mice with no parasitemia after IS and negative PCR results are considered cured.[48] As expected, mice treated with compound **16** in the acute phase exhibited the lowest reactivation after IS, and the presence of parasites by PCR was negative for most of the analyzed organs. Interestingly, mice treated with compound **16** in the chronic phase showed similar results, also being the compound that obtained the best results.

It should be noted that assessment of clinical cure is debatable because of the lack of a reliable test to ensure parasite elimination.[49] The PCR technique to identify cure is an intricate question, and its main utility is to verify the failure of clinical cure because even consistently negative results (for which PCR is able to detect a single parasite in 5 mL of blood) are insufficient to ratify the absence of parasites in tissues.[50,51] In this regard, TaqMan technology has improved the detection by specific PCR (using sequences of constant regions and variables of minicircles of kinetoplast DNA, fluorogenic probes and real-time amplification reaction), and it is quite useful to assess the parasitic load in earlier and later-treated chronic patients and for the coming establishment of a suitable criterion for the curing of patients submitted to therapy.[52] Concerning animal testing, IS is the formula employed to prove cure,[53] and we assess the establishment of cure using a double confirmation based on IS and PCR. At present, sensitive bioluminescence imaging model techniques are used to demonstrate cure.[31] However, we can provide evidence of curation (or a considerable decrease in the parasite load) found on the results of three independent samples by IS and PCR.

According to the mechanism of action, it is well-known that the observed accumulation of succinate, pyruvate and malate could be the result of a mitochondrial dysfunction[35] by causing a blockade of the glycolytic pathway. Moreover, the observed increase in the excretions of glycerol and ethanol are the result of that the parasite used glycosomal and cytoplasmic alternative catabolic routes, respectively, in energy deficient conditions, such as mitochondrial dysfunction that was subsequently analyzed.[33] In addition, a decrease in the mitochondrial membrane potential could produce an imbalance in the NADH/NAD^+ and ATP/ADP ratios,[33] which could be the cause of the observed decrease in DNA and RNA levels of the parasite. Thus, we suggest that the trypanocidal activity of compound **16** could be related to its mitochondrial effect.

Conclusions

The trypanocidal properties of new 5-nitroindazole derivatives were evaluated both in vitro and in vivo. Compound **16** exhibited higher efficiency and lower toxicity than the reference drug BZN, in both the acute and chronic phase treatments, as showed PCR and IS assays. To achieve a total cure and due to the lack of toxicity at the dose tested, compound **16** will be evaluated at higher doses and/or modifying the treatment schedule for a better exposure. Action mechanism studies were performed in parallel, which showed that its antiprotozoal activity could be related to a mitochondrial effect. Inhibition studies will be performed at the level of both trypanothione reductase and respiratory chain, as these are possible targets. Consequently, we present compound **16** as a promising, simple and low-cost therapeutic alternative for the development of a new antiprotozoal agent against CD to be implemented in a further step within the preclinical phase.

Experimental Section

Chemistry

General methods: Melting points (mp) were determined in a Stuart Scientific melting point apparatus SMP3. ^{1}H (300 MHz) and ^{13}C (75 MHz) NMR spectra were recorded on a Bruker Avance 300 spectrometer. The chemical shifts are reported in parts per million (ppm) from TMS (δ scale) but were measured against the solvent signal ([D$_6$]DMSO: $\delta_H = 2.49$, $\delta_C = 39.50$ ppm). The assignments were performed by means of different standard homonuclear and heteronuclear correlation experiments (NOE, gHSQC and gHMBC). To simplify the description of the NMR spectra, bis(indazolylethyl)-amines have been numbered as simple compounds. Electron impact (EI) and electrospray (ES^+) mass spectra were obtained on a Hewlett Packard 5973 MSD (70 eV) and on a Hewlett–Packard 1100 MSD spectrometer, respectively. DC-Alufolien silica gel 60 PF_{254} (Merck, layer thickness 0.2 mm) was used for TLC, and silica gel 60 (Merck, particle size 0.040–0.063 mm) for flash column chromatography. Solvents and reagents were obtained from different commercial sources and used without further purification. Microanalyses were performed on a Heraeus CHN-*O*-RAPID analyzer and were within $\pm$0.3% of the theoretical values.

Preparation of 3-alkoxy-1-(2-bromoethyl)-5-nitro-1*H*-indazoles (13, 14) and related compounds (15–18): A mixture of the corresponding 3-alkoxyindazole (**11**, **12**)[26] (24.0 mmol), 1,2-dibromoethane (22.54 g, 120.0 mmol) and potassium carbonate (3.73 g, 27.0 mmol) in acetone (300 mL) was held at reflux overnight. The solvent was then evaporated and the residue extracted with chloroform (4×100 mL). The organic phase was concentrated and applied to the top of a flash chromatography column; elution with chloroform afforded the corresponding 1-vinyl derivatives (**15**, **16**) and then the required 1-(2-bromoethyl)indazoles (**13**, **14**); further elution with chloroform/acetone mixtures (50:1 to 30:1) afforded the corresponding 1,1′-ethylenebis(3-alkoxyindazoles) (**17**, **18**).

3-Alkoxy-1-vinylindazoles **15**, **16** could also be prepared alternatively as follows: a mixture of the corresponding 1-(2-bromoethyl)indazole (**13**, **14**) (4.0 mmol) and potassium carbonate (1.00 g, 7.2 mmol) in 1-propanol (50 mL) was held at reflux for 3 h. The solvent was then evaporated to dryness and the solid residue extracted with chloroform (4×25 mL). Evaporation of the extraction solvent afforded pure (TLC, ^{1}H NMR) 1-vinylindazoles **15**, **16**.

2-(3-Methoxy-5-nitro-1*H*-indazol-1-yl)ethyl bromide (13): Yield: 5.40 g (75%); mp: 135–137 °C (2-propanol); ^{1}H NMR ([D$_6$]DMSO): $\delta = 8.46$ (d, $J = 2.1$ Hz, 1H, 4′-H), 8.19 (dd, $J = 9.2$, 2.1 Hz, 1H, 6′-H), 7.76 (d, $J = 9.2$ Hz, 1H, 7′-H), 4.72 (t, $J = 6.1$ Hz, 2H, 2-CH_2), 4.05 (s, 3H, OCH_3), 3.89 ppm (t, $J = 6.1$ Hz, 2H, 1-CH_2); ^{13}C NMR ([D$_6$]DMSO):

© 2018 Wiley-VCH Verlag GmbH & Co. KGaA, Weinheim

δ = 157.83 (C3′), 143.36 (C7′a), 140.49 (C5′), 122.24 (C6′), 117.39 (C4′), 110.65 (C3′a), 110.55 (C7′), 56.57 (OCH_3), 49.55 (C2), 31.94 ppm (C1); MS (EI) *m/z* (%): 301 (17) $[M+2]^+$, 299 (17) $[M]^+$, 277 (1), 220 (2), 207 (11), 206 (100), 190 (1), 174 (2), 160 (38), 149 (3), 103 (7); Elemental analysis calcd (%) for $C_{10}H_{10}BrN_3O_3$ (300.11): C 40.02, H 3.36, N 14.00, found: C 39.87, H 3.23, N 14.23.

2-(3-Benzyloxy-5-nitro-1*H*-indazol-1-yl)ethyl bromide (14): Yield: 6.05 g (67%); mp: 145–147 °C (2-propanol); ^{1}H NMR ([D$_6$]DMSO): δ = 8.52 (d, *J* = 2.2 Hz, 1H, 4′-H), 8.21 (dd, *J* = 9.3, 2.2 Hz, 1H, 6′-H), 7.79 (d, *J* = 9.3 Hz, 1H, 7′-H), 7.55 (m, 2H, Ph 2-, 6-H), 7.38 (m, 3H, Ph 3-, 4-, 5-H), 5.44 (s, 2H, OCH_2), 4.74 (t, *J* = 5.9 Hz, 2H, 2-CH_2), 3.90 ppm (t, *J* = 5.9 Hz, 2H, 1-CH_2); ^{13}C NMR ([D$_6$]DMSO): δ = 157.08 (C3′), 143.31 (C7′a), 140. 59 (C5′), 136.13 (Ph C1), 128.41 (Ph C3, C5), 128.20 (2 overlapped signals; Ph C2, C4, C6), 122.28 (C6′), 117.48 (C4′), 110.88 (C3′a), 110.61 (C7′), 70.65 (OCH_2), 49.60 (C2), 31.95 ppm (C1); MS (EI) *m/z* (%): 377 (100) $[M+2]^+$, 375 (100) $[M]^+$, 277 (22), 149 (37), 109 (51), 107 (38); Elemental analysis calcd (%) for $C_{16}H_{14}BrN_3O_3$ (376.20): C 51.08, H 3.75, N 11.17, found: C 51.28, H 3.60, N 11.12.

3-Methoxy-5-nitro-1-vinyl-1*H*-indazole (15): Yield: 263 mg (5%) (from alkylation of compound **11** with 1,2-dibromoethane; 0.87 g (99%) from compound **13**; mp: 127–128 °C (ethanol) (lit., mp: 127–129 °C).[26]

3-Benzyloxy-5-nitro-1-vinyl-1*H*-indazole (16): Yield: 283 mg (4%) (from alkylation of compound **12** with 1,2-dibromoethane; 1.16 g (98%) from compound **14**; mp: 116–118 °C (acetonitrile); ^{1}H NMR ([D$_6$]DMSO): δ = 8.50 (d, *J* = 2.2 Hz, 1H, 4-H), 8.26 (dd, *J* = 9.3, 2.2 Hz, 1H, 6-H), 7.93 (d, *J* = 9.3 Hz, 1H, 7-H), 7.63 (dd, *J* = 15.1, 8.7 Hz, 1H, 1′-H), 7.58 (m, 2H, Ph 2-, 6-H), 7.39 (m, 3H, Ph 3-, 4-, 5-H), 5.51 (d, *J* = 15.1 Hz, 1H, 2′-H_{trans}), 5.49 (s, 2H, OCH_2), 4.85 ppm (d, *J* = 8.7 Hz, 1H, 2′-H_{cis}); ^{13}C NMR ([D$_6$]DMSO): δ = 158.17 (C3), 141.51, 141.18 (C5, C7a), 135.88 (Ph C1), 129.46 (C1′), 128.43 (Ph C3, C5), 128.33 (Ph C2, C6), 128.30 (Ph C4), 123.31 (C6), 117.38 (C4), 112.56 (C3a), 110.45 (C7), 97.71 (C2′), 70.84 ppm (OCH_2); MS (EI) *m/z* (%): 295 (100) $[M]^+$, 280 (1), 204 (7), 158 (7), 150 (4), 117 (4), 104 (8); Elemental analysis calcd (%) for $C_{16}H_{13}N_3O_3$ (295.29): C 65.08, H 4.44, N 14.23, found: C 65.35, H 4.23, N 14.51.

1,1′-Ethylenebis(3-methoxy-5-nitro-1*H*-indazole) (17): Yield: 445 mg (9%); mp: 249–252 °C (nitromethane) (lit., mp: 247–250 °C).[26]

1,1′-Ethylenebis(3-benzyloxy-5-nitro-1*H*-indazole) (18): Yield: 1.15 g (17%); mp: 188–191 °C (butanone); ^{1}H NMR ([D$_6$]DMSO): δ = 8.24 (d, *J* = 2.3 Hz, 2H, 4-, 4′-H), 7.85 (dd, *J* = 9.3, 2.3 Hz, 2H, 6-, 6′-H), 7.47 (m, 4H, Ph 2-, 6-, 2′-, 6′-H), 7.38 (m, 6H, Ph 3-, 4-, 5-, 3′-, 4′-, 5′-H), 7.02 (d, *J* = 9.3 Hz, 2H, 7-, 7′-H), 5.25 (s, 4H, OCH_2), 4.65 ppm (s, 4H, NCH_2); ^{13}C NMR ([D$_6$]DMSO): δ = 157.13 (C3, C3′), 143.00 (C7a, C7′a), 140.22 (C5, C5′), 136.17 (Ph C1, C1′), 128.47 (Ph C3, C5, C3′, C5′), 128.30 (Ph C4, C4′), 128.21 (Ph C2, C6, C2′, C6′), 121.75 (C6, C6′), 117.06 (C4, C4′), 111.05 (C3a, C3′a), 109.51 (C7, C7′), 70.54 (OCH_2), 47.78 ppm (NCH_2); MS (EI) *m/z* (%): 295 (100) $[M]^+$, 280 (1), 204 (7), 158 (7), 150 (4), 117 (4), 104 (8); Elemental analysis calcd (%) for $C_{30}H_{24}N_6O_6$ (564.55): C 63.82, H 4.28, N 14.89, found: C 64.07, H 4.20, N 14.60.

Preparation of *N*-methyl-2-(3-alkoxy-5-nitro-1*H*-indazol-1-yl)-ethylamines 3 and 5: A suspension of the corresponding 2-bromoethyl derivative (**13**, **14**) (4.0 mmol) in a methylamine solution (33% *w/w* in ethanol) (50 mL) was stirred at RT for 24 h. The mixture was evaporated to dryness and, after addition of 0.2 M aqueous hydrochloric acid (100 mL), the corresponding vinyl derivatives (**15**, **16**) were extracted with diethyl ether (3×100 mL). The acid solution was then basified with an excess of solid potassium carbonate and evaporated to dryness; extraction of the solid residue with a 20:1 chloroform/methanol mixture (4×50 mL) followed by evaporation of the solvent afforded free amines **3** and **5**, which were converted into the corresponding hydrochlorides by treatment with 36% aqueous hydrochloric acid (1 mL) in ethanol (20 mL) followed by evaporation to dryness.

***N*-Methyl-2-(3-methoxy-5-nitro-1*H*-indazol-1-yl)ethylamine hydrochloride hemihydrate (3·HCl·$^1/_2$ H$_2$O)**: Yield: 1.07 g (90%) [53 mg (6%) of 1-vinylindazole **15** was also obtained]; mp: 199–202 °C (ethanol); ^{1}H NMR ([D$_6$]DMSO): δ = 9.32 (br s, 2H, $^+NH_2$), 8.48 (d, *J* = 2.1 Hz, 1H, 4′-H), 8.22 (dd, *J* = 9.3, 2.1 Hz, 1H, 6′-H), 7.83 (d, *J* = 9.3 Hz, 1H, 7′-H), 4.68 (t, *J* = 6.1 Hz, 2H, 2-CH_2), 4.06 (s, 3H, OCH_3), 3.35 (t, *J* = 6.1 Hz, 2H, 1-CH_2), 2.55 ppm (s, 3H, NCH_3); ^{13}C NMR ([D$_6$]DMSO): δ = 157.95 (C3′), 143.05 (C7′a), 140.58 (C5′), 122.30 (C6′), 117.33 (C4′), 111.24 (C3′a), 110.39 (C7′), 56.64 (OCH_3), 47.03 (C1), 44.42 (C2), 32.46 ppm (NCH_3); MS (ES^+) *m/z* (%): 251 (100) $[M-Cl]^+$; Elemental analysis calcd (%) for $C_{11}H_{14}N_4O_3$·HCl·$^1/_2$ H_2O (295.72): C 44.68, H 5.45, N 18.95, found: C 44.73, H 5.26, N 19.11.

***N*-Methyl-2-(3-benzyloxy-5-nitro-1*H*-indazol-1-yl)ethylamine hydrochloride (5·HCl)**: Yield: 1.31 g (90%) [83 mg (7%) of 1-vinylindazole **16** was also obtained]; mp: 202–205 °C (ethanol); ^{1}H NMR ([D$_6$]DMSO): δ = 9.34 (br s, 2H, $^+NH_2$), 8.53 (d, *J* = 2.1 Hz, 1H, 4′-H), 8.23 (dd, *J* = 9.3, 2.1 Hz, 1H, 6′-H), 7.85 (d, *J* = 9.3 Hz, 1H, 7′-H), 7.55 (m, 2H, Ph 2-, 6-H), 7.40 (m, 3H, Ph 3-, 4-, 5-H), 5.46 (s, 2H, OCH_2), 4.70 (t, *J* = 6.1 Hz, 2H, 2-CH_2), 3.37 (t, *J* = 6.1 Hz, 2H, 1-CH_2), 2.55 ppm (s, 3H, CH_3); ^{13}C NMR ([D$_6$]DMSO): δ = 157.23 (C3′), 142.97 (C7′a), 140.67 (C5′), 136.14 (Ph C1), 128.45 (Ph C3, C5), 128.20 (Ph C4), 128.13 (Ph C2, C6), 122.34 (C6′), 117.42 (C4′), 111.43 (C3′a), 110.45 (C7′), 70.72 (OCH_2), 47.07 (C1), 44.45 (C2), 32.47 ppm (CH_3); MS (ES^+) *m/z* (%): 327 (100) $[M-Cl]^+$; Elemental analysis calcd (%) for $C_{17}H_{18}N_4O_3$·HCl (362.81): C 56.28, H 5.28, N 15.44, found: C 56.37, H 5.18, N 15.38.

Preparation of 2-(3-alkoxy-5-nitro-1*H*-indazol-1-yl)ethylamines 4 and 6: A stirred suspension of the corresponding 2-bromoethyl derivative (**13**, **14**) (4.0 mmol) in a saturated solution of ammonia in methanol (50 mL) was heated in an autoclave at 70 °C for 3 days. The mixture was evaporate to dryness and the obtained solid triturated with chloroform (20 mL); the insoluble material was recovered by filtration and washed with chloroform (3×5 mL) and ethanol (2×5 mL) to afford the corresponding primary amine hydrobromide (**4** or **6**·HBr). If desired, additional amount of primary amines (**4**, **6**), together with the corresponding 1-vinylindazoles (**15**, **16**) and secondary amines (**8**, **10**) also produced in the reaction, could be obtained as follows: after separation and washing of the corresponding primary amine hydrobromide, the combined organic filtrate was mixed with 10% aqueous potassium carbonate and evaporated to dryness. The resulting solid was extracted with chloroform/methanol (10:1) mixture (ca. 100 mL) and the solution evaporated to dryness and applied to the top of a flash chromatography column; elution with chloroform afforded the corresponding 1-vinylindazoles (**15**, **16**), and further elution with chloroform/ethanol mixtures (30:1 to 5:1) afforded secondary amines (**8**, **10**) followed by primary amines (**4**, **6**); the latter were converted into the corresponding hydrobromides by treatment with hydrobromic acid in ethanol.

2-(3-Methoxy-5-nitro-1*H*-indazol-1-yl)ethylamine hydrobromide (4·HBr): Yield: 0.91 g (72%) [1.00 g (79%) after column chromatography] [53 mg (6%) of 1-vinylindazole **15** and 45 mg (5%) of secondary amine **8** could also be obtained]; mp: 205–207 °C (1-propa-

© 2018 Wiley-VCH Verlag GmbH & Co. KGaA, Weinheim

nol); ^{1}H NMR ([D$_6$]DMSO): δ = 8.50 (d, J = 2.1 Hz, 1H, 4′-H), 8.24 (dd, J = 9.3, 2.1 Hz, 1H, 6′-H), 7.98 (brs, 3H, $^+$NH$_3$), 7.73 (d, J = 9.3 Hz, 1H, 7′-H), 4.55 (t, J = 5.9 Hz, 2H, 2-CH$_2$), 4.07 (s, 3H, OCH$_3$), 3.29 ppm (t, J = 5.9 Hz, 2H, 1-CH$_2$); ^{13}C NMR ([D$_6$]DMSO): δ = 157.97 (C3′), 143.10 (C7′a), 140.57 (C5′), 122.35 (C6′), 117.38 (C4′), 111.30 (C3′a), 110.33 (C7′), 56.67 (OCH$_3$), 45.63 (C2), 38.32 ppm (C1); MS (ES$^+$) m/z (%): 237 (100) [M−Br]$^+$; Elemental analysis calcd (%) for C$_{10}$H$_{12}$N$_4$O$_3$·HBr (317.14): C 37.87, H 4.13, N 17.67, found: C 37.88, H 4.10, N 17.79.

2-(3-Benzyloxy-5-nitro-1*H*-indazol-1-yl)ethylamine hydrobromide (6·HBr): Yield: 1.09 g (69%) [1.28 g (81%) after column chromatography] [35 mg (3%) of 1-vinylindazole **16** and 146 mg (12%) of secondary amine **10** could also be obtained]; mp: 189–191 °C (water); ^{1}H NMR ([D$_6$]DMSO): δ = 8.55 (d, J = 2.1 Hz, 1H, 4′-H), 8.26 (dd, J = 9.3, 2.1 Hz, 1H, 6′-H), 7.99 (brs, 3H, $^+$NH$_3$), 7.75 (d, J = 9.3 Hz, 1H, 7′-H), 7.55 (m, 2H, Ph 2-, 6-H), 7.40 (m, 3H, Ph 3-, 4-, 5-H), 5.46 (s, 2H, OCH$_2$), 4.57 (t, J = 5.8 Hz, 2H, 2-CH$_2$), 3.31 ppm (t, J = 5. Hz, 2H, 1-CH$_2$); ^{13}C NMR ([D$_6$]DMSO): δ = 157.28 (C3′), 143.04 (C7′a), 140.68 (C5′), 136.15 (Ph C1), 128.49 (Ph C3, C5), 128.25 (Ph C4), 128.16 (Ph C2, C6), 122.40 (C6′), 117.48 (C4′), 111.48 (C3′a), 110.39 (C7′), 70.73 (OCH$_2$), 45.66 (C2), 38.39 ppm (C1); MS (ES$^+$) m/z (%): 313 (100) [M−Br]$^+$; Elemental analysis calcd (%) for C$_{16}$H$_{16}$N$_4$O$_3$·HBr (393.24): C 48.87, H 4.36, N 14.25, found: C 48.60, H 4.18, N 14.24.

Preparation of *N*-methylbis[2-(3-alkoxy-5-nitro-1*H*-indazol-1-yl)-ethyl]amines 7 and 9 and bis[2-(3-alkoxy-5-nitro-1*H*-indazol-1-yl)ethyl]amines 8 and 10: A mixture of the corresponding amine salt (3–6·HCl or ·HBr) (2.0 mmol), 2-bromoethyl derivative (**13**, **14**) (2.2 mmol) and potassium carbonate (0.69 g, 5.0 mmol) in acetonitrile (100 mL) was held at reflux for 3 days (for **7**, **9**) or for 7 days (for **8**, **10**). The solvent was then evaporated and the residue extracted with chloroform (4×50 mL). The organic phase was concentrated and applied to the top of a flash chromatography column which was eluted first with chloroform to afford the corresponding 1-vinyl derivatives (**15**, **16**) and the excess of 2-bromoethyl derivative (**13**, **14**), and then with chloroform/ethanol (50:1 to 20:1) (for **8**, **10**) or chloroform/acetone mixtures (50:1 to 5:1) (for **7**, **9**) to yield the desired amines. The latter were converted into the corresponding hydrochlorides by treatment with 36% aqueous hydrochloric acid (1 mL) in ethanol (20 mL) followed by evaporation to dryness. Hydrochlorides of amines **7**, **8**, and **10** were recrystallized from an appropriate solvent; crude 9·HCl was triturated with acetone to afford pure salt as an amorphous solid.

***N*-Methylbis[2-(3-methoxy-5-nitro-1*H*-indazol-1-yl)ethyl]amine hydrochloride (7·HCl)**: Yield: 0.92 g (91%) [38 mg (8%) of 1-vinylindazole **15** was also obtained]; mp: 224–227 °C (methanol); ^{1}H NMR ([D$_6$]DMSO): δ = 11.80 (brs, 1H, $^+$NH), 8.43 (d, J = 2.1 Hz, 2H, 4′-H), 8.18 (dd, J = 9.3, 2.1 Hz, 2H, 6′-H), 7.79 (d, J = 9.3 Hz, 2H, 7′-H), 4.79 (brs, 4H, 2-CH$_2$), 4.04 (s, 6H, OCH$_3$), 3.61 (brs, 4H, 1-CH$_2$), 2.88 ppm (s, 3H, NCH$_3$); ^{13}C NMR ([D$_6$]DMSO): δ = 157.85 (C3′), 142.81 (C7′a), 140.70 (C5′), 122.40 (C6′), 117.36 (C4′), 111.14 (C3′a), 110.40 (C7′), 56.59 (OCH$_3$), 53.38 (C1), 42.96 (C2), 39.96 ppm (NCH$_3$); MS (ES$^+$) m/z (%): 470 (100) [M−Cl]$^+$; Elemental analysis calcd (%) for C$_{21}$H$_{23}$N$_7$O$_6$·HCl (505.91): C 49.86, H 4.78, N 19.38, found: C 49.81, H 4.70, N 19.19.

Bis[2-(3-methoxy-5-nitro-1*H*-indazol-1-yl)ethyl]amine hydrochloride monohydrate (8·HCl·H$_2$O): Yield: 0.81 g (79%) [82 mg (17%) of 1-vinylindazole **15** were also obtained]; mp: 231–234 °C (water) (previous loss of water at 135–140 °C); ^{1}H NMR ([D$_6$]DMSO): δ = 9.59 (brs, 2H, $^+$NH$_2$), 8.46 (d, J = 2.1 Hz, 2H, 4′-H), 8.20 (dd, J = 9.3, 2.1 Hz, 2H, 6′-H), 7.78 (d, J = 9.3 Hz, 2H, 7′-H), 4.68 (t, J = 6.0 Hz, 4H, 2-CH$_2$), 4.02 (s, 6H, OCH$_3$), 3.44 ppm (brs, 4H, 1-CH$_2$); ^{13}C NMR ([D$_6$]DMSO): δ = 157.90 (C3′), 142.94 (C7′a), 140.61 (C5′), 122.34 (C6′), 117.33 (C4′), 111.21 (C3′a), 110.33 (C7′), 56.58 (OCH$_3$), 45.87 (C1), 44.43 ppm (C2); MS (ES$^+$) m/z (%): 456 (100) [M−Cl]$^+$; Elemental analysis calcd (%) for C$_{20}$H$_{21}$N$_7$O$_6$·HCl·H$_2$O (509.90): C 47.11, H 4.74, N 19.23, found: C 47.17, H 4.62, N 19.36.

***N*-Methylbis[2-(3-benzyloxy-5-nitro-1*H*-indazol-1-yl)ethyl]amine hydrochloride (9·HCl)**: Yield: 1.00 g (76%) [80 mg (12%) of 1-vinylindazole **16** was also obtained]; amorphous solid; ^{1}H NMR ([D$_6$]DMSO): δ = 11.46 (brs, 1H, $^+$NH), 8.47 (d, J = 2.2 Hz, 2H, 4′-H), 8.20 (dd, J = 9.0, 2.2 Hz, 2H, 6′-H), 7.82 (d, J = 9.0 Hz, 2H, 7′-H), 7.49 (m, 4H, Ph 2-, 6-H), 7.36 (m, 6H, Ph 3-, 4-, 5-H), 5.37 (s, 4H, OCH$_2$), 4.81 (brs, 4H, 2-CH$_2$), 3.65 (brs, 4H, 1-CH$_2$), 2.89 ppm (s, 3H, CH$_3$); ^{13}C NMR ([D$_6$]DMSO): δ = 157.10 (C3′), 142.75 (C7′a), 140.79 (C5′), 135.98 (Ph C1), 128.42 (Ph C3, C5), 128.22 (Ph C4), 128.08 (Ph C2, C6), 122.46 (C6′), 117.45 (C4′), 111.34 (C3′a), 110.47 (C7′), 70.68 (OCH$_2$), 53.38 (C1), 43.02 (C2), 39.77 ppm (CH$_3$); MS (ES$^+$) m/z (%): 622 (100) [M−Cl]$^+$; Elemental analysis calcd (%) for C$_{33}$H$_{31}$N$_7$O$_6$·HCl (658.10): C 60.23, H 4.90, N 14.90, found: C 60.53, H 5.02, N 14.98.

Bis[2-(3-benzyloxy-5-nitro-1*H*-indazol-1-yl)ethyl]amine hydrochloride (10·HCl): Yield: 0.97 g (75%) [84 mg (13%) of 1-vinylindazole **16** were also obtained]; mp: 205–207 °C (nitromethane); ^{1}H NMR ([D$_6$]DMSO): δ = 9.63 (brs, 2H, $^+$NH$_2$), 8.48 (d, J = 2.1 Hz, 2H, 4′-H), 8.20 (dd, J = 9.3, 2.1 Hz, 2H, 6′-H), 7.80 (d, J = 9.3 Hz, 2H, 7′-H), 7.50 (m, 4H, Ph 2-, 6-H), 7.37 (m, 6H, Ph 3-, 4-, 5-H), 5.37 (s, 4H, OCH$_2$), 4.70 (t, J = 5.7 Hz, 4H, 2-CH$_2$), 3.47 ppm (brs, 4H, 1-CH$_2$); ^{13}C NMR ([D$_6$]DMSO): δ = 157.20 (C3′), 142.87 (C7′a), 140.69 (C5′), 135.99 (Ph C1), 128.42 (Ph C3, C5), 128.22 (Ph C4), 128.12 (Ph C2, C6), 122.37 (C6′), 117.42 (C4′), 111.38 (C3′a), 110.39 (C7′), 70.69 (OCH$_2$), 45.88 (C1), 44.47 ppm (C2); MS (ES$^+$) m/z (%): 608 (100) [M−Cl]$^+$; Elemental analysis calcd (%) for C$_{32}$H$_{29}$N$_7$O$_6$·HCl (644.08): C 59.67, H 4.69, N 15.22, found: C 59.95, H 4.72, N 15.28.

Biology

Parasite strain culture: Three different *T. cruzi* strains were evaluated in this work: *T. cruzi* SN3 strain (IRHOD/CO/2008/SN3, DTU I) isolated from domestic *Rhodnius prolixus* from Guajira, Colombia;[54] *T. cruzi* Arequipa strain (MHOM/Pe/2011/Arequipa, DTU V) isolated from a human from Arequipa, Peru; and *T. cruzi* Tulahuen strain (TINF/CH/1956/Tulahuen, DTU VI) isolated from Tulahuen, Chile. Epimastigote culture forms were grown at 28 °C in RPMI (Gibco®) with 10% (*v*/*v*) fetal bovine serum (heat-inactivated), 0.5% (*w*/*v*) trypticase (BBL) and 0.03 M hemin.[55]

In vitro activity assays; epimastigote forms: *T. cruzi* epimastigotes (strains SN3, Arequipa and Tulahuen) were collected in the exponential growth phase by centrifugation at 400 *g* for 10 min. The compounds to be tested were dissolved in DMSO at a concentration of 0.01% (*v*/*v*) and assayed as nontoxic or without inhibitory effects on parasite growth. Trypanocidal activity was determined in our laboratory using a previously described method[56] with some modifications. Assays were performed in microtiter plates (96-well plates) at 5×10^5 parasites per mL, and after addition of the compounds at dosages of 100 to 0.1 μM and cultured in 200 μL per well volumes at 28 °C. Growth controls and BZN were also included. After a 48 h incubation, 20 μL (0.125 mg mL^{-1}) of resazurin sodium salt (Sigma–Aldrich) was added, and the plates were incubated for a further 24 h. Finally, 5 μL (10% *w*/*v*) of sodium dodecyl sulfate (SDS) was added, and after 10 min, the trypanocidal activity of the compounds on the plates was assessed by absorbance measurements (Sunrise, TECAN) at 570 and 600 nm.[57] The trypanocidal effect was determined using GraphPad Prism and is expressed as the IC$_{50}$, i.e., the concentration required to result in

© 2018 Wiley-VCH Verlag GmbH & Co. KGaA, Weinheim

50% inhibition. Each drug concentration was tested in triplicate in three separate determinations.

Vero cells culture and cytotoxicity tests: Vero cells (EACC number 84113001) from monkey kidney were grown in humidified 95% air, 5% CO_2 atmosphere at 37 °C in RPMI (Gibco®) with 10% (*v*/*v*) fetal bovine serum (heat-inactivated).[58] Vero cells were collected first by trypsinization and then by centrifugation at 400 *g* for 10 min. The compounds to be tested were dissolved as mentioned above. Cytotoxicity against Vero cells was assessed using microtiter plates (96-well plates) at 1.25×10^4 cells per mL, and after addition of the compounds at dosages of 2000 to 1 μM and cultured in 200 μL per well volumes in RPMI with 1% (*v*/*v*) fetal bovine serum (heat-inactivated). Growth controls and BZN were also included. After a 48 h incubation, the same procedure as described to determine the trypanocidal activity was followed.

Transformation of epimastigotes to metacyclic forms: *T. cruzi* strains SN3, Arequipa and Tulahuen were grown as epimastigote forms at 28 °C.[59] Metacyclic trypomastigotes (aged epimastigote cultures) were induced by culturing a seven-day-old culture of epimastigote forms in Grace's Insect Medium (Gibco®) with 10% (*v*/*v*) fetal bovine serum (heat-inactivated) at 28 °C for 7 days.[60] The parasites were then harvested by centrifugation at 400 *g* for 10 min and incubated at 5×10^8 parasites per mL in TAU medium (190 mM NaCl, 17 mM KCl, 2 mM $MgCl_2$, 2 mM $CaCl_2$, 8 mM phosphate buffer, pH 6.0) for 2 h at 28 °C. Thereafter, the parasites were incubated at 5×10^6 parasites per mL in TAU3AAG medium (TAU supplemented with 10 mM L-proline, 50 mM L-sodium glutamate, 2 mM L-sodium aspartate and 10 mM D-glucose) for 4 days at 28 °C.[61] Subsequently, this metacyclic trypomastigotes were used to infect Vero cells in humidified 95% air, 5% CO_2 atmosphere at 37 °C in RPMI (Gibco®) with 10% (*v*/*v*) fetal bovine serum (heat-inactivated) for 5 to 7 days.[62] Finally, the culture-derived trypomastigotes were collected by centrifugation at 3000 *g* for 5 min and used to infect BALB/c albino mice.

In vitro activity assays; amastigote forms: Vero cells (EACC number 84113001) from monkey kidney were grown in humidified 95% air, 5% CO_2 atmosphere at 37 °C in RPMI (Gibco®) with 10% (*v*/*v*) fetal bovine serum (heat-inactivated)[58] and were collected first by trypsinization and then by centrifugation at 400 *g* for 10 min. Assays were performed in microtiter plates (24-well plates) at 1×10^4 Vero cells per well with rounded coverslips on the bottom; 24 h later the cells were infected with culture-derived trypomastigotes of *T. cruzi* (strains SN3, Arequipa and Tulahuen) at a multiplicity of infection (MOI) ratio of 1:10 during 24 h. Non-phagocyted parasites were removed by washing, and after addition of the compounds at dosages of 50 to 0.1 μM, cultured in 500 μL per well volumes in RPMI with 1% (*v*/*v*) fetal bovine serum (heat-inactivated) in a humidified 95% air, 5% CO_2 atmosphere at 37 °C. Growth controls and BZN were also included. After a 72 h incubation, the trypanocidal effect was assessed based on the number of amastigotes in treated and untreated cultures in methanol-fixed and Giemsa-stained preparations. The number of amastigotes was established by analyzing 500 host cells distributed in randomly chosen microscopic fields. The trypanocidal effect was determined using GraphPad Prism and it is expressed as the IC_{50}, i.e., the concentration required to result in 50% inhibition. Each drug concentration was tested in triplicate in three separate determinations.

In vitro activity assays; trypomastigote forms: *T. cruzi* blood trypomastigotes (strains SN3, Arequipa and Tulahuen) were obtained by cardiac puncture from BALB/c albino mice during the parasitemia peak after infection and diluted in RPMI (Gibco®) with 10% (*v*/*v*) fetal bovine serum (heat-inactivated). Trypanocidal activity was determined in our laboratory according to a described method[63] with certain modifications. Assays were performed in microtiter plates (96-well plates) at 2×10^6 parasites per mL, and after addition of the compounds at dosages of 50 to 0.1 μM, cultured in 200 μL per well volumes in humidified 95% air, 5% CO_2 atmosphere at 37 °C. Growth controls and BZN were also included. After a 24 h incubation, 20 μL (0.125 mg mL^{-1}) of resazurin sodium salt (Sigma–Aldrich) was added, and the plates were incubated for 4 h. Finally, the same procedure as described to determine the trypanocidal activity was followed.

In vivo trypanocidal activity assays

Mice: These experiments were approved by the University of Granada Ethics Committee on Animal Experimentation (RD53/2013) and performed under the rules and principles of the international guide for biomedical research in experimental animals. Female BALB/c mice (8–10 weeks old and 20–25 g) were used to perform these experiments, maintained under standard conditions (12 h dark/light cycle and 22±3 °C temperature) and provided with water and standard chow ad libitum.

Mice infection and treatment: Groups of three mice were infected via intraperitoneal inoculation with 5×10^5 BTs of *T. cruzi* Arequipa strain (obtained from previously infected mice with metacyclic trypomastigotes) in 0.2 mL phosphate-buffered saline (PBS). The mice were divided, in acute and chronic phases, as follows: 0, negative control group (uninfected and untreated); I, positive control group (infected and untreated); II, BZN group (infected and treated with BZN); III, study group (infected and treated with the compounds under study). BZN and the compounds under study were prepared at 2 mg mL^{-1} in an aqueous suspension vehicle containing 5% (*v*/*v*) DMSO and 0.5% (*w*/*v*) hydroxypropyl methylcellulose.[53] Drugs were administered by the oral route (≈200 μL) once daily for five consecutive days, and vehicle only was administered in the negative and positive control groups. Therefore, doses of 20 mg kg^{-1} per day were administered for five consecutive days. Administration of the tested compounds was initiated on the 10^{th} day post-infection (once the infection was confirmed) in mice treated in acute phase and on the 75^{th} day post-infection (it is established that the animals had entered the chronic phase of the experiment) in the mice treated in the chronic phase.

Parasitemia levels in the acute phase treatment: Peripheral blood from each mouse treated in acute phase was obtained from the mandibular vein (5 μL samples) and diluted 1:100 in PBS. The number of BTs (parasitemia levels) was quantified every two or three days from 7^{th} day post-infection until the day parasitemia was not detected. This counting was performed using a Neubauer chamber, and the number of BTs was expressed as parasites per mL.[47]

Cyclophosphamide-induced IS: After 100^{th} day post-infection, the groups of mice treated in the acute and chronic phases with significantly decreased parasitemia levels and established to be in the chronic phase of the experiment, regardless of the treatment and undetectable by fresh blood microscopy examination, were immunosuppressed with cyclophosphamide monohydrate (ISOPAC®) as follows: one intraperitoneal injection every four days with a dose of 200 mg kg^{-1}, for a maximum of three doses.[53] The efficacy of such an IS procedure for assessing cryptic infection was verified by the high parasitemia in chronically untreated mice. Within one week after the last cyclophosphamide monohydrate injection, parasitemia was evaluated according the procedure described for par-

© 2018 Wiley-VCH Verlag GmbH & Co. KGaA, Weinheim

asitemia levels in acute phase to quantify the presence or absence of BTs as the reactivation rate.

Organs DNA extraction, PCR and electrophoresis: After cyclophosphamide-induced IS, mice were bled out under gaseous anesthesia (CO_2) via heart puncture, and blood was collected. Our previous in vivo studies using the *T. cruzi* Arequipa strain revealed its tropism for the following organs: adipose tissue, bone marrow, brain, esophagus, heart, lung, muscle, spleen and stomach. Therefore, these nine organs were harvested and immediately perfused with pre-warmed PBS to avoid contamination of the tissue with BTs.[64] In addition, spleen was weighed to evaluate inflammation of this organ in the different groups of mice. Finally, the target organs were thawed and ground up using a Potter-Elvehjem, and DNA extraction was performed using Wizard® Genomic DNA Purification Kit (Promega).[47]

PCR was performed based on the published sequence of the enzyme SOD *T. cruzi* CL Brenner (GenBank accession No. XM_808937) using two primers designed in our laboratory that allow the detection of *T. cruzi* DNA in different biological samples. These primers amplify a fragment belonging to SOD gene b of *T. cruzi* consisting of approximately 300 base pairs (bp). The amplifications were performed using a Thermal Cycler™ MyCycler thermal cycler (Bio-Rad) with the following reaction mixture: 1 μL of DMSO, 200 nM iSODd, 200 nM iSODr, 10 mM Tris·HCl (pH 9.0), 1.5 mM $MgCl_2$, 50 mM KCl, 0.01% gelatin, 0.1% Triton X-100, 100 mM of each dNTP, 0.5 U of Taq DNA polymerase, 1 μg of DNA, and HPLC water, in a final volume of 20 μL; and with the following routine: 95 °C/3 min, 30 cycles of 95 °C/30 s, 55.5 °C/45 s, 72 °C/30 s, and 72 °C/7 min. Finally, the amplification products were subjected to electrophoresis on a 2% agarose gel for 90 min at 90 V, containing 1:10 000 GelRed nucleic acid gel stain.

ELISA: Serum samples were obtained 2 days after treatment, 1 day before IS and on the day of necropsy for the mice treated in acute phase, and 2 days after treatment and on the day of necropsy (sera post-IS) for the mice treated in the chronic phase. To obtain serum, blood was incubated in a glass tube for 2 h at 37 °C to allow clotting and then 16 h at 4 °C for retraction of the clot. The serum was collected and centrifuged at 2700 *g* for 20 min at 4 °C. The serum was used for ELISA and biochemical analysis as explained later in this paper. SOD excreted (SODe) from the parasites, extracted and purified as subsequently described, was used as the antigen fraction. Circulating antibodies in serum against *T. cruzi* Arequipa strain were qualitatively and quantitatively evaluated by ELISA. The serum from whole blood was diluted 1:80 in PBS, and all serum samples were analyzed in triplicate in polystyrene 96-well microtiter plates. The absorbance was read at 492 nm using a microplate reader (Sunrise, TECAN). Mean and standard deviations of the optical densities of the negative control sera were used to calculate the cut-off value (mean plus three times the standard deviation).[47]

Toxicity tests by biochemical analysis: Serum samples were obtained at 2 days after treatment and on the day of necropsy (sera post-IS) both for mice treated in the acute and chronic phases. These sera were sent to the Biochemical Service of the University of Granada, where a series of parameters were measured using commercial kits from Cromakit® with the BS-200 Chemistry Analyzer Shenzhen Mindray (Bio-medical Electronics Co., LTD). Mean values and standard deviations were calculated using the levels obtained for different populations of sera ($n=6$, $n=3$), and the confidence interval for the mean normal populations were also c calculated using the levels obtained for different populations of sera ($n=6$, $n=3$), and the confidence interval for the mean normal populations were also calculated based on a confidence level of 95% [$100\times(1-\alpha)=100\times(1-0.05)$]. Figure 12 shows the timeline for all in vivo experiments in acute and chronic phases.

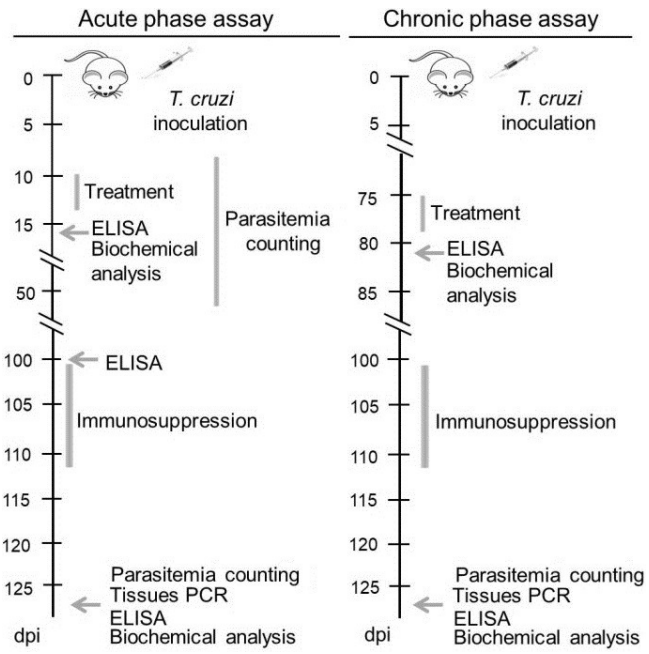

Figure 12. Timeline for all in vivo experiments in acute and chronic phases. dpi = day post-infection.

Studies of the mechanism of action

Metabolite excretion: *T. cruzi* Arequipa strain was grown and collected in the epimastigote form at 28 °C[59] in the exponential growth phase by centrifugation at 400 *g* for 10 min. The compounds to be tested were dissolved as mentioned above. The assays were performed in cell culture flasks (surface area, 25 cm^2) at 5×10^5 parasites per mL and after the addition of the compounds at IC_{25} concentrations at 28 °C. Non-treated parasites were also included. After a 72 h incubation, treated and non-treated parasites were centrifuged at 800 *g* for 10 min to collect the supernatants to determine the excreted metabolites by ^{1}H NMR.

Chemical shifts were expressed in ppm using sodium 2,2-dimethyl-2-silapentane-5-sulfonate as the reference signal. The ^{1}H NMR spectra were acquired with a VARIAN DIRECT DRIVE 400 MHz Bruker spectrometer with an AutoX probe using D_2O. The assignments of metabolites were based on their ^{1}H NMR spectra. The chemical shifts used to identify the respective metabolites were consistent with those described previously by our group[65] and with the human metabolome database. The spectral region of 1.0–5.5 ppm was bucketed into a frequency window of 0.1 ppm. The peak (2.6 ppm) corresponding to DMSO was removed before binning, and the regions corresponding to water (4.5–5.5 ppm) and glucose (3.4–3.8 ppm) were excluded during binning to avoid artefacts due to pre-saturation. The aromatic region was excluded because the signal-to-noise ratio in this region was poorer than in the aliphatic region. The resulting integrals were normalized to the working region (1.0–3.4) ppm of the spectrum to correct for inter-sample differences in dilution. The binning and normalizations were achieved using Mestrenova 9.0 software. The matrix obtained in Mes-

© 2018 Wiley-VCH Verlag GmbH & Co. KGaA, Weinheim

trenova was imported into Microsoft Excel for further data analyses.

Rho 123 and AO assays: *T. cruzi* Arequipa strain was grown and collected as epimastigote forms at 28 °C[59] in the exponential growth phase by centrifugation at 400 *g* for 10 min. The compounds to be tested were dissolved as mentioned above. The assays were performed in cell culture flasks (surface area, 25 cm^2) at 5×10^5 parasites per mL, and after the addition of the compounds at IC_{25} concentration at 28 °C. Untreated parasites were also included. After a 72 h incubation, treated and untreated parasites were collected by centrifugation at 400 *g* for 10 min, and the pellets of parasites were washed three times with PBS. Subsequently, the parasites were resuspended in 0.5 mL PBS with 10 μg mL^{-1} Rho 123 (Sigma–Aldrich) or 10 μg mL^{-1} AO (Sigma–Aldrich) for 20 min.[66] Finally, the samples were washed twice with ice-cold PBS, dispersed in 1 mL of PBS and immediately analyzed by flow cytometry (Becton Dickinson FACSAria III). The data were captured and analyzed using BD FACSDiva v8.01 software (Becton Dickinson Biosciences, 2350 Qume Drive, San Jose, CA, USA). The fluorescence intensities for Rho 123 (mitochondrial membrane potential) and AO (DNA and RNA) were quantified based on the forward (FSC) and side (SSC) scatter, for which a total of 10000 events were acquired in the previously established region corresponding to *T. cruzi* epimastigotes.[67] Alterations in the fluorescence intensities of AO (APC-A) or Rho 123 (FITC-A) were quantified by the index of variation (IV) obtained using the equation (TM-CM)/CM, where TM is the median fluorescence for treated parasites and CM is the median fluorescence for non-treated parasites (control).[66]

Extraction/purification of the SODe and SOD inhibition studies: *T. cruzi* Arequipa strain was grown as the epimastigote form at 28 °C in RPMI (Gibco®) with 10% (*v*/*v*) fetal bovine serum (heat-inactivated), 0.5% (*w*/*v*) trypticase (BBL) and 0.03 M hemin[55] in the exponential growth phase. The parasites were collected by centrifugation at 400 *g* for 10 min, and the pellet was resuspended at 5×10^9 parasites per mL in the same medium without fetal bovine serum in cell culture flasks (surface area, 75 cm^2). After a 28 h incubation at 28 °C, the culture was centrifuged at 800 *g* for 10 min at 4 °C, and the supernatant was collected and filtered with 0.45 μm pore size filters. Protein was precipitated by addition of ammonium sulfate and centrifugation at 10000 *g* for 20 min at 4 °C to maintain the 35–85% protein fraction, which was re-dissolved in 2.5 mL of 20 mM potassium phosphate buffer (pH 7.8) containing 1 mM EDTA. Finally, this fraction was desalted by gel filtration using a Sephadex G-25 column,[68] and the protein concentration was determined using the Bradford method (Sigma Immunochemical, St. Louis, MO, USA) with bovine serum albumin as a standard.[69] Fe-SODe and commercial CuZn-SOD (Sigma–Aldrich) activities were determined using the method described by Beyer and Fridovich.[43]

Acknowledgements

This work was supported by the Spanish Ministry of Economy, Industry and Competitiveness (MINEICO), project reference SAF2015-66690-R and Consolider Ingenio CSD2010-00065, by FONDECYT (Chile), project reference 11150559, and by the Junta de Andalucía, project reference P11-CTS-07187. R.M.-E. is grateful for a FPU Grant (FPU14/01537) from the Ministry of Education of Spain. E.M.-C. acknowledges a predoctoral fellowship from Junta de Andalucia.

Conflict of interest

The authors declare no conflict of interest.

Keywords: antiprotozoal agents · Chagas disease · drug discovery · nitroheterocycles · *Trypanosoma cruzi*

[1] P. J. Hotez, D. H. Molyneux, A. Fenwick, J. Kumaresan, S. E. Sachs, J. D. Sachs, L. Savioli, *N. Engl. J. Med.* **2007**, *357*, 1018–1027.
[2] C. Bern, *N. Engl. J. Med.* **2015**, *373*, 456–466.
[3] J. Manne-Goehler, C. A. Umeh, S. P. Montgomery, V. J. Wirtz, *PLoS Neglected Trop. Dis.* **2016**, *10*, e0005033.
[4] C. Roca, M. J. Pinazo, P. López-Chejade, J. Bayó, E. Posada, J. López-Solana, M. Gállego, M. Portús, J. Gascón, *PLoS Neglected Trop. Dis.* **2011**, *5*, e1135.
[5] J. A. Pérez-Molina, F. Norman, R. López-Vélez, *Curr. Infect. Dis. Rep.* **2012**, *14*, 263–274.
[6] H. B. Tanowitz, L. M. Weiss, S. P. Montgomery, *PLoS Neglected Trop. Dis.* **2011**, *5*, e1136.
[7] P. C. Pereira, E. C. Navarro, *J. Venomous. Anim. Toxins Incl. Trop. Dis.* **2013**, *19*, 34.
[8] Á. Moncayo, A. C. Silveira in *American Trypanosomiasis, Chagas Disease, One Hundred Years of Research*, 2nd Ed. (Eds: J. Telleria, M. Tibayrenc), Elsevier, Amsterdam, **2017**, pp. 17–30.
[9] M. D. Lewis, A. F. Francisco, M. C. Taylor, J. M. Kelly, *J. Biomol. Screening* **2015**, *20*, 36–43.
[10] A. J. Romanha, S. L. de Castro, M. N. C. Soeiro, J. Lannes-Vieira, I. Ribeiro, A. Talvani, B. Bourdin, B. Blum, B. Olivieri, C. Zani, C. Spadafora, E. Chiari, E. Chatelain, G. Chaves, J. E. Calzada, J. M. Bustamante, L. H. Freitas-Junior, L. I. Romero, M. T. Bahia, M. Lotrowska, M. Soares, S. G. Andrade, T. Armstrong, W. Degrave, Z. A. Andrade, *Mem. Inst. Oswaldo Cruz* **2010**, *105*, 233–238.
[11] A. Rassi, Jr., A. Rassi, J. A. Marin-Neto, *Lancet* **2010**, *375*, 1388–1402.
[12] A. F. Henao-Martínez, D. A. Schwartz, I. V. Yang, *Trans. R. Soc. Trop. Med. Hyg.* **2012**, *106*, 521–527.
[13] E. Dumonteil, *Infect. Genet. Evol.* **2009**, *9*, 1075–1082.
[14] S. R. Wilkinson, J. M. Kelly, *Expert Rev. Mol. Med.* **2009**, *11*, e31.
[15] J. A. Marin-Neto, A. Rassi, Jr., A. Avezum, Jr., A. C. Mattos, A. Rassi, *Mem. Inst. Oswaldo Cruz* **2009**, *104*, 319–324.
[16] Y. Jackson, E. Alirol, L. Getaz, H. Wolff, C. Combescure, F. Chappuis, *Clin. Infect. Dis.* **2010**, *51*, e69–e75.
[17] M.-J. Pinazo, L. Guerrero, E. Posada, E. Rodriguez, D. Soy, J. Gascon, *Antimicrob. Agents Chemother.* **2013**, *57*, 390–395.
[18] S. R. Wilkinson, M. C. Taylor, D. Horn, J. M. Kelly, I. Cheeseman, *Proc. Natl. Acad. Sci. USA* **2008**, *105*, 5022–5027.
[19] A. M. Mejia, B. S. Hall, M. C. Taylor, A. Gómez-Palacio, S. R. Wilkinson, O. Triana-Chávez, J. M. Kelly, *J. Infect. Dis.* **2012**, *206*, 220–228.
[20] A. I. Porrás, Z. E. Yadon, J. Altcheh, C. Britto, G. C. Chaves, L. Flevaud, O. A. Martins-Filho, I. Ribeiro, A. G. Schijman, M. A. Shikanai-Yasuda, S. Sosa-Estani, E. Stobbaerts, F. Zicker, *PLoS Neglected Trop. Dis.* **2015**, *9*, e0003697.
[21] V. J. Arán, C. Ochoa, L. Boiani, P. Buccino, H. Cerecetto, A. Gerpe, M. González, D. Montero, J. J. Nogal, A. Gómez-Barrio, A. Azqueta, A. López de Ceráin, O. E. Piro, E. E. Castellano, *Bioorg. Med. Chem.* **2005**, *13*, 3197–3207.
[22] L. Boiani, A. Gerpe, V. J. Arán, S. Torres de Ortiz, E. Serna, N. Vera de Bilbao, L. Sanabria, G. Yaluff, H. Nakayama, A. Rojas de Arias, J. D. Maya, J. A. Morello, H. Cerecetto, M. González, *Eur. J. Med. Chem.* **2009**, *44*, 1034–1040.
[23] J. Rodríguez, A. Gerpe, G. Aguirre, U. Kemmerling, O. E. Piro, V. J. Arán, J. D. Maya, C. Olea-Azar, M. González, H. Cerecetto, *Eur. J. Med. Chem.* **2009**, *44*, 1545–1553.
[24] J. Rodríguez, V. J. Arán, L. Boiani, C. Olea-Azar, M. L. Lavaggi, M. González, H. Cerecetto, J. D. Maya, C. Carrasco-Pozo, H. S. Cosoy, *Bioorg. Med. Chem.* **2009**, *17*, 8186–8196.
[25] B. Muro, F. Reviriego, P. Navarro, C. Marín, I. Ramírez-Macías, M. J. Rosales, M. Sánchez-Moreno, V. J. Arán, *Eur. J. Med. Chem.* **2014**, *74*, 124–134.

© 2018 Wiley-VCH Verlag GmbH & Co. KGaA, Weinheim

[26] M. M. Alho, R. N. García-Sánchez, J. J. Nogal-Ruiz, J. A. Escario, A. Gómez-Barrio, A. R. Martínez-Fernández, V. J. Arán, *ChemMedChem* **2009**, *4*, 78 – 87.
[27] P. González, C. Marín, I. Rodríguez-González, A. B. Hitos, M. J. Rosales, M. Reina, J. G. Díaz, A. González-Coloma, M. Sánchez-Moreno, *Int. J. Antimicrob. Agents* **2005**, *25*, 136 – 141.
[28] S. Espuelas, D. Plano, P. Nguewa, M. Font, J. A. Palop, J. M. Irache, C. Sanmartín, *Curr. Med. Chem.* **2012**, *19*, 4259 – 4288.
[29] H. Kayama, K. Takeda, *Microbes Infect.* **2010**, *12*, 511 – 517.
[30] A. El Bouhdidi, C. Truyens, M.-T. Rivera, H. Bazin, Y. Carlier, *Parasite Immunol.* **1994**, *16*, 69 – 76.
[31] A. F. Francisco, M. D. Lewis, S. Jayawardhana, M. C. Taylor, E. Chatelain, J. M. Kelly, *Antimicrob. Agents Chemother.* **2015**, *59*, 4653 – 4661.
[32] M. L. Ginger, *Protist* **2005**, *156*, 377 – 392.
[33] F. Bringaud, L. Rivière, V. Coustou, *Mol. Biochem. Parasitol.* **2006**, *149*, 1 – 9.
[34] J. J. Cazzulo, *FASEB J.* **1992**, *6*, 3153 – 3161.
[35] I. G. Kirkinezos, C. T. Moraes, *Semin. Cell Dev. Biol.* **2001**, *12*, 449 – 457.
[36] W. Lee, F. Thévenod, *Am. J. Physiol. Cell Physiol.* **2006**, *291*, C195 – C202.
[37] X. J. Shang, G. Yao, J. P. Ge, Y. Sun, W. H. Teng, Y. F. Huang, *J. Androl.* **2009**, *30*, 122 – 126.
[38] N. K. Verma, G. Singh, C. S. Dey, *Exp. Parasitol.* **2007**, *116*, 1 – 13.
[39] W. N. Hunter, M. S. Alphey, C. S. Bond, A. W. Schüttelkopf, *Biochem. Soc. Trans.* **2003**, *31*, 607 – 610.
[40] L. Piacenza, M. P. Zago, G. Peluffo, M. N. Alvarez, M. A. Basombrio, R. Radi, *Int. J. Parasitol.* **2009**, *39*, 1455 – 1464.
[41] L. Maes, D. Van den Berghe, N. Germonprez, L. Quirijnen, P. Cos, N. De Kimpe, L. Van Puyvelde, *Antimicrob. Agents Chemother.* **2004**, *48*, 130 – 136.
[42] N. Germonprez, L. Maes, L. Van Puyvelde, M. Van Tri, D. A. Tuan, N. De Kimpe, *J. Med. Chem.* **2005**, *48*, 32 – 37.
[43] W. F. Beyer, I. Fridovich, *Anal. Biochem.* **1987**, *161*, 559 – 566.
[44] R. Don, J. R. Ioset, *Parasitology* **2014**, *141*, 140 – 146.
[45] D. F. De Suasnábar, E. Arias, M. Streiger, M. Piacenza, M. Ingaramo, M. Del Barco, N. Amicone, *Rev. Inst. Med. Trop. Sao Paulo* **2000**, *42*, 99 – 109.
[46] J. A. Urbina, *Curr. Pharm. Des.* **2002**, *8*, 287 – 295.
[47] F. Olmo, C. Rotger, I. Ramírez-Macías, L. Martínez, C. Marín, L. Carreras, K. Urbanová, M. Vega, G. Chaves-Lemaur, A. Sampedro, M. J. Rosales, M. Sánchez-Moreno, A. Costa, *J. Med. Chem.* **2014**, *57*, 987 – 999.
[48] D. M. Santos, T. A. F. Martins, I. S. Caldas, L. F. Diniz, G. L. L. Machado-Coelho, C. M. Carneiro, R. P. de Oliveira, A. Talvani, M. Lana, M. T. Bahia, *Acta Trop.* **2010**, *113*, 134 – 138.
[49] L. Murcia, B. Carrilero, F. Ferrer, M. Roig, F. Franco, M. Segovia, *Eur. J. Clin. Microbiol. Infect. Dis.* **2016**, *35*, 1819 – 1827.
[50] A. Requena-Méndez, E. Aldasoro, E. de Lazzari, E. Sicuri, M. Brown, D. A. Moore, J. Gascon, J. Muñoz, *PLoS Neglected Trop. Dis.* **2015**, *9*, e0003540.
[51] A. L. Basquiera, A. Sembaj, A. M. Aguerri, M. Omelianiuk, S. Guzmán, J. Moreno Barral, T. F. Caeiro, R. J. Madoery, O. A. Salomone, *Heart* **2003**, *89*, 1186 – 1190.
[52] C. Britto, M. A. Cardoso, P. Marques, O. Fernandes, C. M. Morel, *Mem. Inst. Oswaldo Cruz* **1999**, *94*, 305 – 306.
[53] A. F. Francisco, S. Jayawardhana, M. D. Lewis, K. L. White, D. M. Shackleford, G. Chen, J. Saunders, M. Osuna-Cabello, K. D. Read, S. A. Charman, E. Chatelain, J. M. Kelly, *Sci. Rep.* **2016**, *6*, 35351.
[54] J. Téllez-Meneses, A. M. Mejía-Jaramillo, O. Triana-Chávez, *Acta Trop.* **2008**, *108*, 26 – 34.
[55] G. Kendall, A. F. Wilderspin, F. Ashall, M. A. Miles, J. M. Kelly, *EMBO J.* **1990**, *9*, 2751 – 2758.
[56] M. Rolón, C. Vega, J. A. Escario, A. Gómez-Barrio, *Parasitol. Res.* **2006**, *99*, 103 – 107.
[57] S. N. Rampersad, *Sensors* **2012**, *12*, 12347 – 12360.
[58] G. Pless-Petig, M. Metzenmacher, T. R. Türk, U. Rauen, *BMC Biotechnol.* **2012**, *12*, 73.
[59] M. T. Bahia, I. M. de Andrade, T. A. Fontes Martins, Á. F. da Silva do Nascimiento, L. F. de Diniz, I. S. Caldas, A. Talvani, B. B. Trunz, E. Torreele, I. Ribeiro, *PLoS Neglected Trop. Dis.* **2012**, *6*, e1870.
[60] E. L. Isola, E. M. Lammel, S. M. González Cappa, *Exp. Parasitol.* **1986**, *62*, 329 – 335.
[61] J. Cardoso, M. J. Soares, *Mem. Inst. Oswaldo Cruz* **2010**, *105*, 1026 – 1032.
[62] V. T. Contreras, J. M. Salles, N. Thomas, C. M. Morel, S. Goldenberg, *Mol. Biochem. Parasitol.* **1985**, *16*, 315 – 327.
[63] M. Faundez, L. Pino, P. Letelier, C. Ortiz, R. López, C. Seguel, J. Ferreira, M. Pavani, A. Morello, J. D. Maya, *Antimicrob. Agents Chemother.* **2005**, *49*, 126 – 130.
[64] X. Ye, J. Ding, X. Zhou, G. Chen, S. F. Liu, *J. Exp. Med.* **2008**, *205*, 1303 – 1315.
[65] C. Fernández-Becerra, M. Sánchez-Moreno, A. Osuna, F. R. Opperdoes, *J. Eukaryotic Microbiol.* **1997**, *44*, 523 – 529.
[66] J. M. Sandes, A. Fontes, C. G. Regis-da-Silva, M. C. A. Brelaz De Castro, C. G. Lima-Junior, F. P. L. Silva, M. L. A. A. Vasconcellos, R. C. B. Q. Figueiredo, *PLoS One* **2014**, *9*, e93936.
[67] N. Hussein, H. Amawi, C. Karthikeyan, F. S. Hall, R. Mittal, P. Trivedi, C. R. Ashby, A. K. Tiwari, *Cancer Lett.* **2017**, *396*, 167 – 180.
[68] Á. López-Céspedes, E. Villagrán, K. Briceño Álvarez, J. A. de Diego, H. L. Hernández-Montiel, C. Saldaña, M. Sánchez-Moreno, C. Marín, *Sci. World J.* **2012**, 914129.
[69] M. M. Bradford, *Anal. Biochem.* **1976**, *72*, 248 – 254.

Manuscript received: July 31, 2018
Accepted manuscript online: August 11, 2018
Version of record online: September 4, 2018

© 2018 Wiley-VCH Verlag GmbH & Co. KGaA, Weinheim

6. DISCUSSION

6.1. Novel fluorescent parasites-based method

Currently, screening assays based on counting using Neubauer Chambers[215,230] or fluorescence/absorbance measurements based on colorimetric reagents[209,231] are the methods used for the evaluation of trypanocidal drugs against extracellular forms. For intracellular forms, assays are based on counting of stained samples using nucleic acids dyes[232,233] and/or image analysis algorithms[234–237]. This novel fluorescence-based method allows the evaluation of trypanocidal drugs against any of the parasite forms, either extra- or intracellular, in a shorter time (faster) and with fewer steps in the procedure (simpler) as no additional indicator reagents, enzymatic post-processes or laborious counting are required), and with faster data collection and processing. Moreover, this method has more precision and accuracy than any of the techniques mentioned above, especially those based on counting. In addition, the stability of the fluorescence is maintained for weeks.

Regarding High-throughput Screening (HTS) based on the automated fluorescence image analysis system for amastigote forms after nuclei acids dye stain[234–236], this allows differentiate intracellular amastigote forms and host cells based on significant differences of sizes between kinetoplasts and host nuclei, respectively, but the fluorescence discrimination has to be performed using algorithm in non-conventional microplate readers. In this regard, the novel fluorescent parasites-based method do not use any dye for the parasite detection and all fluorescence is only due to parasites, so conventional microplate readers can be used. Moreover, the possible problem in the false spot detection, that could result in an over estimation of infection, does not happen using fluorescence. Alternatively, the imagen analysis system is a highly sensitive method but detection of amastigotes is done by acquiring a certain number of images, and is not based on the entire well. The novel fluorescence-based method allows the

detection in the whole well, so the sensitivity is even higher, especially to determine very low infection following drug treatment. This is a really important point for the potential pharmacological consideration of drugs.

Finally, this novel fluorescence-based method provided by the NeonGreen protein has higher sensitivity than the previous ones, whose fluorescence come from other fluorescent proteins, such as tomato fluorescent protein or green fluorescent protein[228,238,239]. In addition, this dual-expresser parasite (fluorescence and bioluminescence) can be used in both *in vitro* and *in vivo* assays.

In summary, it is a highly reproducible, sensible, precise, simple and fast method that allows the evaluation of trypanocidal drugs against all three morphological forms of *T. cruzi*, either extra- or intracellular. Moreover, this method allows continuous monitoring of treated cultures over time, and this is able to predict/distinguish between slow- or fast-acting, short- or long-lasting, and static or cidal drugs after performing the so-called time to kill, length for action, and washout/reversibility assays, respectively. This is an important fact since fast-acting, long-lasting and cidal drugs are urgently needed[208]. These assays have been well defined for other parasitic diseases[240,241], but not for CD.

6.2. Trypanocidal drug candidates

6.2.1. Screening strategy

Drug discovery is a time-consuming and high-investment process used to identify new drugs for different disciplines, including biology, chemistry and pharmacology[242]. According to the Eastern Research Group (ERG)[243], it usually takes 10-15 years to develop a new drug, and its success rate is only 2.01 %[244]. As demonstrated the Food and Drug Administration (FDA), the number of drugs approved has been declining since 1995[245], but the investment in drug development has been increasing[246]. Therefore, it is urgent to find a new strategy for the development of new drugs.

The strategy of screening and identification of trypanocidal drug candidates, in both *in vitro* and *in vivo*, has been improved in this doctoral thesis. The methodology has been also improved according the instrumentation available[247–249]. Regarding *in vitro* strategy:

- Considering the widely genetic diversity of this parasite, the variable drug resistance to current treatments[52,250,251], and the TPP established by the DND*i*[2], three different strains, belonging to three different DTUs – I, V, and VI –, with different genotype, phenotype, tropism, and drug resistance, and from different host and location[210] were used for the *in vitro* screening. The primary reason for the high variability in the efficacy of BZN has been attributed to the broad genetic diversity of *T. cruzi* strains[251].
- Compounds were evaluated against the three morphological forms of the parasite, using the replicative extracellular epimastigote forms as a primary screening owing to its easy-to-handle cell culture. Active compounds were then tested against the relevant forms from a clinical viewpoint – trypomastigote and amastigote forms –, since they are the responsible for the acute and chronic phases of CD[250].
- The *in vitro* screening was performed in two steps following the criteria shown in **Scheme 6A**.These criteria were agreed according to criteria established by other authors: I) $IC_{50} < 5$ μM, selectivity index (SI) > 10[208]; II) $IC_{50} \leq 10$ μM, SI > 10[252]; III) $IC_{50} < 1$ μg·ml^{-1}, SI > 50[253]; IV) $IC_{50} \leq$ BZN, SI ≥ 50[229]. In addition, another criterion was that compounds had to be active against the three *T. cruzi* strains to avoid drug resistance.

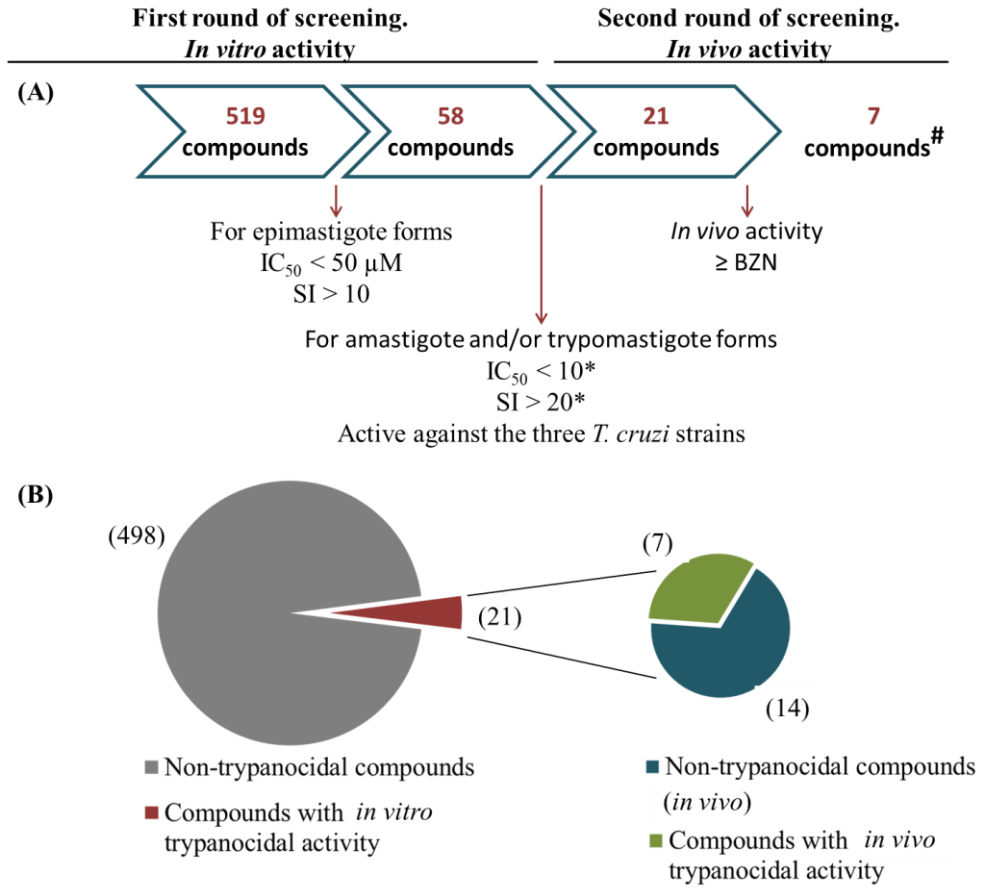

Scheme 6. Screening of trypanocidal compounds. (A) Strategy followed to select drug candidates for the treatment of CD. (B) Distribution of compounds after the first and second rounds of screening. IC_{50}, inhibitory concentration 50; SI, selectivity index; BZN, benznidazole; *At least for one of the parasite forms in vertebrate hosts for the three *T. cruzi* strains; #3 of them are included in this doctoral thesis.

The *in vivo* strategy, thanks to the *in vivo* approach for CD chemotherapy using BALB/c mice[247–249] (see *section 5.2*), was as follows (**Scheme 7**):

- Owing to the different effectiveness of current drugs, especially limited during the chronic-phase of CD[208,254,255], compounds were evaluated in both the acute and chronic phases of CD. Most *in vivo* testing has focused on acute-phase of CD because it is simpler to monitor parasite infection, but chronic-phase infections should be the main research focus in animal models[2].

- Drugs were administered orally because it is the preferred route for the treatment of parasitic diseases in developing countries, it leads to better patient compliance, and it has a low cost[2,256].
- Given that a compound that achieves parasitaemia reduction in infected mice following 5 days of treatment can be defined as a lead compound[208], the treatment guideline was for 5 consecutive days. Moreover, to evaluate if tested compounds showed higher trypanocidal activity than BZN in the first *in vivo* screening phase[229], the treatment was at subcurative doses of BZN (20 mg·kg^{-1} per day).
- The treatment efficacy or experimental cure in infected mice was evaluated using a double test-of-cure widely used in animal models: parasitaemia reactivation after cyclophosphamide-induced IS, and PCR of nested parasites in the target organs/tissues[210,213,215,257,258].
- Finally, the *in vivo* screening was carried out according to the following criteria: compound activity ≥ BZN activity[229] (**Scheme 6**).

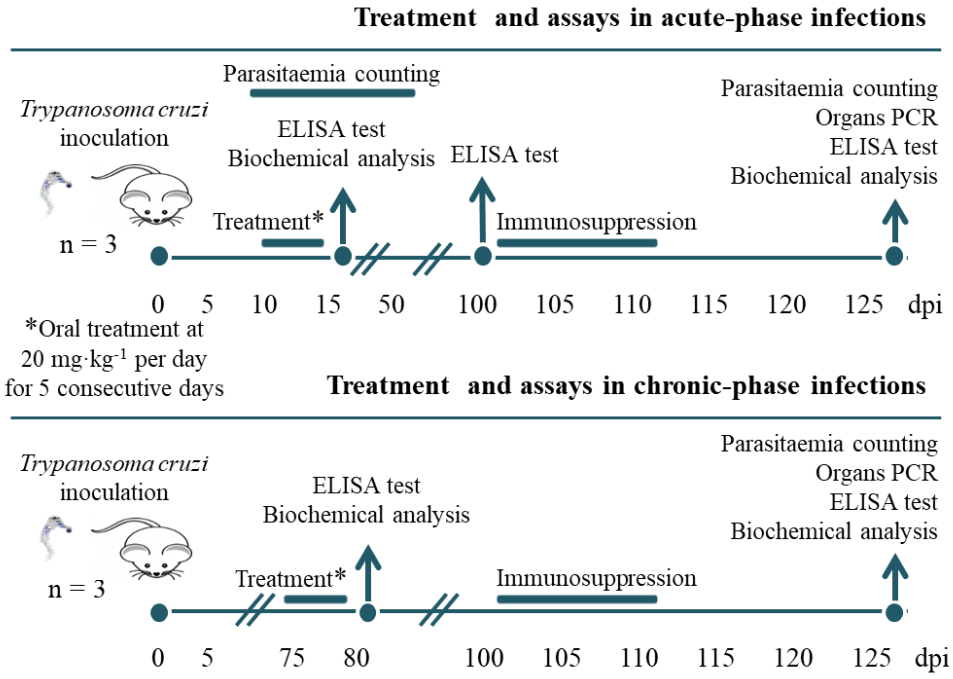

Scheme 7. Timeline for all *in vivo* assays in the acute and chronic phases of Chagas Disease. dpi, days post-infections.

6.2.2. Evaluation of trypanocidal compounds

A total of 519 compounds belonging to different chemical families have been evaluated during the pre-doctoral period, identifying 21 compounds (4.0 %) with high *in vitro* activity. The *in vivo* activity of these 21 compounds was then tested in a second round of screening, and 7 of them (1.3 %) were identified as trypanocidal drug candidates for the treatment of CD (**Scheme 6B**).

3 drug candidates are included in this doctoral thesis. **Table 6** summarizes the *in vitro* activity, the *in vivo* efficacy, and the suggested MoA of the 3 drug candidates. Data of the reference drug BZN are also included. In general, trypanocidal drug candidates show improved *in vitro* activities against the relevant forms from a clinical viewpoint, and enhanced *in vivo* efficacy compared to BZN. Other authors have reported trypanocidal activity of nitroindazole[259–261] and polyamine[168,262] compounds, but as far as we know no squaramide[202] compounds with trypanocidal activity have been reported by other authors.

These trypanocidal drug candidates fulfilled the most stringent *in vitro* requirements stablished for ideal drugs against CD: efficacy against a panel of different strains, fast time to kill behaviour (mentioned below), and higher trypanocidal activity and lower citotoxicity than BZN[208,229,252,253]. Moreover, these compounds met the majority of the *in vivo* criteria of the TPP[2]: activity after oral administration, activity in both the acute and chronic phases of CD, and higher *in vivo* efficacy and lower toxicity than BZN. In addition, the results suggested a hopeful *in vivo* ADMET profile (abbreviation in pharmacokinetics and pharmacology for "absorption, distribution, metabolism, excretion and toxicity").

Table 6. *In vitro* activity, *in vivo* efficacy, and suggested mechanism of action of the 3 trypanocidal drug candidates and the reference drug benznidazole.

Compound and Publication	Chemical structure	*In vitro* IC_{50} (µM) values		*In vivo* treatment efficacy			Suggested MoA
		Amastigote forms (DTU)	Trypomastigote forms (DTU)	Parasitaemia peak in the acute-phase (parasites·mL^{-1})	Parasitaemia reactivation (%) after IS	Infected target organs/tissues*	
Benznidazole	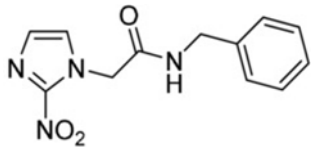	16.6 ± 1.4 (I) 8.3 ± 0.7 (V) 10.0 ± 0.8 (VI)	36.1 ± 3.1 (I) 12.4 ± 1.1 (V) 15.1 ± 1.3 (VI)	1.3 ×10^6	75.0 (A) 51.2 (C)	6/9 (A) 4/9 (C)	Damage to macromolecules (proteins, lipids and nucleic acids)[263,264]
Squaramide 7. [1] (*section 5.3.1*)	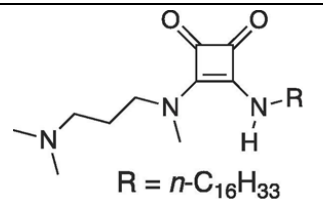	18.9 ± 1.4 (I) 0.2 ± 0.0 (V) 6.4 ± 0.5 (VI)	5.4 ± 0.4 (I) 4.4 ± 0.3 (V) 4.7 ± 0.3 (VI)	1.0 ×10^6	26.1 (A) 21.0 (C)	3/9 (A) 2/9 (C)	Mitochondrial-dependent manner
Polyamine 7. [2] (*section 5.3.2*)	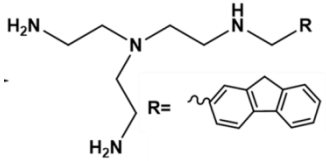	19.7 ± 2.7 (I) 4.8 ± 0.4 (V) 15.1 ± 1.3 (VI)	12.4 ± 1.1 (I) 14.7 ± 1.2 (V) 17.6 ± 1.4 (VI)	1.4 ×10^6	16.3 (A) 5.9 (C)	2/9 (A) 1/9 (C)	Glycosomal-dependent manner
Nitroindazole 16. [3] (*section 5.3.3*)	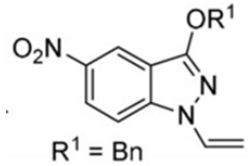	5.8 ± 0.6 (I) 7.4 ± 0.4 (V) 12.4 ± 1.3 (VI)	4.6 ± 0.5 (I) 5.4 ± 0.6 (V) 6.1 ± 0.6 (VI)	1.4 ×10^6	30.1 (A) 35.1 (C)	3/9 (A) 3/9 (C)	Mitochondrial-dependent manner

*By PCR of nested parasites in the 9 target organs/tissues. I, *T. cruzi* SN3 strain (Discrete Typing Unit (DTU) I); V, *T. cruzi* Arequipa strain (DTU V); VI, *T. cruzi* Tulahuen strain (DTU VI); IS, immunosuppression; A, after acute-phase treatment; C, after chronic-phase treatment; MoA, mechanism of action; Bn, benzyl group.

It should be noted that the 3 trypanocidal drug candidates did not obtain a sterile cure after treatment at subcurative doses of BZN, and different organs/tissues maintained the infection after treatment in the acute and chronic phases of CD. It is proposed that the different effectiveness in the different phases is related to inadequate pharmacokinetics/pharmacodynamics between the compounds and the tissue localization of nested parasites during the chronic-phase[265]. Alternatively, compounds and BZN showed higher efficacy in the chronic-phase than in the acute-phase, probably because the parasite burden is significantly low and limited to far few locations[257]. However, a massive reduction in the parasitic load in these first *in vivo* screening phase is considered an important advance towards the identification of new tripanocidal drugs[229]. In overall, the absence of toxicity allows these compounds to be tested at higher doses, establishing improved treatment guidelines based on pharmacokinetic/pharmacodynamics studies, even combined therapies using compounds with different MoA, in order to achieve sterile cure.

Regarding infected target organs/tissues, it has to be highlighted that the adipose tissue and the heart are the organs/tissues that most maintained the infection after treatment using the drug candidates, including BZN. Concerning adipose tissue, many of the current potential candidates for the treatment of CD show nested parasites in this tissue after treatment[266,267267], and lesser drug accessibility or parasite susceptibility in a lipid rich environment could be the reasons for the lower efficacy[96,266]. For the heart, it could be because of the tissue contamination with BTs due to the difficulty of removing all blood by perfusion.

Assessment of cure in CD is controversial due to the absence of irrefutable tests to ensure parasite elimination, and PCR techniques are mainly used to ascertain the failure of clinical treatments – even consistently negative results using blood are not sufficient

to confirm parasite elimination[268,269]. For animal models, the double test-of-cure[210,213,215,257,258] is widely used to evaluate the treatment efficacy or experimental cure in infected animals: mice whose parasitaemia remains negative after IS and with negative PCR results for target organs/tissues are considered cured[213,257]. It has to be highlighted that the PCR determination of the presence of nested parasites in organs/tissues shows better sensitivity than any other blood methodology[268]. Recently, new bioluminescence *in vivo* imaging models using transgenic parasites facilitate research in terms of monitoring the course and the dynamic of the infection – even the spatiotemporal dynamic distribution of the parasite during the chronic-phase, with foci that appear/disappear over the course of even a single day[222] –, reducing the number of animal and generating data with superior accuracy[222,270,271]. Nevertheless, results of six independent samples can provide evidence of cure, or a considerable reduction in the parasitic load, substantiated on the double test-of-cure (and supported by the immune response determination and the splenomegaly observation, which are linked with the parasitic load, reflect the infection rates and verify the efficacy attributed to the treatment[210,216,272]).

Finally, the MoA analyses were initiated at the energy metabolism level owing to the fast-acting activity showed by the tested compounds: *in vitro* screening were carried out for 72 and 24 h (endpoints for amastigote and trypomastigote forms, respectively) in order to select only the compounds that were able to show activity in short time treatments, as BZN[204]. The time of action is an important feature to predict the exposure needed to avoid any relapse after chemotherapy, and it is questionable whether slow-acting drugs are desirables[208]: slow-acting drugs as posaconazole often act by inhibiting parasite replication, so the sensitivity of quiescent or dormant amastigote forms is null. It seems that it is necessary to target each of these forms to eradicate an infection[62].

Therefore, glycosomal and mitochondrial were the levels analysed since these are the main organelles/routes of *T. cruzi* for obtaining energy[74,273–275]. As stated before (**Table 7**), MoA analyses suggested that the fast-acting activities could be explained by a bioenergetic collapse caused by a mitochondrial membrane depolarisation (for squaramide 7 and nitroindazole 16)[248,249] and a reduction on the catabolic glucose metabolism (for polyamine 7)[247], inducing *T. cruzi* death by necrosis:

- On the one hand, it is well-known that the mitochondrion plays an imperative role in cell death decisions, and an active pumping of H^+ is produced in the mitochondrial membrane to maintain its electrochemical gradient, integrity and function[276]. Disturbances produced in this potential (as caused by squaramide 7[248] and nitroindazole 16[249]) may cause imbalances in NADH/NAD^+ and adenosine triphosphate (ATP)/ adenosine diphosphate (ADP) ratios, compromising nucleic acid levels and causing apoptosis and/or necrosis[273,277,278].
- On the other hand, alterations on the catabolic glucose metabolism can slowdown the NADH reoxidation system, especially if there is a reduction in the production of L-alanine and succinate[80] (as caused by polyamine 7[247]). NADH is an essential coenzyme for biosynthetic pathways and also for protection against oxidative stress, due to ROS[81].

However, the therapeutic targets were not elucidated since the only target evaluated was the Fe-SOD of *T. cruzi*, and the activity of the drug candidates could not be ascribed to the inhibition of this enzyme. This enzyme was tested since the trypanosomatid exclusive Fe-SOD presents structural and biochemical differences with respect to the human SOD[279,280], it is a key enzyme in the elimination of ROS and in the protection from the damage produced by oxidative stress[281,282], and its inhibition could explain the suggested MoA[283]. Other alternative homologue/parasite-specific enzymes, such as

trypanothione reductase[73,284], can be studied to determine the molecular targets for these compounds.

Enzymes involved in the glucose metabolism are also candidate enzymes to be a target for polyamine 7 – especially those with the lowest maximum velocity (Vmax) since they are enzymes with high control on the pathway fluxes and are not highly regulated, as hexokinase in *T. cruzi*[73,75]. In addition, hexokinase is a key enzyme since it is encoded by all morphological forms of *T. cruzi*[74]. Alternatively, it has been determined that glucose transporter has the highest control of glycolysis in different cells, doing this transporter another target protein for polyamine 7[73].

Synthesis of ergosterol and polyamine transporter are also candidates to be inhibited for nitroindazole 16 (as a nitrogen heterocycle)[30,167] and for polyamine 7 (as an analogue of other polyamines such as putrescine or spermine)[168], respectively. Therefore, these possible MoA should not be discarded.

Finally, it should be noted that these compounds could act against enzymes involved in the synthesis of these key enzymes, causing the same effect as being inhibitors[285–288].

In short, a more focused view is required in order to know the molecular targets, and if the disturbances observed are the cause of the parasite death or a consequence of its action at another levels. In addition, the possibility of multitarget activity should not be rejected.

Simultaneously, the bioenergetic collapse could be the cause of the cidal, and not static, activity observed by these drug candidates: they did not only inhibit the infection growth by prolonging the growth rate of the parasite (static activity), but reduced both the number of infected cells and the number of amastigote forms per cell compared to the primary infection by eradicating *T. cruzi* infection (cidal activity)[234,289] in 72 h (data not shown). Wash-out/recovery assays are required as the ultimate tests to confirm if

there is any regrowth of the parasites once one stops drug pressure[208]. However, it should be mentioned that the assay performed against amastigote forms can already give this information if no parasites can be identified after drug treatment. For trypomastigote forms, the design of the assay and the non-replicative nature of these forms mean that the differences observed with respect to the controls are solely due to the cidal activity of these compounds.

The importance of assessing cidality of compounds is a main feature, along with the time to kill, in order to avoid any recovery after treatment[290]. Moreover, both features can help to predict the exposure needed to achieve sterile cure *in vivo*[208], a critical prerequisite for new drug candidates for CD. In 2014, the prerequisite of cidality was notably supported by clinical studies where most patients eventually relapsed after apparent total clearance of infection at the end of treatment using two triazoles, posaconazole and fosravuconazole (a prodrug of ravuconazole)[151,291], in contrast to the relatively low treatment failure observed with BZN[292]. This fact demonstrates that these drugs are unable to achieve a sterile cure, even being active at significantly lower concentrations than BZN *in vitro* (nanomolar range)[292–294]. In 2016, it has been demonstrated by wash-out assays that these drugs maintain residual infected cells after treatment, but viable and infective[292]. In addition, dormant forms of *T. cruzi* that allows the infection to persist after treatment were identified in 2018: these dormant amastigote forms appear spontaneously (arresting the replication), they are often observed soon after host cell infection, and they resume replication days to weeks after entering dormancy[251]. This objection could be related to the MoA of these triazoles: they are ergosterol biosynthesis inhibitors, a crucial component for the proliferation of the replicative stages of *T. cruzi*[295,296], which means that these drugs inhibit cell division and growth of *T. cruzi* (static, and not cidal, activity) and are time-dependent drugs

(slow-acting)[297,298]. Therefore, parasites with reduced metabolism activity (dormant amastigote forms) and non-replicative stages (trypomastigote forms) have reduced susceptibility to such drugs[208,251,299]. Shortly, new fast-acting and cidal candidates, capable of killing dormant amastigotes, are needed to avoid treatment failures.

In summary, new fast-acting and trypanocidal drug candidates against different *T. cruzi* strains and with higher efficacy and lower toxicity than BZN in both the acute and chronic CD are presented. These drug candidates meet the majority of the *in vitro* and *in vivo* requirements stablished for ideal drugs against CD, and the results suggest a hopeful ADMET profile. Therefore, these compounds provide a step forward in the development of new cost-effective anti-Chagas drugs. It is worth considering higher doses and/or prolonged treatment duration, and improved treatment guidelines based on pharmacokinetic/pharmacodynamics studies, even improved formulations and combined therapies, with the aim of reaching sterile cure. Among them, polyamine 7 is the best candidate for combined therapy with the reference drug BZN as it is the most effective compound *in vivo*, at the doses tested. In addition, polyamine 7 seems to have a different MoA than BZN, which may enhance the combined activity.

7. CONCLUSIONS/CONCLUSIONES

1. The screening strategy during the pre-doctoral period identified 21 compounds with *in vitro* activity out a total of 519 compounds, and 7 of them were selected after *in vivo* screening.
2. The 3 drug candidates included in this doctoral thesis have been identified for the development of new trypanocidal agents against Chagas Disease: they showed enhanced *in vitro* activities and *in vivo* efficacies in both the acute and chronic phases of Chagas Disease compared to the reference drug benznidazole, at the tested doses.
3. The drug candidates met the majority of the *in vitro* and *in vivo* requirements stablished for ideal drugs against Chagas Disease, such as trypanocidal activity against different *Trypanosoma cruzi* strains, efficacy after oral administration, and higher efficacy and lower toxicity than benznidazole in both the acute and chronic phases of Chagas Disease.
4. The drug candidates showed fast-acting and cidal activities that could be explained by a bioenrgetic collapse caused by a mitochondrial membrane depolarisation (for squaramide 7 and nitroindazole 16) and a reduction on the catabolic glucose metabolism (for polyamine 8).
5. A highly reproducible, sensible, precise, simple, and improved fluorescence-based method has been developed for the *in vitro* drug screening against all morphological forms of *Trypanosoma cruzi*.
6. This research provides a step forward in the development of new cost-effective anti-Chagas drugs.

/

1. La estrategia de cribado identificó 21 compuestos con actividad *in vitro* de un total de 519 compuestos, y 7 de ellos se seleccionaron después del cribado *in vivo*.

2. Los 3 potenciales compuestos incluidos en esta tesis doctoral se presentan para el desarrollo de nuevos agentes tripanocidas frente a la Enfermedad de Chagas: mostraron mejores actividades *in vitro* y eficacias *in vivo* tanto en la fase aguda como en la fase crónica de la enfermedad en comparación con el fármaco de referencia Benznidazol.
3. Los potenciales compuestos cumplieron la mayoría de los requerimientos *in vitro* e *in vivo* establecidos para fármacos ideales frente a la Enfermedad de Chagas, como actividad tripanocida frente a diferentes cepas de *Trypanosoma. cruzi*, eficacia tras una administración oral, y mayor eficacia y menor toxicidad que el benznidazol tanto en la fase aguda como en la fase crónica de la enfermedad.
4. Los potenciales compuestos mostraron actividades cidal y de acción rápida que podrían explicarse por un colapso bioenergético causado por una despolarización de la membrana mitocondrial (para la escuaramida 7 y el nitroimidazol 16) y una reducción en el metabolismo catabólico de la glucosa (para la poliamina 8).
5. Se ha desarrollado un método basado en fluorescencia altamente reproducible, sensible, preciso, simple y mejorado para el cribado *in vitro* de compuestos contra todas las formas morfológicas de *Trypanosoma cruzi*.
6. Esta investigación supone un paso adelante en el desarrollo de nuevos fármacos rentables frente a la Enfermedad de Chagas.

8. FUTURE DIRECTIONS

1. Apply the novel methodology based on the fluorescence produced by the *T. cruzi* CL-Luc:Neon/Cas9 strain for all parasite forms to improve *in vitro* screening of trypanocidal compounds (time to kill, time of action, and washout/recovery assays).
2. Implement the highly sensitive *in vivo* imaging system based on bioluminescent *T. cruzi* strains to monitor the infection caused by this parasite.
3. Conduct new *in vivo* trials by increasing treatment doses, prolonging treatment duration, and/or combining drug candidates in order to achieve a sterile cure.
4. Design new formulations to improve their pharmacokinetics/pharmacodynamics and ADMET profiles with the aim of administering the shortest and lowest effective treatment guideline to achieve a sterile cure.
5. Perform PCR of the target organs based on the *T. cruzi* splice leader (SL) region, a tandem repeated intergenic region, in order to increase the technique sensitivity (not applicable if point 2).
6. Perform new assays to deepen the mechanism of action of the potential compounds.
    6.1. To determine apoptosis: measure nucleosome formation, DNA fragmentation (laddering), caspase activation, mitochondrial respiration and/or mitochondrial cytochrome c release.
    6.2. To determine the molecular target: cloning candidate targets (Fe-SOD, trypanothione reductase, cruzipain, pyruvate kinase and hexokinase genes, among others) from *T. cruzi* into plasmids for the overexpression and purification of high-yield proteins. Once produced, characterise the compound-protein binding/inhibition kinetics by isothermal titration calorimemtry (ITC) techniques in order to determine the catalytic constants.

9. APPENDICES

9.1. Appendix 1: personal contribution

- Cellular cultures
    - Parasite culture
    - Mammalian cell culture
- *In vitro* assays
    - Obtaining parasite metacyclic forms
    - Screening tests against extra- and intracellular parasite forms
    - Cytotoxicity tests
    - Development of the novel fluorescence-based *in vitro* screening method*
- *In vivo* assays
    - Establishment of a new *in vivo* murine model for CD
    - Mice Care and Maintenance
    - Mice infection and treatment
    - Parasitaemia counting
    - Cyclophosphamide-induced IS
    - Tissues harvesting
    - DNA extraction, PCR and electrophoresis
    - ELISA tests
    - Samples preparation for the determination of toxicity by biochemical analyses using the BS-200 Chemistry Analyzer Shenzhen Mindray
- MoA assays
    - Samples preparation for the determination of metabolites by nuclear magnetic resonance (NMR)
    - Samples preparation for the determination of mitochondrial membrane potential and nucleic acid levels by flow cytometry

- SOD inhibition tests

- Processing of data and analysis
- Writing of published works

*Performed at the London School of Hygiene and Tropical Medicine (LSHTM) under the supervision of Dr J. Kelly.

9.2. Appendix 2: other works published during the doctoral thesis

1. **Martín-Escolano, R.**, Cebrian, R., Maqueda, M., Romero, D., Rosales, M.J., Sánchez-Moreno, M., Marín, C., 2020. Assessing the effectiveness of AS-48 in experimental mice models of Chagas Disease. J. Adv. Res. Epub ahead of print. https://doi.org/10.1093/jac/dkaa030.
2. Martín-Montes, Á., Aguilera-Venegas, B., Mª Morales-Martín, R., **Martín-Escolano, R.**, Zamora-Ledesma, S., Marín, C., Arán, V.J., Sánchez-Moreno, M., 2019. *In vitro* assessment of 3-alkoxy-5-nitroindazole-derived ethylamines and related compounds as potential antileishmanial drugs. Bioorg. Chem. 92, 103274. https://doi.org/10.1016/j.bioorg.2019.103274.
3. Cebrián, R., Rodríguez-Cabezas, M.E., **Martín-Escolano, R.**, Rubiño, S., Garrido-Barros, M., Montalbán-López, M., Rosales, M.J., Sánchez-Moreno, M., Valdivia, E., Martínez-Bueno, M., Marín, C., Gálvez, J., Maqueda, M., 2019. Preclinical studies of toxicity and safety of the AS-48 bacteriocin. J. Adv. Res. 20, 129–139. https://doi.org/10.1016/j.jare.2019.06.003.
4. Paucar, R., **Martín-Escolano, R.**, Moreno-Viguri, E., Cirauqui, N., Marín, C., Sánchez-Moreno, M., Pérez-Silanes, S., 2019. Antichagasic profile of a series of Mannich base-type derivatives: Design, synthesis, *in vitro* evaluation, and computational studies involving iron superoxide dismutase. ChemistrySelect. 4, 8112–8121. https://doi.org/10.1002/slct.201901108.

5. Paucar, R., **Martín-Escolano, R.**, Moreno-Viguri, E., Azqueta, A., Cirauqui, N., Marín, C., Sánchez-Moreno, M., Pérez-Silanes, S., 2019. Rational modification of Mannich base-type derivatives as novel antichagasic compounds: Synthesis, *in vitro* and *in vivo* evaluation. Bioorg. Med. Chem. 27, 3902–3917. https://doi.org/10.1016/j.bmc.2019.07.029.
6. **Martín-Escolano, R.**, Cebrián, R., Martín-Escolano, J., Rosales, M.J., Maqueda, M., Sánchez-Moreno, M., Marín, C., 2019. Insights into Chagas treatment based on the potential of bacteriocin AS-48. Int. J. Parasitol. Drugs Drug Resist. 10, 1–8. https://doi.org/10.1016/j.ijpddr.2019.03.003.
7. Urbanová, K., Ramírez-Macías, I., **Martín-Escolano, R.**, Rosales, M.J., Cussó, O., Serrano, J., Company, A., Sánchez-Moreno, M., Costas, M., Ribas, X., Marín, C., 2019. Effective tetradentate compound complexes against *Leishmania* spp. that act on critical enzymatic pathways of these parasites. Molecules. 24, E134. https://doi.org/10.3390/molecules24010134.
8. Paucar, R., **Martín-Escolano, R.**, Moreno-Viguri, E., Cirauqui, N., Rodrigues, C.R., Marín, C., Sánchez-Moreno, M., Pérez-Silanes, S., Ravera, M., Gabano, E., 2019. A step towards development of promising trypanocidal agents: Synthesis, characterization and *in vitro* biological evaluation of ferrocenyl Mannich base-type derivatives. Eur. J. Med. Chem. 163, 569–582. https://doi.org/10.1016/j.ejmech.2018.12.005.
9. Medina-Carmona, E., Rizzuti, B., **Martín-Escolano, R.**, Pacheco-García, J.L., Mesa-Torres, N., Neira, J.L., Guzzi, R., Pey, A.L., 2019. Phosphorylation compromises FAD binding and intracellular stability of wild-type and cancer-associated NQO1: Insights into flavo-proteome stability. Int. J. Biol. Macromol. 125, 1275–1288. https://doi.org/10.1016/j.ijbiomac.2018.09.108.

10. **Martín-Escolano, R.**, Moreno-Viguri, E., Santivañez-Veliz, M., Martin-Montes, A., Medina-Carmona, E., Paucar, R., Marín, C., Azqueta, A., Cirauqui, N., Pey, A.L., Pérez-Silanes, S., Sánchez-Moreno, M., 2018. Second generation of Mannich base-type derivatives with *in vivo* activity against *Trypanosoma cruzi*. J. Med. Chem. 61, 5643–5663. https://doi.org/10.1021/acs.jmedchem.8b00468.
11. Martin-Montes, A., Santivañez-Veliz, M., Moreno-Viguri, E., **Martín-Escolano, R.**, Jiménez-Montes, C., Lopez-Gonzalez, C., Marín, C., Sanmartín, C., Gutiérrez Sánchez, R., Sánchez-Moreno, M., Pérez-Silanes, S., 2017. *In vitro* antileishmanial activity and iron superoxide dismutase inhibition of arylamine Mannich base derivatives. Parasitology. 144, 1783–1790. https://doi.org/10.1017/S0031182017001123.
12. Martín-Montes, Á., Plano, D., **Martín-Escolano, R.**, Alcolea, V., Díaz, M., Pérez-Silanes, S., Espuelas, S., Moreno, E., Marín, C., Gutiérrez-Sánchez, R., Sanmartín, C., Sánchez-Moreno, M., 2017. Library of seleno-compounds as novel agents against *Leishmania* species. Antimicrob. Agents Chemother. 61, e02546-16. https://doi.org/10.1128/AAC.02546-16.
13. Martín-Montes, Á., Ballesteros-Garrido, R., **Martín-Escolano, R.**, Marín, C., Guitiérrez-Sánchez, R., Abarca, B., Ballesteros, R., Sanchez-Moreno, M., 2017. Synthesis and *in vitro* leishmanicidal activity of novel [1,2,3]triazolo[1,5-a]pyridine salts. RSC Adv. 7, 15715–15726. https://doi.org/10.1039/C7RA01070B.
14. Moreno-Viguri, E., Jiménez-Montes, C., **Martín-Escolano, R.**, Santivañez-Veliz, M., Martin-Montes, A., Azqueta, A., Jimenez-Lopez, M., Zamora Ledesma, S., Cirauqui, N., López de Ceráin, A., Marín, C., Sánchez-Moreno, M., Pérez-Silanes, S., 2016. *In vitro* and i*n vivo* anti-*Trypanosoma cruzi* activity of

new arylamine Mannich base-type derivatives. J. Med. Chem. 59, 10929–10945. https://doi.org/10.1021/acs.jmedchem.6b00784.

9.3. Appendix 3: fellowships & research stays

- Fellowships
    - International mobility fellowship (STF8080, 2019) from the European Molecular Biology Organization (EMBO).
    - International mobility fellowship (EMR, 2018/2019) from the University of Granada (UGR).
    - International mobility fellowship (EST16/00218) from the Ministerio de Educación, Cultura y Deporte (MECD), Gobierno de España.
    - FPU fellowship (FPU14/01537) from the Ministerio de Educación, Cultura y Deporte (MECD), Gobierno de España.
- Research stays
    - School of Biosciences, University of Kent, Canterbury, United Kingdom. Period: 29/04/2019 to 28/10/2019.
    - London School of Hygiene and Tropical Medicine (LSHTM), London, United Kingdom. Period: 18/09/2017 to 17/12/2017.

10. ABBREVIATIONS

ADMET, absorption, distribution, metabolism, excretion and toxicity; **ADP**, adenosine diphosphate; **AIDS**, acquired immune deficiency syndrome; **AO**, acridine orange; **ASP-2**, amastigote surface protein-2; **ATP**, adenosine triphosphate; **BZN**, benznidazole; **BTs**, bloodstream trypomastigotes; **Cas9**, CRISPR associated protein 9; **CCRP**, Chagas Clinical Research Platform; **CD**, Chagas Disease; **CDC**, Centers for Disease Control and Prevention; **CNS**, central nervous system; **CO_2**, carbon dioxide; **CP**, cyclophosphamide monohydrate; **CRA**, cytoplasmic repetitive antigen; **CSF**, cerebral spinal fluid; **DAPI**, 4′,6-diamidino-2-phenylindole; **DMEM**, Dulbecco's Modified Eagle Medium; **DMSO**, dimethyl sulfoxide; **DNA**, deoxyribonucleic acid; **DND*i***; Drugs for Neglected Diseases *Initiative;* **dpi**, day post-infection; **DTU**, discrete typing unit; **DSC**, differential scanning calorimetry; **EDTA**, ethylenediaminetetraacetic acid; **ELISA**, enzyme-linked immunosorbent assay; **ERG**, Eastern Research Group; **FBS**, foetal bovine serum; **FDA**, Food and Drug Administration; **FRA**, flagellar repetitive antigen; **FSC**, forward scatter; **gRNA**, guide RNA; **HIV**, human immunodeficiency virus; **HTS**, High-throughput Screening; **IC_{50}**, inhibitoy concentration 50; **IFA**, indirect immunofluorescence assay; **Ig**, immunoglobulin; **IL**, interleukin; **IS**, immunosuppression; **JCR**, Journal Citation Reports; **kDNA**, kinetoplast DNA; **Luc:Neon**, Luciferase:NeonGreen**; LSHTM**, London School of Hygiene Tropical Medicine; **MoA**, mechanism of action; **MILT**, miltefosine; **MOI**, multiplicity of infection; **MSF**, Médecins sans Frontières; **NADH**, nicotinamide adenine dinucleotide; **NADPH**, nicotinamide adenine dinucleotide phosphate; **NFX**, nifurtimox; **NMR**, nuclear magnetic resonance; **NTD**, neglected tropical disease; **NTR**, nitroreductase; **rDNA**, ribosomal DNA; **RNA**, ribonucleic acid; **ROS**, reactive oxygen species; **rRNA**, ribosomal RNA; **RPMI**, Roswell Park Memorial Institute; **SOD**, superoxide dismutase; **TcSP**, *T. cruzi* transsialidase superfamily; **TDR**, Tropical Diseases Research; **TGF-*β*,** transforming growth factor β; **TNF*α***, tumour

necrosis factor α; **TPP**, target product profile; **TSA-1**, trypomastigotes surface antigen 1; **PAHO**, Pan American Health Organization**; PBS**, phosphate-buffered saline; **PCR**, polymerase chain reaction; **PEP**, phosphoenolpyruvate; **PEPCK**, phosphoenolpyruvate carboxykinase; **PFA**, paraformaldehyde; **PFR**, paraflagellar rod protein; **PIP3**, phosphatidylinositol-3,4,5-triphosphate; **PK**, pyruvate kinase; **PPDK**, pyruvate phosphate dikinase; **ppm**, parts per million; **PPP**, pentose phosphate pathway; **PV**, parasitophorus vacuole; **R**, Pearson correlation coefficient; **Rho**, Rhodamine 123; **SDS**, sodium dodecyl sulphate; **SI**, selectivity index; **SL**, splice leader; **SSC**, side scatter; **TCA**, tricarboxylic acid; $\mathbf{V_{max}}$, maximum velocity; **WHO**, World Health Organization.

11. REFERENCES

1. Chagas, C. Nova tripanozomiaze humana: estudios sobre a morfolojia e o ciclo evolutivo do *Schizotrypanum cruzi* n. gen., n. sp., ajente etiolojico de nova entidade mórbida do homen. *Mem. Inst. Oswaldo Cruz* **1**, 159–218 (1909).
2. DNDi. Drugs for Neglected Diseases Initiative. Diseases & projects – Chagas disease (2018). Available at: https://www.dndi.org/diseases-projects/chagas/. (Accessed: 10th December 2019)
3. Miles, M. A. The discovery of Chagas Disease: Progress and prejudice. *Infect. Dis. Clin. North Am.* **18**, 247–260 (2004).
4. Viotti, R., Vigliano, C. & Armenti, A. Nothing goes on forever Chagas Disease. *Rev. Esp. Cardiol.* **62**, 1332–1333 (2009).
5. Segovia, J. C. Un caso de trypanosomiasis. *Arch Hosp Rosales En San Salvador* **8**, 249–254 (1913).
6. Ayulo, V. M. & Herrer, A. Estudios sobre trypanosomiasis americana en el Perú: I. Observaciones en el departamento de Arequipa. *Rev. Peru. Med. Exp. Salud Publica* **3**, 96–117 (1944).
7. Tejera, E. La trypanosomose americaine ou maladie de Chagas au Venezuela. *Bull. Soc. Pathol. Exot.* **12**, 509–513 (1919).
8. de Araujo-Jorge, T. C., Telleria, J. & Rios-Dalenz, J. *History of the Discovery of American Trypanosomiasis (Chagas Disease)*. (Elsevier Inc., 2010). doi:10.1016/B978-0-12-384876-5.00001-0
9. León Gómez, A. et al. La Enfermad de Chagas en Honduras. *Rev. Med. Hondureña* **28**, 78–83 (1960).
10. Gasic, G. & Bertin, V. Epidemiologia de la Enfermedad de Chagas en Chile. *Rev. Chil. Pediatr.* **11**, 561–584 (1940).

11. Steverding, D. The history of Chagas Disease. *Parasites and Vectors* **7**, 317 (2014).

12. Guhl, F., Jaramillo, C., Yockteng, R., Vallejo, G. A. & Cárdenas-Arroyo, F. *Trypanosoma cruzi* DNA in human mummies. *Lancet* **349**, 1370 (1997).

13. Lidani, K. C. F. et al. Chagas Disease: From discovery to a worldwide health problem. *Front. Public Health* **7**, 166 (2019).

14. Pérez-Molina, J. A. & Molina, I. Chagas Disease. *Lancet* **391**, 82–94 (2018).

15. Pinto Dias, J. C. et al. 2nd Brazilian Consensus on Chagas Disease, 2015. *Rev. Soc. Bras. Med. Trop.* **49**, 3–60 (2016).

16. WHO. World Health Organization. Chagas disease (American trypanosomiasis). World Health Organ Fact Sheet 340 (2019). Available at: http://www.who.int/mediacentre/factsheets/fs340/en/. (Accessed: 12th December 2019)

17. Coura, J. R. Chagas Disease: Control, elimination and eradication. Is it possible? *Mem. Inst. Oswaldo Cruz* **108**, 962–967 (2013).

18. Coura, J. R., Viñas, P. A. & Junqueira, A. C. V. Ecoepidemiology, short history and control of Chagas Disease in the endemic countries and the new challenge for non-endemic countries. *Mem. Inst. Oswaldo Cruz* **109**, 856–862 (2014).

19. Moncayo, A. & Silveira, A. C. *Current Epidemiological Trends of Chagas Disease in Latin America and Future Challenges: Epidemiology, Surveillance, and Health Policies. American Trypanosomiasis Chagas Disease: One Hundred Years of Research: Second Edition* (Elsevier Inc., 2017). doi:10.1016/B978-0-12-801029-7.00004-6

20. Belaunzarán, M. L. Chagas Disease: Globalization and new hope for its cure. *Rev. Argent. Microbiol.* **47**, 85–87 (2015).

21. Imaz-Iglesia, I. et al. Economic evaluation of Chagas Disease screening in Spain. *Acta Trop.* **148**, 77–88 (2015).

22. Jackson, Y., Pinto, A. & Pett, S. Chagas Disease in Australia and New Zealand: Risks and needs for public health interventions. *Trop. Med. Int. Health.* **19**, 212–218 (2014).

23. Pinazo, M. J. & Gascon, J. The importance of the multidisciplinary approach to deal with the new epidemiological scenario of Chagas Disease (global health). *Acta Trop.* **151**, 16–20 (2015).

24. Bonney, K. M. Chagas Disease in the 21st Century: A public health success or an emerging threat? *Parasite* **21**, 11 (2014).

25. CDC. Centers for Disease Control and Prevention. Parasites - American Trypanosomiasis (also known as Chagas Disease) (2019). Available at: https://www.cdc.gov/parasites/chagas/. (Accessed: 18th December 2019)

26. PAHO. Pan American Health Organization. Chagas Disease (2018). Available at: https://www.paho.org/hq/index.php?option=com_topics&view=article&id=10&Itemid=40743&lang=en. (Accessed: 20th December 2019)

27. Pérez-Molina, J. A., Norman, F. & López-Vélez, R. Chagas Disease in non-endemic countries: Epidemiology, clinical presentation and treatment. *Curr. Infect. Dis. Rep.* **14**, 263–274 (2012).

28. Strasen, J. et al. Epidemiology of Chagas Disease in Europe: Many calculations, little knowledge. *Clin. Res. Cardiol.* **103**, 1–10 (2014).

29. Lee, B. Y., Bacon, K. M., Bottazzi, M. E. & Hotez, P. J. Global economic burden of Chagas Disease: A computational simulation model. *Lancet Infect. Dis.* **13**, 342–348 (2013).

30. Urbina, J. A. Specific chemotherapy of Chagas Disease: Relevance, current limitations and new approaches. *Acta Trop*. **115**, 55–68 (2010).

31. Rassi Jr, A., Rassi, A. & Marin-Neto, J. A. Chagas Disease. *Lancet* **375**, 1388–1402 (2010).

32. Bern, C. Chagas' disease. *N. Engl. J. Med.* **373**, 456–466 (2015).

33. de Araújo, C. A. C., Mayer, C., Waniek, P. J., Azambuja, P. & Jansen, A. M. Differentiation of *Trypanosoma cruzi* I (TcI) and *T. cruzi* II (TcII) genotypes using genes encoding serine carboxypeptidases. *Parasitol. Res.* **115**, 4211–4219 (2016).

34. Tyler, K. M., Olson, C. L. & Engman, D. M. *The Life Cycle of Trypanosoma cruzi. American Trypanosomiasis. World Class Parasites*, vol 7. (Springer, 2003). doi:10.1007/978-1-4419-9206-2_1

35. Teixeira, D. E., Benchimol, M., Crepaldi, P. H. & de Souza, W. Interactive multimedia to teach the life cycle of *Trypanosoma cruzi*, the causative agent of Chagas Disease. *PLoS Negl. Trop. Dis.* **6**, e1749 (2012).

36. de Souza, W. A short review on the morphology of *Trypanosoma cruzi*: from 1909 to 1999. *Mem. Inst. Oswaldo Cruz* **94**, 17–36 (1999).

37. de Melo, L. D. et al. Evolutionary conservation of actin-binding proteins in *Trypanosoma cruzi* and unusual subcellular localization of the actin homologue. *Parasitology* **135**, 955–965 (2008).

38. Cevallos, A. M. et al. *Trypanosoma cruzi*: Multiple actin isovariants are observed along different developmental stages. *Exp. Parasitol.* **127**, 249–259 (2011).

39. Soares, M. J., Souto-Padron, T. & De Souza, W. Identification of a large pre-lysosomal compartment in the pathogenic protozoon *Trypanosoma cruzi*. *J. Cell Sci*. **102**, 157–167 (1992).

40. Macedo, A. M., Machado, C. R., Oliveira, R. P. & Pena, S. D. J. *Trypanosoma cruzi*: Genetic structure of populations and relevance of genetic variability to the pathogenesis of Chagas Disease. *Mem. Inst. Oswaldo Cruz* **99**, 1–12 (2004).

41. Manoel-Caetano, F. D. S. & Silva, A. E. Implications of genetic variability of *Trypanosoma cruzi* for the pathogenesis of Chagas Disease. *Cad. Saude Publica* **23**, 2263–2274 (2007).

42. Dvorak, J. A. et al. *Trypanosoma cruzi*: Flow cytometric analysis. I. Analysis of total DNA/organism by means of mithramycin-induced fluorescence. *J. Protozool.* **29**, 430–437 (1982).

43. Lewis, M. D. et al. Flow cytometric analysis and microsatellite genotyping reveal extensive DNA content variation in *Trypanosoma cruzi* populations and expose contrasts between natural and experimental hybrids. *Int. J. Parasitol*. **39**, 1305–1317 (2009).

44. Briones, M. R., Souto, R. P., Stolf, B. S. & Zingales, B. The evolution of two *Trypanosoma cruzi* subgroups inferred from rRNA genes can be correlated with the interchange of American mammalian faunas in the Cenozoic and has implications to pathogenicity and host specificity. *Mol. Biochem. Parasitol.* **104**, 219–232 (1999).

45. Brisse, S. et al. Evidence for genetic exchange and hybridization in *Trypanosoma cruzi* based on nucleotide sequences and molecular karyotype. *Infect. Genet. Evol.* **2**, 173–183 (2003).

46. Machado, C. A. & Ayala, F. J. Nucleotide sequences provide evidence of genetic exchange among distantly related lineages of *Trypanosoma cruzi*. *Proc. Natl. Acad. Sci. U. S. A.* **98**, 7396–7401 (2001).

47. Sturm, N. R., Vargas, N. S., Westenberger, S. J., Zingales, B. & Campbell, D. A. Evidence for multiple hybrid groups in *Trypanosoma cruzi*. *Int. J. Parasitol.* **33**, 269–279 (2003).

48. Messenger, L. A. & Miles, M. A. Evidence and importance of genetic exchange among field populations of *Trypanosoma cruzi*. *Acta Trop*. **151**, 150–155 (2015).

49. Gaunt, M. W., Yeo, M., Frame, I. A. & Stothard, J. R. Mechanism of genetic exchange in American trypanosomes. *Nature* **421**, 936–939 (2003).

50. Bingle, L. E., Eastlake, J. L., Bailey, M. & Gibson, W. C. A novel GFP approach for the analysis of genetic exchange in trypanosomes allowing the *in situ* detection of mating events. *Microbiology* **147**, 3231–3240 (2001).

51. Romano, A. et al. Cross-species genetic exchange between visceral and cutaneous strains of *Leishmania* in the sand fly vector. *Proc. Natl. Acad. Sci. U. S. A.* **111**, 16808–16813 (2014).

52. Zingales, B. *Trypanosoma cruzi* genetic diversity: Something new for something known about Chagas Disease manifestations, serodiagnosis and drug sensitivity. *Acta Trop*. **184**, 38–52 (2018).

53. Tibayrenc, M. & Ayala, F. J. The clonal theory of parasitic protozoa: 12 years on. *Trends Parasitol.* **18**, 405–410 (2002).

54. Recommendations From a Satellite Meeting. *Mem. Inst. Oswaldo Cruz* **94**, 429–432 (1999).

55. Di Noia, J. M., Buscaglia, C. A., De Marchi, C. R., Almeida, I. C. & Frasch, A. C. C. A *Trypanosoma cruzi* small surface molecule provides the first immunological evidence that Chagas' disease is due to a single parasite lineage. *J. Exp. Med.* **195**, 401–413 (2002).

56. Freitas, J. M., Lages-Silva, E., Crema, E., Pena, S. D. J. & Macedo, A. M. Real time PCR strategy for the identification of major lineages of *Trypanosoma cruzi* directly in chronically infected human tissues. *Int. J. Parasitol.* **35**, 411–417 (2005).

57. Brisse, S., Dujardin, J. C. & Tibayrenc, M. Identification of six *Trypanosoma cruzi* lineages by sequence-characterised amplified region markers. *Mol. Biochem. Parasitol.* **111**, 95–105 (2000).

58. El-Sayed, N. M. et al. The genome sequence of *Trypanosoma cruzi*, etiologic agent of Chagas Disease. *Science* **309**, 409–415 (2005).

59. de Freitas, J. M. et al. Ancestral genomes, sex, and the population structure of *Trypanosoma cruzi*. *PLoS Pathog*. **2**, e24 (2006).

60. Zingales, B. et al. A New Consensus for *Trypanosoma cruzi* intraspecific nomenclature: Second revision meeting recommends TcI to TcVI. *Mem. Inst. Oswaldo Cruz* **104**, 1051–1054 (2009).

61. Barnabé, C., Mobarec, H. I., Jurado, M. R., Cortez, J. A. & Brenière, S. F. Reconsideration of the seven discrete typing units within the species *Trypanosoma cruzi*, a new proposal of three reliable mitochondrial clades. *Infect. Genet. Evol.* **39**, 176–186 (2016).

62. Francisco, A. F., Jayawardhana, S., Lewis, M. D., Taylor, M. C. & Kelly, J. M. Biological factors that impinge on Chagas Disease drug development. *Parasitology* **144**, 1871–1880 (2017).

63. Zingales, B. et al. The revised *Trypanosoma cruzi* subspecific nomenclature: Rationale, epidemiological relevance and research applications. *Infect. Genet. Evol.* **12**, 240–253 (2012).

64. Miles, M. A. et al. The molecular epidemiology and phylogeography of *Trypanosoma cruzi* and parallel research on *Leishmania*: Looking back and to the future. *Parasitology* **136**, 1509–1528 (2009).

65. Izeta-Alberdi, A., Ibarra-Cerdeña, C. N., Moo-Llanes, D. A. & Ramsey, J. M. Geographical, landscape and host associations of *Trypanosoma cruzi* DTUs and lineages. *Parasites and Vectors* **9**, 631 (2016).

66. Mejia, A. M. et al. Benznidazole-resistance in *Trypanosoma cruzi* is a readily acquired trait that can arise independently in a single population. *J. Infect. Dis.* **206**, 220–228 (2012).

67. Villarreal, D., Barnabe, C., Sereno, D. & Tibayrenc, M. Lack of correlation between *in vitro* susceptibility to Benznidazole and phylogenetic diversity of *Trypanosoma cruzi*, the agent of Chagas Disease. *Exp. Parasitol*. **108**, 24–31 (2004).

68. Moreno, M. et al. *Trypanosoma cruzi* benznidazole susceptibility *in vitro* does not predict the therapeutic outcome of human Chagas Disease. *Mem. Inst. Oswaldo Cruz* **105**, 918–924 (2010).

69. Toledo, M. J. et al. Chemotherapy with Benznidazole and Itraconazole for mice infected with different *Trypanosoma cruzi* clonal genotypes. *Antimicrob. Agents Chemother.* **47**, 223–230 (2003).

70. Cazzulo, J. J., Franke de Cazzulo, B. M., Engel, J. C. & Cannata, J. J. B. End products and enzyme levels of aerobic glucose fermentation in trypanosomatids. *Mol. Biochem. Parasitol.* **16**, 329–343 (1985).

71. Von Brand, T. *Biochemistry and Physiology of Endoparasites*. (Elsevier, 1979).

72. Cazzulo, J. J. Aerobic fermentation of glucose by trypanosomatids. *FASEB J.* **6**, 3153–3161 (1992).

73. Saavedra, E., Zabdi, G.-C., Moreno-Sánchez, R. & Michels, P. A. M. Drug target selection for *Trypanosoma cruzi* metabolism by metabolic control analysis and kinetic modeling. *Curr. Med. Chem.* **26**, 6652–6671 (2019).

74. Mauregi, D. A., Cannata, J. J. B. & Cazzulo, J.-J. Glucose metabolism in *Trypanosoma cruzi*. *Essays Biochem.* **51**, 15–30 (2011).

75. Sanz-Rodríguez, C. E., Concepción, J. L., Pekerar, S., Oldfield, E. & Urbina, J. A. Bisphosphonates as inhibitors of *Trypanosoma cruzi* hexokinase: Kinetic and metabolic studies. *J. Biol. Chem.* **282**, 12377–12387 (2007).

76. Desjardins, M. & Descoteaux, A. Inhibition of phagolysosomal biogenesis by the *Leishmania* lipophosphoglycan. *J. Exp. Med.* **185**, 2061–2068 (1997).

77. Haanstra, J. R. et al. Compartmentation prevents a lethal turbo-explosion of glycolysis in trypanosomes. *Proc. Natl. Acad. Sci. U. S. A.* **105**, 17718–17723 (2008).

78. Frydman, B., de los Santos, C., Cannata, J. J. B. & Cazzulo, J. J. Carbon-13 nuclear magnetic resonance analysis of [1-13C]glucose metabolism in *Trypanosoma cruzi*. *Eur. J. Biochem.* **192**, 363–368 (1990).

79. Urbina, J. A., Osorno, C. E. & Rojas, A. Inhibition of phosphoenolpyruvate carboxykinase from *Trypanosoma* (*Schizotrypanum*) *cruzi* epimastigotes by 3-mercaptopicolinic acid: *in vitro* and *in vivo* studies. *Arch. Biochem. Biophys.* **282**, 91–99 (1990).

80. Cazzulo, J. J. Intermediate Metabolism in *Trypanosoma cruzi*. *J. Bioenerg. Biomembr.* **26**, 157–165 (1994).

81. Krauth-Siegel, R. L. & Comini, M. A. Redox control in trypanosomatids, parasitic protozoa with trypanothione-based thiol metabolism. *Biochim. Biophys. Acta* **1780**, 1236–1248 (2008).

82. Esteve, M. I. & Cazzulo, J. J. The 6-phosphogluconate dehydrogenase from *Trypanosoma cruzi*: The absence of two inter-subunit salt bridges as a reason for enzyme instability. *Mol. Biochem. Parasitol*. **133**, 197–207 (2004).

83. Dardonville, C. et al. Synthesis and biological evaluation of substrate-based inhibitors of 6-phosphogluconate dehydrogenase as potential drugs against African trypanosomiasis. *Bioorganic Med. Chem.* **11**, 3205–3214 (2003).

84. Tetaud, E., Bringaud, F., Chabas, S., Barrett, M. P. & Baltz, T. Characterization of glucose transport and cloning of a hexose transporter gene in *Trypanosoma cruzi*. *Proc. Natl. Acad. Sci. U. S. A.* **91**, 8278–8282 (1994).

85. Silber, A. M. et al. Glucose uptake in the mammalian stages of *Trypanosoma cruzi*. *Mol. Biochem. Parasitol.* **168**, 102–108 (2009).

86. Gonçalves, C. S., Ávila, A. R., de Souza, W., Motta, M. C. M. & Cavalcanti, D. P. Revisiting the *Trypanosoma cruzi* metacyclogenesis: Morphological and ultrastructural analyses during cell differentiation. *Parasites and Vectors* **11**, 83 (2018).

87. Jimenez, V. Dealing with environmental challenges: Mechanisms of adaptation in *Trypanosoma cruzi*. *Res. Microbiol*. **165**, 155–165 (2014).

88. Kollien, A. & Schaub, G. The development of *Trypanosoma cruzi* in Triatominae. *Trends Parasitol*. **16**, 381–387 (2000).

89. Tyler, K. M. & Engman, D. M. The life cycle of *Trypanosoma cruzi* revisited. *Int. J. Parasitol*. **31**, 472–481 (2001).

90. Ferreira, L. R., Dossin, F. M., Ramos, T. C., Freymüller, E. & Schenkman, S. Active transcription and ultrastructural changes during *Trypanosoma cruzi* metacyclogenesis. *An. Acad. Bras. Cienc.* **80**, 157–166 (2008).

91. Noireau, F., Diosque, P. & Jansen, A. M. *Trypanosoma cruzi*: Adaptation to its vectors and its hosts. *Vet. Res.* **40**, 26 (2009).

92. de Souza, W., de Carvalho, T. M. U. & Barrias, E. S. Review on *Trypanosoma cruzi*: Host cell interaction. *Int. J. Cell Biol*. **2010**, 295394 (2010).

93. Kurup, S. P. & Tarleton, R. L. The *trypanosoma cruzi* flagellum is discarded via asymmetric cell division following invasion and provides early targets for protective CD8+ T cells. *Cell Host Microbe* **16**, 439–449 (2014).

94. Kessler, R. L. et al. Recently differentiated epimastigotes from *Trypanosoma cruzi* are infective to the mammalian host. *Mol. Microbiol*. **104**, 712–736 (2017).

95. Gutierrez, F. R. S., Guedes, P. M. M., Gazzinelli, R. T. & Silva, J. S. The role of parasite persistence in pathogenesis of Chagas heart disease. *Parasite Immunol.* **31**, 673–685 (2009).

96. Nagajyothi, F. et al. Mechanisms of *Trypanosoma cruzi* persistence in Chagas Disease. *Cell. Microbiol.* **14**, 634–643 (2013).

97. Tanowitz, H. B. et al. Cytokine Gene Expression of Endothelial Cells Infected With *Trypanosoma Cruzi*. *J. Infect. Dis.* **3**, 598–603 (1992).

98. Huang, H. et al. Infection of endothelial cells with *Trypanosoma cruzi* activates NF-κB and induces vascular adhesion molecule expression. *Infect. Immun*. **67**, 5434–5440 (1999).

99. Teixeira, M. M., Gazzinelli, R. T. & Silva, J. S. Chemokines, inflammation and *Trypanosoma cruzi* infection. *Trends Parasitol.* **18**, 262–265 (2002).

100. De Pablos, L. M. & Osuna, A. multigene families in *Trypanosoma cruzi* and their role in infectivity. *Infect. Immun.* **80**, 2258–2264 (2012).

101. Norris, K. A., Bradt, B., Cooper, N. R. & So, M. Characterization of a *Trypanosoma cruzi* C3 binding protein with functional and genetic similarities to

the human complement regulatory protein, decay-accelerating factor. *J. Immunol.* **147**, 2240–2247 (1991).

102. Zambrano-Villa, S., Rosales-Borjas, D., Carrero, J. C. & Ortiz-Ortiz, L. How protozoan parasites evade the immune response. *Trends Parasitol.* **18**, 272–278 (2002).

103. Paulnock, D. M. & Coller, S. P. Analysis of macrophage activation in African trypanosomiasis. *J. Leukoc. Biol.* **69**, 685–690 (2001).

104. Bogdan, C. & Röllinghoff, M. How do protozoan parasites survive inside macrophages? *Parasitol. Today* **15**, 22–28 (1999).

105. de Diego, J., Punzón, C., Duarte, M. & Fresno, M. Alteration of macrophage function by a *Trypanosoma cruzi* membrane mucin. *J. Immunol.* **159**, 4983–4989 (1997).

106. Doyle, P. S. et al. The *Trypanosoma cruzi* protease cruzain mediates immune evasion. *PLoS Pathog.* **7**, e1002139 (2011).

107. Silva, J. S., Twardzik, D. R. & Reed, S. G. Regulation of *Trypanosoma cruzi* infections *in vitro* and *in vivo* by transforming growth factor beta (TGF-beta). *J. Exp. Med.* **174**, 539–545 (1991).

108. Hunter, C. A. et al. IL-10 is required to prevent immune hyperactivity during infection with *Trypanosoma cruzi*. *J. Immunol.* **158**, 3311–3316 (1997).

109. Malechar, J. R. & Kierszenbaum, F. Inhibition of mitogen-induced proliferation of mouse T and B lymphocytes by bloodstream forms of *Trypanosoma cruzi*. *J. Immunol.* **130**, 908–911 (1983).

110. Ortiz-Ortiz, L., Parks, D. E., Rodriguez, M. & Weigle, W. O. Polyclonal B lymphocyte activation during *Trypanosoma cruzi* infection. *J. Immunol*. **124**, 121–126 (1980).

111. Lauria-Pires, L. & Teixeira, A. R. Virulence and pathogenicity associated with diversity of *Trypanosoma cruzi* stocks and clones derived from Chagas' disease patients. *Am. J. Trop. Med. Hyg.* **55**, 304–310 (1996).

112. Eugenia Giorgi, M. & De Lederkremer, R. M. Trans-sialidase and mucins of *Trypanosoma cruzi*: An important interplay for the parasite. *Carbohydr. Res.* **346**, 1389–1393 (2011).

113. Previato, J. O. et al. Structural characterization of the major glycosylphosphatidylinositol membrane-anchored glycoprotein from epimastigote forms of *Trypanosoma cruzi* Y-strain. *J. Biol. Chem.* **270**, 7241–7250 (1995).

114. Gazzinelli, R. T., Pereira, M. E., Romanha, A., Gazzinelli, G. & Brener, Z. Direct lysis of *Trypanosoma cruzi*: A novel effector mechanism of protection mediated by human anti-Gal antibodies. *Parasite Immunol.* **13**, 345–356 (1991).

115. Pereira-Chioccola, V. L. et al. Mucin-like molecules form a negatively charged coat that protects *Trypanosoma cruzi* trypomastigotes from killing by human anti-α-galactosyl antibodies. *J. Cell Sci.* **113**, 1299–1307 (2000).

116. Alcaide, P. & Fresno, M. The *Trypanosoma cruzi* membrane mucin AgC10 inhibits T cell activation and IL-2 transcription through L-selectin. *Int. Immunol.* **16**, 1365–1375 (2004).

117. Schenkman, S., Jiang, M. S., Hart, G. W. & Nussenzweig, V. A novel cell surface trans-sialidase of *Trypanosoma cruzi* generates a stage-specific epitope required for invasion of mammalian cells. *Cell* **65**, 1117–1125 (1991).

118. Dvorak, J. A. & Schmunis, G. A. *Trypanosoma cruzi*: Interaction with mouse peritoneal macrophages. *Exp. Parasitol.* **32**, 289–300 (1972).

119. Wilkowsky, S. E., Barbieri, M. A., Stahl, P. D. & Isola, E. L. Regulation of *Trypanosoma cruzi* invasion of nonphagocytic cells by the endocytically active GTPases dynamin, Rab5, and Rab7. *Biochem. Biophys. Res. Commun*. **291**, 516–521 (2002).

120. Andrews, N. W. From lysosomes into the cytosol: The intracellular pathway of *Trypanosoma cruzi*. *Braz. J. Med. Biol. Res.* **27**, 471–475 (1994).

121. Campbell, D. A., Westenberger, S. J. & Sturm, N. R. The determinants of Chagas Disease: Connecting parasite and host genetics. *Curr. Mol. Med.* **4**, 549–562 (2004).

122. Torrico, F. et al. Maternal *Trypanosoma cruzi* infection, pregnancy outcome, morbidity, and mortality of congenitally infected and non-infected newborns in Bolivia. *Am. J. Trop. Med. Hyg.* **70**, 201–209 (2004).

123. de Bona, E. et al. Autoimmunity in chronic Chagas Disease: A road of multiple pathways to cardiomyopathy? *Front. Immunol.* **9**, 1842 (2018).

124. Rassi, A. J., Rassi, A. & Little, W. C. Chagas' Heart Disease. *Clin. Cardiol.* **23**, 883–889 (2000).

125. Marin Neto, J. A., Simões, M. V & Sarabanda, A. V. Chagas' Heart Disease. *Arq. Bras. Cardiol.* **72**, 247–280 (1999).

126. Braz, L. M. A., Amato Neto, V. & Okay, T. S. Reactivation of *Trypanosoma cruzi* infection in immunosuppressed patients: Contributions for the laboratorial diagnosis standardization. *Rev. Inst. Med. Trop. Sao Paulo* **50**, 65–66 (2008).

127. WHO. World Health Organization. Chagas disease (American trypanosomiasis) (2020). Available at: https://www.who.int/chagas/. (Accessed: 15th January 2020)

128. Andrade, Z. A. Immunopathology of Chagas Disease. *Mem. Inst. Oswaldo Cruz* **94**, 71–80 (1999).

129. Aliberti, J. C. S. et al. Interleukin-12 mediates resistance to *Trypanosoma cruzi* in mice and is produced by murine macrophages in response to live trypomastigotes. *Infect. Immun*. **64**, 1961–1967 (1996).

130. Silva, J. S. et al. The Role of IL-12 in experimental *Trypanosoma cruzi* Infection. *Braz. J. Med. Biol. Res.* **31**, 111–115 (1998).

131. Martins, G. A., Vieira, L. Q., Cunha, F. Q. & Silva, J. S. Gamma interferon modulates CD95 (Fas) and CD95 ligand (Fas-L) expression and nitric oxide-induced apoptosis during the acute phase of *Trypanosoma cruzi* infection: A possible role in immune response control. *Infect. Immun.* **67**, 3864–3871 (1999).

132. Gutierrez, F. R. S., Mineo, T. W. P., Pavanelli, W. R., Guedes, P. M. M. & Silva, J. S. The effects of nitric oxide on the immune system during *Trypanosoma cruzi* infection. *Mem. Inst. Oswaldo Cruz* **104**, 236–245 (2009).

133. Reed, S. G. et al. IL-10 mediates susceptibility to *Trypanosoma cruzi* infection. *J. Immunol.* **153**, 3135–3140 (1994).

134. Tarleton, R. L. *Trypanosoma Cruzi and Chagas Disease: Cause and Effect.* (Kluwer Academic Publishers, 2003). doi: 10.1007/978-1-4419-9206-2_10

135. Kierszenbaum, F. Mechanisms of pathogenesis in Chagas Disease. *Acta Parasitol*. **52**, 1–12 (2007).

136. Bonney, K. M., Luthringer, D. J., Kim, S. A., Garg, N. J. & Engman, D. M. Pathology and pathogenesis of rheumatic heart disease. *Annu. Rev. Pathol*. **14**, 421–447 (2019).

137. Scares, M. B. P., Pontes-De-Carvalho, L. & Ribeiro-Dos-Santos, R. The pathogenesis of Chagas' disease: When autoimmune and parasite-specific immune responses meet. *An. Acad. Bras. Cienc*. **73**, 546–559 (2001).

138. Marin-Neto, J. A., Cunha-Neto, E., Maciel, B. C. & Simões, M. V. Pathogenesis of chronic Chagas heart disease. *Circulation* **115**, 1109–1123 (2007).

139. Minoprio, P. Parasite polyclonal activators: New targets for vaccination approaches? *Int. J. Parasitol*. **31**, 588–591 (2001).

140. Cunha-Neto, E. et al. Induction of cardiac autoimmunity in Chagas heart disease: A case for molecular mimicry. *Autoimmunity* **39**, 41–54 (2006).

141. Gironès, N. et al. Dominant T- and B-cell epitopes in an autoantigen linked to Chagas' disease. *J. Clin. Invest*. **107**, 985–993 (2001).

142. Gomes, Y. M., Lorena, V. M. B. & Luquetti, A. O. Diagnosis of Chagas Disease: What has been achieved? what remains to be done with regard to diagnosis and follow up studies? *Mem. Inst. Oswaldo Cruz* **104**, 115–121 (2009).

143. Diez, C. N., Manattini, S., Zanuttini, J. C., Bottasso, O. & Marcipar, I. The value of molecular stues for the diagnosis of congenital Chagas Disease in northeastern Argentina. *Am. J. Trop. Med. Hyg*. **78**, 624–627 (2008).

144. Bern, C. et al. Evaluation and treatment of chagas disease in the United States: A systematic review. J. *Am. Med. Assoc*. **298**, 2171–2181 (2007).

145. Britto, C. C. Usefulness of PCR-based assays to assess drug efficacy in Chagas Disease chemotherapy: Value and limitations. *Mem. Inst. Oswaldo Cruz* **104**, 122–135 (2009).

146. Lidani, K. C. F., Bavia, L., Ambrosio, A. R. & de Messias-Reason, I. J. The complement system: A prey of *Trypanosoma cruzi*. *Front. Microbiol*. **8**, 607 (2017).

147. Schijman, A. G. et al. International study to evaluate PCR methods for detection of *Trypanosoma cruzi* DNA in blood samples from Chagas Disease patients. *PLoS Negl. Trop. Dis*. **5**, e931 (2011).

148. Moncayo, Á. & Silveira, A. C. Current epidemiological trends of Chagas Disease in Latin America and future challenges in epidemiology, surveillance, and health policy. *Mem. Inst. Oswaldo Cruz* **104**, 17–30 (2009).

149. Hashimoto, K. & Yoshioka, K. Review: Surveillance of Chagas Disease. *Adv. Parasitol.* **79**, 375–428 (2012).

150. Morillo, C. A. et al. Benznidazole and posaconazole in eliminating parasites in asymptomatic *T. cruzi* carriers: The STOP-CHAGAS Trial. *J. Am. Coll. Cardiol*. **69**, 939–947 (2017).

151. Molina, I. et al. Randomized trial of posaconazole and benznidazole for chronic Chagas' disease. *N. Engl. J. Med*. **370**, 1899–1908 (2014).

152. Aldasoro, E. et al. What to expect and when: Benznidazole toxicity in chronic Chagas' disease treatment. *J. Antimicrob. Chemother*. **73**, 1060–1067 (2018).

153. Menezes, J. C. L. et al. Synthesis and anti-*Trypanosoma cruzi* activity of diaryldiazepines. *Molecules* **20**, 43–51 (2014).

154. Dias, J. C. P. et al. II Consenso Brasileiro em Doença de Chagas, 2015. *Epidemiol. Serv. Saude* **25**, 7–86 (2016).

155. Fabbro, D. L. et al. Trypanocide treatment among adults with chronic Chagas Disease living in Santa Fe City (Argentina), over a mean follow-up of 21 years: Parasitological, serological and clinical evolution. *Rev. Soc. Bras. Med. Trop*. **40**, 1–10 (2007).

156. Viotti, R. et al. Side effects of benznidazole as treatment in chronic Chagas Disease: Fears and realities. *Expert Rev. Anti. Infect. Ther*. **7**, 157–163 (2009).

157. Ribeiro, A. L., Nunes, M. P., Teixeira, M. M. & Rocha, M. O. C. Diagnosis and management of Chagas Disease and cardiomyopathy. *Nat. Rev. Cardiol*. **9**, 576–589 (2012).

158. Rassi, A., Rassi, S. G. & Rassi, A. Sudden death in chagas' disease. *Arq. Bras. Cardiol*. **76**, 86–96 (2001).

159. Fiorelli, A. I. et al. Heart transplantation in 107 cases of Chagas' disease. *Transplant. Proc*. **43**, 220–224 (2011).

160. Matsuda, N. M., Miller, S. M. & Evora, P. R. B. The chronic gastrointestinal manifestations of Chagas Disease. *Clinics* **64**, 1219–1224 (2009).

161. Herbella, F. A. M. et al. Treatment of achalasia: Lessons learned with Chagas'disease. *Dis. Esophagus* **21**, 461–467 (2008).

162. Garcia, R. L. S., De Matos, B. M. R., Féres, O. & Da Rocha, J. J. R. Surgical treatment of Chagas megacolon. Critical analysis of outcome in operative methods. *Acta Cir. Bras*. **23**, 83–92 (2008).

163. Hotez, P. J., Bottazzi, M. E., Franco-Paredes, C., Ault, S. K. & Periago, M. R. The neglected tropical diseases of Latin America and the Caribbean: A review of disease burden and distribution and a roadmap for control and elimination. *PLoS Negl. Trop. Dis.* **2**, e300 (2008).

164. Swinney, D. C. & Anthony, J. How were new medicines discovered? *Nat. Rev. Drug Discov*. **10**, 507–519 (2011).

165. Jin, G. & Wong, S. T. C. Toward better drug repositioning: Prioritizing and integrating existing methods into efficient pipelines. *Drug Discov. Today* **19**, 637–644 (2014).

166. Apt, W. Current and developing therapeutic agents in the treatment of Chagas Disease. *Drug Des. Devel. Ther.* **4**, 243–253 (2010).

167. WHO. World Health Organization. *Research Priorities for Chagas Disease, Human African Trypanosomiasis and Leishmaniasis*. World Health Organization technical report series (2012).

168. Reigada, C., Phanstiel, O., Miranda, M. R. & Pereira, C. A. Targeting polyamine transport in *Trypanosoma cruzi*. *Eur. J. Med. Chem.* **147**, 1–6 (2018).

169. National Library of Medicine. Available at: https://clinicaltrials.gov/. (Accessed: 8th January 2020)

170. Torrico, F. et al. Treatment of adult chronic indeterminate Chagas Disease with benznidazole and three E1224 dosing regimens: a proof-of-concept, randomised, placebo-controlled trial. *Lancet Infect. Dis*. **18**, 419–430 (2018).

171. DNDi. Drugs for Neglected Diseases initiative. CLINICAL TRIALS. Chagas Disease (2018). Available at: https://www.dndi.org/2016/clinical-trials/clinical-trials-chagas/. (Accessed: 11th January 2020)

172. Morillo, C. A. et al. Randomized trial of benznidazole for chronic chagas' cardiomyopathy. *N. Engl. J. Med*. **373**, 1295–1306 (2015).

173. Rodríguez-Morales, O. et al. Experimental vaccines against Chagas Disease: A journey through history. *J. Immunol. Res*. **2015**, 489758 (2015).

174. Sánchez-Valdéz, F. J., Pérez Brandán, C., Ferreira, A. & Basombrio, M. Á. Gene-deleted live-attenuated *Trypanosoma cruzi* parasites as vaccines to protect against Chagas Disease. *Expert Rev. Vaccines* **14**, 681–697 (2015).

175. Introini, M. V, Basso, B. & Moretti, E. Experimental Chagas' Disease: I. Study of different immunization conditions in the infection course. *Bol. Chil. Parasitol.* **53**, 45–51 (1998).

176. Basso, B., Moretti, E. & Fretes, R. Vaccination with epimastigotes of different strains of *Trypanosoma rangeli* protects mice against *Trypanosoma cruzi* infection. *Mem. Inst. Oswaldo Cruz* **103**, 370–374 (2008).

177. Breganó, J. W. et al. *Phytomonas serpens*, a tomato parasite, shares antigens with *Trypanosoma cruzi* that are recognized by human sera and induce protective immunity in mice. *FEMS Immunol. Med. Microbiol*. **39**, 257–264 (2003).

178. Ruiz, A. M., Esteva, M., Cabeza Meckert, P., Laguens, R. P. & Segura, E. L. Protective immunity and pathology induced by inoculation of mice with different subcellular fractions of *Trypanosoma cruzi*. *Acta Trop.* **42**, 299–309 (1985).

179. Snary, D. Cell surface glycoproteins of *Trypanosoma cruzi*: protective immunity in mice and antibody levels in human chagasic sera. *Trans. R. Soc. Trop. Med. Hyg.* **77**, 126–129 (1983).

180. Araujo, F. G. & Morein, B. Immunization with *Trypanosoma cruzi* epimastigote antigens incorporated into iscoms protects against lethal challenge in mice. *Infect. Immun*. **59**, 2909–2914 (1991).

181. Gomes, Y. M. et al. Partial protection of mice against *Trypanosoma cruzi* after immunizing with the TcY 72 antigenic preparation. *Mem. Inst. Oswaldo Cruz* **94**, 167–172 (1999).

182. Brandan, C. P., Padilla, A. M., Xu, D., Tarleton, R. L. & Basombrio, M. A. Knockout of the dhfr-ts gene in *Trypanosoma cruzi* generates attenuated parasites able to confer protection against a virulent challenge. *PLoS Negl. Trop. Dis*. **5**, e1418 (2011).

183. Pereira, V. R. et al. Antibody isotype responses in Balb/c mice immunized with the cytoplasmic repetitive antigen and flagellar repetitive antigen of *Trypanosoma cruzi*. *Mem. Inst. Oswaldo Cruz* **98**, 823–825 (2003).

184. Luhrs, K. A., Fouts, D. L. & Manning, J. E. Immunization with recombinant paraflagellar rod protein induces protective immunity against *Trypanosoma cruzi* infection. *Vaccine* **21**, 3058–3069 (2003).

185. Cazorla, S. I. et al. Redirection of the immune response to the functional catalytic domain of the cystein proteinase cruzipain improves protective immunity against *Trypanosoma cruzi* Infection. *J. Infect. Dis.* **202**, 136–144 (2010).

186. Bontempi, I. A. et al. Efficacy of a trans-sialidase-ISCOMATRIX subunit vaccine candidate to protect against experimental Chagas Disease. *Vaccine* **33**, 1274–1283 (2015).

187. Dutton, J. L. et al. A novel DNA vaccine technology conveying protection against a lethal herpes simplex viral challenge in mice. *PLoS One* **8**, e76407 (2013).

188. Lu, G. et al. Alpha-galactosylceramide enhances protective immunity induced by DNA vaccine of the SAG5D gene of *Toxoplasma gondii*. *BMC Infect. Dis*. **14**, 3862 (2014).

189. Dong, B., Zarlenga, D. S. & Ren, X. An overview of live attenuated recombinant pseudorabies viruses for use as novel vaccines. *J. Immunol. Res*. **2014**, 824630 (2014).

190. Salgado-Jiménez, B., Arce-Fonseca, M., Baylón-Pacheco, L., Talamás-Rohana, P. & Rosales-Encina, J. L. Differential immune response in mice immunized with the A, R or C domain from TcSP protein of *Trypanosoma cruzi* or with the coding DNAs. *Parasite Immunol.* **35**, 32–41 (2013).

191. Arce-Fonseca, M. et al. A DNA vaccine encoding for TcSSP4 induces protection against acute and chronic infection in experimental Chagas Disease. *Int. J. Biol. Sci*. **7**, 1230–1238 (2011).

192. Nogueira, R. T. et al. Recombinant yellow fever viruses elicit CD8+ T cell responses and protective immunity against *Trypanosoma cruzi*. *PLoS One* **8**, e59347 (2013).

193. Cazorla, S. I., Frank, M. F. & Malchiodi, E. L. Vaccination approaches against *Trypanosoma cruzi* infection. *Expert Rev. Vaccines* **8**, 921–935 (2009).

194. Dumonteil, E. et al. Accelerating the development of a therapeutic vaccine for human Chagas Disease: Rationale and prospects. *Expert Rev. Vaccines* **11**, 1043–1055 (2012).

195. Bivona, A. E., Alberti, A. S., Cerny, N., Trinitario, S. N. & Malchiodi, E. L. Chagas Disease vaccine design: the search for an efficient *Trypanosoma cruzi* immune-mediated control. *Biochim. Biophys. Acta - Mol. Basis Dis*. 165658 (2020). doi:10.1016/j.bbadis.2019.165658

196. Duschak, V. G. & Couto, A. S. Cruzipain, the major cysteine protease of *Trypanosoma cruzi*: A sulfated glycoprotein antigen as relevant candidate for vaccine development and drug target. A review. *Curr. Med. Chem.* **16**, 3174–3202 (2009).

197. Allaoui, A., François, C., Zemzoumi, K., Guilvard, E. & Ouaissi, A. Intracellular growth and metacyclogenesis defects in *Trypanosoma cruzi* carrying a targeted deletion of a Tc52 protein-encoding allele. *Mol. Microbiol*. **32**, 1273–1286 (1999).

198. Rappuoli, R. Reverse vaccinology. *Curr. Opin. Microbiol*. **3**, 445–450 (2000).

199. Bhatia, V., Sinha, M., Luxon, B. & Garg, N. Utility of the *Trypanosoma cruzi* sequence database for identification of potential vaccine candidates by *in silico* and *in vitro* screening. *Infect. Immun.* **72**, 6245–6254 (2004).

200. Costa, F. C. et al. Expanding the toolbox for *Trypanosoma cruzi*: A parasite line incorporating a bioluminescence-fluorescence dual reporter and streamlined CRISPR/Cas9 functionality for rapid *in vivo* localisation and phenotyping. *PLoS Negl. Trop. Dis.* **12**, e0006388 (2018).

201. Kendall, G., Wilderspin, A. F., Ashall, F., Miles, M. A. & Kelly, J. M. *Trypanosoma cruzi* glycosomal glyceraldehyde-3-phosphate dehydrogenase does not conform to the 'hotspot' topogenic signal model. EMBO J. **9**, 2751–2758 (1990).

202. Olmo, F. et al. Synthesis and biological evaluation of N, N ′-squaramides with high *in vivo* efficacy and low toxicity: Toward a low-cost drug against Chagas Disease. *J. Med. Chem*. **57**, 987–999 (2014).

203. Ye, X., Ding, J., Zhou, X., Chen, G. & Liu, S. F. Divergent roles of endothelial NF-κB in multiple organ injury and bacterial clearance in mouse models of sepsis. *J. Exp. Med.* **205**, 1303–1315 (2008).

204. MacLean, L. M. et al. Development of *Trypanosoma cruzi in vitro* assays to identify compounds suitable for progression in Chagas' disease drug discovery. *PLoS Negl. Trop. Dis.* **12**, e0006612 (2018).

205. Franco, C. H., Alcântara, L. M., Chatelain, E., Freitas-Junior, L. & Moraes, C. B. Drug discovery for Chagas Disease: Impact of different host cell lines on assay performance and hit compound selection. *Trop. Med. Infect. Dis.* **4**, 82 (2019).

206. Andrade, L. O. et al. Differential tissue tropism of *Trypanosoma cruzi* strains: An *in vitro* study. *Mem. Inst. Oswaldo Cruz* **105**, 834–837 (2010).

207. Duran-Rehbein, G. A., Vargas-Zambrano, J. C., Cuéllar, A., Puerta, C. J. & Gonzalez, J. M. Mammalian cellular culture models of *Trypanosoma cruzi* infection: A review of the published literature. *Parasite* **21**, 38 (2014).

208. Chatelain, E. Chagas Disease drug discovery: Toward a new era. *J. Biomol. Screen*. **20**, 22–35 (2015).

209. Rolón, M., Vega, C., Escario, J. A. & Gómez-Barrio, A. Development of resazurin microtiter assay for drug sensibility testing of *Trypanosoma cruzi* epimastigotes. *Parasitol. Res.* **99**, 103–107 (2006).

210. Martín-Escolano, R. et al. Second generation of Mannich base-type derivatives with *in vivo* activity against *Trypanosoma cruzi. J. Med. Chem*. **61**, 5643–5663 (2018).

211. Rodriguez, H. O. et al. *Trypanosoma cruzi* strains cause different myocarditis patterns in infected mice. *Acta Trop*. **139**, 57–66 (2014).

212. Toledo, M. J. O. et al. Effects of specific treatment on parasitological and histopathological parameters in mice infected with different *Trypanosoma cruzi* clonal genotypes. *J. Antimicrob. Chemother*. **53**, 1045–1053 (2004).

213. Santos, D. M. et al. Benznidazole alters the pattern of cyclophosphamide-induced reactivation in experimental *Trypanosoma cruzi*-dependent lineage infection. *Acta Trop*. **113**, 134–138 (2010).

214. Caldas, S. et al. *Trypanosoma cruzi*: Acute and long-term infection in the vertebrate host can modify the response to benznidazole. *Exp. Parasitol.* **118**, 315–323 (2008).

215. Moreno-Viguri, E. et al. *In vitro* and *in vivo* anti-*Trypanosoma cruzi* activity of new arylamine Mannich base-type derivatives. *J. Med. Chem*. **59**, 10929–10945 (2016).

216. Francisco, A. F. et al. Limited ability of posaconazole to cure both acute and chronic *Trypanosoma cruzi* infections revealed by highly sensitive *in vivo* imaging. *Antimicrob. Agents Chemother*. **59**, 4653–4661 (2015).

217. Francisco, A. F., Jayawardhana, S., Taylor, M. C., Lewis, M. D. & Kelly, J. M. Assessing the effectiveness of curative benznidazole treatment in preventing chronic cardiac pathology in experimental models of Chagas Disease. *Antimicrob. Agents Chemother*. **62**, e00832-18 (2018).

218. Henriques, C., Henriques-Pons, A., Meuser-Batista, M., Ribeiro, A. S. & De Souza, W. *In vivo* imaging of mice infected with bioluminescent *Trypanosoma cruzi* unveils novel sites of infection. *Parasites and Vectors* **7**, 89 (2014).

219. Lewis, M. D. et al. Imaging the development of chronic Chagas Disease after oral transmission. *Sci. Rep*. **8**, 11292 (2018).

220. Lewis, M. D. & Kelly, J. M. Putting infection dynamics at the heart of Chagas Disease. *Trends Parasitol*. **32**, 899–911 (2016).

221. Tibayrenc, M. & Telleria, J. *American Trypanosomiasis: Chagas Disease: One Hundred Years of Research*. (Elsevier, 2010).

222. Lewis, M. D. et al. Bioluminescence imaging of chronic *Trypanosoma cruzi* infections reveals tissue-specific parasite dynamics and heart disease in the absence of locally persistent infection. *Cell. Microbiol*. **16**, 1285–1300 (2014).

223. Lewis, M. D., Francisco, A. F., Taylor, M. C., Jayawardhana, S. & Kelly, J. M. Host and parasite genetics shape a link between *Trypanosoma cruzi* infection dynamics and chronic cardiomyopathy. *Cell. Microbiol*. **18**, 1429–1443 (2016).

224. Guarner, J. et al. Mouse model for Chagas Disease: Immunohistochemical distribution of different stages of *Trypanosoma cruzi* in tissues throughout infection. *Am. J. Trop. Med. Hyg*. **65**, 152–158 (2001).

225. Bilate, A. M. B. & Cunha-Neto, E. Chagas Disease cardiomyopathy: Current concepts of an old disease. *Rev. Inst. Med. Trop. Sao Paulo* **50**, 67–74 (2008).

226. Chatelain, E. & Konar, N. Translational challenges of animal models in Chagas Disease drug development: A review. *Drug Des. Devel. Ther.* **9**, 4807–4823 (2015).

227. Buckner, F. S. Experimental chemotherapy and approaches to drug discovery for *Trypanosoma cruzi* infection. *Adv. Parasitol.* **75**, 89–119 (2011).

228. Canavaci, A. M. C. et al. *In vitro* and *in vivo* high-throughput assays for the testing of anti-*Trypanosoma cruzi* compounds. *PLoS Negl. Trop. Dis.* **4**, e740 (2010).

229. Romanha, A. J. et al. *In vitro* and *in vivo* experimental models for drug screening and development for Chagas Disease. *Mem. Inst. Oswaldo Cruz* **105**, 233–238 (2010).

230. Olmo, F. et al. An *in vitro* iron superoxide dismutase inhibitor decreases the parasitemia levels of *Trypanosoma cruzi* in BALB/c mouse model during acute phase. *Int. J. Parasitol. Drugs Drug Resist.* **5**, 110–116 (2015).

231. Sola, I. et al. Synthesis and biological evaluation of N-cyanoalkyl-, N-aminoalkyl-, and N-guanidinoalkyl-substituted 4-aminoquinoline derivatives as potent, selective, brain permeable antitrypanosomal agents. *Bioorganic Med. Chem.* **24**, 5162–5171 (2016).

232. Olmo, F. et al. Tetradentate polyamines as efficient metallodrugs for Chagas Disease treatment in murine model. *J. Chemother.* **29**, 83–93 (2017).

233. Reviriego, F. et al. Simple dialkyl pyrazole-3,5-dicarboxylates show *in vitro* and *in vivo* activity against disease-causing trypanosomatids. *Parasitology* **9**, 1133–1143 (2017).

234. De Rycker, M. et al. Identification of trypanocidal activity for known clinical compounds using a new *Trypanosoma cruzi* hit-discovery screening cascade. *PLoS Negl. Trop. Dis.* **10**, e0004584 (2016).

235. Alonso-Padilla, J. et al. Automated high-content assay for compounds selectively toxic to *Trypanosoma cruzi* in a myoblastic cell line. *PLoS Negl. Trop. Dis.* **9**, e0003493 (2015).

236. Sykes, M. L. & Avery, V. M. Development and application of a sensitive, phenotypic, high-throughput image-based assay to identify compound activity against *Trypanosoma cruzi* amastigotes. *Int. J. Parasitol. Drugs Drug Resist*. **5**, 215–228 (2015).

237. Engel, J. C. et al. Image-based high-throughput drug screening targeting the intracellular stage of *Trypanosoma cruzi*, the agent of Chagas' disease. *Antimicrob. Agents Chemother*. **54**, 3326–3334 (2010).

238. Guevara, P. et al. Expression of fluorescent genes in *Trypanosoma cruzi* and *Trypanosoma rangeli* (Kinetoplastida: Trypanosomatidae): Its application to parasite-vector biology. *J. Med. Entomol*. **42**, 48–56 (2005).

239. Kessler, R. L. et al. Stage-regulated GFP expression in *Trypanosoma cruzi*: Applications from host-parasite interactions to drug screening. *PLoS One* **8**, e67441 (2013).

240. Sanz, L. M. et al. *P. falciparum in vitro* killing rates allow to discriminate between different antimalarial mode-of-action. *PLoS One* **7**, e30949 (2012).

241. Nare, B. et al. Discovery of novel orally bioavailable oxaborole 6-carboxamides that demonstrate cure in a murine model of late-stage central nervous system African trypanosomiasis. *Antimicrob. Agents Chemother.* **54**, 4379–4388 (2010).

242. Xue, H., Li, J., Xie, H. & Wang, Y. Review of drug repositioning approaches and resources. *Int. J. Biol. Sci.* **14**, 1232–1244 (2018).

243. Sertkaya, A., Birkenbach, A., Berlind, A. & Eyraud, J. *Examination of Clinical Trial Costs and Barriers for Drug Development* (2014).

244. Yeu, Y., Yoon, Y. & Park, S. Protein localization vector propagation: a method for improving the accuracy of drug repositioning. *Mol. Biosyst.* **11**, 2096–2102 (2015).

245. PhRMA. Pharmaceutical Research and Manufacturers of America. *PhRMA 2015 Biopharmaceutical Research Industry Profile* (2015).

246. FDA. U.S. Food and Drug Administration. Development & Approval Process | Drugs (2019). Available at: https://www.fda.gov/Drugs/default.htm. (Accessed: 18th November 2019)

247. Martín-Escolano, R. et al. New polyamine drugs as more effective antichagas agents than benznidazole in both the acute and chronic phases. *Eur. J. Med. Chem*. **164**, 27–46 (2019).

248. Martín-Escolano, R. et al. Synthesis and biological evaluation of new long-chain squaramides as anti-chagasic agents in the BALB/c mouse model. Bioorganic Med. Chem. **27**, 865–879 (2019).

249. Martín-Escolano, R. et al. Synthesis and biological *in vitro* and *in vivo* evaluation of 2-(5-nitroindazol-1-yl)ethylamines and related compounds as potential therapeutic alternatives for Chagas Disease. *ChemMedChem* **13**, 2104–2118 (2018).

250. Zingales, B. et al. Drug discovery for Chagas Disease should consider *Trypanosoma cruzi* strain diversity. *Mem. Inst. Oswaldo Cruz* **109**, 828–833 (2014).

251. Sánchez-Valdéz, F. J., Padilla, A., Wang, W., Orr, D. & Tarleton, R. L. Spontaneous dormancy protects *Trypanosoma cruzi* during extended drug exposure. *Elife* **7**, e34039 (2018).

252. Don, R. & Ioset, J. R. Screening strategies to identify new chemical diversity for drug development to treat kinetoplastid infections. *Parasitology* **141**, 140–146 (2014).

253. Nwaka, S. et al. Integrated dataset of screening hits against multiple neglected disease pathogens. *PLoS Negl. Trop. Dis.* **5**, e1412 (2011).

254. Wilkinson, S. R., Taylor, M. C., Horn, D., Kelly, J. M. & Cheeseman, I. A mechanism for cross-resistance to nifurtimox and benznidazole in trypanosomes. *Proc. Natl. Acad. Sci. USA* **105**, 5022–5027 (2008).

255. Scarim, C. B. et al. Current advances in drug discovery for Chagas Disease. *Eur. J. Med. Chem*. **155**, 824–838 (2018).

256. Espuelas, S. et al. Innovative lead compounds and formulation strategies as newer kinetoplastid therapies. *Curr. Med. Chem.* **19**, 4259–4288 (2012).

257. Francisco, A. F. et al. Nitroheterocyclic drugs cure experimental *Trypanosoma cruzi* infections more effectively in the chronic stage than in the acute stage. *Sci. Rep*. **6**, 35351 (2016).

258. Rangel-Gamboa, L. et al. *Trypanosoma cruzi* infection associated with atypical clinical manifestation during the acute phase of the Chagas Disease. *Parasites and Vectors* **12**, 506 (2019).

259. Fonseca-Berzal, C. et al. Antichagasic, leishmanicidal, and trichomonacidal activity of 2-benzyl-5-nitroindazole-derived amines. *ChemMedChem* **13**, 1246–1259 (2018).

260. Fonseca-Berzal, C. et al. Biological approaches to characterize the mode of action of two 5-nitroindazolinone prototypes on *Trypanosoma cruzi* bloodstream trypomastigotes. *Parasitology* **143**, 1469–1478 (2016).

261. Fonseca-Berzal, C. et al. Antichagasic and trichomonacidal activity of 1-substituted 2-benzyl-5-nitroindazolin-3-ones and 3-alkoxy-2-benzyl-5-nitro-2H-indazoles. *Eur. J. Med. Chem.* **115**, 295–310 (2016).

262. Wang, J., Kaiser, M. & Copp, B. R. Investigation of indolglyoxamide and indolacetamide analogues of polyamines as antimalarial and antitrypanosomal agents. *Mar. Drugs* **12**, 3138–3160 (2014).

263. Maya, J. D. et al. Mode of action of natural and synthetic drugs against *Trypanosoma cruzi* and their interaction with the mammalian host. *Comp. Biochem. Physiol. - A Mol. Integr. Physiol*. **146**, 601–620 (2007).

264. Romanha, A. J. et al. Experimental chemotherapy against *Trypanosoma cruzi* infection: Essential role of endogenous interferon-γ in mediating parasitologic cure. *J. Infect. Dis.* **186**, 823–828 (2002).

265. Urbina, J. A. Chemotherapy of Chagas Disease. *Curr. Pharm. Des.* **8**, 287–295 (2002).

266. Galloway, D. A., Laimins, L. A., Division, B. & Hutchinson, F. Adipose tissue - a safe haven for parasites? *Trends Parasitol*. **33**, 276–284 (2016).

267. Ferreira, A. V. M. et al. Evidence for *Trypanosoma cruzi* in adipose tissue in human chronic Chagas Disease. *Microbes Infect*. **13**, 1002–1005 (2011).

268. Martins, H. R., Figueiredo, L. M., Carneiro, C. M., Bahia, M. T. & Pesquisas, D. Persistence of PCR-positive tissue in benznidazole-treated mice with negative blood parasitological and serological tests in dual infections with *Trypanosoma*

cruzi stocks from different genotypes. J. *Antimicrob. Chemother.* **61**, 1319–1327 (2008).

269. Williams, J. T. et al. Polymerase chain reaction detection of *Trypanosoma cruzi* in *Macaca fascicularis* using archived tissues. *Am. J. Trop. Med. Hyg*. **81**, 228–234 (2009).

270. Andriani, G., Chessler, A. C., Courtemanche, G. & Burleigh, B. A. Activity *in vivo* of anti-*Trypanosoma cruzi* compounds selected from a high throughput screening. *PLoS Negl. Trop. Dis*. **5**, e1298 (2011).

271. Lewis, M. D., Francisco, A. F., Taylor, M. C. & Kelly, J. M. A new experimental model for assessing drug efficacy against *Trypanosoma cruzi* infection based on highly sensitive *in vivo* imaging. *J. Biomol. Screen*. **20**, 36–43 (2015).

272. Kayama, H. & Takeda, K. The innate immune response to *Trypanosoma cruzi* infection. *Microbes Infect.* **12**, 511–517 (2010).

273. Bringaud, F., Rivière, L. & Coustou, V. Energy metabolism of trypanosomatids: Adaptation to available carbon sources. *Mol. Biochem. Parasitol.* **149**, 1–9 (2006).

274. Cannata, J. J. B. & Cazzulo, J. J. The aerobic fermentation of glucose by *Trypanosoma cruzi*. *Comp. Biochem. Physiol. -- Part B Biochem*. **79**, 297–308 (1984).

275. Sanchez-moreno, M., Fernandez-becerra, M. C., Castilla-calvente, J. J. & Osuna, A. Metabolic studies by 1H NMR of different forms of *Trypanosoma cruzi* as obtained by *'in vitro'* culture. *FEMS Microbiol. Lett.* **133**, 119–125 (1995).

276. Lee, W. K. & Thévenod, F. A role for mitochondrial aquaporins in cellular life-and-death decisions? *Am. J. Physiol. Cell Physiol.* **291**, C195-202 (2006).

277. Michels, P. A. M., Bringaud, F., Herman, M. & Hannaert, V. Metabolic functions of glycosomes in trypanosomatids. *Biochim. Biophys. Acta - Mol. Cell Res.* **1763**, 1463–1477 (2006).

278. Verma, N. K., Singh, G. & Dey, C. S. Miltefosine induces apoptosis in arsenite-resistant *Leishmania donovani* promastigotes through mitochondrial dysfunction. *Exp. Parasitol.* **116**, 1–13 (2007).

279. Perry, J. J. P. et al. The structural biochemistry of the superoxide dismutases. *Biochim. Biophycs Acta* **1804**, 245–262 (2010).

280. Rodriguez-Ciria, M. et al. 1,4-Bis(alkylamino)benzo[g]phthalazines able to form dinuclear complexes of Cu(II) which as free ligands behave as SOD inhibitors and show efficient in vitro activity against *Trypanosoma cruzi*. *Bioorg. Med. Chem.* **15**, 2081–2091 (2007).

281. Maes, L. et al. *In vitro* and *in vivo* activities of a triterpenoid saponin extract (PX-6518) from the plant *Maesa balansae* against visceral *Leishmania* species. *Antimicrob. Agents Chemother.* **48**, 130–136 (2004).

282. Germonprez, N. et al. *In vitro* and *in vivo* anti-leishmanial activity of triterpenoid saponins isolated from *Maesa balansae* and some chemical derivatives. *J. Med. Chem*. **48**, 32–37 (2005).

283. Kirkinezos, I. G. & Moraes, C. T. Reactive oxygen species and mitochondrial diseases. *Semin. Cell Dev. Biol.* **12**, 449–457 (2001).

284. Soeiro, M. N. & de Castro, S. L. *Trypanosoma cruzi* targets for new chemotherapeutic approaches. *Expert Opin. Ther. Targets* **13**, 105–121 (2009).

285. Osorio-Méndez, J. F. & Cevallos, A. M. Discovery and genetic validation of chemotherapeutic targets for Chagas' disease. *Front. Cell. Infect. Microbiol.* **8**, 439 (2019).

286. Wyllie, S. et al. Dissecting the essentiality of the bifunctional trypanothione synthetase-amidase in *Trypanosoma brucei* using chemical and genetic methods. *Mol. Microbiol.* **74**, 529–540 (2009).

287. Patterson, S. et al. Dihydroquinazolines as a novel class of *Trypanosoma brucei* trypanothione reductase inhibitors: Discovery, synthesis, and characterization of their binding mode by protein crystallography. *J. Med. Chem*. **54**, 6514–6530 (2011).

288. Spinks, D. et al. Design, synthesis and biological evaluation of *Trypanosoma brucei* Trypanothione Synthetase inhibitors. *ChemMedChem* **7**, 95–106 (2012).

289. Mckerrow, J. H. et al. Two approaches to discovering and developing new drugs for Chagas Disease. *Mem. Inst. Oswaldo Cruz* **104**, 263–269 (2009).

290. Roquero, I. et al. Novel chemical starting points for drug discovery in leishmaniasis and Chagas Disease. *Int. J. Parasitol. Drugs Drug Resist*. **10**, 58–68 (2019).

291. Urbina, J. A. Recent clinical trials for the etiological treatment of chronic Chagas Disease: Advances, challenges and perspectives. *J. Eukaryot. Microbiol*. **62**, 149–156 (2015).

292. Cal, M., Ioset, J. R., Fügi, M. A., Mäser, P. & Kaiser, M. Assessing anti-*T. cruzi* candidates *in vitro* for sterile cidality. *Int. J. Parasitol. Drugs Drug Resist*. **6**, 165–170 (2016).

293. Buckner, F. S. & Urbina, J. A. Recent developments in sterol 14-demethylase inhibitors for Chagas Disease. *Int. J. Parasitol. Drugs Drug Resist*. **2**, 236–242 (2012).

294. de Nazaré Correia Soeiro, M. et al. *In vitro* and *in vivo* studies of the antiparasitic activity of sterol 14α-demethylase (CYP51) INHIBITOR VNI against drug-

resistant strains of *Trypanosoma cruzi*. *Antimicrob. Agents Chemother*. **57**, 4151–4163 (2013).

295. Lepesheva, G. I., Villalta, F. & Waterman, M. R. Targeting *Trypanosoma cruzi* Sterol 14α-Demethylase (CYP51). *Adv. Parasitol.* **75**, 65–87 (2011).

296. Urbina, J. A. et al. Antiproliferative effects and mechanism of action of SCH 56592 against *Trypanosoma* (*Schizotrypanum*) *cruz*i: *In vitro* and *in vivo* studies. *Antimicrob. Agents Chemother*. **42**, 1771–1777 (1998).

297. Lepesheva, G. I. Design or screening of drugs for the treatment of Chagas Disease: What shows the most promise? *Expert Opin. Drug Discov*. **8**, 1479–1489 (2013).

298. Molina, I., Salvador, F. & Sánchez-Montalvá, A. The use of posaconazole against Chagas Disease. *Curr. Opin. Infect. Dis*. **28**, 397–407 (2015).

299. Cançado, J. R. Long term evaluation of etiological treatment of Chagas Disease with benznidazole. *Rev. Inst. Med. Trop. Sao Paulo* **44**, 29–37 (2002).